University of Piraeus
Department of Industrial Management &Technology

Πανεπιστήμιο Πειραιώς
Τμήμα Βιομηχανικής Διοίκησης & Τεχνολογίας

Ph.D. Dissertation

Contribution in technical problem-solving using Life Cycle Analysis and Multi-criteria Decision-Making Models: Applications to the energy sector

Διδακτορική Διατριβή

Συμβολή στην ανάπτυξη τεχνικών λύσεων χρησιμοποιώντας Ανάλυση Κύκλου Ζωής και Πολυκριτηριακά Μοντέλα Λήψης Αποφάσεων: Εφαρμογές στον ενεργειακό τομέα

ΑΓΓΕΛΙΚΗ ΣΑΓΑΝΗ
MSc Μηχανολόγος Μηχανικός Ε.Μ.Π

Επιβλέπων Καθηγητής: Βασίλειος Δεδούσης

Δεκέμβριος 2025

Στην οικογένειά μου,
η οποία είναι πάντα δίπλα μου και με στηρίζει ανιδιοτελώς.

Στον σκύλο μου, Λουκουμά,
πηγή ανόθευτης χαράς και σιωπηλής συντροφιάς.

Acknowledgements

This Ph.D. thesis represents the culmination of many years of academic inquiry, sustained effort, and profound intellectual and personal development. Its successful completion would not have been possible without the invaluable support, guidance, and encouragement of numerous individuals, to whom I am deeply and sincerely indebted.

First and foremost, I would like to express my deepest gratitude to my supervisor, Professor Emeritus Vassilis Dedoussis, for his outstanding scientific expertise, unwavering patience, and continuous guidance throughout the entirety of this research. His insightful feedback and constant availability were invaluable at every stage of the doctoral process. He consistently engaged in thoughtful and constructive discussions regarding the challenges encountered, offering clear perspectives and well-founded advice that greatly enhanced the quality of this research. His extensive knowledge in energy modelling and optimization profoundly shaped the direction of this research, providing a robust framework for addressing complex analytical and methodological issues. Beyond his technical contributions, his commitment to academic excellence and integrity was deeply influential. His mentorship was instrumental to the successful completion of this dissertation, for which I am sincerely grateful.

I would also like to express my sincere appreciation to the members of my examining committee, Professor Dimitrios Sidiras of the University of Piraeus and Professor Athanasios Tolis of the National Technical University of Athens (NTUA), for the time and expertise they devoted to the thorough evaluation of this dissertation. Their insightful comments, constructive observations, and rigorous questions contributed significantly to improving the clarity, scientific rigor, and overall quality of this research work. I gratefully acknowledge the remaining members of the committee, namely Professor Dimitrios Georgakellos, Dr. Panagiotis Grammelis, Professor Eleni Didaskalou, and Professor Konstantinos Evangelinos, for agreeing to serve on the seven-member committee for my dissertation.

I am particularly grateful to Professor Stella Sofianopoulou of University of Piraeus for her valuable guidance and support in the section of this dissertation associated with multi-criteria decision analysis. Her extensive expertise in the development of metaheuristic algorithms, as well as in the application of Data Envelopment Analysis (DEA) techniques to advanced energy systems played a decisive role in shaping this part research and in ensuring its methodological rigor.

Furthermore, I gratefully acknowledge the Centre for Research and Technology Hellas (CERTH), where I have been conducting research alongside my Ph.D. studies. I would like to extend special recognition to Dr. Dimitrios Kourkoumpas, Senior Research Engineer at CERTH, whose ongoing collaboration, profound expertise, and exceptional guidance in Life Cycle Analysis (LCA) were indispensable to this research work. His constant confidence in my abilities, combined with his thoughtful mentorship and insightful feedback, significantly enhanced both the overall quality of this dissertation and my professional development. Through my participation in numerous European-funded research projects under his supervision, I gained invaluable practical experience and deepened my knowledge in LCA. I am truly grateful for his generosity

and encouragement, which have greatly enriched my experience and inspired me to pursue new challenges in research. I would also like to express my heartfelt appreciation to my dear colleague at CERTH, Ioanna Marina Anagnostara, for her unwavering support and friendship throughout this journey. Her expertise in programming was a constant source of inspiration, motivating me to further develop my own skills and methodological approaches. Her insightful comments, steady encouragement, and collaborative spirit continually enriched my research experience. Additionally, I am grateful to my colleagues at CERTH, Aliki Zioga, Aikaterini-Maria Zarogianni, and Thanos Kerchoulas, who, together with Ioanna, fostered a supportive and intellectually enriching research environment, and whose encouragement and collegial spirit I will always remember with sincere appreciation. Building on this collaborative atmosphere, I would like to extend my thanks to the students who carried out their undergraduate and postgraduate theses under my guidance.

Last, but certainly not least, I extend my deepest and most heartfelt gratitude to my parents, my sister, my brother-in-law, and my nephew. Their immeasurable love, patience, and steadfast belief in me were my greatest source of strength throughout this demanding journey, constantly reminding me that challenges also carry opportunities for growth. Their encouragement, care, and constant presence offered not only support but also inspiration, enabling me to persevere through the most difficult moments. This dissertation is dedicated to them, with all my love and profound gratitude, for standing by me unwaveringly and supporting me unconditionally at every step of this journey.

Angeliki Sagani

Athens, December 2025

Επιβλέπων Καθηγητής

Δρ. Βασίλειος Δεδούσης
Ομότιμος Καθηγητής Πανεπιστήμιου Πειραιώς

Τριμελής Συμβουλευτική Επιτροπή

Δρ. Βασίλης Δεδούσης
Ομότιμος Καθηγητής Πανεπιστήμιου Πειραιώς

Δρ. Δημήτριος Σιδηράς
Καθηγητής Πανεπιστήμιου Πειραιώς

Δρ. Αθανάσιος Τόλης
Καθηγητής Ε.Μ.Π

Επταμελής Εξεταστική Επιτροπή

Δρ. Βασίλειος Δεδούσης
Ομότιμος Καθηγητής Πανεπιστήμιου Πειραιώς

Δρ. Δημήτριος Σιδηράς
Καθηγητής Πανεπιστήμιου Πειραιώς

Δρ. Αθανάσιος Τόλης
Καθηγητής Ε.Μ.Π

Δρ. Δημήτριος Γεωργακέλλος
Καθηγητής Πανεπιστήμιου Πειραιώς

Δρ. Παναγιώτης Γραμμέλης
Ερευνητής Α' ΕΚΕΤΑ/ΙΔΕΠ

Δρ. Ελένη Διδασκάλου
Καθηγήτρια Πανεπιστημίου Πειραιώς

Δρ. Κωνσταντίνος Ευαγγελινός
Καθηγητής Πανεπιστημίου Αιγαίου

Σύνοψη

Η μετάβαση προς χαμηλού άνθρακα και οικονομικά αποδοτικά ενεργειακά συστήματα αποτελεί στρατηγική προτεραιότητα για την Ελλάδα, μια χώρα με σημαντικό δυναμικό Ανανεώσιμων Πηγών Ενέργειας. (ΑΠΕ). Τα αιολικά και τα φωτοβολταϊκά συστήματα συνιστούν βασικούς πυλώνες για την πλήρη απανθρακοποίηση της ηλεκτροπαραγωγής, στο πλαίσιο της κυκλικής οικονομίας. Ωστόσο, παρά τις τεχνολογικές εξελίξεις, εξακολουθούν να υφίστανται σημαντικά κενά γνώσης και πρακτικοί περιορισμοί. Οι περισσότερες μελέτες Ανάλυσης Κύκλου Ζωής (ΑΚΖ) των συστημάτων ΑΠΕ επικεντρώνονται κυρίως στο στάδιο της λειτουργίας τους, παραβλέποντας τη σημαντική πρωτογενή κατανάλωση ενέργειας και τις εκπομπές των αερίων του θερμοκηπίου που σχετίζονται με τα στάδια παραγωγής, μεταφοράς, εγκατάστασης και διαχείρισης στο τέλος ζωής των συστημάτων. Επιπρόσθετα, τα διαθέσιμα δεδομένα προσαρμοσμένα στην ελληνική αγορά είναι περιορισμένα, ενώ η περιβαλλοντική απόδοση προηγμένων τεχνολογιών, όπως τα φωτοβολταϊκά τρίτης γενιάς, οι υπεράκτιες ανεμογεννήτριες και τα υβριδικά συστήματα ηλεκτροπαραγωγής πολλαπλών πηγών (συμβατικών και ανανεώσιμων), έχει αξιολογηθεί ελλιπώς. Παράλληλα, οι υποδομές ανακύκλωσης ή/και επαναχρησιμοποίησης παραμένουν ανεπαρκείς, ενώ η έλλειψη ολοκληρωμένων πολιτικών πλαισίων περιορίζει περαιτέρω την εφαρμογή των αρχών της κυκλικής οικονομίας και την ευρεία διάδοση των τεχνολογιών ανανεώσιμης ενέργειας.

Η παρούσα Διδακτορική Διατριβή αποσκοπεί στην αντιμετώπιση των ανωτέρω προκλήσεων μέσω της ανάπτυξης ενός ολοκληρωμένου, πολυδιάστατου μεθοδολογικού πλαισίου για την αξιολόγηση και τη βελτιστοποίηση της παραγωγής ηλεκτρικής ενέργειας από συμβατικά ορυκτά καύσιμα και ανανεώσιμες πηγές. Η προτεινόμενη μεθοδολογία ενσωματώνει το σχεδιασμό, τη μοντελοποίηση και τη βελτιστοποίηση ενεργειακών συστημάτων, εμπεριστατωμένη οικονομική και περιβαλλοντική αξιολόγηση βάσει των αρχών του κύκλου ζωής, καθώς και πολυκριτηριακή λήψη αποφάσεων. Η ολοκληρωμένη αυτή προσέγγιση απο-σκοπεί στον καθορισμό των τεχνολογικών διαμορφώσεων υβριδικών συστημάτων παραγωγής ενέργειας, την προσομοίωση της λειτουργίας τους υπό πραγματικά μετεωρολογικά δεδομένα και περιορισμούς του δικτύου, εφαρμόζοντας τη στρατηγική παρακολούθησης φορτίου (load-following dispatch). Η οικονομική ανάλυση βιωσιμότητας αξιολογεί τις ενεργειακές επενδύσεις ενσωματώνοντας βασικούς δείκτες απόδοσης όπως η Καθαρή Παρούσα Αξία (Net Present Value, NPV), ο Εσωτερικός Βαθμός Απόδοσης (Internal Rate of Return, IRR), και το Σταθμισμένο Κόστος Παραγωγής Ενέργειας (Levelized Cost of Energy, LCOE). Η Ανάλυση Κύκλου Ζωής (Life Cycle Assessment, LCA) είναι ένα σημαντικό εργαλείο περιβαλλοντικής διαχείρισης που αξιολογεί την περιβαλλοντική απόδοση σε όλα τα στάδια ζωής του συστήματος (σχεδιασμός, κατασκευή, εγκατάσταση, λειτουργία και απόσυρση), βοηθώντας στη λήψη βιώσιμων αποφάσεων και συγκρίνοντας εναλλακτικές λύσεις. Το σύνολο των επιπτώσεων αξιολογείται ποσοτικά σε τομείς ιδιαίτερου περιβαλλοντικού ενδιαφέροντος, όπως η κλιματική αλλαγή, η χρήση μη ανανεώσιμης ενέργειας, η καταστροφή του όζοντος, η ανθρώπινη υγεία, η εξάντληση των ορυκτών πόρων, κτλ. Τέλος, η πολυκριτηριακή λήψη αποφάσεων (Multi-Criteria Decision Making, MCDM) παρέχει συστηματική αξιολόγηση ανταγωνιστικών στόχων και προτεραιοτήτων των ενδιαφερόμενων μερών, διευκολύνοντας τη βιώσιμη επιλογή στρατηγικών. Το ολοκληρωμένο αυτό πλαίσιο αποτελεί ένα ευέλικτο εργαλείο, ικανό να

υποστηρίζει τόσο την ανάλυση σε επίπεδο έργου όσο και τον στρατηγικό ενεργειακό σχεδιασμό σε εθνικό επίπεδο.

Η εφαρμογή του προτεινόμενου μεθοδολογικού πλαισίου σε πολλαπλές περιπτώσεις μελέτης, σε διάφορες κλίμακες, έδειξε ότι σε ***επίπεδο κτιρίου*** τα συνδεδεμένα με το δίκτυο φωτοβολταϊκά συστήματα ισχύος 5 - 10 kW_p είναι οικονομικά βιώσιμα, ενώ παράλληλα συμβάλλουν σε σημαντικό βαθμό στη μείωση των εκπομπών των αερίων του θερμοκηπίου και την κατανάλωση πρωτογενούς ενέργειας καθ' όλη τη διάρκεια ζωής τους. Τα συστήματα με εγκατεστημένη ισχύ που δεν ξεπερνά τα 5 KW_p κρίθηκαν μη οικονομικά αποδοτικά λόγω υψηλού αρχικού κόστους και χαμηλών τιμών ηλεκτρικής ενέργειας, τονίζοντας την ανάγκη μείωσης του κόστους κατασκευής των φωτοβολταϊκών πάνελ, καθώς και του εξοπλισμού «Ισορροπίας Συστήματος», σε συνδυασμό με μηχανισμούς στήριξης που θα παρέχουν κίνητρα στους παραγωγούς να ανταποκριθούν στις εξελίξεις της αγοράς. Τα πλήρως αυτόνομα υβριδικά συστήματα, που ενσωματώνουν φωτοβολταϊκά, γεννήτρες ντίζελ, συστήματα αποθήκευσης, και θερμική ενέργεια από βιομάζα, κρίθηκαν ως οι πλέον κατάλληλες λύσεις για αποκεντρωμένη ηλεκτροπαραγωγή σε απομακρυσμένα νοικοκυριά, προσφέροντας υψηλή τεχνική απόδοση, ενεργειακή ασφάλεια και αξιοπιστία, καθώς και βελτιωμένη περιβαλλοντική απόδοση.

Σε ***επίπεδο κοινότητας***, οι υβριδικοί σταθμοί παραγωγής ηλεκτρικής ενέργειας που συνδυάζουν αιολική και ηλιακή ενέργεια, συσσωρευτές και γεννήτριες ντίζελ, παρέχουν αξιόπιστες, οικονομικά αποδοτικές και βιώσιμες λύσεις για τα απομονωμένα νησιά του Αιγαίου. Στη Λέσβο, την Κάρπαθο και την Αστυπάλαια, η ανανεώσιμη παραγωγή καλύπτει πάνω από 90% της ηλεκτρικής ενέργειας, ενώ η γεννήτρια ντίζελ λειτουργεί ως εφεδρεία. Τα συστήματα αποθήκευσης (συσσωρευτές) εξισορροπούν τη μεταβλητότητα παραγωγής και ζήτησης, ενώ η ύπαρξη σημαντικού πλεονάσματος ηλεκτρικής ενέργειας άνω του 40% υπογραμμίζει τη δυνατότητα για επιπλέον αποθήκευση ή ευέλικτη χρήση. Τα συστήματα αυτά επιτυγχάνουν ανταγωνιστικό κόστος παραγόμενης ενέργειας, το οποίο κυμαίνεται μεταξύ 0.12–0.15 €/kWh_e, ενώ, παράλληλα, μειώνουν τις εκπομπές των αερίων του θερμοκηπίου άνω του 92%, υποστηρίζοντας τη νέα εποχή ενεργειακής μετάβασης και το «πρασίνισμα» / απανθρακοποίηση των μη διασυνδεδεμένων νησιών.

Σε ***επίπεδο εθνικού δικτύου***, οι θερμικοί σταθμοί ηλεκτροπαραγωγής παραμένουν οι κύριοι παράγοντες περιβαλλοντικών επιπτώσεων, κυρίως όσον αφορά στην κλιματική αλλαγή πλανήτη και τη χρήση μη ανανεώσιμης ενέργειας, ενώ οι ανανεώσιμες πηγές, όπως η αιολική, η ηλιακή, τα μικρά υδροηλεκτρικά και οι μονάδες βιομάζας, παρέχουν μετρήσιμη αλλά σημαντική δυνατότητα μείωσης των εκπομπών. Σενάρια με υψηλή διείσδυση ανανεώσιμης ενέργειας υποδεικνύουν σημαντικές μειώσεις στις εκπομπές των αερίων του θερμοκηπίου και της πρωτογενούς κατανάλωσης ενέργειας, αναδεικνύοντας τη σημασία του βέλτιστου σχεδιασμού, και στρατηγικών βασισμένων στον κύκλο ζωής. Οι υποδομές μεταφοράς και οι απώλειες στο δίκτυο συνεισφέρουν σημαντικά στις περιβαλλοντικές επιπτώσεις, αν και η συμβολή τους παραμένει μικρότερη σε σχέση με τις επιπτώσεις από την παραγωγή ενέργειας στην ηπειρωτική χώρα και τα αυτόνομα Ελληνικά νησιά.

Κρίσιμο στοιχείο για την επίτευξη βιώσιμων ενεργειακών μεταβάσεων αποτελεί η ***φάση τέλους ζωής των ανανεώσιμων τεχνολογιών παραγωγής ενέργειας***. Η διάθεση, η ανακύκλωση ή η επαναχρησιμοποίηση π.χ. των πτερυγίων των ανεμογεννητριών, επηρεάζει σημαντικά την περιβαλλοντική και οικονομική τους απόδοση. Η συνδυαστική εφαρμογή της Ανάλυσης Κύκλου Ζωής και της Πολυκριτηριακής Μεθοδολογίας

Λήψης Αποφάσεων κατέδειξε ότι η επαναχρησιμοποίηση των σύνθετων υλικών των πτερυγίων, καθώς και η μηχανική ανακύκλωση του σκυροδέματος θεμελίωσης των ανεμογεννητριών, αποτελούν τις πιο αποτελεσματικές στρατηγικές στο τέλος ζωής, μειώνοντας τις εκπομπές των αερίων του θερμοκηπίου, την κατανάλωση πρωτογενούς ενέργειας, τη χρήση γης, και το κόστος διαχείρισης αποβλήτων. Η ενεργοβόρα χημική ή θερμική ανακύκλωση, ιδίως όταν περιλαμβάνει μεταφορές σε μεγάλες αποστάσεις, αποδείχθηκε λιγότερο αποδοτική. Η ενσωμάτωση στρατηγικών επαναχρησιμοποίησης, σχεδίασης για ανακύκλωση, και πρόληψης δημιουργίας αποβλήτων δύναται να ελαχιστοποιήσει τη χρήση φυσικών πόρων, και να μειώσει την απώλεια βιοποικιλότητας. Η εφαρμογή οικονομικών κινήτρων μπορεί περαιτέρω να ενισχύσει την υιοθέτηση αυτών των πρακτικών.

Εν κατακλείδι, η επίτευξη βιώσιμων ενεργειακών μεταβάσεων δεν περιορίζεται στην ανάπτυξη καθαρών μορφών ενέργειας, αλλά απαιτεί μια ολιστική προσέγγιση που ενσωματώνει το σχεδιασμό και την τεχνολογική βελτιστοποίηση, τις αρχές της κυκλικής οικονομίας, τη στρατηγική διαχείριση των συστημάτων αποθήκευσης, την εφαρμογή κατάλληλων οικονομικών κινήτρων και τη λήψη αποφάσεων βάσει ανάλυσης κύκλου ζωής. Η παρούσα διατριβή συμβάλλει ουσιαστικά στη βελτιστοποίηση και αξιολόγηση ενεργειακών συστημάτων σε πολλαπλές κλίμακες, παρέχοντας εμπεριστατωμένα στοιχεία για μια οικονομικά αποδοτική, αξιόπιστη και καθοδηγούμενη από τις αρχές της κυκλικής οικονομίας απανθρακοποίηση, από το επίπεδο των κτιρίων και των κοινοτήτων έως τα νησιωτικά μικροδίκτυα και το εθνικό ηλεκτρικό δίκτυο.

Abstract

The transition towards low-carbon and cost-effective energy systems is a strategic priority of Greece, a country endowed with abundant renewable energy potential. Solar energy conversion units and wind power systems constitute key pillars for the decarbonization of the electricity sector under a circular economy framework. Despite their potential, significant knowledge gaps and practical limitations remain. Most of life cycle environmental performance evaluation studies focus primarily on the operational phase of renewable energy technologies, often neglecting Greenhouse Gas (GHG) emissions and non-renewable energy use associated with the stages of manufacturing, transportation, installation, and end-of-life management. Region-specific data are scarce, emerging technologies, including third-generation solar Photovoltaics (PVs), offshore wind turbines, and hybrid systems, have been poorly evaluated, and recycling and reuse infrastructures remain insufficient. The absence of comprehensive policy frameworks further constrains the implementation of circular economy principles, alongside the widespread deployment of renewable energy technologies.

The current Ph.D. dissertation addresses these shortcomings by developing a holistic, multi -dimensional methodological framework for the assessment and optimization of both conventional and renewable energy systems. The framework developed integrates energy system design and modelling, economic analysis, Life Cycle Assessment (LCA), and Multi-Criteria Decision Making (MCDM). The energy modelling component captures system configurations and technology interactions, as well as operational behaviour under realistic meteorological data and grid constraints, encompassing load-following dispatch strategies. The economic analysis evaluates the economic viability of systems, employing key performance indicators, such as the Levelized Cost of Energy (LCOE), Net Present Value (NPV), Internal Rate of Return (IRR), and Cost-Benefit Ratio (CBR). From an environmental perspective, the LCA assesses the adverse impacts across all life cycle stages, i.e., from manufacturing and operation to end-of-life treatment, quantifying climate change impact, fossil and nuclear energy use, resource consumption, and other environmental pressures. Finally, the MCDM approach evaluates competing objectives and stakeholder priorities, aiming at supporting sustainable decision-making regarding technology selection, system configurations, and end-of-life strategies. This integrated framework constitutes a flexible, scalable, and future-ready tool, able to facility both project-level analysis and long-term strategic energy planning.

Application of the framework at multiple scales yielded important insights.

At the ***building level***, grid-connected solar PV systems with capacities of 5-10 kW_p were found to be economically viable, and achieved significant life cycle reductions in GHG emissions and non-renewable energy use. However, systems below 5 kW_p were cost-ineffective, due to high upfront costs and low electricity prices, highlighting the need for cost reductions in module manufacturing and balance-of-system components, alongside supportive policies such as investment incentives, feed-in tariffs, and credit trading mechanisms. Fully autonomous hybrid systems, integrating solar PV arrays, energy (battery) storage, diesel generators, and biomass-based heating, were identified as the most suitable solutions for decentralized energy supply in remote households, offering both technical reliability and improved sustainability.

Sensitivity analysis emphasized the influence of load management and fuel prices on economic feasibility, underscoring the importance of both operational optimization and policy support.

At the ***community level***, hybrid electricity supply systems combining wind, solar, battery storage, and diesel generators provide robust, cost-effective, and sustainable solutions for isolated Aegean Islands. In Lesvos, Karpathos, and Astypalaia, renewable generation supplies over 90% of electricity, with diesel generator as a backup, while batteries align fluctuating generation with demand and stabilize the grid. A significant surplus of electricity, exceeding 40% in all three Islands, highlights the opportunities for additional storage or flexible use. From an economic perspective, these hybrid systems achieve competitive LCOE (0.12–0.15 €/kWh) compared to the current diesel-based systems on the islands, despite higher up-front investments. From an economic point of view, the substitution of diesel generators can decrease GHG emissions by over 92%, to below 71 gCO_{2eq}/kWh, providing a circular economy-driven solution towards the deep decarbonization of non-interconnected islands.

At the ***grid scale***, thermal power plants remain the major contributor to environmental impacts, especially in terms of global warming potential and non-renewable energy use. In contrast, large hydro and renewable energies, including wind, solar, small hydro, and biomass systems, provide a modest but significant mitigation potential. Future scenarios with higher renewable energy penetration suggest substantial reductions in climate change impact, emphasizing the importance of systemic planning and life cycle-informed strategies for decarbonization. Transmission infrastructure, including lines and substations, as well as grid power losses, also represent a notable share of life cycle environmental impacts; however, their contribution is small compared to the adverse impacts from the electricity generation sector.

Critically, achieving sustainable energy transitions requires attention to the ***end-of-life phase of renewable technologies***. The disposal, recycling, or repurposing of components, such as wind turbine blades, significantly affects both environmental and economic performance. Combined LCA and MCDM analyses demonstrated that mechanical recycling of wind turbine concrete foundations and repurposing of composite materials were the most effective end-of-life strategies, reducing global warming potential, non-renewable energy use, land occupation, and waste costs. Energy-intensive chemical or thermal recycling, particularly when involving long-distance transport, proved less efficient. Integrating remanufacturing, and design-for-recycling, along with waste prevention strategies, support a circular economy, while financial incentives can further enhance adoption of renewable technologies.

In summary, the achievement of sustainable energy transitions requires more than just deploying renewable energy technologies; it strongly depends on the combination of technological optimization, circular economy integration, storage management, policy incentives, and life cycle-informed decision-making. This Ph.D. thesis specifically contributes by assessing and optimizing across multiple scales, providing valuable insights for cost-effective, reliable, and sustainable decarbonization from buildings and communities to island microgrids and national grids.

Preface

My name is Angeliki Sagani. I am a Research Engineer at the Centre for Research and Technology Hellas (CERTH) / Chemical Process & Energy Resources Institute (CPERI), where I have been employed since 2020. I hold a Dipl. Ing. Degree in Mechanical Engineering from the National Technical University of Athens (NTUA) and an MSc Degree in Energy Management and Environmental Protection Systems, jointly awarded by the National Technical University of Athens (NTUA) and the University of Piraeus. My research interest focuses on the development, integration, and application of life cycle thinking models, encompassing Life Cycle Assessment (LCA) and Life Cycle Cost Analysis (LCCA),within decision-support tools for the simulation, optimization, and evaluation of advanced energy systems. I have participated in numerous European -funded research projects, contributing to the advancement of methodologies for sustainable and optimized energy systems. I have also served as a Paper Reviewer Expert and as a member of the Programme Committee of the 34th European Biomass Conference and Exhibition. All research activities have led to the publication of articles in high-impact peer-reviewed journals and international conference proceedings. Among these publications, four journal articles and four conference papers stem from the present dissertation, namely:

Publications in International Journals:

- **Sagani A**, Mihelis J, Dedoussis V. Techno-economic analysis and life cycle environmental impacts of small-scale building-integrated PV systems in Greece. Energy Buildings 2017;139:277–90. https://doi.org /10.1016/j.enbuild.2017.01.022.
- **Sagani A**, Vrettakos G, Dedoussis V. Viability assessment of a combined hybrid electricity and heat system for remote household applications. Solar Energy 2017;151:33–47. https://doi.org/10.1016/j.solener.2017.05.011.
- Orfanos N, Mitzelos D, **Sagani A**, Dedoussis V. Life cycle environmental performance assessment of electricity generation and transmission systems in Greece. Renewable Energy 2019;139:1447–62. https://doi.org/10.1016/j.renene.2019.03.00.
- Gennitsaris S, **Sagani A**, Sofianopoulou S, Dedoussis V. Integrated LCA and DEA approach for circular economy-driven performance evaluation of wind turbine end-of-life treatment options. Applied Energy 2023;339:120951. https://doi.org/10.1016/j.apenergy.2023.120951.

Publications in Conferences:

- Sofianopoulou, S., **Sagani A.** Circular economy-driven performance assessment of electricity generation options for decarbonization of islands. ACEM24, Seoul, Korea: 2024.
- Dedoussis, V., **Sagani A.** Life cycle GHG emissions assessment of hybrid power systems for off-grid electrification of remote islands. ACEM24, Seoul, Korea: 2024.
- **Sagani**, A., Dedoussis V. An integrated analysis of Hybrid Energy Systems for decarbonization of off-grid islands based on life cycle thinking. Striving for Stability in a Highly Uncertain Energy World, Maroussi Plaza Centre, Athens: HAEE Energy Transition Symposium: 2024.
- **Sagani, A.**, Gennitsaris, S., Sofianopoulou, S., Dedoussis V. Sustainability Assessment of End-of-Life Wind Turbine Management using LCA and TOPSIS. 6th International Congress of Environment (ICE), Osaka, Japan: 2025.

Contents

List of Tables

List of Figures

Abbreviations

AC	Alternating Current
a-Si	Amorphous Silicon
BaU	Business-as-Usual
BoS	Balance of System
CCS	Carbon Capture and Storage
CdTe	Cadmium Telluride
CF	Capacity Factor
CHP	Combined Heat and Power
CIGS	Copper Indium Gallium Selenide
CRF	Capital Recovery Factor
c-Si	Crystalline Silicon
DAPEEP	Electricity Market and Guarantees of Origin
DC	Direct Current
DEA	Data Envelopment Analysis
DG	Diesel Generator
DMU	Decision-Making Unit
EPBT	Energy Payback Time
EoL	End-of-Life
EU	European Union
FU	Functional Unit
GHG	Greenhouse Gas
GRP	Glass-Reinforced Plastic
GWP	Global Warming Potential
HEDNO	Hellenic Electricity Distribution Network Operator
HOMER	Hybrid Optimization of Multiple Energy Resources
IPTO	Independent Power Transmission Operator
IRR	Internal Rate of Return
LA	Lead-Acid
LCA	Life Cycle Assessment
LCI	Life Cycle Inventory
LCIA	Life Cycle Impact Assessment
LCOE	Levelized Cost of Energy
Li-Ion	Lithium-Ion
LF	Load Following
MCDM	Multi-Criteria Decision Making
mono-Si	Monocrystalline Silicon
MPP	Maximum Power Point
NOCT	Nominal Operating Cell Temperature
NPC	Net Present Cost
NPV	Net Present Value

O&M	Operating and Maintenance
OpRE	Operating Reserve
PBP	Payback Period
poly-Si	Polycrystalline Silicon
PPC	Public Power Corporation
PV	Photovoltaic
REF	Renewable Energy Fraction
RES	Renewable Energy Sources
SoC	State of Charge
STP	Standard Temperature and Pressure
TCI	Total Capital Investment
TEA	Techno-Economic Analysis
TOPSIS	Technique for Order Preference by Similarity to an Ideal Solution
VRS	Variable Returns to Scale

Chapter 1
Introduction

The global energy sector is undergoing a period of important transformation driven by the imperatives of ensuring adequate energy access and maintaining high levels of reliability and quality of energy supply, as well as enhancing the sustainability of power generation technologies [1,2]. In light of these challenges, the European Union (EU) has established ambitious targets, encompassing: (i) the mitigation of Greenhouse Gas (GHG) emissions by at least 55% by 2030 compared to 1990 levels, and (ii) achieving climate neutrality by 2050 [3]. The attainment of these goals calls for the accelerated deployment of non-polluting renewable energy systems, particularly solar Photovoltaic (PV) and wind power, which have emerged as the most cost-effective and scalable alternative solutions towards the decarbonization of electricity generation [4]. The transition to greener energy offers a dual benefit of reducing the environmental pollution caused by fossil fuel-based power generation, and addressing the energy demand in a circular economy-aligned approach [1].

Greece, as an EU Member State with substantial renewable energy potential, is pursuing a transformative energy transition under its National Energy and Climate Plan. This Plan initially aimed for a 40% reduction in GHG emissions compared with 1990 levels (over 55% relative to 2005). The revised Plan implements new objectives, namely, a 58% reduction by 2030, an 80% reduction by 2040, and full carbon neutrality by 2050 [3,4]. The successful achievement of these targets is underpinned by the distinctive geographic and climate conditions of the country, comprising high solar irradiation levels, substantial wind resources, abundant agricultural biomass potential, and an extensive archipelago. These features create both opportunities and challenges for the deployment of robust renewable energy-based supply-demand systems that guarantee energy security, reliability, and resilience across multiple scales [5,6]. Certain regions, such as the Aegean islands, exhibit wind speeds exceeding 10 m/s at 30 m height, with solar energy potential reaching 1,900 kWh/m^2 [7,8]. In parallel, the ever-increasing demand for electricity, heat and transport fuels, in conjunction with the retirement of aging conventional thermal power stations, highlights the need for efficient, low-carbon generation in Greece [9]. This necessity is particularly pronounced for remote and rural areas in the country, such as the non-interconnected Greek islands, which currently depend almost exclusively on heavy fuel oil imports and diesel-based generation. The frequent start-ups and shut-downs of electric diesel generators increase both fuel consumption and maintenance costs, and decrease operational efficiency, outlining the key role of renewable energy penetration [6]. Nonetheless, the availability of suitable sites for large-scale installations is increasingly limited, and local opposition constitutes a further serious handicap to the renewable energy deployment [10,11]. Furthermore, the energy output of solar PVs and wind turbines is inherently dependent on local weather conditions, which can adversely affect the reliability of continuous electricity supply [12].

Hybrid electricity generating systems that incorporate more than one type of renewable power sources, optionally supplemented with fossil fuel generators and storage or backup options, have therefore emerged

as promising configurations to ensure uninterrupted electricity supply in high renewable energy scenarios [13–17]. It is reasonable to expect that hybrid power systems result in higher power supply reliability and lower generation costs compared to systems relying on a single energy source [18]. Hybrid power systems, however, often need a substantial surplus of renewable capacity to guarantee energy sufficiency [19,20]. To this end, island interconnections are essential for reducing the dependence on fossil fuels and effectively eliminating the associated GHG impact. Linking off-grid islands to the mainland or with one another through the implementation of hybrid electricity generating stations, improves islands' strategic position within domestic and regional energy systems, while notably expanding the "green margin" available for further renewable energy development [21].

Despite the considerable benefits of hybrid power systems combined with island interconnections in terms of improved energy security, reliability, and sustainability, current analytical approaches for evaluating such systems remain fragmented. Technical optimization, techno-economic evaluation, life cycle environmental assessment, and multi-criteria decision analysis are often conducted as independent or partially connected components. Furthermore, most published studies are limited to a single spatial scale and do not preserve methodological consistency across hierarchical system levels. As a result, cross-scale comparisons are affected by differing modelling assumptions rather than by structural differences inherent to the system scales. An additional limitation concerns the definition of the system boundaries. Electricity transmission infrastructure, comprising transmission lines, substations, and related material requirements, is frequently excluded from sustainability assessments despite its material intensity and contribution to operational losses. Likewise, the waste management phase of renewable energy technologies is often explored using simplified assumptions that neglect recycling pathways, material recovery potential, and context-specific disposal impacts. The aforementioned omissions restrict the completeness and policy relevance of sustainability assessments. Addressing these limitations requires the development of a holistic, scalable and consistent methodological framework that incorporates system optimization with environmental and economic evaluation, and structured decision support within harmonized life cycle system boundaries and modelling assumptions.

Building on the identified methodological gaps, this Ph.D. thesis develops and implements a unified multi-layer framework for the optimization and economic and environmental performance assessment of electricity generation systems composed of fossil fuel-based and renewable energy technologies. At the core of the framework lies an advanced optimization model that establishes the structural foundation of the evaluation process by determining feasible and optimal system configurations under technical, operational, and reliability constraints. The resulting optimized configurations serve as the basis for the subsequent economic and environmental evaluations. Techno-economic indicators and life cycle impact categories are derived directly from the optimized system using harmonized system boundaries, aligned functional units, and consistent modelling assumptions, thereby ensuring methodological coherence across all analytical layers. A major scientific contribution of this dissertation is the consistent application of this methodological approach across three hierarchical spatial scales, i.e., building-scale systems, community-scale island systems, and national grid-scale systems. The modelling structure, decision variables, and economic and environmental metrics remain conceptually invariant across scales, while scale-specific parameters and boundary conditions are adjusted accordingly. This design enables the systematic identification of scale-

dependent effects, such as aggregation benefits, infrastructure constraints, network interdependencies, and spatial resource variability, without introducing inconsistencies in modelling assumptions.

The dissertation further extends conventional system boundaries by explicitly incorporating electricity transmission infrastructure into both economic and environmental assessments. Transmission assets are considered as integral components of the system, with embodied material impacts and network losses internalized within the life cycle framework. This approach results in a more realistic comparison between decentralized and centralized configurations. Moreover, the structured modelling of the End-of-Life (EoL) treatment phase of renewable technologies is introduced, with particular focus on wind turbine systems. Recycling, reuse, and disposal pathways are represented within the life cycle framework and evaluated through multi-criteria decision analysis. By embedding EoL processes into the integrated assessment structure, the framework captures long-term material flows and circular economy implications in a systematic manner. Overall, the scientific contribution of this thesis lies in establishing a scalable and coherent analytical architecture that bridges building-, community- and grid-scale electricity system assessment within a single optimization-driven framework. By preserving methodological consistency, while extending system boundaries to infrastructure and waste management considerations, the proposed approach enhances the robustness, transparency, and policy relevance of sustainability-based energy planning.

The proposed framework is applied to distinct case studies in Greece to evaluate electricity generation systems across multiple spatial scales. Through these applications, the Ph.D. thesis investigates how different system configurations perform under varying operational contexts and infrastructural conditions while identifying synergies and trade-offs among technical, economic, and environmental dimensions. The research is aligned with the strategic objectives of the Greek National Energy and Climate Plan and broader European Union decarbonization targets. By providing a structured analytical tool for evaluating alternative transition pathways, the dissertation supports evidence-based planning for renewable deployment and infrastructure expansion. Beyond methodological advancement, the proposed framework offers direct decision-support value for policy makers, system planners, utility operators, and project developers. It is particularly relevant for enhancing energy autonomy in isolated islands, optimizing hybrid renewable configurations, investigating transmission expansion strategies, and formulating sustainable environmental policies, including structured strategies for waste management and decommissioning of wind turbines.

This Ph.D. thesis is structured about the aforementioned main topics and organized into eight chapters, following a progressive scale from technology-level assessment to system-level planning and policy relevance. **Chapter 2** investigates the environmental performance of PVs and wind power technologies via a thorough synthesis of Life Cycle Assessment (LCA) studies. The chapter identifies key methodological trends, environmental hotspots, improvement strategies, and existing knowledge gaps, thereby informing future research and supporting a deeper understanding of the sustainability implications associated with these renewable energy technologies.

Building on the thorough environmental insights derived in Chapter 2, **Chapter 3** develops a structured and transparent methodological framework for evaluating the performance of both conventional and renewable electricity generation technologies, with and without energy storage or backup options. This framework

integrates advanced energy systems modelling and optimization with rigorous economic viability analyses, enabling a holistic evaluation of alternative electricity supply system configurations. The specific chapter establishes the methodological foundation applied consistently across the subsequent case studies.

Transitioning from the methodological framework to applied assessments, **Chapter 4** focuses on the design and performance evaluation of hybrid electricity supply systems for both grid-connected and autonomous / isolated building-scale applications. Particular emphasis is placed on solar PV systems, evaluating their technical and economic performance, alongside their life cycle environmental impacts, across fabrication, installation, operation, and maintenance. The integration of solar PV production and operational data with LCA enables the identification of key environmental hotspots and the evaluation of alternative PV design and deployment strategies at the building scale. These alternatives are further evaluated using multi-criteria decision analysis methods, which allow the simultaneous assessment of technical, economic, and environmental criteria, enabling the identification of optimal solutions from different stakeholder perspectives. In addition to stand-alone PV systems, the chapter investigates the design, techno-economic optimization, and performance evaluation of hybrid electricity supply systems combining solar PVs, wind turbines, battery energy storage, and fossil fuel–based backup generation, addressing the operational and reliability constraints of isolated and off-grid buildings. The optimization of these hybrid configurations is coupled with life cycle global warming impact assessment, enabling a comparative evaluation of alternative system architectures in terms of supply security, cost-efficiency, GHG emissions reduction potential, and fully alignment with decarbonization objectives.

Chapter 5 extends the analysis from building-scale systems to the community level, investigating the performance of hybrid electricity supply systems in isolated, non-interconnected islands of different scale. This approach captures the diversity of off-grid/autonomous energy systems and supports the formulation of dedicated, scale-sensitive energy transition and sustainability policies. The chapter assesses community - scale systems, integrating wind turbines, solar PV technologies, battery energy storage, and diesel backup generation, emphasizing on technological feasibility, economic optimization, and GHG emissions impact during the operational phase. The proposed approach is demonstrated through real-world case studies on three non-interconnected islands in the Aegean Sea, namely, Lesvos, Karpathos, and Astypalaia, representing large-, medium-, and small-scale isolated systems, respectively. All cases are characterized by abundant renewable energy potential and a strong dependence on heavy fuel oil-based electricity generation.

Leveraging the insights gained from isolated and community-scale applications, **Chapter 6** further scales up the assessment to the national electricity grid level. By explicitly accounting for both generation and transmission of electricity and considering a diverse portfolio of renewable and thermal power systems, this chapter provides a holistic evaluation of the environmental footprint of electricity supply in Greece. The transition from decentralized systems to the interconnected national grid ensures methodological continuity, and address system-wide interactions, thus, supporting evidence-based policy development and long-term strategic planning for national decarbonization.

With the operational performance of electricity generation systems established across multiple scales, **Chapter 7** focuses specifically on the EoL stage of renewable technologies, particularly, wind turbines. This

chapter applies a hybrid multi-criteria decision analysis approach to evaluate alternative EoL pathways, such as recycling, reuse, and disposal, by simultaneously considering technical feasibility, environmental impacts, and costs. The analysis of Chapter 7, which is exclusively devoted to the EoL assessment of wind turbines, provides deeper insights into circular economy strategies and their contribution to the overall sustainability of wind power systems.

Lastly, **Chapter 8** presents the overarching conclusions of this Ph.D. thesis and discusses future research directions. It synthesizes the key findings from the building-, community-, and national-level analyses, highlighting the contributions of the integrated methodological framework to the assessment, optimization, and sustainable planning of electricity supply systems. The chapter also identifies remaining knowledge gaps and proposes avenues for further research to enhance energy system sustainability, decarbonization strategies, and policy development, thereby providing a roadmap for future work in this field.

Chapter 2
Critical Review of the Life Cycle Environmental Performance of Solar PV and Wind Power Systems

This chapter presents a comprehensive investigation of the environmental performance of renewable energy technologies, with a particular focus on solar PV and wind power systems. Both technologies entail distinct manufacturing processes, material and energy requirements, performance characteristics, as well as waste management procedures, all of which strongly influence their environmental sustainability. Based on the thorough review of LCA studies, this chapter intends to synthesize key findings and demonstrate both methodological consistencies and discrepancies in current research. It also discusses environmental hotspots from a life cycle perspective, proposes potential improvement strategies, and outlines existing knowledge gaps. The overarching objective is to identify future research avenues, as well as to support a deeper understanding of the sustainability implications of deploying wind power and solar energy conversion technologies.

2.1 State-of-the-art

The large-scale penetration of Renewable Energy Sources (RES) and associated technologies into existing power generation systems constitutes a pivotal strategy in the global effort to decarbonize the electricity sector and promote long-term sustainability, fully aligned with the circular economy principles [22]. Among the different renewable technologies available, solar PV and wind energy have emerged as the most mature and rapidly scalable options. Their widespread geographical potential, in conjunction with their non-depleting nature and the negligible GHG emissions during the operation phase, have positioned them at the forefront of the energy transition [23]. Over the past decade, the global installed capacities of solar PV and wind energy have exhibited substantial growth, with average annual growth rates of approximately 27% and 13%, respectively [24–26]. This rapid expansion has been driven by: (i) the continuous technological innovation, (ii) the significant decreases in cost of energy, and (iii) the strong policy incentives (feed-in-tariffs and investment subsidies), particularly within the European markets [24,25].

Decentralized solar PV and wind power systems present significant advantages over centralized fossil fuel-based electricity generation, comprising important reduction in GHG emissions, improved energy security through localized power production, more efficient resource exploitation and a stronger alignment with sustainable development targets [27]. Nevertheless, the acceleration of the global deployment of these technologies needs a comprehensive environmental performance evaluation from a life cycle perspective. Current sustainability analyses tend to concentrate on the operation stage, often evaluating the GHG

emissions reduction to be achieved by the substitution of fossil fuel-based energy systems [28]. This narrow approach overlooks the considerable material and energy requirements associated with the manufacturing stages of solar PV and wind power systems, as well as their EoL management and material recovery. Consequently, it prevents the identification of key opportunities for improving material use, refining system design, and advancing circular economy principles throughout the technologies' entire lifespan [29].

To explore the actual environmental profile of solar and wind power systems, the LCA methodological framework should be applied. LCA emerged as a methodology in the late 1960s and early 1970s and has since evolved into a universally accepted and standardized methodology, significantly influenced by the ISO 14040 and 14044 Standards [30,31]. The LCA framework serves as a robust integrated tool or technique to assess the adverse effects of a system, while aligning with sustainability goals within a circular economy framework [32]. It can adopt a cradle-to-grave approach, systematically encompassing all life cycle stages, i.e., raw materials acquisition, component manufacturing, transportation, installation, operation and maintenance, decommissioning, and EoL management processes, such as recycling, repurposing, or disposal [33]. A key strength of LCA lies in its ability to establish essential linkages between environmental interventions, demonstrated in the Life Cycle Inventory (LCI), and their potential effects on human health, ecosystem quality, and resource depletion. This holistic approach is essential for informed, evidence-based decision-making in the sustainable deployment of renewable energy technologies, offering valuable insights that extend beyond operational emissions alone. An additional valuable feature of LCA is its ability to enable comparative benchmarking of alternative technologies and to support the formulation of effective impact mitigation strategies. These strategies mainly include the application of eco-design principles, process optimization, material, all of which are fundamental to the responsible and efficient development of low-carbon energy technologies aligned with ambitious decarbonization goals.

Building on this imperative, the following sections synthesize current knowledge on LCA applications for solar PV and wind power technologies, focusing on three key criteria: (i) variation in system boundaries, (ii) quantitative assessment of environmental impacts, and (iii) sufficient methodological detail to facilitate critical analysis. This extensive review covers traditional crystalline silicon (c-Si) and emerging thin-film solar PV technologies, as well as different wind turbine configurations, including onshore and offshore installations. Through a systematic examination of the published literature, we aim at identifying critical research priorities and methodological enhancements needed to advance the field towards standardized and holistic environmental assessment frameworks, ultimately promoting the sustainable deployment of renewable energy technologies (from individual buildings to communities and their integration into the electricity grid).

2.2 Critical review of the current LCA studies on solar PV systems

2.2.1 Review outputs regarding methodological issues

System Boundaries and Functional Unit

The state-of-the-art demonstrates the importance of conducting holistic LCAs of solar PV systems in order to comprehensively evaluate their impacts across all the life cycle stages, as well as to identify potential

opportunities for energy and environmental optimization. These impacts are directly related to raw material acquisition, energy and fuel consumption, emissions and waste generation. The literature reveals that most LCA studies implement a cradle-to-gate approach, comprising activities from the extraction and processing of raw materials to the fabrication of solar cells, modules/panels and balance of system components. This methodological choice is primarily dictated by practical considerations, notably the scarcity of reliable data for EoL stages. Nevertheless, restricting analysis to the manufacturing stage may lead to incomplete outcomes potentially underestimating environmental impacts, particularly when considering variations in geographic and/or climatic conditions. To address this limitation, the adoption of a cradle-to-grave perspective is recommended, extending the environmental evaluation to include installation, operation and maintenance, decommissioning, and EoL management, as demonstrated in the recent studies [34–36].

Methodological heterogeneity in the selection of the unit of analysis (Functional Unit, FU) primarily affects the consistency and comparability of results across LCA studies, rather than generating uncertainty in the estimates themselves. Factors such as temporal assumptions, performance degradation rates, and geographical variability can substantially influence estimates of net environmental performance. A FU referred to electricity generation (expressed in kWh_e) is generally considered to be the most suitable option for comparing the environmental profile of solar PV and fossil fuel–based electricity generation. However, this metric is sensitive to the system lifetime, typically assumed to range from 20 to 30 years, and to the annual performance degradation of PV panels, estimated at 0.6-0.7% per year [37]. Geographic and climatic variations, solar radiation, in particular, also influence the energy payback time (EPBT). On the other hand, the normalization of impacts by installed capacity (in KW_p), instead of electricity generation, might lead to misleading comparisons, particularly across technologies with different efficiencies or deployment conditions. Incorporating site-specific irradiance data, in conjunction with accurate estimates of both system losses and degradation rates, is thus fundamental to ensure robust and meaningful environmental assessments.

Impact Categories

Climate change, also expressed as Global Warming Potential (GWP) in CO_2-equivalent, is the most frequently evaluated impact category for renewable energy technologies, including solar energy conversion units [34,35]. This is attributed to their contribution to GHG emissions reduction. The climate change impact accounts for emissions from silicon purification, module/panel fabrication, transportation, installation, and EoL treatment, which are offset by the clean electricity generated during the operation phase. Fossil and nuclear energy consumption is also commonly assessed, given the substantial energy intensity of manufacturing processes, i.e., silicon purification and cell fabrication, which rely heavily on fossil fuel-based electricity grids. The quantification of the primary energy requirements is critical for estimating the EPBT, defined as the period required for operational electricity generation to offset the environmental impacts of the PV system's life cycle [34]. Other impact categories, although less frequently reported, remain important for robust and thorough evaluation. Mineral resource scarcity reflects the depletion of critical raw materials, while human toxicity potential considers the health risks from emissions of hazardous substances during semiconductor manufacturing. Terrestrial acidification stems from electricity - intensive upstream processes (e.g., silicon purification and aluminium frame production), typically

powered by conventional energy systems. Marine and freshwater eutrophication captures nutrient enrichment from nitrogen and phosphorus emissions. The selection of impact categories generally follows established Life Cycle Impact Assessment (LCIA) methods, including IMPACT World+, ReCiPe, or CML, supporting comparability across studies and informed decision-making for sustainable energy transitions [38–41].

2.2.2 Review outputs per technology type

First-Generation Crystalline Silicon Technologies

Extensive research is devoted to the environmental implications of fist-generation c-Si PV systems, encompassing either monocrystalline (mono-Si) or polycrystalline (poly-Si) technologies, which currently account for over 80% of the global solar PV market [42]. Their dominance stems from the attractive characteristics that these technologies exhibit, namely, material abundance, high energy conversion efficiencies (up to 26%) and cost-effectiveness [43,44].

The production of solar-grade polysilicon is pivotal in elucidating the environmental sustainability of these technologies, since it represents one of the most energy-intensive stages within the solar PV manufacturing chain. Two main production routes dominate the industrial production of solar-grade polysilicon: (i) the modified Siemens process and (ii) the metallurgical route. The Siemens Process, which represents the majority of global polysilicon production, relies on chemical vapor deposition at temperatures of about 1,500 to 2,000°C. This high-temperature processing step, which is required for refining the metallurgical-grade silicon into high-purity polysilicon, contributes substantially to the embodied energy of PV modules and constitutes a notable source of GHG emissions, particularly in regions where the electricity generation remains highly dependent on fossil fuels [45–47]. LCA studies [48] demonstrate that the Siemens process entails higher energy demand and emissions compared to polysilicon produced via the metallurgical route, which can decrease the total environmental impact by approximately 4.5 times. Given that a standard 60-cell module contains roughly 660 g of silicon, this stage contributes substantially to the overall GHG emissions of the panel [49].

Following the polysilicon production phase, the manufacturing stage involves ingot and wafer production, cell fabrication, and module assembly. LCA studies consistently showcase that this stage represents the most impact-intensive phase of the entire life cycle, particularly change and fossil energy use [29]. This poor environmental performance is attributed mainly to the energy-intensive processes required to convert raw quartz into high-purity, semiconductor-grade silicon. For instance, Fu et al. [50] reports a fossil energy use of approximately 0.514 MJ/kWh$_e$ and an associated EPBT of six years for mono-Si systems, highlighting the key role of silicon purification in determining their overall environmental performance. Similarly, Kato et al. [21] noted GHG emissions of 315 tn CO_{2eq}/year from the use of low-grade recycled silicon, emphasizing the impact of material quality.

The energy requirements differ significantly between poly-Si and mono-Si ingots. Notably, the poly-Si ingots require considerably less energy than the corresponding mono-Si ones, which are produced through the high-temperature Czochralski process; specifically, mono-Si wafer production consumes roughly 3.5 times more energy [51]. As reported in [52] and [53], within solar PV manufacturing, polysilicon extraction, cell

fabrication, and module assembly contribute significantly (29%, 18%, and 33%, respectively) to the overall environmental impact. Moreover, the fabrication processes, e.g., wafer texturing, junction formation, anti-reflective coating deposition, in conjunction with the aluminium frames, impose additional energy requirements, thereby affecting the overall environmental footprint of PV modules.

Despite the fact that solar PV modules are the principal focus of LCA studies, Balance of System (BoS) components, including inverters, mounting structures, transformers, and related electrical infrastructure, also result in significant life cycle environmental impacts. Mounting structures, for example, which are typically composed of aluminium or galvanized steel, require energy-intensive manufacturing processes, and the material selection markedly affects the overall environmental profile. The expansion of the system boundaries beyond the PV module further highlights these additional impacts. Stylos and Koroneos [54] found that encompassing inverters, steel foundations and batteries in poly-Si systems result in GHG emissions between 12.3 and 58.8 gCO_{2eq}/kWh_e. This range accounts for differences in systems configurations, components specifications, as well as regional grid electricity mixes. Fukurozaki et al. [55], in a study of a 1.2 kW_p rooftop mono-Si system in Brazil, reported GHG emissions fluctuating from 14.5 to 18.7 gCO_{2eq}/kWh_e, and EPBTs between 2.5 and 3.1 years, outlining the considerable influence of the local irradiance on the environmental profile.

Despite the importance of EoL considerations, comprehensive cradle-to-grave LCAs remain scarce. Research works that incorporate these stages, such as by Fthenakis and Kim [29], Kannan et al. [56], Muneer et al. [57] and Jungbluth et al. [58,59], showcase the critical impact of selecting system boundaries on robust and reliable environmental performance evaluations. For example, Fthenakis and Kim [29] reported EPBTs of 1.5-2 years and GHG emissions of 20-25 gCO_{2eq}/kWh_e for the module manufacturing stage, which increased to about 3 years and 50 gCO_{2eq}/kWh_e when BoS components, transport, installation, and EoL stages are taken into account. Kannan et al. [56] estimated a fossil energy use of 2.2 MJ/kWh_e, while Muneer et al. [57], in a similar case study for medium-sized installation, reported an EPBT between 2.5 and 3.5 years and GHG emissions ranging from 30 to 40 gCO_{2eq}/kWh_e. In line with these results, Jungbluth et al. [58,59] in their investigation of twelve 3 kW_p grid-connected poly-Si systems, found EBPT figures between 3 and 6 years and GHG emissions varying from 39 to 110 gCO_{2eq}/kWh_e. All the aforementioned studies consistently indicate that broader system boundaries yield higher reported environmental impacts, underscoring the necessity of cradle-to-grave assessments for robust evaluations.

Second- and Third-Generation PV Technologies

In parallel with the environmental assessment of c-Si PV systems, growing attention is being directed towards second- and third-generation PV technologies, which are widely regarded as promising and potentially more sustainable alternatives. Second-generation systems comprise thin-film technologies, including cadmium telluride (CdTe), copper indium gallium selenide (CIGS), and amorphous silicon (a-Si) [60], whereas third-generation systems involve non-silicon-based technologies, such as organic PVs [61]. As noted by Al-Ali et al. [62] and Cellura et al. [34], these technologies offer advantages over conventional c-Si options, such as lower material intensity, reduced manufacturing energy requirements, and improved design flexibility, all of which contribute to a more favourable environmental profile. However, they continue to deal with significant limitations, most notably regarding the long-term operational stability, technological

maturity, conversion efficiency, and scalability, which collectively hinder their broader penetration into the prevailing solar PV market [63].

Several LCA studies have examined the environmental benefits of innovative second- and third- generation PV technologies compared to conventional c-Si systems. Hondo [64] outlined that replacing poly-Si modules with a-Si could decrease the GWP from 53.4 to 26.0 gCO_{2eq}/kWh_e, mainly because of the lower material requirements and the reduced thermal processing during the manufacturing stage. Similarly, Pacca et al. [65], evaluated a 33 kW_p rooftop installation and showed that implementing a-Si technology leads to an EPBT of 3.2 years, which is less than half the 7.5 years associated with poly-Si modules. Complementing these findings, Mohr et al. [66] compared poly-Si, a-Si, and advanced thin film modules, such as gallium arsenide and gallium indium phosphide. Results of this study indicate that while poly-Si and a-Si systems exhibited slightly shorter EPBTs (about 4.2 years) than the thin-film modules, the latter achieved up to 4.9 times lower GHG emissions when powered by renewable (solar) electricity. These outcomes highlight the environmental advantages of combining less energy-intensive PV technologies with renewable energy inputs. Nonetheless, the apparent energy and environmental benefits of both second- and third-generation PV systems should be interpreted cautiously, due to the fact that several LCAs of emerging technologies omit energy-intensive components (e.g., BoS components), and/or exclude decommissioning stages, potentially overstating their environmental advantages relative to established commercial technologies.

2.2.3 Environmental optimization strategies

Building on the previous sections' review on LCA studies and their reported energy and environmental findings for first-, second-, and third-generation PV technologies, it is evident that important opportunities arise through improvements in fabrication processes, material innovation, and systemic policy frameworks. Although LCA studies demonstrate the dominant influence of the upstream processes, particularly, silicon purification, wafer production, metallization, and aluminium framing, emerging research and industry trends indicate that targeted interventions across these stages could significantly enhance the sustainability of PV systems. The following integrated analysis synthesizes these improvement pathways, considering both recent literature and industry commitments to outline a comprehensive roadmap for reducing fossil energy use, GHG emissions, and resource consumption.

Continued technological innovation plays a fundamental role in mitigating the environmental impacts of PV module manufacturing. Several optimization pathways have been identified, including shifting to renewable - based electricity for all energy-intensive production steps, adopting lower-impact purification routes, and reducing wafer thickness and kerf loss during sawing. Transitioning to RES alone has been found to significantly decrease (50-70%) manufacturing-related climate change impacts, under-scoring the substantial influence of electricity consumption and grid carbon intensity [67]. Sensitivity analyses consistently identify the electricity mix as a critical factor in determining the environmental profile. Correspondingly, multiple studies, encompassing Alsema et al. [68], and Kim et al. [69], emphasize the importance of powering silicon purification and wafer production with renewable electricity in order to decrease cumulative energy demand (fossil energy use) and emissions. In particular, Alsema et al. [68] points out that using dedicated solar-grade purification routes powered by renewable energy can offer even

greater reductions in embodied energy compared with conventional electronic-grade silicon production. Industry-wide commitments to sourcing 100% renewable electricity by the year 2050 further suggest that the environmental profile of future PV manufacturing will enhance substantially. Additional manufacturing improvements involve enhanced recycling and recovery processes, specifically the reclamation of silicon lost during cutting and processing, thereby reducing the need for newly refined material. Interest is also growing in the utilization of lower-grade or secondary material, such as off-specification industrial silicon and recycled aluminium, without compromising module performance. Hong et al. [70] reported that using secondary (recycled) aluminium, improving energy efficiency and reducing wafer consumption for the cell fabrication can collectively reduce emissions by more than 25%.

Moreover, advancements in cell efficiency result in lowering life cycle impacts per unit of electricity generated. Higher-efficiency technologies, including perovskite/silicon tandem solar cells, achieve module efficiencies of 25–30%, compared to the 15–20% typical of c-Si technologies [71]. These efficiency improvements can lead to 20-30% reduction in overall environmental impacts per kilowatt-hour when normalized for energy output [72]. Material-focused improvements within PV systems, such as reducing silver consumption through advanced metallization techniques or implementing copper-based contacts, further decrease environmental burdens. Environmental performance is also influenced by geographic and operational context. Site-specific irradiance strongly affects EPBT and GWP. Sumper et al. [73] reported EPBT values of 3.5-5 years for a 200 kW_p rooftop system in Catalonia, Spain, depending on the local solar irradiation levels. Akinyele et al. [74] found GHG emissions ranging from 37.3 to 72.2 gCO_{2eq}/kWh_e and EPBT of 0.82–2.3 years for c-Si PV systems under fluctuating environmental conditions. Similarly, Zhai et al. [75] confirmed that regions with high annual irradiance (about 1,700 kWh/m^2) demonstrate significantly lower EPBTs of about 2.2 years. These findings underscore the importance of incorporating geographic variability into life cycle analyses to ensure accurate representation of PV sustainability across different deployment contexts.

Last, but not least, waste management, and recycling in particular, can significantly improve the environmental sustainability of PV systems. Proper recycling not only minimizes resources depletion and reduces GWP but also enables the recovery of high-value materials, such as silicon, aluminium, and silver, which can be reintegrated into new module production. The incorporation of waste management strategies complements upstream improvements (material efficiency, renewable-powered manufacturing, and wafer optimization), creating a closed-loop system that enhances the circularity of PV supply chains. According to Daniela-Abigail et al. [52], recycling processes can reduce environmental impacts by 25–50% across multiple impact categories compared to landfill disposal and can lower mineral resource scarcity by up to 89%, enabling recovery of valuable materials such as silicon, aluminium, and silver. Especially when combined with advances in cell efficiency and site-specific deployment strategies, robust recycling practices ensure that environmental gains are realized throughout the entire life cycle, from production to final disposal, ultimately supporting truly sustainable solar energy deployment [76]. However, supportive policy frameworks, encompassing recycled content mandates and incentives for clean domestic production, are essential to fully realize these benefits, paving the way for an integrated and environmentally sustainable roadmap for solar energy deployment.

2.3 Critical review of the current LCA studies on wind power systems

The preceding analysis highlighted the key environmental hotspots and improvement opportunities linked to PV systems from a life cycle perspective. The discussion now shifts to wind energy technologies. A thorough review of the literature demonstrates a substantial body of LCA studies focusing on wind power generation [77–79]. These investigations mainly focus on examining production conditions, manufacturing processes, turbine design and size, local wind characteristics, as well as waste management strategies, including decommissioning, refurbishment, and repowering [80,81]. While early LCAs primarily aimed to benchmark the environmental performance of wind power systems against fossil-fuel-based electricity generation, more recent research works have been dedicated to the optimization of the manufacturing processes so as to align with the EU regulations on energy efficiency and climate change impact reduction. More specifically, resource and energy optimization has emerged as a major concern in the design and construction of wind turbines, with the dual target to decrease energy consumption and mitigate the GHG emissions [82,83]. This evolution reflects a broader transition from comparative assessments towards proactive strategies that significantly improve the environmental sustainability of wind energy systems across their entire life cycle.

2.3.1 Review outputs regarding methodological issues

System Boundaries and Functional Unit

Applying comprehensive system boundaries when conducting LCAs of wind energy systems is essential to ensure that all relevant environmental impacts across key processes are captured and that opportunities for optimization are accurately identified. Environmental impacts of wind turbines derive from raw materials extraction, manufacturing of turbine components, transportation, installation, operation and maintenance, and, ultimately, EoL treatment [84]. Similar to solar PV technologies, most of the published studies adopt a cradle-to-gate approach, encompassing all activities from the acquisition of raw materials and the fabrication of components (particularly, towers, blades, nacelles, foundations, cabling, and substations) to transportation and installation [85]. Cradle-to-gate performance evaluations effectively indicate the major contributors to life cycle impacts, particularly material production and components manufacturing, which account for above 80% of total GHG emissions [77–79,86]. Additionally, they enable robust evaluation of design parameters, site-specific operational conditions, and manufacturing improvements. The prevalence of these system boundaries is also driven by data availability constraints, especially concerning the waste management stage, where recycling pathways for composite materials still remain uncertain, evolving, and geographically variable [87,88].

Nevertheless, as observed in PV systems, restricting the analysis introduces notable limitations. The exclusion of EoL stage fails to provide an integrated perspective on the long-term sustainability of wind power systems, leading to underestimating total impacts, and potentially misinforming practitioners and LCA decision-makers [89–91]. This gap is especially critical given the emerging waste management challenges directly related to the large-scale decommissioning of wind turbines, as well as the technical difficulties associated with the recycling of composite blades. Several authors report that the relatively low

apparent contribution of waste treatment to total environmental burdens may lead to incomplete modelling, inconsistent reporting, or excessively simplistic waste management assumptions [89].

These uncertainties underscore the necessity for implementing cradle-to-grave approaches so as to include operation/maintenance, decommissioning, and waste management adequately capturing the implications of circular economy strategies. Such strategies include advanced composite recycling, material recovery, and component repurposing [90,92,93]. When recycling credits are applied, accounted for avoided impacts linked to the recovery of metals, and, potentially, composite materials, the net life cycle impacts can be significantly decreased by 15-40% [94–96]. Furthermore, repurposing strategies can substantially minimize the amount of waste sent to landfills or incineration facilities, leading to more sustainable waste management practices [97]. These reductions are particularly important for turbines with high proportions of steel and aluminium, as well as for emerging thermoplastic blade technologies that enable closed-loop material recirculation. It is worth mentioning that sensitivity analyses consistently demonstrate that the transportation distances from manufacturing sites to installation locations have a stronger influence on overall life cycle emissions than the distances from the operational sites to waste processing facilities. This finding highlights the strategic importance of regionalized supply chains and localized manufacturing capacity, particularly for large offshore components.

The selection of an appropriate FU is an additional methodological aspect that notably affects the robustness and comparability of LCA findings. In the case of wind energy systems, electricity generation, typically expresses as kWh_e delivered to thee gird, is widely considered as the most suitable unit of the analysis. This choice not only enables the direct comparison with fossil fuel-based electricity production, but also allows performance differences across wind turbine sizes, types and locations to be meaningfully evaluated. However, it is important to mention that this FU is sensitive to key assumptions, such as the Capacity Factor (CF) and the annual energy yield, all of which are affected by site-specific wind resources, hub height, turbine design, and meteorological condition. For example, the GHG impact intensity, expressed in gCO_{2eq}/kWh_e, is strongly influenced by the annual energy yield. Normalizing the environmental impacts by installed capacity (expressed in kW_p) might result in misleading interpretations when comparing turbines of different rated power, rotor diameters, or efficiency. Consequently, this FU choice appears less appropriate except for design-focused analyses. Accounting for accurate wind speed distributions, site-specific losses, and technology-specific performance degradation is fundamental to ensure robust and reliable evaluations of wind power systems performance.

Impact Categories

Climate change, typically expressed as GHG emissions (in CO_{2eq}), is the most frequently assessed impact category in LCA studies, reflecting the substantial contribution of wind energy towards the decarbonization of the electricity sector [98]. The energy intensive fabrication processes, i.e., steel and concrete production for the towers and the relevant foundations, composite fabrication for blades, and the utilization of rare earth elements in generators, are the main contributors to the GHG impact. On the other hand, the stages of transportation, installation and operation are smaller contributors to the GWP. Fossil and nuclear energy use is also a key impact category because of the high embodied energy of structural and mechanical components [99]. The quantification of the non-renewable energy use provides valuable information on the

benefits of the wind turbines design optimization. Comprehensive LCAs also comprise a broader range of environmental impacts, such as mineral resources use associated e.g., with the alloying elements utilized in structural components, human toxicity and ecotoxicity related to metal extraction and refining, as well as terrestrial and aquatic acidification, eutrophication, photochemical ozone formation, and particulate matter formation stem from the energy intensive manufacturing processes. In the case of the offshore installations, additional categories include marine ecosystem impacts. Additionally, wind energy directly contributes to land-use change and occupation, since construction and site preparation require permanent conversion of areas for wind turbine foundations, access roads, and supporting infrastructure [98]. Standardized Life LCIA methodologies, including IMPACT World+, ReCiPe, or CML provide regionalized characterization factors and facilitate multi-impact evaluation, supporting comparability across studies and informed decision-making regarding material selection, turbine design, manufacturing improvements, and circular economy strategies for waste management [38–41].

2.3.2 Review outputs focusing on system boundaries

The literature consistently underscores that resource and energy optimization has been a key priority in wind turbine design and construction, with the objective to mitigate both energy demand and GHG emissions [77–79]. Morozovska [86] identifies the production of raw materials, such as steel, iron, copper, aluminium and their alloys, polymers, glass- and carbon-fibre components, together with the manufacturing of major components (towers, nacelles, foundations, blades, internal and external cables, and substations), as the principal contributors to environmental impacts. A thorough LCA of electricity generation from a 15 MW offshore wind plant [100] further clarifies the processes and life cycle stages driving the climate change impact and the non-renewable energy consumption. The study demonstrates that the manufacturing stage is the predominant contributor, with foundations (25%), the tower (13%), blades (9%), site cables (9%), the nacelle (7%), the gear and main shaft (5%), and offshore substations (3%) accounting for the highest shares of GHG emissions. These outcomes are consistent with Kouloumpis et al. [79], who report that carbon-intensive materials used in turbine support represent more than 60% of total GHG emissions. A similar pattern emerges for fossil energy use, where the foundation (19%), tower (10%), blades (10%), site cables (10%), and nacelle (6%) constitute the most energy-intensive components of the manufacturing phase.

In response to these environmental burdens, several studies propose strategies to reduce the adverse impact of the manufacturing stage. Zajicek et al. [101] and Martínez et al. [102] suggest integrating secondary or reused materials in towers and nacelles, while other authors [102,103] propose the substitution of carbon-intensive materials with less energy-intensive alternatives that maintain equivalent performance without compromising turbine efficiency. Beyond manufacturing, subsequent life cycle stages also play a notable role. The plant set-up (installation) phase and maintenance activities, involving preventive maintenance, oil changes, lubrication, and equipment replacement, contribute considerably to overall impacts, particularly through the use of marine gas oil by service vessels. During operation, this accounts for 24% of total fossil energy consumption, with installation vessels used in the plant set-up phase contributing an additional 6% [100].

Although these stages collectively shape the environmental profile of wind power systems, the EoL phase has received comparatively less attention. Studies generally find that waste management has a relatively low influence on total life cycle impacts [80]. However, broader aspects of wind turbine waste disposal remain unclear, inconsistent, or non-transparent, underscoring the need for more comprehensive and harmonized assessments of EoL practices [80,92,104–106].

2.3.3 Review outputs focusing on wind turbines design parameters

Onshore versus offshore installations

Comprehensive comparative assessment show important differences in the environmental performance of onshore and offshore wind turbines. According to the 2014 IPCC Fifth Assessment Report [107], the life cycle GHG emissions of onshore installations are estimated at 7-11 $gCO_{2eq}/kWh_{e,}$ whereas offshore installations reach 8-14 $gCO_{2eq}/kWh_{e.}$ These figures are both substantially lower than ones of coal-fired electricity, estimated at 900 gCO_{2eq}/kWh_e. The relatively higher GHG emissions of offshore turbines are mainly attributed to the additional steel and other carbon-intensive raw materials required for floating platforms, monopile foundation, subsea cabling and substations, as well as the energy-intensive installation and maintenance activities involving vessels and helicopters [108]. Several studies further demonstrate these differences. Gor instance, Bonou et al. [90] estimated onshore GHG emissions below 7 gCO_{2eq}/kWh_e versus 11 gCO_{2eq}/kWh_e for offshore wind power systems, consistent with Jungbluth et al. [109], who evaluated 11gCO_{2eq}/kWh_e and 13 gCO_{2eq}/kWh_e for onshore and offshore systems, respectively. To mitigate the higher offshore impacts, increasing the recycled steel content has been identified as an effective strategy, potentially reducing life cycle GHG emissions by up to 49% [84].

Horizontal versus vertical axis configurations

Beyond the onshore-offshore comparison, research on the relative environmental performance of vertical-axis and horizontal-axis wind turbines remains limited. Uddin and Kumar [94], who carried out an integrated environmental evaluation of vertical- versus horizontal-axis turbines, outlined that vertical-axis grid-connected turbines are more energy- and emissions-intensive. Nevertheless, the authors highlighted that material reuse exhibits substantial benefits; studies show reductions of more than 50% in embodied energy and relevant emissions when reused components are employed. Concerning material substitution, some LCA assessments point out that substituting aluminium with thermoplastic or glass-fibre composites can decrease embodied energy by 40% [77,110,111]. All the aforementioned studies emphasize the substantial potential for impact mitigation via the selection of low-carbon materials and the deployment of systematic recycling strategies.

Rated capacity, hub height and site-specific factors

From the perspective of turbine size, Demir and Taşkin [112] investigated the trade-offs between rated capacities, hub heights and environmental impacts. In detail, they performed a comparative assessment of three medium-scale (330 kW, 500 kW and 810 kW) and two large-scale (2050 kW and 3020 kW) wind turbines with hub heights of 50 m, 80 m and 100 m. Their results indicate that the GHG impact ranges from 15.1 to 38.3 gCO_{2eq}/kWh_e, outlining that higher hub and greater rated power generally result in enhanced

environmental performance from the viewpoint of GWP. Similar findings were reported by Crawford [113], Kabir et al. [114], and Tremeac and Meunier [115], who confirmed that as wind turbine size increases, electricity generation rises, and, thereby, environmental impacts per unit of electricity generated decrease. Bhandari et al. [116] further explored the correlation between onshore wind turbine environmental impacts and multiple factors, including CF, rated power, hub height, and rotor diameter. The authors concluded that larger turbines or power systems, and higher annual energy yields, are associated with lower GHG impact. Other variables were either collinear with annual energy yield or presented weak correlations. Lenzen and Munksgaard [117] further showed that the energy intensity is strongly influenced by the country of manufacture and the waste treatment strategy, while the GWP is additionally affected by the national electricity mix. Notably, the distance between manufacturing facilities and wind farm sites has a greater impact on life cycle GHG emissions than the distance from operational sites to EoL processing facilities, indicating that developing regional manufacturing capacity is a key strategy for minimizing environmental impacts.

2.4 Lessons learnt, gaps and challenges

The LCA literature on solar PV and wind power systems provides valuable insights into their strategic role in decarbonizing the electricity sector. This is due to the fact that these technologies produce near-zero emissions during operation. Nonetheless, robust sustainability assessments require a full life cycle perspective, since substantial energy use and GHG emissions occur during their manufacturing, transport, installation, and disposal /EoL treatment. For PVs, silicon purification and module assembly are the primary contributors to environmental burdens, whereas for wind turbines, the production of steel and concrete for towers and foundations dominates life cycle impacts. These outcomes underscore the importance of transitioning manufacturing processes to RES and adopting more resource-efficient production methods. From an EoL perspective, circular economy approaches, involving material recycling, component repurposing, and design optimization, can significantly reduce non-renewable energy use, GHG emissions and landfill waste. In addition, national energy policies that increase the share of renewables in the electricity mix can further enhance sustainability by lowering the embedded emissions of renewable technologies, highlighting the interconnectedness of technological innovation and policy measures.

Despite substantial progress, important knowledge gaps still exist. Region-specific LCI data remain limited, constraining the accuracy of environmental assessments across contexts with differing manufacturing practices, supply chains, and electricity mixes. Recycling and repurposing pathways for both PV modules and wind turbine components are also underdeveloped, particularly at the scale required to support projected deployment levels. Moreover, most research is dedicated to first generation (c-Si PVs) and onshore wind power systems, whilst emerging technologies, such as third generation PVs, offshore wind, and hybrid renewable energy systems, have received comparatively limited environmental evaluation. Robust and holistic frameworks that integrate circular economy principles throughout the entire life cycle of renewable energy technologies do not exist, leaving room for optimization in both design and policy. Another challenge is the dependence of PV and wind power systems on critical raw materials. c-Si PVs require large amounts of silver, and several advanced PVs rely heavily on scarce elements, e.g., tellurium

and indium. BoS components also contain aluminium, copper, and rare earth elements, while wind generators typically depend on neodymium and dysprosium. The extraction and processing of the aforementioned materials can create adverse environmental impacts, thus complicating long-term sustainability goals. Addressing these constraints requires advances in material substitution, resource-efficient design, and circular strategies that enable recovery of critical elements at EoL, supported by policies that align rapid renewable energy deployment with responsible material management.

In order to advance the environmental sustainability of solar and wind power systems, several priority strategies emerge. Manufacturing should increasingly operate on "greener" energy inputs, and adopt higher-efficiency production techniques, complemented by material optimization and the implementation of recycled or low-impact alternatives. Circular economy strategies, including advanced recycling processes for composite materials (e.g., wind turbine blades) and components repurposing, should be also incorporated into the EoL stages. In addition, the development of holistic, region-specific datasets across all life cycle stages, alongside the incorporation of future energy scenarios in environmental performance evaluations, are essential to support accurate assessments, and inform technological optimization and policy development. The incorporation of economic dimensions, such as the Levelized Cost of Energy (LCOE), will further enhance the holistic understanding of renewable energy sustainability. Last, but not least, well-designed policy frameworks are fundamental to coordinate these efforts. Incentives, regulations, and long-term planning should jointly promote the large-scale deployment of renewable energy technologies, as well as the sustainable material management, and innovation in circular practices and advanced technologies. By integrating technological advancements with circular economy approaches and supportive policy measures, the renewable energy sector can progress towards climate-neutral electricity generation while minimizing resource utilizations and adverse environmental impacts across the entire life cycle.

Chapter 3
Methodological Framework for Energy System Modelling, Economic Analysis & Multi-Criteria Decision-Making

This chapter introduces a holistic methodological framework developed for the analysis and performance evaluation of renewable energy systems. The objective is to establish a structured and transparent approach that enables the rigorous assessment of alternative energy system configurations. To achieve this, three complementary methodological components are integrated into a unified framework. The first component, the energy system modelling framework, is devoted to developing robust mathematical models that could represent the configuration, performance, and interactions of technologies within the system, supporting design, evaluation and grid integration. The second component, the economic modelling framework, quantifies costs, revenues, and key economic indicators, enabling assessment of the financial viability of system configurations for both short- and long-term planning. The third component, the multi-criteria decision analysis framework, implements a hybrid methodology for selecting alternatives by integrating criteria and stakeholder preferences while generating robust rankings.

3.1 Energy system modelling framework

The accurate modelling of renewable energy technologies, particularly solar PV and wind power systems, constitutes a significant prerequisite for the reliable prediction of their electrical output under diverse environmental and operational conditions. The development of robust mathematical models is fundamental for the optimal system design and sizing, as well as integrated technical, economic and environmental system evaluation, and informed grid integration planning. By identifying the nonlinear interactions among resource availability, component-level technical and economic specifications, and operational constraints, these models provide valuable insights for researchers, engineers, system planners, and policy makers, thus supporting the optimization of system performance in terms of resources utilization, energy efficiency, system reliability, cost-effectiveness, and environmental sustainability. This section provides a detailed description of the mathematical models employed to simulate energy generation in PV and wind power systems, with the aim to establish the analytical foundation for the case studies examined in Chapters 4 and 5.

3.1.1 Photovoltaic system modelling

PV modules generate Direct Current (DC) electricity, which is proportional to the incident solar radiation [118,119]. The simulation of solar PV systems relies on two main categories of input data: (i) environmental data, and (ii) system-related inputs (design specifications or actual design parameters) [120]. Environmental variables, including solar irradiation, ambient temperature, wind speed and relative humidity, are inherently variable and uncertain but essential for the accurate modelling of the system's performance over extended periods. For instance, the electrical efficiency of the PV module decreases with increasing cell temperature, leading to an important trade-off between higher irradiance levels and elevated operating temperatures [119]. Conversely, system-related inputs, encompassing technical specifications of both PV module and inverters, system configuration and orientation, tracking mechanisms, and shading conditions, are constant or predictable [121,122]. Beyond defining these inputs, a systematic methodology is necessary for reliable modelling and energy yield prediction of a PV installation, incorporating operational performance parameters, such as CF, module and inverter efficiency, availability and degradation rates [120]. This methodology, encompassing multiple sequential steps - from site assessment to final system energy output evaluation and grid integration - is presented in detail in the following paragraphs.

Step 1: Site evaluation & data compilation process

An accurate energy assessment begins with a thorough site evaluation and systematic data compilation. Environmental data, employed to simulate real-world system operation over daily, seasonal, and long-term timeframes, are retrieved from reliable solar databases, including the NASA Surface Meteorology and Solar Energy Database, RETScreen, PVGIS, HMIRS, as well as validated atmospheric models [123]. On the other hand, system-related inputs are directly provided by the equipment manufacturer. Integrating the validated environmental datasets and the manufacturer-provided system specifications enables the assessment of the expected PV energy output, as well as the identification of the potential losses, and the estimation of the overall system efficiency and reliability, along with the implications for grid integration.

Step 2: System configuration and component modelling

Following the compilation of site-specific environmental and system-related data, the next step involves determining the PV system configuration, particularly, defining the number of PV modules, string and array configurations, inverter capacity and efficiency, mounting structures, and potential tracking mechanisms. This step is essential as it characterizes the electrical behavior of the system and strongly affects the energy output under fluctuating environmental/meteorological conditions.

Component modelling incorporates current-voltage characteristics, temperature-dependent performance coefficients, and degradation rates. The Maximum Power Point (MPP) of a module, defined as the maximum power available at one specific operating condition, in determined by Equation 1 [124]. It should be noted that PV modules should operate as close as possible to their MPP in order to maximize energy yield and ensure optimal system performance.

$$P_{MPP} = V_{MPP} \times I_{MPP} \quad (1)$$

$P_{MPP}(W)$ denotes the maximum power output, while $V_{MPP}(V)$ and $I_{MPP}(A)$ represent the voltage and the current at maximum power point, respectively.

The temperature of a PV cell significantly influences its efficiency and performance; elevated temperatures typically result in reduced power output due to increased internal resistance and lower voltage. Considering that the MPP is directly related to the cell temperature, T_c (°C), the electrical efficiency of the PV module, η_p, can be expressed as a function of T_c, as presented in Equation 2 [125].

$$\eta_p = \eta_r \times \left[1 - \beta_p \times \left(T_c - T_{ref}\right)\right] \quad (2)$$

T_{ref} is the reference temperature (25°C), η_r is the module efficiency at the T_{ref}, and β_p (%/°C) is the β_p (%/°C), representing the percentage decrease in PV output for each degree Celsius increase above the reference temperature. The cell temperature, T_c (°C), is not directly measured but calculated using the nominal operating cell temperature figure, as shown in Equation 3 [125,126].

$$T_c = T_a + \left[(219 + 832 \times K_t) \times \left(\frac{NOCT-20}{80}\right)\right] \quad (3)$$

T_a (°C) is the ambient temperature, *NOCT* (°C) is the nominal operating cell temperature, K_t is the clearness index, representing atmospheric clarity (ranging from 0 under cloudy to 1 under clear conditions), and 219, 832, and 80 are empirical constants used for estimating cell temperature.

Step 3: PV system energy output estimation

Following the methodology proposed by Almonacid et al. [126], Kumar et al. [127] and Skoplaki and Palyvos [125], the energy output of the PV system, $E_P\ (kWh)$, over a time internal Δt, is calculated using Equation 4.

$$E_P(t) = \sum_t H_t \times \eta_p \times (1 - \lambda_p) \times S \times \Delta t \quad (4)$$

S (m^2) is the PV surface area, H_t(kWh) is the solar radiation on the tilted surface, η_p is the PV module electrical efficiency, and λ_p represents the miscellaneous PV losses.

The energy available to the load, $E_A(kWh)$, over a time internal Δt, accounts for system conditioning losses, λ_c, and is quantified employing Equation 5.

$$E_A(t) = \sum_t E_P \times (1 - \lambda_c) \times \Delta t \quad (5)$$

Finally, the inverter converts the DC from the PV modules to Alternating Current (AC) for grid compatibility. The energy exported to the grid, $E_{grid}(kWh)$, over a time internal Δt, is derived from E_A, taking into account the inverter efficiency, η_{inv}, as shown in Equation 6.

$$E_{grid}(t) = \sum_t E_A \times \eta_{inv} \times \Delta t \quad (6)$$

Implementing this simulation framework enables the assessment of PV system performance alongside grid integration, thereby optimizing energy production, system efficiency, and ensuring reliable connection to the electrical network. The energy flow diagram for a typical grid-connected PV system is presented in Figure 1.

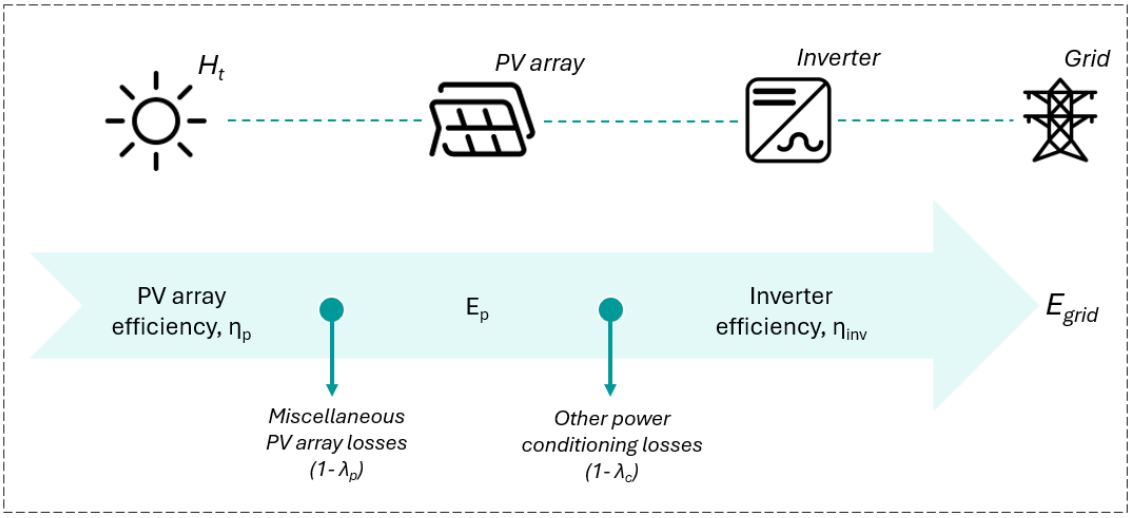

Figure 1 Flowchart for grid-interconnected PV model

3.1.2 Wind power system modelling

The primary function of a wind generator is to convert the kinetic energy of the wind into Alternating -Current (AC) electricity [128]. At the turbine-level, the power output of a wind turbine is influenced by three main factors: (i) the wind speed distribution at the installation site, (ii) the tower height, and (iii) the power output curve of the wind turbine; the latter is determined by the aerodynamic power efficiency, the mechanical transmission efficiency, and the generator efficiency. A wind turbine starts generating electricity when the wind speed ranges from 2 to 4 m/s, which initiates the rotation of the turbine blades. It continues generating power up to wind speeds of 25–30 m/s, though these values may vary depending on the manufacturer and model [129]. The output power of a wind turbine at Standard Temperature and Pressure (STP) conditions, $P_{WT,STP}$ (kW), is estimated as follows [130,131]:

$$P_{WT,STP}(V) = \begin{cases} P_r \cdot (V - V_{cin})/V_r - V_{cin}, & V_{cin} \le V \le V_r \\ P_r, & V_r \le V \le V_c \\ 0, & V \le V_{cin} \; and \; V \ge V_c \end{cases} \quad (7)$$

P_r denotes the rated power of the wind turbine, and V_{cin} (m/s), V_r (m/s) and V_c (m/s) represent the cut-in velocity, the rated velocity and the cut-out velocity, respectively.

The wind velocity at the hub height, U_{hub} (m/s), is estimated using the power law equation [132,133]:

$$U_{hub} = U_{anem} \cdot (Z_{hub}/Z_{anem})^{\alpha} \quad (8)$$

U_{anam} (m/s) denotes the wind speed at the anemometer height, Z_{hub} (m) and Z_{anam} (m) are the height at the hub of the wind turbine and at the anemometer position, respectively, and α represents the power law exponent. As reported in [134], α is assumed to be 0.143 for moderately rough terrain.

To account for actual conditions, the output power at STP conditions (see Equation 7) is multiplied by the air density ratio, as shown in Equation 9 [135].

$$P_{WT} = P_{WT,STP} \cdot \left(\rho/\rho_o\right) \quad (9)$$

$P_{WT}(kW)$ denotes the wind turbine power output, ρ (kg/m^3) is the actual air density, and ρ_o is the air density at STP (1.225 kg/m^3).

While the performance assessment of individual wind turbines remains essential, research is increasingly devoted to simulating wind power systems within a comprehensive framework, incorporating: (i) system - wide (grid) integration, (ii) operational challenges arising from the intermittent and fluctuating nature of wind power (load balancing and reserve capacity requirements), and (iii) long-term planning considerations. At the core of wind energy system modelling is capacity planning, which determines the optimal sizing of power capacity, identifies appropriate geographical deployment, and assesses transmission infrastructure requirements [136,137]. Capacity planning informs decisions on the optimal location, while considering both technical and economic parameters/constraints. Furthermore, it serves as the basis for grid integration modelling, which addresses the operational challenges, such as system flexibility, reserve requirements, and impacts on grid stability, frequency regulation, voltage control, and reactive power management. Models also incorporate forecast accuracy, probabilistic generation scenarios, and correlations with electricity demand, while considering seasonal and interannual variations so as to ensure both short-term reliability and long-term system planning. Complementing these technical assessments, economic and market models are also implemented to evaluate the effects of wind power on electricity prices, operator revenues, and capacity credit, thereby providing a holistic view of the operational and economic implications of large-scale wind energy integration.

3.1.3 Storage integration

In order to strengthen grid and market operations and mitigate the impacts of the intermittent and fluctuating nature of solar and wind power, energy storage systems are increasingly deployed, providing operational flexibility, balancing supply and demand, and enhancing the overall system reliability. Batteries, in particular, serve as a backup in the system providing a continuous and uninterrupted electricity supply during periods when power is unavailable from both solar PV and wind power systems. They also provide support in the event of breakdown or scheduled shutdown of fossil fuel-based generation units (e.g., diesel generators), thereby reinforcing system stability and operational resilience.

The most widely applied approach for managing battery storage systems is the “generic State of Charge (SOC)-based model”, which monitors changes in the battery’s SOC due to power inflows or outflows [138].

SOC, expressed as a percentage from 0% (fully discharged) to 100% (fully charged), denotes the battery's energy level relative to its total capacity. Assuming constant battery voltage, SOC is calculated as the ratio of the energy stored in the battery to its maximum capacity. Temporal variations in SOC are tracked as a discrete time series, with increases indicating charging and decreases indicating discharging. The SOC at each time step is determined using Equation 10 [139].

$$SOC_t = SOC_{t-1} + \frac{\left(P_{bat_{ch,t}} \cdot \eta_{ch} - P_{bat_{disch},t}/\eta_{disch}\right) \cdot \Delta t}{EC_{bat}} \quad (10)$$

$P_{bat_{ch,t}}(kW)$ and $P_{bat_{disch,t}}(kW)$ denote the charging and discharging power of the battery energy storage system, respectively, and η_{ch}andη_{disch}represent the corresponding charging and discharging efficiencies. $EC_{bat}(kWh)$is the total energy capacity of the battery bank, and $\Delta t\ (hrs)$ indicates the duration of each time step.

SOC constraints for batteries are significant for ensuring safe and efficient operation of batteries [140]. These constraints include minimum and maximum SOC limits, as presented in Equation 11.

$$SOC_{min} \leq SOC(t) \leq SOC_{max} \quad (11)$$

$SOC(t)$denotes the battery's SOC at time t, SOC_{min} represents the minimum allowable SOC, preventing deep discharge that could damage the battery, while SOC_{max} indicates the maximum allowable SOC, avoiding overcharging that could reduce battery lifespan. Concerning Lead-Acid (LA) batteries, SOC_{min} and SOC_{max} figures typically range between 30-50% and 80-90%, respectively [141].

3.1.4 Load following dispatch strategy

Accurate monitoring and management of SOC provides the foundation for implementing effective load dispatch strategies for ensuring reliable and efficient electricity supply. Specifically, dispatch strategies are a set of rules/regulations employed to control system operation when renewable energy technologies (wind and solar energy conversion units) cannot meet the load requirements, optimizing the operation of available generation and storage assets [142]. Among various dispatch strategies, the Load Following (LF) dispatch strategy is a fundamental mechanism in power system simulations for ensuring that electricity demand is met at all times, while minimizing system costs and maintaining reliability. This approach recognizes the important distinction between RES, which are characterized by variable and non-dispatchable output, and conventional generation technologies (Diesel Generators - DG) that offer controllable power delivery. Under this strategy, the conventional power technology (diesel generator) is activated only to produce the exact amount of power required to meet excess load demands. Lower-priority tasks, such as charging battery storage elements, are assigned to RES, namely wind turbines and PV modules. It is highlighted that this strategy is particularly well-suited for off-grid or isolated systems with abundant renewable energy potential. By utilizing excess renewable energy to charge batteries, the approach reduces the surplus energy, decreases both the total Net Present Cost (NPC) and system emissions, and improves the overall operational efficiency. Consequently, the integration of energy storage, combined with effective SOC

management and implementation of the LF dispatch strategy can ensure system balance, operational reliability, and economic viability. The relevant LF dispatch strategy is shown diagrammatically in Figure 2.

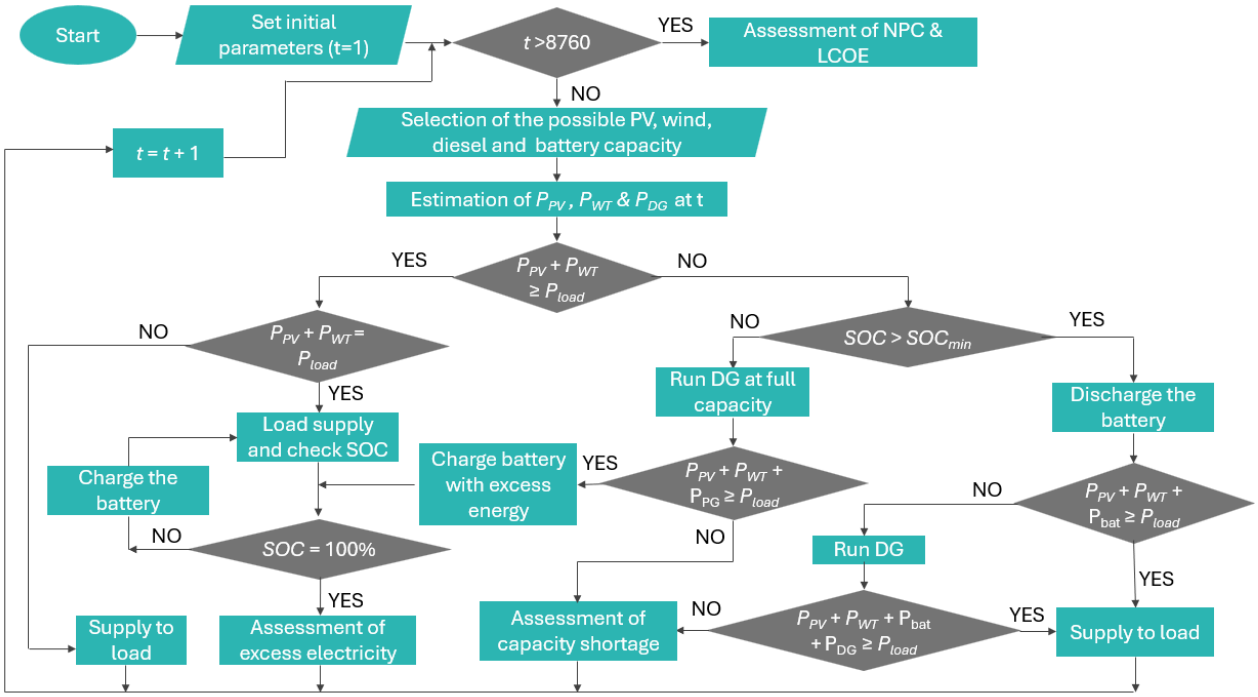

Figure 2 Flowchart of LF dispatch strategy applied in this analysis

In detail, first, the customized system controller continuously monitors wind power generation, P_{WT}, solar PV power generation, P_{PV}, load demand, P_{load}, and batteries state of charge, SOC. In ordinary situations, both the wind turbines and PV modules meet the load requirements. However, their output strongly depends on the variations in wind speed and solar radiation. The system controller determines whether the power generated by wind turbines and PV modules is sufficient to meet the load demand at that moment (t). When it exceeds the load demand, the SOC of batteries is evaluated to determine whether it can absorb the excess power. If the storage (battery) bank has sufficient capacity, it stores the surplus energy until it is fully charged. Conversely, if solar and wind energy are insufficient to meet the load requirements, the SOC of battery is assessed to determine whether the battery can discharge in order to supply the remaining required power. The batteries will discharge only if they have sufficient capacity ($SOC > SOC_{min}$). If the batteries cannot fully fill the load gap, the diesel generator (P_{DG}) operates in order to meet the remaining demand, a situation that typically occurs at night.

The concept of Operating Reserve (OpRe) is also considered as it is critical for grid stability, especially in hybrid and renewable-based energy systems where power generation can be variable. OpRe refers to the surplus operating capacity that ensures a reliable electricity supply in unexpected situations, including sudden increases in load demand or abrupt decreases or failures in renewable power output. As demonstrated in [15], OpRe is set to be 10%, 25% and 50%, as a percentage of hourly load, solar power

output and wind power output, respectively. The relevant mathematical expression applied to evaluate the OpRe is provided by Equation 12 [15].

$$OpRe = (0.10 \cdot E_L) + (0.25 \cdot E_{PV}) + (0.50 \cdot E_{WT}) \quad (12)$$

E_L is the energy required by the load, E_{PV} is the energy generated by the PV modules and E_{WT} is the energy generated by the wind turbine.

In summary, the aforementioned modelling approach provides valuable insight into the operation of hybrid power systems that integrate RES, supporting the determination of optimal component sizing. Furthermore, it enables a comprehensive evaluation of system performance across diverse scenarios, thereby ensuring a well-informed assessment of both efficiency and reliability.

3.2 Economic modelling framework

Assessing the economic viability of renewable energy systems, comprising solar energy conversion units and/or wind turbines, integrated with conventional energy systems, with or without energy storage, requires a comprehensive modelling framework that demonstrates the interactions between capital investments, operating and maintenance costs, revenue streams, and long-term economic performance. Unlike stand-alone conventional systems, renewable energy projects introduce important economic challenges, such as high upfront costs, variable output profiles, technology-specific degradation, and evolving policy incentives, which can impact on the overall system economics. This section offers a systematic methodological approach for evaluating integrated energy systems using standardized cost structures and performance indicators. It helps determine whether the combined renewable and conventional energy investment delivers sufficient value relative to its costs, while offering decision-makers the appropriate quantitative tools for technology comparison, optimal system design, and investment planning.

3.2.1 Cost structure components

A rigorous economic assessment of renewable energy projects requires a comprehensive understanding of both costs and revenues that determine the long-term viability.

Total Capital Investment

The Total Capital Investment (TCI) covers direct costs, indirect costs, land, and working capital [143], forming the basis for project economics. For solar PV installations, direct costs primarily consist of equipment costs (typically over 70%), including PV modules, inverters, mounting structures, cables, monitoring and safety systems, as well as costs related to installation labour, transport, logistics, and construction materials. On the other hand, indirect costs account for 10-15% of the TCI and cover engineering, both system and electrical design, as well as tendering, contracting, and construction supervision or project management [144–146]. It is worth mentioning that the evaluation of potential risks, uncertainties, and unforeseen costs that may arise during the construction phase is fundamental to accurately estimate both direct and indirect costs. Other costs, including land, working capital and

contingency funds are also key components of the TCI. Land represents 5-10% of the TCI, reflecting site acquisition and preparation, whereas working capital and contingency funds account for 5-10%, corresponding to spare parts, maintenance reserves, and operational readiness throughout the system's lifetime [144–146]. This breakdown points out that while equipment and installation represent the dominant costs, indirect costs, land, and working capital are quite critical in assessing the economic viability of the project.

For onshore wind energy projects, the largest share of the TCI (typically about 55%) is associated with the principal generating components, i.e., the rotor assembly, nacelle and tower [147]. The BoS, which covers electrical interconnections, foundations, and site access, accounts for roughly 30% of overall expenditure. Lastly, other costs, encompassing planning, permitting, and other administrative or development-related activities, comprise the remaining 15% (Figure 3). This distribution outlines the multifaceted nature of costs related to wind energy projects, emphasizing that while the turbine hardware dominates expenditure, a substantial portion of the investment is dedicated to enabling infrastructure and project development processes essential for the realization of a fully operational wind farm.

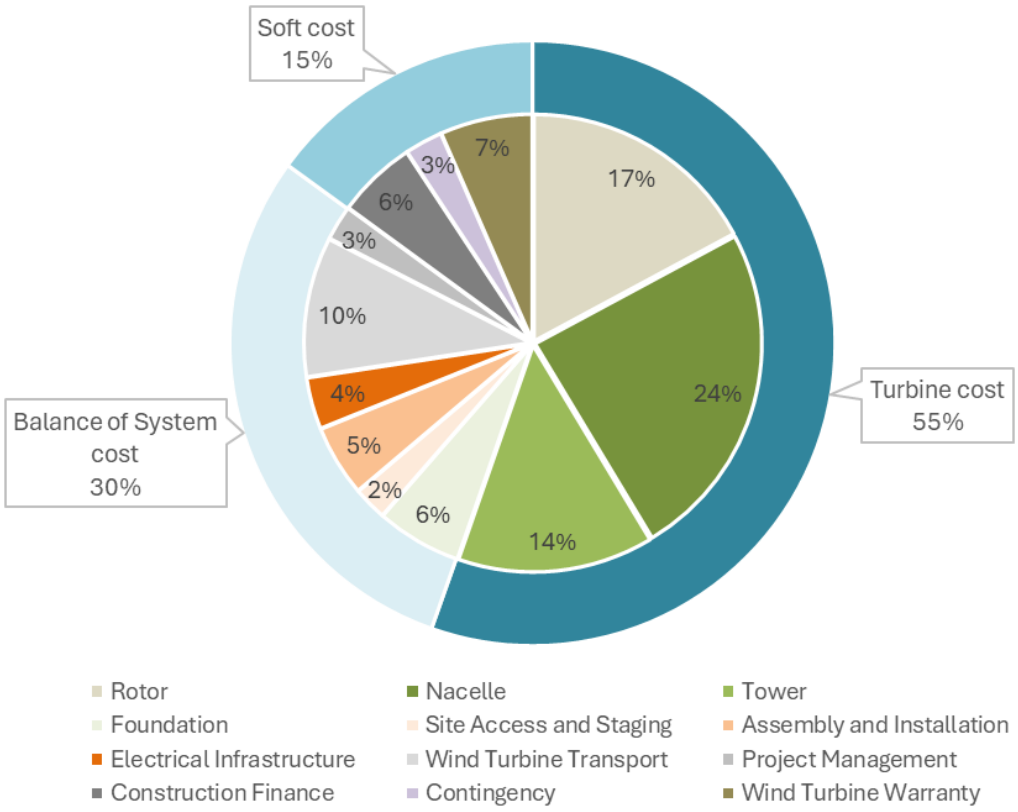

Figure 3 Breakdown of TCI for an onshore wind turbine

Operating and Maintenance Costs

Wind turbines and solar energy conversion units exhibit distinct Operating and Maintenance (O&M) cost profiles, reflecting differences in technology and maintenance requirements. O&M costs include insurance, regular maintenance, repair, spare parts, and contingencies. For PV systems, O&M costs typically account for 0.5-2.0% of the TCI [144,148]. These costs are mainly related to module cleaning to maintain efficiency and basic electrical maintenance. Monitoring systems support the early detection of underperforming panels or electrical issues, thereby eliminating the need for extensive troubleshooting [148]. Onshore wind turbines exhibit O&M costs of approximately 2.0-4.0% of the TCI annually, which are higher than the ones of PV systems. Offshore wind turbines are associated with even greater O&M requirements, mainly because of more challenging maintenance conditions and specialized vessel requirements. Wind turbine O&M costs also vary significantly by technology type and location, being strongly influenced by drivetrain design and distance from maintenance infrastructure [149]. It should be noted that for both wind turbines and PV systems, potential increases in O&M costs are expected as systems age.

Replacement cost

Replacement cost refers to the expenditure required to substitute system components whose operational lifetime is shorter than the total project assessment period. In the case of solar PV applications, this most commonly applies to the BoS components, particularly inverters, due to shorter lifespans (approximately 10-15 years) than PV modules and require one or more replacements to ensure continuous and efficient system performance. Similarly, in wind turbines, high-stress components, encompassing gearboxes, generators, and power electronics may require replacement or major refurbishment during the project horizon because of mechanical wear and performance degradation. The accurate consideration of replacement costs is fundamental to ensure both reliable long-term operation and realistic life cycle cost evaluations.

Salvage Value

The salvage value is fundamental in long-term economic viability evaluations, particularly for renewable energy projects such as PV systems and wind turbines since it offers a realistic adjustment to net present costs and can affect investment decisions. For both PV technologies and wind turbines, it represents the residual worth of the components at the end of the project lifetime, based on their remaining useful life. The salvage value, S, is determined using the following equation [150]:

$$S = C_{rep} \times {}^{R_{rem}}\!/_{R_{comp}} \quad (13)$$

C_{rep} $\left({}^{€}\!/_{year}\right)$ reflects the replacement cost of the component, R_{rem} $(years)$ denotes the remaining lifetime of the component at the end of the project lifetime, and R_{comp} $(years)$ represents the lifetime of the component.

It is worth mentioning that since the salvage value is derived from the replacement cost, these two figures are inherently interconnected; specifically, a higher future replacement cost of a component leads to a greater proportional salvage value if that component retains useful life at the end of the project period.

3.2.2 Economic evaluation parameters

Different methods have been widely applied by researchers to evaluate the economic feasibility and cost-effectiveness of renewable energy systems, particularly hybrid configurations that incorporate solar PVs, wind turbines, diesel generators, and storage. These methods require the inclusion of all relevant cost categories presented in detail in Section 3.2.1, allowing for an integrated assessment of the key economic performance indicators, which are described in the following paragraphs. These indicators also enable comparative analyses with other investment opportunities [151,152], providing decision-makers with a solid foundation for assessing the long-term economic viability of renewable energy projects relative to conventional options.

Net Present Cost and Net Present Value

The total NPC of a system denotes the present value of all the expenditures incurred over its lifetime, minus the present value of any revenues earned. In energy systems, the cost structure typically includes the TCI, C_{inv} $(€)$, incurred at the beginning of the project, along with recurring annual costs, including O&M costs, $C_{O\&M}$ $(€/year)$, replacement costs for components with shorter lifetimes (e.g., inverters and batteries), C_{rep} $(€/year)$, and fuel costs, $C_{fuel}(€/year)$, in the case of conventional or hybrid systems. Depending on the system configuration and regulatory framework, additional expenditures may arise, covering emission penalties or expenditures for purchasing electricity from the grid. The salvage value, S $(€)$, is incorporated as a negative cost, discounted to its present value at the end of the project lifetime, thereby reducing the total net present cost. Conversely, revenues consist of income arise from selling excess electricity to the grid at market prices [150,153]. The general expression of the total $NPC(€)$ is written as follows [154–156]:

$$NPC\ (€) = C_{inv} + \sum_{n=1}^{N} \frac{C_{O\&M,n} + C_{rep,n} + C_{fuel,n}}{(1 + i_{real})^n} - \frac{S_N}{(1 + i_{real})^N} \quad (14)$$

i_{real} is the real discount rate, n is the year index (it goes from 1 to N), and N is the project lifespan. Note that S_n is zero for all $n < N$, with S_N being the only positive term. i_{real} is determined as follows [154,155]:

$$i_{real} = \frac{1 + i}{1 + f} - 1 \quad (15)$$

i denotes the nominal discount rate, and f represents the inflation rate.

The Total Annualized Cost, NPC_{ann} $(€/year)$ converts the total *NPC* into an equivalent constant annual cost over the project lifetime, N, using the Capital Recovery Factor (*CRF*), as follows [157]:

$$NPC_{ann}\ (€/year) = NPC \times CRF \quad (16)$$

where

$$CRF = \frac{i_{real} \cdot (1 + i_{real})^N}{(1 + i_{real})^n - 1} \tag{17}$$

The Net Present Value (NPV), in turn, denotes the difference between the present values of cash inflows (revenues) and the present value of cash outflows (costs) associated with an investment project (refer to Equation 18) [158–160]. By performing a discounted cash flow analysis, NPV provides a comprehensive assessment of economic viability: a positive NPV indicates that the expected returns exceed the initial investment costs, thereby signifying that the project is economically feasible and potentially profitable. Conversely, a negative NPV suggests that the projected revenues fall short of covering the investment, therefore rendering the project economically unviable [160].

$$NPV\ (€) = -\ C_{inv} + \sum_{n=1}^{N} \frac{CF_n}{(1 + r_{real})^n} \tag{18}$$

CF_n represents the cash flow in year n, determined by the following equation:

$$CF_n(€/year) = Rev_n + S_n - C_{O\&M,n} - C_{rep,n} - C_{fuel,n} \tag{19}$$

Rev_n denotes the revenues in year n.

Levelized Cost of Energy

The LCOE is closely related to the concepts of NPC and NPV which are widely used in techno-economic analyses. LCOE expresses the lifetime cost per unit of electricity generated, effectively converting NPC into a per-energy metric. It is evaluated by dividing the annualized cost, $NPC_{ann}\ (€/year)$, by the gross yearly load, $E_{load}\ (kWh/year)$, (Equation 20) [157,161].

$$LCOE\ (€/kWh) =\ NPC_{ann}\ /\ E_{load} \tag{20}$$

This approach allows for a direct comparison of different energy technologies, irrespective of scale or lifetime, by providing a single, normalized cost metric in €/MWh or €/kWh. When considered in conjunction with NPV, LCOE enables a robust and multidimensional assessment of the economic viability of renewable energy systems, supporting informed decision-making for both investors and policy makers.

Internal Rate of Return

The Internal Rate of Return (IRR) is a widely used economic metric in investment analysis, defined as the discount rate at which the NPC of projected cash flows equals zero (see Equation 18) [151,161,162]. It denotes the break-even cost of capital and serves as a critical indicator for assessing the profitability of a project. In particular, a project is deemed economically attractive when its IRR exceeds the investor's

minimum acceptable rate of return [163], thereby indicating its cost-effectiveness relative to alternative investment opportunities.

$$NPV(IRR) = -C_{inv} + \sum_{n=1}^{N} \frac{C_{CF_n}}{(1+IRR)^n} = 0 \quad (21)$$

Simple Payback Period (without discounting)

Complementary to IRR, the Payback Period (PBP) is another commonly utilized indicator, which determines the duration required to recover the initial capital investment from net annual cash inflows. The fundamental principle underlying this metric is that investments with shorter PBPs are generally less risky and more appealing, particularly under uncertain market conditions. [164]. As demonstrated in the relevant literature, a PBP substantially shorter than the expected lifespan of the system often signals favourable economic performance [165]. The simple PBP is calculated as follows [161,164,166]:

$$PBP(years) = \frac{C_{inv}}{\sum_{n=1}^{N} CF_n} \quad (22)$$

Benefit-Cost Ratio

In addition to the aforementioned economic performance indicators, the Benefit-Cost Ratio (BCR) serves as a fundamental metric in the economic appraisal of investment projects, particularly in the domain of energy systems. The BCR is defined as the ratio of the present value of total benefits, typically represented by cumulative cash inflows or cost savings, to the present value of total costs, encompassing capital expenditures and operational expenditures, over the entire project life cycle. Mathematically, it can be expressed as [167]:

$$BCR = \frac{\sum_{n=1}^{N}[Rev_n \times \frac{1}{(1+i_{real})^n}]}{C_{inv} + \sum_{n=1}^{N}[(C_{o\&M,n} + C_{rep,n} + C_{fuel,n}) \times \frac{1}{(1+i_{real})^n}]} \quad (23)$$

The BCR provides a dimensionless figure; a BCR greater than 1 indicates that the present value of benefits outweighs the present value of costs, suggesting that the project is economically viable. Conversely, a BCR less than 1 is indicative of a cost-ineffective investment.

3.3 Multi-criteria decision making framework

Building on the energy modelling and economic evaluation framework, an additional layer of analysis is required to enable comprehensive decision-making. Multi-Criteria Decision Making (MCDM) provides a structured approach for incorporating multiple, and often conflicting, criteria into the evaluation of energy system alternatives. It systematically integrates quantitative analysis with stakeholder preferences, value judgments, and cost–benefit considerations, thereby supporting more transparent and balanced decisions [168].

The general framework of the MCDM approach is typically organized into a four-stage process, as illustrated in Figure 4. The first stage, the problem identification, establishes the decision context and the scope of the analysis. Potential alternatives are determined, while clearly infeasible options are excluded based on key factors and constraints, including minimum resource thresholds (e.g., solar irradiation and wind speed), technology readiness, regulatory and environmental requirements, social acceptance, and preliminary economic feasibility. The second stage focuses on engaging diverse stakeholders and refining the set of alternatives. Investors, who primarily emphasize on cost-effectiveness and risk management, help identify economically viable options, while utilities provide input on system reliability and grid integration. Regulators ensure compliance with policy and legal frameworks, whilst communities highlight environmental and social considerations. Based on these perspectives, alternatives are further refined in terms of configuration, capacity, and scale, and constraints are adjusted to reflect technical, economic, environmental, and social aspects, collectively shaping the evaluation of feasible solutions. The third stage, the model formulation, develops the analytical framework for evaluating alternatives. Criteria are clearly defined and quantified, and stakeholder preferences are incorporated using weighting methods such as the pairwise comparison or trade-off analysis, thereby ensuring that the evaluation reflects different priorities. In the fourth stage, which is related to the model resolution and ranking, individual criterion scores are aggregated to produce overall rankings. The robustness of the results can be assessed through sensitivity analysis of weights, criteria, and methods, while outputs may include overall rankings, criterion-specific rankings, and stakeholder-specific rankings, collectively supporting informed decision-making [169].

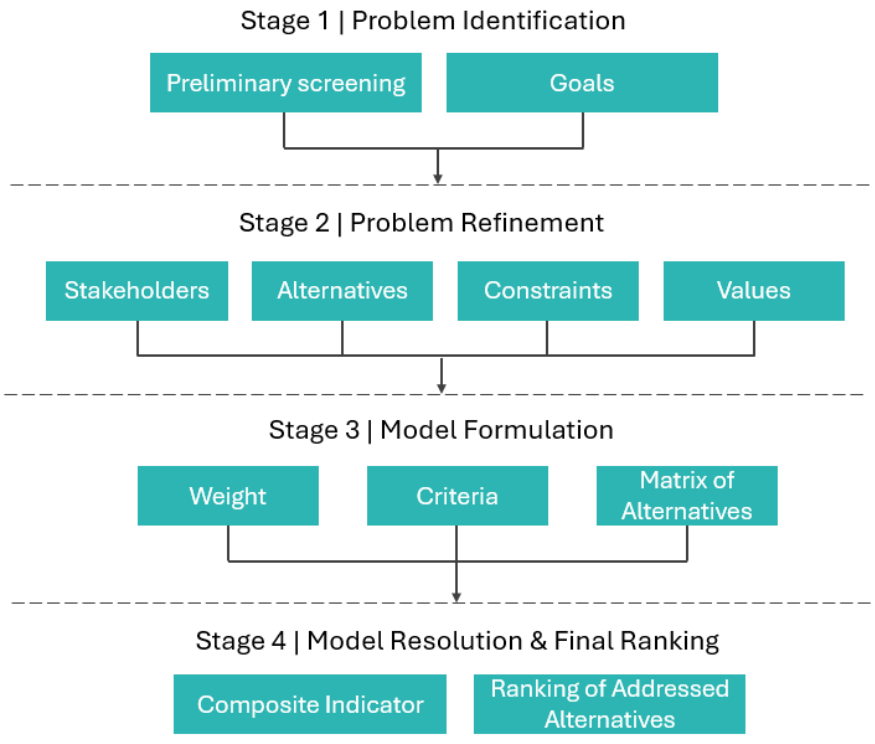

Figure 4 General framework of an MCDM approach

3.3.1 Hybrid DEA-TOPSIS MCDM approach

This comprehensive MCDM framework provides a transparent and stakeholder-inclusive methodology for assessing the performance of renewable energy systems, addressing the complex technical, economic, environmental, and social dimensions inherent in sustainable energy transitions. By integrating quantitative analysis with qualitative stakeholder values, it enables a rigorous yet flexible evaluation that goes beyond purely economic optimization to consider the full spectrum of factors relevant to sustainable energy development.

To operationalize this framework, two widely recognized MCDM methods are employed: Data Envelope Analysis (DEA) [170], and the Technique for Order Preference by Similarity to an Ideal Solution (TOPSIS) [171]. DEA is a data-oriented technique employed for performance evaluation or benchmarking, integrating multi-inputs and output dimensions [172]. Conversely, TOPSIS ranks alternatives by minimizing the Euclidean distance from an ideal solution while maximizing the distance from a negative ideal solution [171]. To fully leverage the strengths of these two methods, this study implements a hybrid DEA-TOPSIS approach. This integrated methodology evaluates the efficiency of alternatives using DEA and subsequently ranks them based on their relative closeness to the ideal solution as determined by TOPSIS. By combining efficiency analysis with preference-based ranking, the hybrid DEA-TOPSIS model ensures a more robust, transparent, and reliable performance assessment of alternatives. The methodological steps for employing this hybrid approach are illustrated in Figure 5.

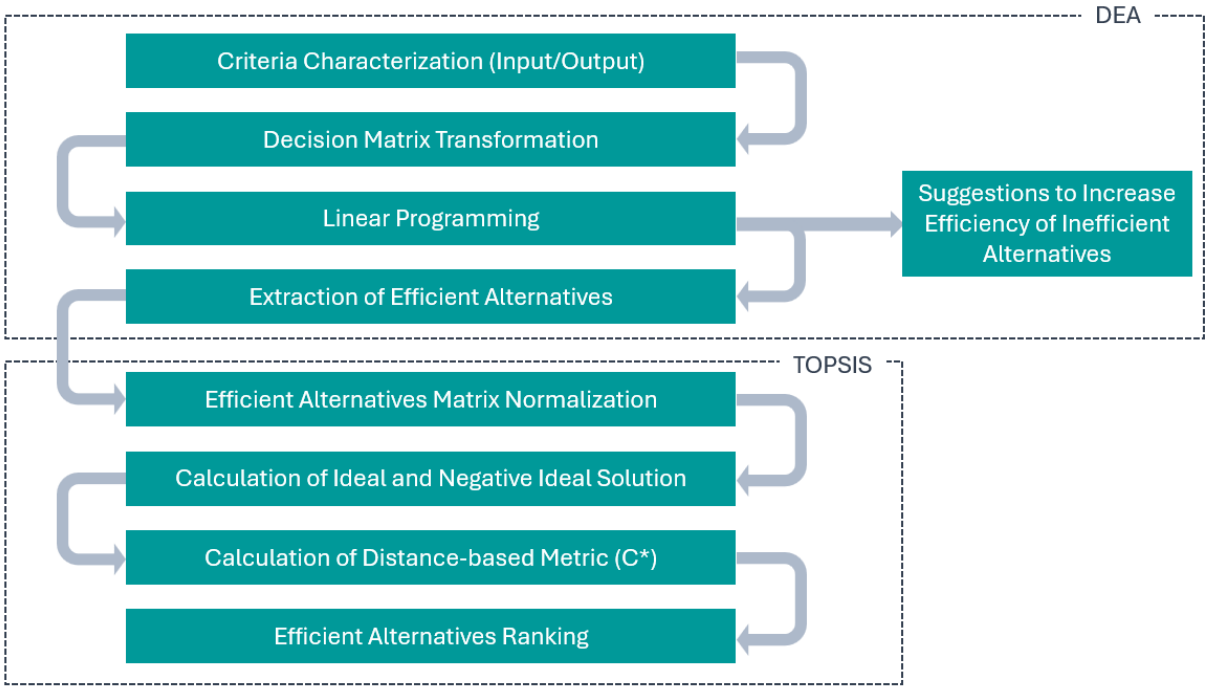

Figure 5 Hybrid DEA-TOPSIS MCDM methodological approach

3.3.2 Data Envelope Analysis component

DEA relies on mathematical programming techniques to measure the efficiency (or inefficiency) of Decision-Making Units (DMUs) that transform several inputs into several outputs/yields. The steps of the DEA component in this hybrid methodology are [173]:

Step 1 Criteria Characterization

Prior to model implementation, the inputs and outputs of the DEA model should be clearly defined. Performance measures for which lower values indicate superior performance are characterized as input criteria. On the other hand, those for which higher values correspond to superior performance are treated as output criteria. This characterization is important for the correct formulation of the optimization problem and ensures theoretical consistency with the underlying DEA principles.

Step 2 Decision Matrix Construction

The decision problem is represented by a pairwise comparison matrix, denoted as *A*, of dimensions $M \times N$. Each element a_{ij} of this matrix corresponds to the performance value of alternative i with respect to criterion j. This matrix structure enables the systematic evaluation of all alternatives across all specified criteria, whether inputs or outputs.

Step 3 Mathematical Problem Formulation

The optimal DMU aims to maximize the outputs while minimizing the inputs, thus, achieving the highest possible efficiency. Assuming each DMU employs N_i inputs to produce N_o outputs, the efficiency of a specific DMU under evaluation, denoted as DMU_o, can be formulated as the following non-linear programming problem, in line with the input-oriented model proposed by Charnes, Cooper, and Rhodes (commonly referred to as the CCR model) [170].

$$\max z = \frac{\sum_{r=1}^{N_o} u_r y_{r_o}}{\sum_{i=1}^{N_i} v_i x_{io}} \tag{24}$$

Subject to constraints:

$$\frac{\sum_{r=1}^{N_o} u_r y_{rj}}{\sum_{i=1}^{N_i} v_i x_{ij}} \leq 1 \quad (j = 1, \dots, M) \tag{25}$$

$$u_r \geq 0 \quad (r = 1, \dots, N_o) \tag{26}$$

$$v_i \geq 0 \quad (i = 1, \dots, N_i) \tag{27}$$

$u_r$represents the weights assigned to output r, v_i denotes the weights assigned to input i, y_{r_o} is the r_{th} output of the DMU under evaluation, and x_{i_o} is the i_{th} input of the DMU under evaluation.

This fractional programming problem possesses infinite optimal solutions, as any proportional scaling of all weights maintains the same efficiency ratios. To remove this indeterminacy and transform the problem into a linear programming formulation, the following normalization constraint is imposed:

$$\sum_{i=1}^{N_i} v_i x_{io} = 1 \tag{28}$$

This constraint fixes the denominator at unity, transforming the fractional program into the following linear programming one:

$$\max z = \sum_{r=1}^{N_o} u_r y_{ro} \tag{29}$$

Subject to constraints:

$$\sum_{r=1}^{N_o} u_r y_{ro} - \sum_{i=1}^{N_i} v_i x_{ji} \leq 0 \tag{30}$$

$$u_r \geq 0 \quad r = 1, \dots, N_o \tag{31}$$

$$v_j \geq 0 \quad i = 1, \dots, N_i \tag{32}$$

Step 4 Apply Linear Programming Solution

In order to ensure computational efficiency and numerical stability, the dual formulation of the linear programming problem is generally preferred. This approach exhibits several advantages, encompassing a more concise representation when the number of DMUs exceeds the number of input and output criteria. Furthermore, the dual formulation offers a direct interpretation of the solution in terms of efficiency scores and reference sets, thus, facilitating the identification of benchmark DMUs and the assessment of relative performance. These features make the dual model particularly suitable for DEA, where both computational tractability and interpretability are critical [174]. The dual problem is solved separately for each DMU under evaluation, as follows:

$$\theta^* = \min \theta \tag{33}$$

$$\sum_{j=1}^{M} \lambda_j x_{ij} \leq \theta x_{io}, \;\; i = 1, 2, \dots, N_i \tag{34}$$

$$\sum_{j=1}^{M} \lambda_j y_{rj} \geq y_{ro}, \;\; r = 1, 2, \dots, N_o \tag{35}$$

$$\sum_{j=1}^{M} \lambda_j = 1 \tag{36}$$

This formulation seeks the minimum proportional reduction in inputs (θ) required to make the DMU under evaluation efficient, while maintaining at least its current output levels. The parameters are interpreted as follows: θ^*represents the optimal efficiency score, indicating the minimum input contraction ratio, and λ_j denotes the intensity variables that indicate the weight of DMU j n constructing the efficient reference point. The convexity constraint $\sum_{j=1}^{M} \lambda_j = 1$ ensures Variable Returns to Scale (VRS), thereby enabling the model to account for non-constant proportional changes in inputs and outputs.

Step 5 Extract Efficient DMUs
In the linear programming solution, the value of θ represents the efficiency score of each DMU. A DMU is considered efficient if $\theta = 1;$ otherwise, if $\theta < 1$, it is considered inefficient.

Step 6 Provide Efficiency Improvement Guidance
The DEA solution provides actionable insights for improving inefficient DMUs through the optimal λ_j values. For efficient DMUs, the $\lambda_j$values in the solution of the linear programming problem for DMU_o are equal to 1 for $j = 0$ and 0 for all $j \neq 0$, indicating that the DMU lies directly on the efficient frontier. On the contrary, for inefficient DMUs, the $\lambda_j$values represent a linear combination of efficient DMUs that projects DMU_oonto the efficient frontier, thus, making it efficient. Through these intensity variables, the efficient DMUs serving as benchmarks for performance improvement can be determined.

3.3.3 Technique for Order Preference by Similarity to an Ideal Solution component

Once the efficient alternatives have been determined through DEA, the subsequent step in our hybrid MCDM approach involves applying the TOPSIS method. The characterization of criteria as inputs and outputs in DEA is preserved in TOPSIS, namely, inputs are characterized as cost criteria, while outputs are characterized as benefit criteria. This distinction enables the determination of ideal and negative ideal solutions, depending on whether higher or lower values indicate superior performance for a given criterion. Assuming that $M_{efficient}$ DMUs have been identified from the DEA analysis, the following steps outline the application of the TOPSIS method [175]:

Step 1 Decision Matrix formulation
A $M_{efficient} \times N$ decision matrix, X, is constructed, where each element x_{ij} represents the performance of efficient alternative i with respect to criterion j. This matrix consists of the rows of the original $M \times N$ decision matrix that correspond to the efficient DMUs identified via DEA.

Step 2 Normalization of the Efficient Decision Matrix
The next step involves normalizing the $M_{efficient} \times N$ decision matrix, X. Normalization transforms the performance values across different criteria into a comparable scale, aiming at ensuring that all criteria contribute proportionally to the subsequent analysis, regardless of their original units [176]. Each element of the efficient decision matrix is normalized by diving it by the square root of the sum of the squares of the values in the respective column, as follows:

$$r_{ij} = \frac{x_{ij}}{\sqrt{\sum_{i=1}^{M} x_{ij}^2}} \tag{37}$$

r_{ij} represents the normalized value of alternative i with respect to criterion j.

Step 3 Weighted Normalized Decision Matrix

The normalized decision matrix is weighted by multiplying each element by the weight of the corresponding criterion:

$$u_{ij} = w_j \times r_{ij} \tag{38}$$

w_j denotes the weight of criterion j.

Step 4 Identification of Ideal and Negative Ideal Solutions

The next step involves determining the ideal solution (V_j^+) and the negative ideal solution (V_j^-) for each criterion *j* (see Equations 39 and 40, respectively). This step ensures that each criterion is evaluated against its most desirable (ideal) and least desirable (negative-ideal) levels.

$$V_j^+ = \begin{cases} max_{i=1}^{N} u_{ij} & for\ benefit\ criteria \\ min_{i=1}^{N} u_{ij} & for\ cost\ criteria \end{cases} \tag{39}$$

$$V_j^- = \begin{cases} min_{i=1}^{N} u_{ij} & for\ benefit\ criteria \\ max\ _{i=1}^{N} u_{ij} & for\ cost\ criteria \end{cases} \tag{40}$$

Step 5 Calculation of Separation Measures

The separation of each alternative from the ideal (S_i^+) and negative ideal (S_i^-) solutions is determined using the Euclidean distance metric. For the i^{th} alternative, the separation measures is calculated as follows:

$$S_i^+ = \sqrt{\sum_{j=1}^{N} \left(u_{ij} - V_j^+\right)^2} \tag{41}$$

$$S_i^- = \sqrt{\sum_{j=1}^{N} \left(u_{ij} - V_j^-\right)^2} \tag{42}$$

Step 6 Determination of Relative Closeness

The relative closeness of the i^{th} alternative to the ideal solution is estimated employing the separation measures obtained in Step 5. It is expressed as:

$$C_i^* = \frac{S_i^-}{S_i^- + S_i^+} \tag{43}$$

Step 7 Ranking of Alternatives

Efficient alternatives are ranked according to their relative closeness values C_i^*. A higher C_i^* indicates greater proximity to the ideal solution, and thus a more desirable alternative. Consequently, the alternative with the highest C_i^* is considered to be the best option.

3.4 Summary and conclusions

This chapter presents a comprehensive framework that integrates energy modelling, economic analysis, and multi-criteria decision analysis, aiming at establishing a robust methodology for the evaluation of the performance of renewable energy systems. By capturing the technical performance of solar PV and wind power systems under realistic meteorological conditions and grid constraints, the framework provides an accurate representation of system behavior, including load-following dispatch strategies. The incorporation of key economic performance indicators, such as LCOE, NPV, IRR, PBP, and CBR, offers decision-makers a clear and rigorous assessment of economic feasibility. Additionally, the implementation of a hybrid DEA-TOPSIS MCDM approach effectively addresses the complexity of renewable energy planning by enabling systematic evaluation of competing objectives and stakeholder priorities. Overall, this integrated framework delivers a flexible, scalable, and future-ready toolset that supports both project-level analyses and long-term strategic energy planning, while remaining adaptable to evolving technologies and policy landscapes. The next chapters will demonstrate the practical application of this framework through distinct case studies, encompassing both building and community-level energy systems as well as grid-level planning, thereby highlighting its versatility and relevance across multiple scales of renewable energy deployment.

Chapter 4
Building-Level Application

Building on the methodological framework for energy optimization, economic evaluation and multi-criteria decision analysis presented in the previous chapter, this chapter advances the analysis by incorporating LCA to estimate the environmental performance of renewable power generating systems alongside their techno-economic characteristics. This methodology is employed pre-dominantly at the building level through selected case studies, illustrating its relevance and versatility for the design, deployment, and management of renewable energy systems. Specifically, this chapter investigates the techno-economic performance and life cycle environmental impacts of solar PV system production and operation, as well as the design, performance, and optimization of hybrid renewable energy systems integrated with fossil fuel generation. By integrating technological, economic, and environmental dimensions, these case studies provide a comprehensive understanding of renewable energy systems, highlighting opportunities for sustainable, efficient, and circular energy solutions at the building scale.

4.1 Case study: Techno-Economic and Life Cycle Assessment of solar Photovoltaic system production and operation

This case study incorporates material that has been partly published in a peer-reviewed scientific journal [177] along with additional original analysis *(Sagani A, Mihelis J, Dedoussis V. Techno-economic analysis and life cycle environmental impacts of small-scale building-integrated PV systems in Greece. Energy Buildings 2017;139:277–90)*.

4.1.1 Case study overview

4.1.1.1 Location and meteorological parameters

The case study focuses on small-scale, grid-connected residential PV systems installed in Athens, the capital and largest city of Greece. Athens is located at a latitude of 37.9° N and a longitude of 23.7° E, and it is characterized by a Mediterranean climate with hot, dry summers and mild, wet winters. The city benefits from abundant and reliable solar resources throughout the year, even during the winter period. Annual global horizontal solar radiation in Athens is approximately 1,569 kWh/m^2 [178]. The annual daily average global solar radiation on a horizontal surface is estimated at 4.6 kWh/m^2. Seasonal variation is significant, with the lowest values observed between November and February and the highest in summer (from June to August), where daily radiation can reach up to 7.5 kWh/m^2 in June. Table 1 summarizes key meteorological parameters for Athens, including average air temperature, global horizontal radiation, relative humidity, and wind speed. On an annual basis, the average ambient temperature, relative humidity, and wind speed are 18.0 °C, 61.3 %, and 3.4 m/s, respectively. These data directly inform the solar radiation values (H_t) utilized in the energy modelling of the solar PV systems, which are obtained from the RETScreen Clean Energy

Management Software [179] and are presented in Figure 6 to illustrate their seasonal distribution and variation throughout the year.

Table 1 Average meteorological data over Athens [180]

Month	Ambient Temperature (°C)	Relative humidity (%)	Daily solar (horizontal) radiation (kWh/m^2)	Wind speed (m/sec)
January	9.9	69.1	2.1	3.3
February	9.8	66.7	2.9	3.6
March	11.7	66.1	4.0	3.5
April	15.2	64.3	5.4	3.0
May	19.9	59.8	6.4	3.0
June	24.7	54.1	7.5	3.3
July	27.6	48.3	7.4	3.7
August	27.6	48.6	6.7	3.8
September	24.0	55.6	5.2	3.3
October	19.2	63.2	3.4	3.2
November	14.6	69.7	2.2	3.2
December	11.2	70.8	1.7	3.4
Annual	18.0	61.3	4.6	3.4

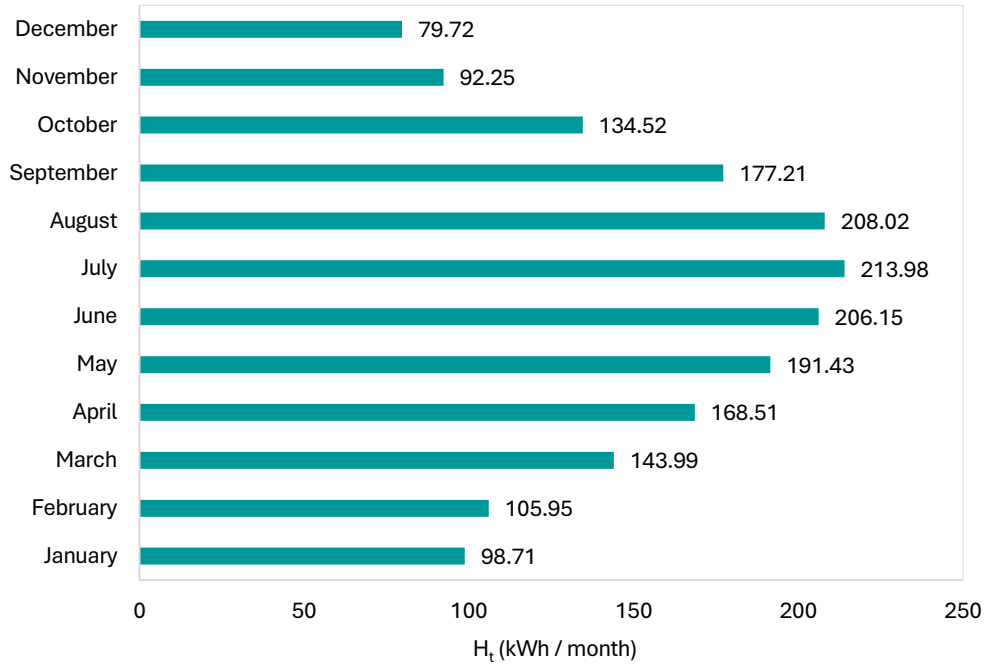

Figure 6 Monthly solar radiation on tilted surface

4.1.1.2 System description

The case study investigates five grid-connected poly-Si PV systems with rated capacities of 2.59 kW$_p$, 4.94 kW$_p$, 7.05 kW$_p$, 8.93 kW$_p$, and 9.87 kW$_p$. All systems are installed on the rooftop of a three-story multifamily residential building, which is representative of common residential buildings in Athens and other European cities. The systems operate in parallel with the Public Power Corporation (PPC) electricity grid, enabling all

electricity generated to be fed directly into the grid and eliminating the need for battery storage. Each installation comprises poly-Si PV modules with nominal peak power ratings between 235.0 W_p to 246.8 W_p, coupled with DC-to-AC inverters that ensure efficient grid integration. Furthermore, control units are incorporated in all systems to regulate and optimize electricity transfer from the PV arrays to the national grid. Component selection was based on performance reliability, cost-effectiveness, and market availability. To maximize annual energy capture, unshaded PV modules are mounted at a fixed tilt angle of 30° and oriented due south. Solar tracking systems (single-axis or dual-axis) are excluded due to their higher capital and maintenance costs and additional operational requirements, which make them less appropriate for small-scale residential applications. The general characteristics of the five PV systems considered in this study are summarized in Table 2, while the detailed specifications of the PV modules are presented in Table 3. The technical specifications of the selected inverters are provided in Table 4. Annual average system losses, including wiring losses, inverter inefficiencies, and dust accumulation, are estimated to be approximately 3% [181].

Table 2 General characteristics of the different PV power systems [182]

PV					
(SHARP) Model/type	poly-Si-ND-235QCJ				
Power capacity	2.59 kW_p	4.94 kW_p	7.05 kW_p	8.93 kW_p	9.87 kW_p
Number of units	11	21	30	38	42
Solar collector area	18 m^2	34 m^2	49 m^2	62 m^2	68 m^2
Miscellaneous losses	3%	3%	3%	3%	3%
Inverter					
(SMA) Model	Sunny Boy 3000TL	Sunny Tripower 5000 TL	Sunny Tripower 7000 TL	Sunny Tripower 9000 TL	Sunny Tripower 10000 TL

Table 3 Technical specifications of the modules considered [182]

Item	Specification
Manufacturer	Sharp
PV model	ND-235QCJ
Solar cell	poly-Si silicon
Cell configuration	60 in series
Maximum power (P_{max})	235.0 (-0/+5%)
Maximum power voltage (V_{pm})	29.3 V
Maximum power current (I_{pm})	8.02 A
Open circuit voltage (V_{oc})	37.2 V
Short circuit current (I_{sc})	8.60 A
Module efficiency	14.4%
Miscellaneous losses	3%
Maximum system (DC) voltage	600.0 V
Temperature coefficient (P_{max})	-0.485%/°C
Temperature coefficient (V_{oc})	-0.36%/°C
Temperature coefficient (I_{sc})	0.053%/°C
Series Fuse Rating	15.0 A
Nominal Operating Cell Temperature (NOCT)	47.5 °C
Length	1,640 mm
Width	994 mm
Thickness	46 mm
Weight	19.0 kg
Number of cells	60 in series
Limited power warranty	25 years

Table 4 Technical specifications of the inverters considered [183,184]

Specifications	Sunny Boy 3000TL	Sunny Tripower 5000TL	Sunny Tripower 7000 TL	Sunny Tripower 9000 TL	Sunny Tripower 10000 TL
Input (DC)					
Max. DC power	3,200 W	5,100 W	7,175 W	9,225 W	10,250 W
Max. DC voltage	3,000 W	1,000 V	1,000 V	1,000 V	1,000 V
DC nominal voltage	400 V	580 V	580 V	580 V	580 V
MPP voltage range	175 – 500 V	245 - 800 V	290 - 800 V	370 - 800 V	370 - 800 V
Min. DC voltage/start voltage	125 V / 150 V	150 V / 188 V	150 V / 188 V	150 V / 188 V	150 V / 188 V
Max. input current input A / input B	15 A / 15 A	11 A / 10 A	15 A / 10 A	15 A / 10 A	18 A / 10 A
Max. input current per string input A / input B	15 A / 15 A	11 A / 10 A	15 A / 10 A	15 A / 10 A	18 A / 10 A
Output (AC)					
Nominal power	3,000 W	5,000 W	7,000 W	9,000 W	10,000 W
Max. AC apparent power	3000 VA	5,000 VA	7,000 VA	9,000 VA	10,000 VA
Nominal AC voltage	220 V	220 / 380 V	220 / 380 V	220 / 380 V	220 / 380 V
	230 V	230 / 400 V	230 / 400 V	230 / 400 V	230 / 400 V
	240 V	240 / 415 V	240 / 415 V	240 / 415 V	240 / 415 V
AC voltage range	180 V – 280 V	160 V - 280 V	160 V - 280 V	160 V - 280 V	160 V - 280 V
AC grid frequency	50 Hz	50/60 Hz	50/60 Hz	50/60 Hz	50/60 Hz
Efficiency					
Max. efficiency/European efficiency	97% / 96%	98% / 97.1%	98% / 97.5%	98% / 97.6%	98% / 97.6%
General Data					
Operating temperature range	-25 °C +60 °C	-25 °C +60 °C	25 °C +60 °C	25 °C +60 °C	25 °C +60 °C
Dimensions (W/H/D) in mm	490/519/185	430 / 730/ 240	430 / 730/ 240	430 / 730/ 240	430 / 730/ 240
Packing weight	26 kg	37 kg	37 kg	37 kg	37 kg

4.1.2 Methodology application

4.1.2.1 Energy modelling and techno-economic analysis

The technical and economic performance of the grid-connected PV systems was assessed employing the RETScreen® Clean Energy Management Software [179]. RETScreen®, which is a widely recognized and freely available software tool. It has been included in this case study due to its established value in the performance evaluation of renewable energy projects, as highlighted in the literature [185]. Its capabilities in estimating energy production, evaluating economic feasibility align directly with the objectives of this research. By incorporating the RETScreen® Software, this case study ensures a thorough and standardized analysis, consistent with methodologies commonly employed in Techno-Economic Analysis (TEA) of solar PV systems.

Specifically, in this case study, RETScreen® was employed to estimate the annual electricity production of the five grid-connected PV systems under investigation, perform TEA, and conduct sensitivity analyses on key technical and economic parameters. The TEA methodological approach, including definitions and calculation methods for indicators such as NPV, IRR, PBP, BCR, and LCOE, was presented in detail in Chapter 2 and is, therefore, not repeated here. The sensitivity analysis provides added value by identifying the key parameters with the greatest impact on PV system performance, assessing the robustness of economic viability under varying conditions, and highlighting potential risks and opportunities. This enables

decision-makers to prioritize critical design and operational factors, evaluate uncertainty, and make more informed and resilient investment and policy decisions [151,152].

The primary objective of this modelling is to estimate the annual electricity exported to the grid and evaluate the efficiency of the PV systems under representative operational and environmental conditions. System efficiency is quantified using the CF, defined as the ratio of the actual energy output over a given period to the theoretical maximum output if the system operated at full capacity continuously [186]. While the study assumes consistent annual energy output over the investment period, actual generation may vary due to hourly, monthly, seasonal, and interannual fluctuations in solar radiation, as well as module degradation. Monthly performance metrics are also calculated for the largest PV system (9.87 kW_p) to account for seasonal variations.

Based on the manufacturer's specifications, the inverter efficiency, η_{inv}, is 97.6% [184] and is assumed to remain nearly constant throughout the year. Economic assumptions for the analysis include a debt ratio of 75% of the initial investment with an interest rate of 7.5 % over a 10-year repayment period, as well as an electricity sale price of 115 €/MWh [141]. The TCI (C_{inv}) for the solar PV systems is determined following the guidelines of Kalfountzou [144], encompassing the combined costs of equipment, installation, and associated expenditures. These values are summarized in Figure 7, which depicts how investment scales with system size.

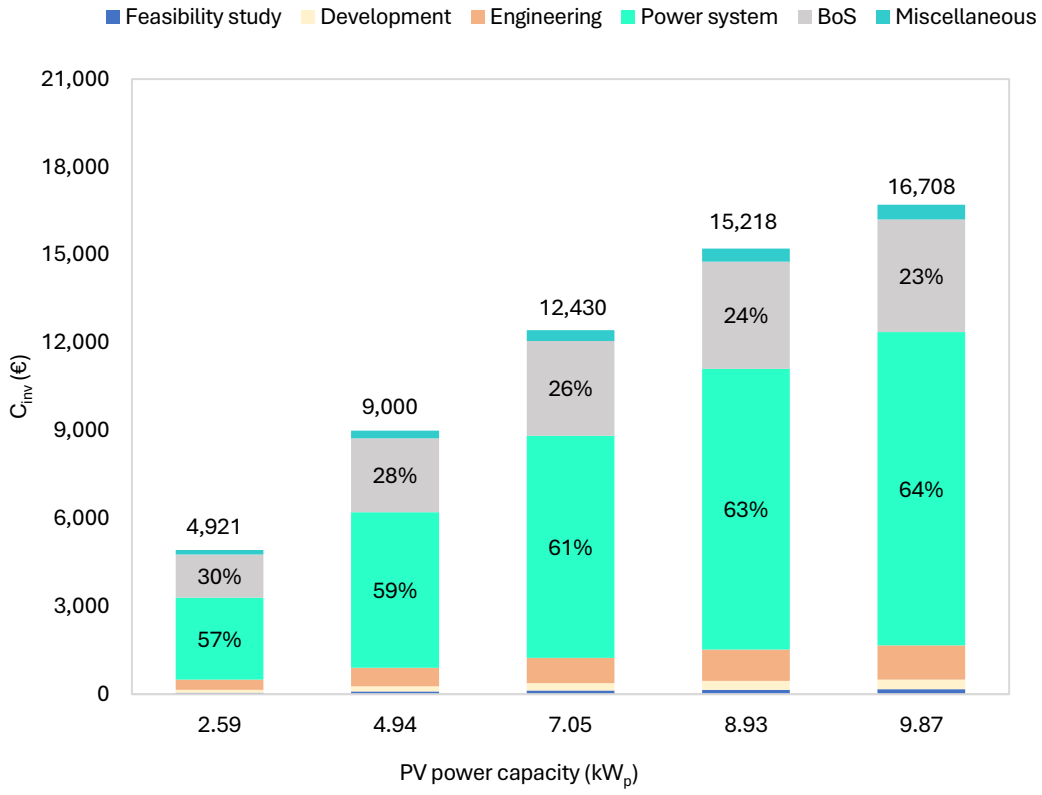

Figure 7 TCI of the PV systems under analysis

It is noted that the cost per installed kilowatt generally decreases with increasing system size, indicating that the 9.87 kW_p system is likely the most cost-effective among those analysed. Annual O&M costs $(C_{O\&M})$ are assumed constant at 0.5% of C_{inv}, without taking into account potential age-related increases. Although the Greek Government has introduced several programs to promote solar energy adoption, potential grants or financial incentives for building-integrated PV systems are not considered in this study. Thus, all economic indicators are reported on a pre-tax basis.

4.1.2.2 Life Cycle Assessment

In addition to the energy and economic analysis, this study presents an assessment of the environmental performance of the five grid-connected PV systems based on life cycle principles. The evaluation is carried out using LCA methodological framework in accordance with ISO 14040 and ISO 14044 Standards [30,31]. The primary objective of the LCA is to inform decision-making by providing scientifically robust insights into critical environmental hotspots across the entire life cycle of solar PV systems, thereby supporting policy formulation for the sustainable transformation of Greece's energy sector. Moreover, the assessment facilitates a comparative evaluation against conventional fossil fuel-based electricity generation systems, underscoring the environmental benefits to be incurred from the deployment of solar PV systems in residential applications. The LCA process involves four interconnected phases: (i) system boundaries identification, (ii) inventory analysis, (iii) impact assessment, and (iv) interpretation of results. These phases are further explored in the following sections.

Phase 1 System Boundaries

The first phase of the LCA involves the definition of the system boundaries, which establishes the scope of the assessment and determines the life cycle stages included in the analysis. In this case study, the system boundaries are defined as cradle-to-gate, encompassing the following life cycle stages: (i) the extraction and production of raw materials, (ii) the processing and purification of materials, (iii) the manufacturing of PV modules and BoS components, and (iv) the installation and operational phase of the PV systems (Figure 8). The production process begins with the extraction of quartz sand, which is subsequently processed and purified to yield silicon suitable for PV applications. During this stage, silica derived from quartz sand is reduced in an arc furnace to produce metallurgical-grade silicon. This intermediate product is then further refined into solar-grade silicon, most commonly through the Siemens process, a step that alone accounts for approximately 30% of the total primary energy demand associated with the production of poly-Si modules [68]. Once purified, the solar-grade silicon is melted and cast into reusable molds, from which silicon wafers are extracted. These wafers undergo further purification and surface treatment, including etching, during the solar cell manufacturing process. Finaly, the solar cells are electrically interconnected in series and parallel configurations to form complete PV modules.

A complete PV system consists of both the PV modules and the BoS components, which include inverters, cabling, and connectors, each considered as discrete sub-assemblies. To enhance structural integrity and facilitate installation, the PV modules are typically mounted within aluminium frames.

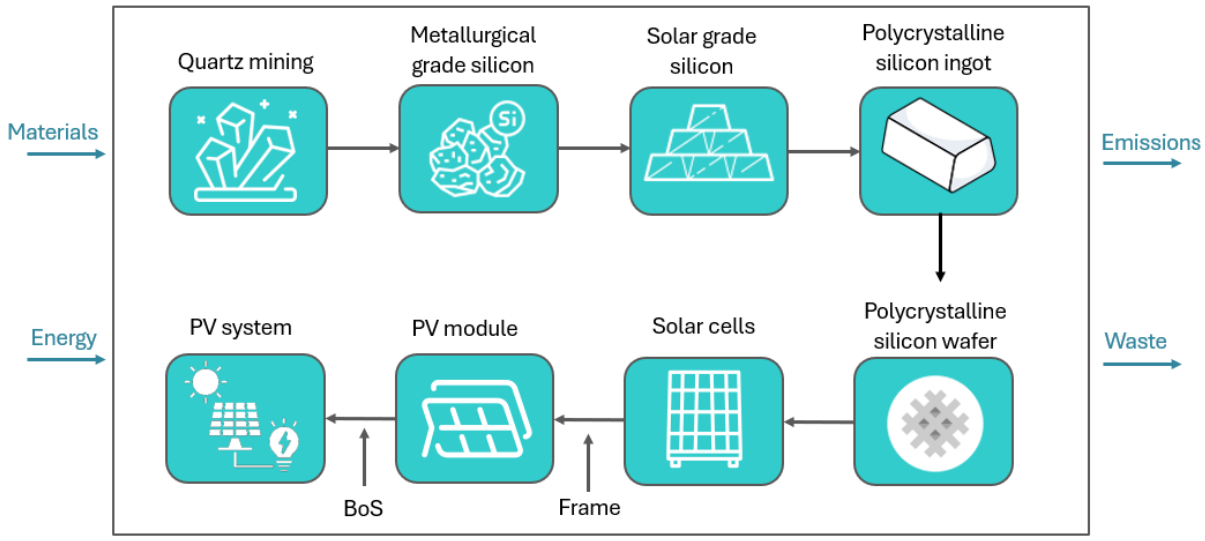

Figure 8 System Boundaries of a poly-Si PV system

Phase 2 Data sources and life cycle inventory

The LCI phase constitutes a fundamental component of the LCA methodology. It involves the systematic collection, quantification, and organization of data concerning raw material and resource inputs, energy and mass flows, emissions to air, water, and soil, as well as solid waste generation across all stages of the PV system life cycle. The integrity and reliability of the LCA model depend heavily on the robustness of the LCI. The use of outdated, incomplete, or inconsistent datasets can compromise the validity of the assessment and lead to potentially misleading interpretations, which in turn may affect decision-making by stakeholders and policy makers.

To ensure transparency, consistency, and data reliability, LCI data were compiled independently for each unit process defined within the system boundaries. This disaggregated approach contributes to greater traceability of inputs and outputs, enabling sensitivity analyses and improving the robustness of the overall life cycle model. Specifically, LCI data for the production of wafers, ingots, solar cells and PV modules were obtained from eleven European- and U.S.-based solar PV manufacturers participating in the European Commission's Crystal-Clear project, which was designed to enhance the environmental performance and competitiveness of PV technologies. The utilization of these industry-sourced datasets not only ensures high representativeness of contemporary production practices but also improves the credibility of the study. These primary datasets have been previously published and validated in the scientific literature, notably by Alsema and de Wild-Scholten [68], and Fthenakis and Kim [29]. For the modelling of metallurgical-grade silicon production, which is a key upstream process in the crystalline silicon PV supply chain, data were retrieved from the Ecoinvent Database [187]. Ecoinvent is one of the most comprehensive and peer-reviewed LCA databases, built on European industrial data with consistent methodological assumptions. It includes over 18,000 datasets spanning energy, materials, agriculture, transport, and waste management across multiple regions. Continuously updated to incorporate new data and technologies, it is widely used in industry and academia, making it essential for credible and reproducible LCA studies. LCI data on the

manufacturing and installation of inverters, mounting structures, and electrical wiring were obtained from the "Life Cycle Inventories and Life Cycle Assessments of Photovoltaic Systems" report [188]. Particularly, inverter data was derived from a survey of three major European manufacturers and represents average technology for the Western European region.

At this point, it is significant to note that the decommissioning phase of the PV systems was excluded from the analysis, mainly due to the lack of available and reliable data. Although this phase may contribute to the overall environmental impact, its omission is not expected to substantially affect the study's results, as prior research demonstrates that EoL impacts for PV systems, encompassing dismantling, disposal, and potential recycling, are generally minor compared to the adverse effects from production processes. Nevertheless, regional variations in recycling practices and material recovery efficiencies could influence these contributions, highlighting an area for future investigation.

Key inventory data for poly-Si PV systems of varying installed capacities, as considered in this study, are summarized in Table 5. Corresponding inventory data for inverters are presented in Table 6, which details the precise energy and material requirements for inverters for systems ranging from 2.5 kW_p to 10 kW_p. Necessary adjustments have been made in the modelling to reflect the specific solar PV system capacities considered in this study.

To ensure that the LCI model accurately accounts for the contemporary European grid electricity supply, a weighted electricity mix was applied across all processes involving electrical energy consumption. Specifically, electricity utilized in the production of wafers, ingots, solar cells, and PV modules, as well as in inverter manufacturing, was modelled based on the average European electricity generation profile for the year 2020 (Figure 9) [189].

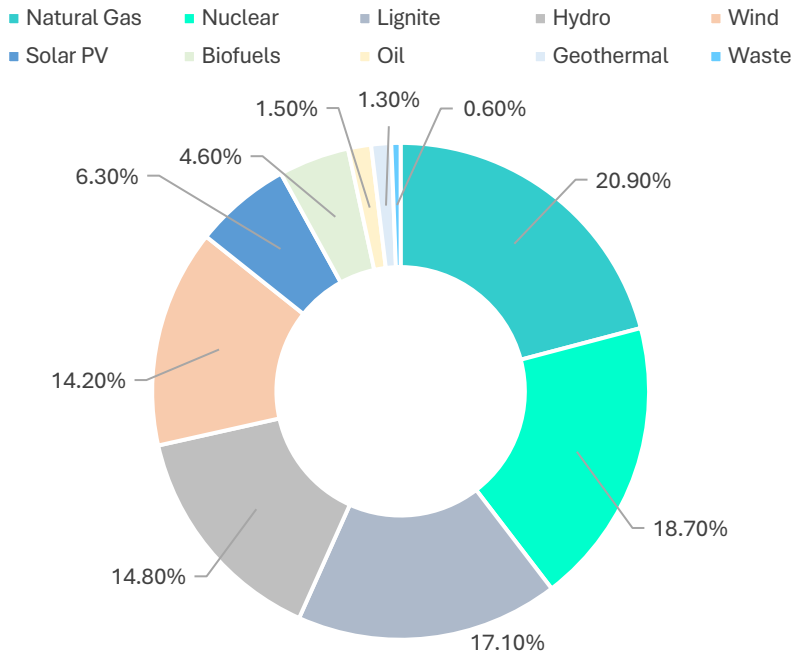

Figure 9 European electricity generation mix (Ref. year 2020) [189]

Table 5 Key parameters of the LCI for manufacturing the poly-Si PV module [29,68,187]

	Unit	Value
Poly-Si, Siemens process	**kg**	**1.00**
Materials		
Metallurgical grade silicon	kg	1.13
Inorganic chemicals	kg	2.00
Heat from natural gas	MJ	185.00
Electricity/heat		
Electricity, from combined cycle plant, gas-fired	kWh	45.00
Electricity, hydropower	kWh	65.00
Poly-Si wafer (156 cm^2)	**m^2**	**1.00**
Materials/Fuels		
Poly-Si	kg	1.30
Quartz crucible	kg	0.39
Glass	kg	0.01
Steel wire	kg	1.49
Silicon carbide (SiC), virgin	kg	0.49
Silicon carbide (SiC), from external recycling	kg	2.14
Nitrogen (N_2)	kg	0.05
Argon (Ar)	kg	0.30
Polyethylene glycol (PEG), virgin	kg	0.11
Polyethylene glycol (PEG), from external recycling	kg	2.60
Dipropylene glycol monomethyl ether (DPM)	kg	0.30
Sodium hydroxide, 50% in H_2O	kg	0.01
Acetic acid, 98% in H_2O	kg	0.04
Water, deionized	kg	65.00
Electricity/heat		
Electricity, medium voltage	kWh	30.00
Natural gas	MJ	4.00
Metallization paste		
Front metallization paste	**kg**	**1.00**
Materials/Fuels		
Silver	kg	0.83
Lead	kg	0.05
Organic chemicals	kg	0.12
Back contact metallization paste	**kg**	**1.00**
Materials/Fuels		
Silver	kg	0.67
Bismuth	kg	0.08
Organic chemicals	kg	0.25
Aluminium back-surface field metallization paste	**kg**	**1.00**
Materials/Fuels		
Aluminium	kg	0.80
Quartz	kg	0.03
Organic chemicals	kg	0.17

Table 5 Continual

	Unit	Value
Poly-Si cells (243 cm^2)	**p**	**1.00**
Resources		
Water, cooling	m^3	$2.43x10^{-2}$
Materials/Fuels		
Poly-Si wafer (156 cm^2)	p	1.06
Front metallization paste	kg	$1.80x10^{-4}$
Back contact metallization paste	kg	$1.20x10^{-4}$
Aluminium back-surface field metallization paste	kg	$1.75x10^{-3}$
Nitrogen (N_2)	kg	$4.51x10^{-2}$
Oxygen (O_2)	kg	$2.48x10^{-3}$
Argon (Ar)	kg	$6.25x10^{-4}$
Ammonia (NH_3)	kg	$1.64x10^{-4}$
Sodium hydroxide, 50% in H_2O (NaOH)	kg	$3.82x10^{-3}$
Acetic acid, 50% in H_2O (CH_3COOH)	kg	$6.88x10^{-5}$
Hydrochloric acid, 30% in H_2O (HCl)	kg	$1.11x10^{-3}$
Hydrogen fluoride (HF) 100%	kg	$9.18x10^{-4}$
Nitric acid, 50% in H_2O (HNO_3)	kg	$6.49x10^{-4}$
$POCl_3$phosphoryl chloride	kg	$5.82x10^{-6}$
Phosphoric acid, industrial grade, 85% in H_20(H3PO4)	kg	$1.85x10^{-4}$
Sodium silicate	kg	$1.82x10^{-3}$
Calcium chloride ($CaCl_2$)	kg	$5.25x10^{-4}$
Isopropanol	kg	$1.92x10^{-3}$
Ethanol	kg	$1.56x10^{-5}$
Solvents, organic, unspecified	kg	$3.49x10^{-5}$
Water, deionized	kg	3.34
Electricity		
Electricity, medium voltage	kWh	$7.36x10^{-1}$
Natural gas	MJ	$1.16x10^{-1}$
Emissions to air		
Aluminium	kg	$1.88x10^{-5}$
Hydrogen chloride	kg	$6.48x10^{-6}$
Hydrogen fluoride	kg	$1.18x10^{-7}$
Lead	kg	$1.88x10^{-5}$
Particulates, unspecified	kg	$6.48x10^{-5}$
Silicon dioxide	kg	$1.77x10^{-6}$
Silver	kg	$1.88x10^{-5}$
Sodium hydroxide	kg	$1.18x10^{-6}$
Tin	kg	$1.88x10^{-5}$
VOC, volatile organic compounds	kg	$4.71x10^{-3}$
Poly-Si PV module	**p**	**1.00**
Materials		
Poly-Si cells (243 cm^2)	p	61.20
Aluminium	kg	4.20
Polyphenylenoxid	kg	0.30
Glass sheet, low iron, tempered	kg	16.10
Ethyl Vinyl acetate	kg	1.60
Copper	kg	0.18
Lead	kg	$0.05x10^{-1}$
Nickel	kg	$0.26x10^{-3}$
Soldering flux	kg	$0.13x10^{-1}$
Cardboard	kg	1.75
Tap water	kg	34.00
Electricity		
Electricity, medium voltage	kWh	10.70

Table 6 Key parameters of the LCI for manufacturing the inverter [188]

Component / Material	Unit	Capacity		
		2.5 kW	5 kW	10 kw
Main Materials				
Aluminium (cast alloy)	kg	4.770	7.640	12.200
Aluminium alloy	kg	0.212	0.339	0.543
Copper	kg	1.910	3.060	4.900
Steel, low-alloyed	kg	0.907	1.450	2.330
Polypropylene granulate	kg	0.882	1.410	2.770
Polycarbonate	kg	0.202	0.324	0.519
Glass fiber reinforced plastic	kg	0.131	0.209	0.335
Electronic components				
Cable, connector for computer	m	0.131	0.210	0.337
Inductor, ring core choke type	kg	0.871	1.400	2.240
Integrated circuit, IC, logic type	kg	0.067	0.106	0.170
Ferrite	kg	0.035	0.056	0.090
Plugs (inlet and outlet)	unit	3.48	5.58	8.93
Printed Board Assembly				
Printed wiring board	m^2	0.101	0.162	0.260
Tin	kg	0.009	0.015	0.025
Inductor, ring core choke type	kg	0.024	0.039	0.063
Inductor, miniature RF chip type	kg	0.131	0.209	0.335
IC, logic type	kg	0.001	0.001	0.003
IC, memory type	kg	0.155	0.249	0.399
Transistor, unspecified	kg	0.002	0.003	0.005
Transistor, SMD type	kg	0.019	0.031	0.107
Diode, glass, SMD type	kg	0.042	0.003	0.005
Capacitors				
Capacitor, film, through-hole	kg	0.166	0.267	0.427
Capacitor, electrolyte > 2 cm height	kg	0.257	0.412	0.660
Capacitor, electrolyte < 2 cm height	kg	0.007	0.011	0.017
Capacitor, SMD type	kg	0.001	0.002	0.003
Resistors				
Resistor, wirewound, through-hole	kg	0.001	0.002	0.003
Resistor, SMD type	kg	0.005	0.007	0.012
Other components				
Transformer, low voltage	kg	0.040	0.064	0.103
Energy consumption				
Electricity, medium voltage	kWh	10.6	16.9	27.1
Natural gas, burned in power plant	MJ	3.57	5.72	9.17
Heat, natural gas	MJ	9.21	14.7	23.6
Light fuel oil	MJ	0.226	0.361	0.579

Phase 3 Life Cycle Impact Assessment

Following the data collection phase for each system component (LCI), the LCA was carried out to quantify the environmental impacts of the PV systems. For the sake of numerical modelling, all stages of the solar PV system assembly were systematically represented with relevant material and energy flows referenced to system capacities of 2.59 kW_p, 4.94 kW_p, 7.05 kW_p, 8.93 kW_p, and 9.87 kW_p, corresponding to active surface areas of 18 m^2, 34 m^2, 49 m^2, 62 m^2, and 68 m^2, respectively. It was assumed that the operation of the solar PV systems contributes negligible environmental impacts, thereby allowing the assessment to focus on the impacts associated with the manufacturing and assembly stages. This structured approach ensures that all critical stages of the PV life cycle are captured and provide a consistent basis for evaluating environmental performance across systems of different sizes and configurations.

The modelling and analysis of the PV systems were carried out employing SimaPro PhD 9.5 [190], a state-of-the-art software platform widely recognized for its thorough capabilities in environmental simulation and LCIA [191]. All relevant processes - from material production and module assembly - were systematically incorporated into the software environment. Environmental performance was evaluated using the Impact World+ methodology [39], with particular emphasis on climate change impacts and fossil and nuclear energy use, since these indicators represent the most critical environmental burdens of poly-Si PV systems, consistent with the literature reviewed in Chapter 2. While other impact categories, including water scarcity, land occupation and transformation, and toxicity, might contribute to the overall footprint, their significance is minor relative to the energy- and carbon-intensive manufacturing stage.

Building on these selected indicators, the EPBT was assessed to provide time-based measures of sustainability. The EPBT compares the fossil and nuclear energy utilized in the system with the annual electricity generation, indicating the period required for the PV system to offset the energy consumed during the production process. In addition, a comparison with conventional energy systems was carried out across different scenarios to evaluate how PV systems perform relative to traditional fossil fuel-based generation in terms of GHG emissions. To evaluate these benefits under real-world conditions, three electricity supply scenarios were considered, linking LCI data to operational performance. The first scenario represents the current Greek electricity mix (see Figure 10). The second scenario assumes electricity generation via diesel electric generators with 68% overall efficiency, which is typical for Greece. The third scenario considers a natural gas-fired turbine, including both system realization and fuel consumption. For all scenarios, fuel-related data were primarily sourced from the Ecoinvent Database and supplemented with literature values where necessary, ensuring consistency, traceability, and reliability across the LCI datasets. This approach enables an integrated, scenario-specific assessment of sustainability, integrating the underlying inventory data, electricity supply scenarios, and the resulting environmental performance indicators.

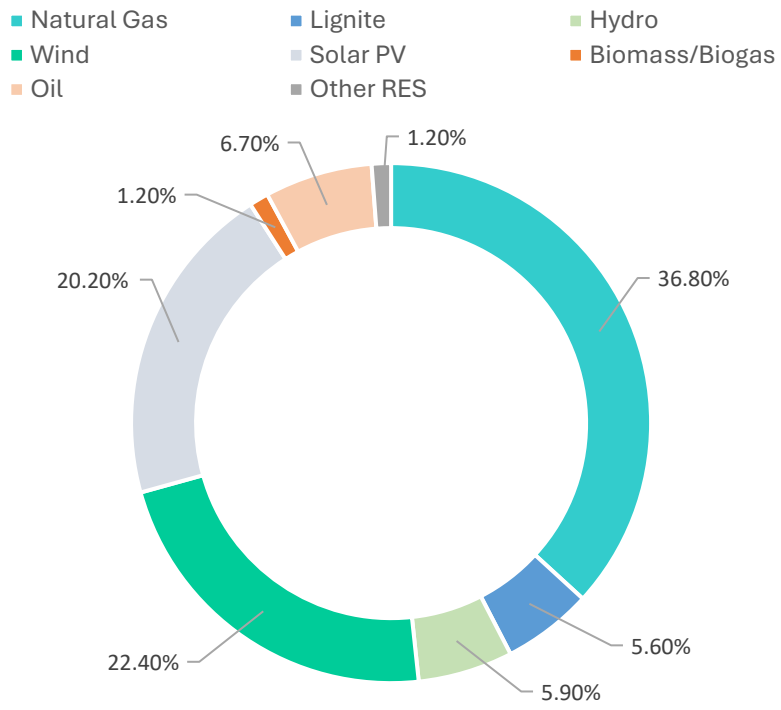

Figure 10 Greek electricity generation mix (Ref. year 2024) [192]

4.1.2.3 Technique for Order Preference by Similarity to an Ideal Solution

Leveraging the results of the TEA and LCA, TOPSIS was employed to rank five grid-connected poly-Si PV systems and determine the optimal PV capacity across multiple weighting schemes representative of diverse stakeholder preferences. The evaluation was based on five selected sub-criteria, namely, (i) GHG emissions, (ii) fossil energy use, (iii) TCI, (iv) IRR, and (v) annual electricity exported to the grid. To ensure comparability among the PV systems, the performance values were normalized and weighted according to their respective sub-criteria weights (see Table 7). Within the environmental dimension, greater emphasis was assigned to GHG emissions (80%), as this indicator directly reflects the contribution of solar PV systems to climate change mitigation and aligns with national and EU decarbonization targets. Fossil energy use was incorporated as a complementary indicator (20%) to quantify the cumulative energy demand associated with the upstream life cycle stages, and to characterize the extent of dependency on fossil energy resources within the PV system value chain. In the economic dimension, higher weight was assigned to the TCI (60%) than the IRR (40%), highlighting the emphasis on upfront financial commitment in the evaluation framework. The technological dimension was defined solely by the capacity of the PV systems to supply electricity to the grid. The resulting weighted values were subsequently aggregated and normalized to derive the overall environmental, economic, and technological performance scores.

Table 7 Criteria and weights for performance assessment

Criteria	Sub-Criteria	Weight	Type
Environmental	GHG emissions	80%	Cost
	Fossil energy use	20%	Cost
Economic	TCI	60%	Cost
	IRR	40%	Benefit
Technological	Electricity exported to the grid	100%	Benefit

The relative importance of each criterion is generally determined by experts. Nevertheless, considering the inherently subjective nature of stakeholder priorities, scenario differentiation is introduced via alternative weighting schemes that capture distinct strategic emphases, encompassing environmental, economic, and technological priorities, as well as a balanced multi-criteria perspective (Table 8). This structured approach not only enables a transparent and systematic evaluation of trade-offs among competing objectives but also preserves methodological consistency across scenarios. By explicitly delineating the weighting schemes, the proposed framework improves comparability, facilitates robustness, and supports informed decision-making under divergent stakeholder preferences. Importantly, this methodology provides a replicable mechanism for integrating subjective judgments within a MCDM process, thereby bridging the gap between expert insight and structured quantitative assessment. It is noted that all weights satisfy the normalization constraints, summing to unity in accordance, ensuring consistency in the MCDM evaluation.

Table 8 Decision scenarios and associated criterion weights

Criteria Category	Environmental Priority	Economic Priority	Technological Priority	Balanced Scenario
Environmental	0.60	0.20	0.20	0.33
Economic	0.20	0.60	0.20	0.33
Technological	0.20	0.20	0.60	0.33
Total	1.00	1.00	1.00	1.00

4.1.3 Simulation results and discussion

4.1.3.1 Economic assessment and sensitivity analysis

The key economic performance indicators are summarized in Table 9. A comparative analysis of the NPV and IRR for the five PV systems with different installed capacities is depicted in Figure 11. Both NPV and IRR figures increase with the system's power capacity, while the LCOE decreases. Among the investigated systems, the 9.87 kW_p PV installation was found to be the most economically attractive, with an NPV of 1,723 €, an IRR of 10.1%, a BCR of 1.41, and an LCOE of 104.67 €/MWh. On the contrary, the 2.59 kW_p PV

system was found to be cost-ineffective, discouraging investment in such small-scale installations. Its high LCOE, estimated at about 122.75 €/MWh, suggests that there is no incentive for grid-interconnected consumers to invest in PV systems with a capacity below 5 kW_p to meet their own electricity demand. An exception might apply to remote regions such as the Greek islands, where electricity supply relies almost exclusively on cost-inefficient heavy and light oil fuel. For PV systems under 5 kW_p, the combination of high specific investment cost (approximately 1,900 €/kW) and the relatively low electricity selling price (115 € / MWh) constitutes the main handicap to their adoption in the residential sector. Therefore, the widespread deployment of grid-connected, building-integrated PV systems would likely require both an increase in the electricity selling price and a reduction in the initial investment cost.

Table 9 Comparison of performance of the different PV power systems

		Power Capacity (kW_p)				
		2.59	4.94	7.05	8.93	9.87
Project costs	Initial investment cost (€)	4,921	9,000	12,430	15,218	16,708
	Operation and Maintenance cost (€)	25	45	62	76	84
Economic Indicators	NPV (€)	-325	137	698	1,452	1,723
	IRR (%)	6.7	8.3	9.1	9.9	10.1
	PBP (years)	15.6	14.3	13.8	13.3	13.2
	Annual life cycle savings (€/year)	-30	13	65	136	161
	BCR (years)	0.74	1.06	1.22	1.38	1.14
	LCOE (€/MWh)	122.75	113.85	109.13	105.38	104.67

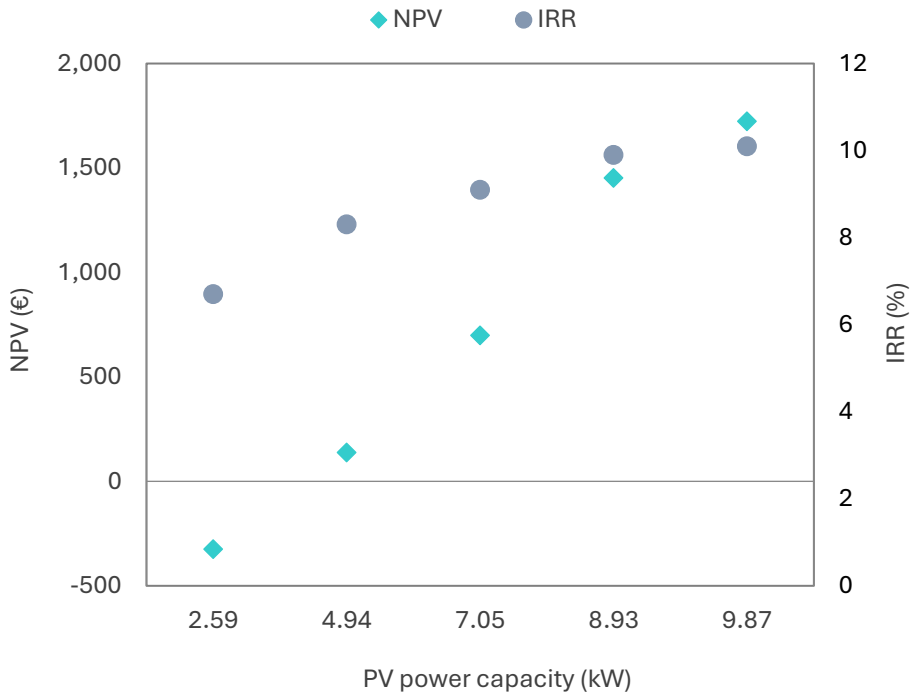

Figure 11 Comparison of the different PV systems in terms of NPV and IRR

The findings of this study demonstrate that the economic viability of small-scale residential PV systems in Greece is highly sensitive to both the electricity selling price and the TCI. To quantify these effects, a sensitivity analysis was conducted to examine how variations in TCI and electricity selling price influence the economic performance of grid-connected solar PV systems. For the analysis, variations of $\pm 15\%$ and $\pm 30\%$ were applied to both parameters. These ranges were selected to represent reasonable fluctuations in market conditions, while capturing both moderate and more pronounced shifts. The $\pm 15\%$ scenarios account for typical short-term market dynamics, for example, minor equipment price changes or adjustments in electricity tariffs, whereas $\pm 30\%$ scenarios correspond to substantial deviations, such as significant technology cost reductions or major policy-driven changes in market remuneration. This approach ensures a robust assessment of system performance under a realistic spectrum of future conditions.

Calculated results indicate that PV system profitability improves notably when the TCI decreases or the selling price of electricity increases. Conversely, even a moderate 15% reduction in the reference selling price of 115 €/MWh, the value used in this study to represent prevailing market conditions at the time of analysis, renders all PV projects economically unattractive. Importantly, this lower-bound case closely reflects current market-based compensation in Greece under the net-billing scheme, where payments for surplus residential PV electricity are approximately 70-75 €/MWh [145]. To illustrate these effects, Figure 12 and Figure 13 present indicative results for the least profitable 2.59 kW_p system and the most cost-effective 9.87 kW_p system, respectively, under the reference case and the four sensitivity scenarios. As shown in Figure 12, a 15% increase in the reference electricity selling price raises the IRR of the 2.59 kW_p system from 6.7% to 9.9%, exceeding the assumed discount rate of 8% and rendering the project profitable. Likewise, a potential 15% decrease in the TCI (estimated at 4,921 €) significantly enhances its economic performance. Figure 13 further demonstrates that for the 9.87 kW_p system, a 15% increase in the base initial investment cost (16,708 €) would reduce the IRR from 10.1% to 7.2%, making the project no longer profitable. Conversely, a 15 % increase in the selling price and/or a 15 % reduction in the TCI would substantially enhance its profitability. These findings highlight the pronounced sensitivity of small-scale PV systems to cost and price fluctuations and emphasize the need for cost-reduction measures and stable remuneration schemes to maintain the economic attractiveness of residential PV investments in Greece.

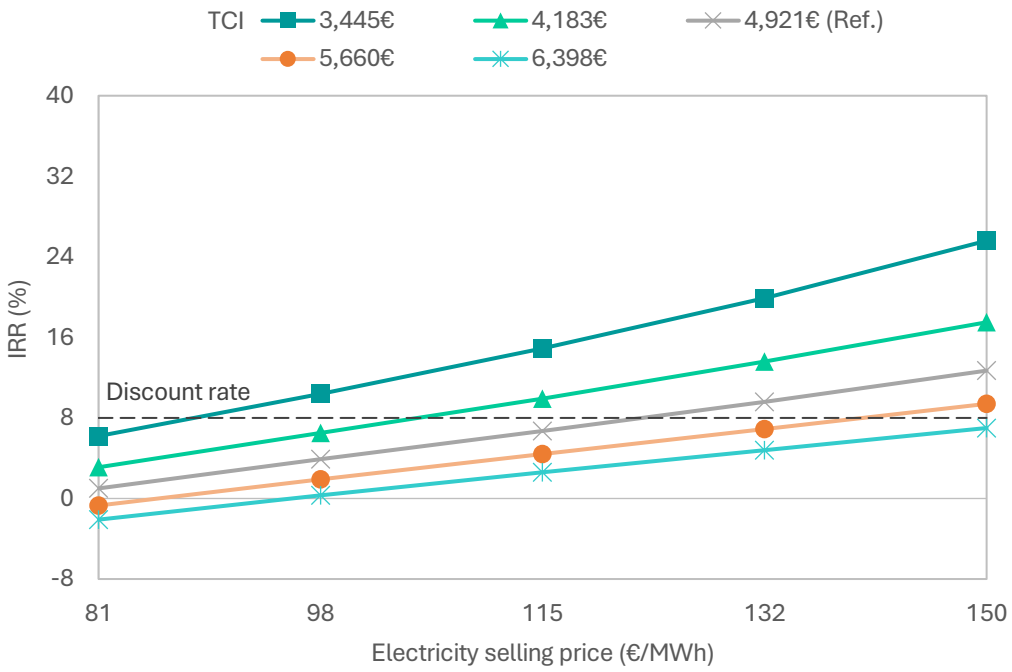

Figure 12 Effect of electricity price on IRR (2.59 kW_p PV system)

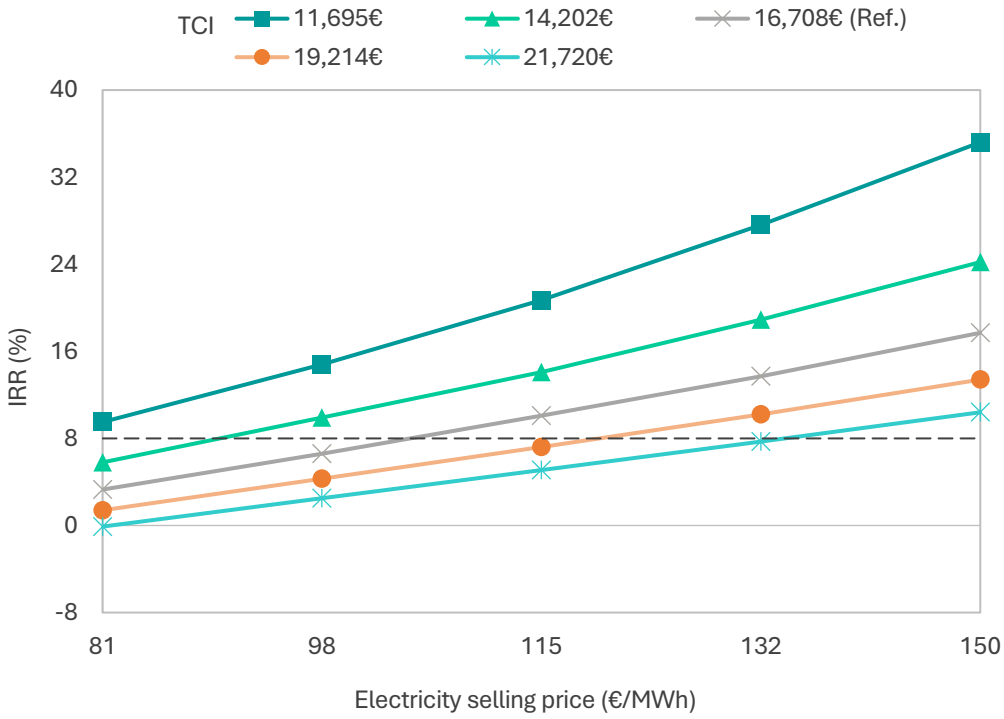

Figure 13 Effect of electricity price on IRR (9.87 kW_p PV system)

4.1.3.2 Electricity output

The annual electricity exported to the grid and the corresponding CF of the PV systems analysed in this case study are illustrated in Figure 14. The annual energy exported to the grid increases with the system's installed capacity, ranging from 3,924 kWh for a 2.59 kW_p system to 15,622 kWh for a 9.87 kW_p system. The associated CF values vary between 17.3% and 18.1% for the 2.59 kW_p and 9.87 kW_p systems, respectively. It is noteworthy that the CF values obtained in this study, approximately 17-18%, lie near the midpoint of the 10-25% range reported in the relevant literature [193]. Considering that the annual electricity demand of a typical four-member household is approximately 3,750 kWh, while the building's total annual energy demand is estimated at 33,750 kWh [125], the analysed PV systems are capable of supplying roughly 12% to 46% of the building's annual energy needs.

In addition to the annual performance indices, monthly performance metrics were evaluated for the most cost-effective and largest system with a capacity of 9.87 kW_p, following the integrated methodology for PV energy modelling presented in Chapter 3 (Figure 15). The results indicate that the monthly energy delivered by the PV array is strongly influenced by solar radiation on the tilted surface. Higher array energy output is observed during months with high solar irradiance, while lower output occurs during months with reduced irradiance. The energy available to the load is consistently lower than the energy delivered by the PV array due to system losses. Monthly energy exported to the grid ranges from 811 kWh in December to 2,347 kWh in July. The total annual energy generated by the system is 15,622 kWh, with an average monthly output of 1,302 kWh. The annual energy yield is 1,583 kWh/kW_p, which can serve as a reference for comparing the performance of PV systems operating under similar climatic conditions and geographic coordinates.

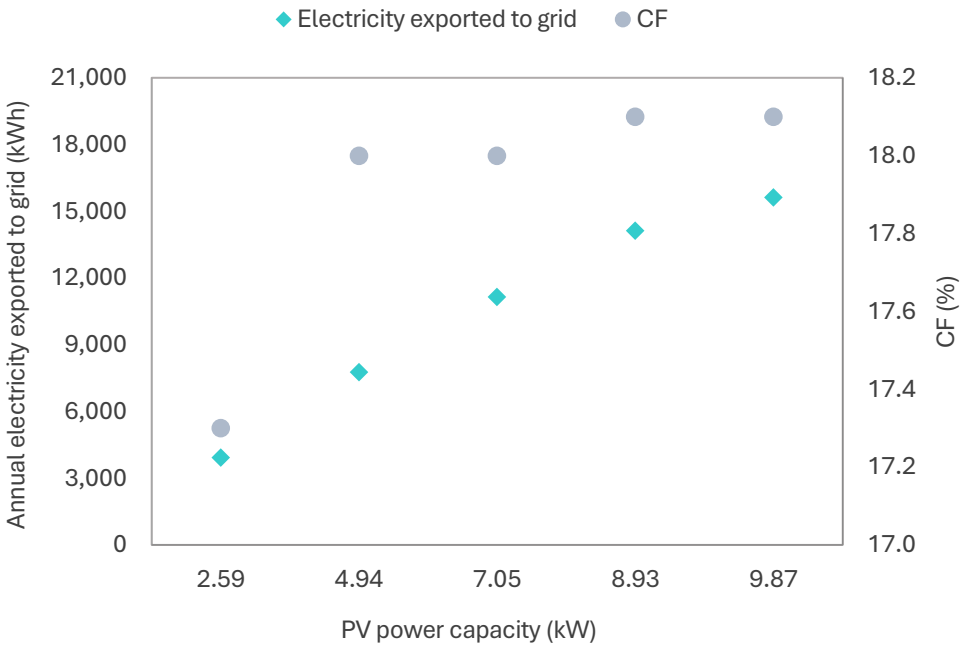

Figure 14 Annual electricity exported to the grid and relevant CF of the different PV systems

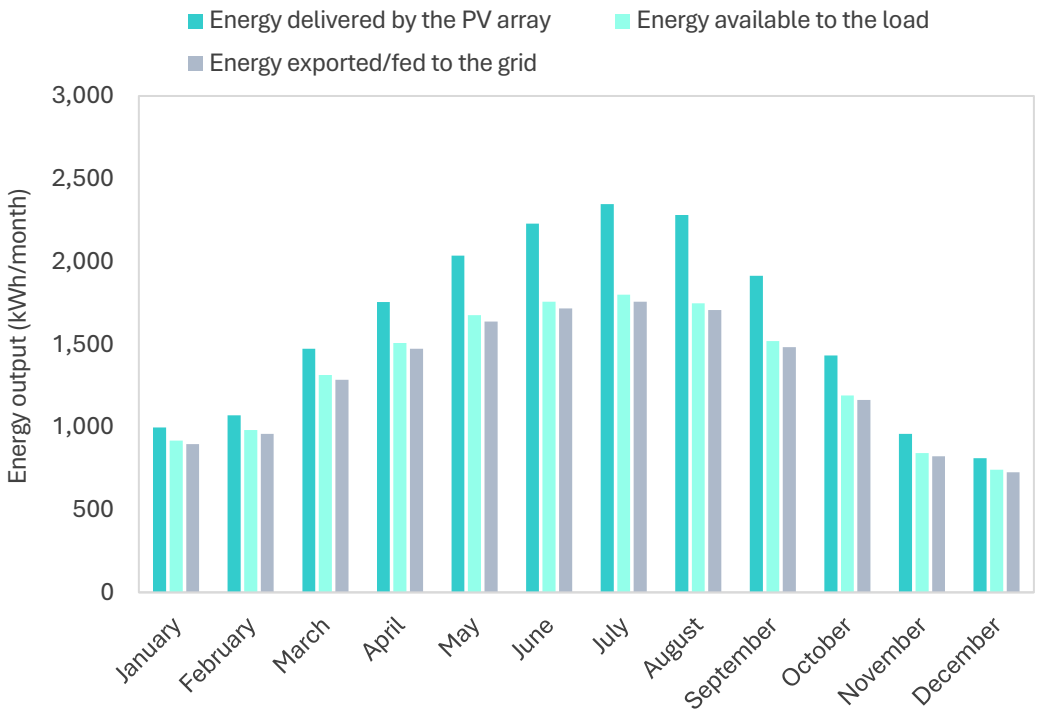

Figure 15 Monthly energy output of the 9.87 kW_p PV system

The monthly PV array and system efficiencies are illustrated in Figure 16. The array efficiency is strongly affected by ambient temperature, with higher efficiency observed during warmer months and lower efficiency during cooler months. The highest array efficiency, approximately 16.3%, is recorded in July, coinciding with relatively high ambient temperatures and solar irradiance. Despite the higher array efficiency observed in summer, the overall system efficiency decreases during this period. This reduction is attributed to increased system losses. PV system efficiency reflects total electrical losses, including those occurring in the DC side (PV array capture losses) and AC side (inverter losses, miscellaneous array losses, and other power conditioning losses) [194].

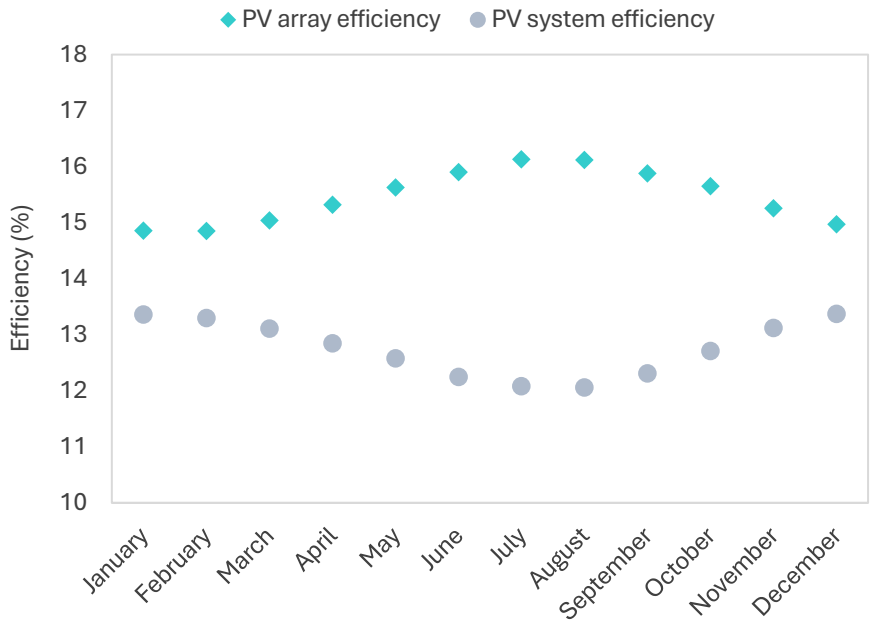

Figure 16 Monthly array and system efficiency of the 9.87 kW_p PV system

It should be noted that, in hot Mediterranean summers, there are periods of high electricity demand, primarily due to the operation of air conditioning systems. Under such conditions, PV cell/module operating temperatures may exceed ambient temperatures, leading to a larger reduction in system efficiency than that calculated using monthly averages. To improve the reliability of the results, the effects of hourly variations in ambient temperature on cell/module operating temperature, array efficiency, and overall system efficiency were investigated. In this analysis, the three hottest days of the summer months in 2016, June 19, July 24, and August 2, were considered. Hourly solar radiation on the tilted surface was estimated from horizontal surface radiation, accounting for the module tilt angle (30°) and local latitude (37.9°), as well as the solar declination angle [195,196]. Hourly PV cell/module temperatures were calculated using the NOCT, hourly ambient temperature data from the Hellenic National Meteorological Service [197], and the relevant hourly clearness index, which strongly depends on the ratio of horizontal solar radiation to extra-terrestrial horizontal radiation [198]. Hourly PV array efficiency was then assessed based on the calculated module temperatures, nominal module efficiency and temperature coefficient. Finally, hourly overall system efficiency was evaluated assuming a constant 3% miscellaneous array loss. The results, presented in Figure 17 show that during summer, PV cell/module operating temperature, array efficiency, and overall system efficiency are strongly influenced by hourly variations in ambient temperature. Higher cell/module temperatures and higher array efficiency are observed during peak-irradiance hours, typically between 12:00 and 15:00. The overall PV system efficiency on the three hottest days ranges from 11.4% (August 2) to 12.6% (July 24), with an average of 12%. This value is very close to the average summer system efficiency of 12.1% calculated using the RETScreen monthly approach (refer to Figure 16), suggesting that RETScreen provides reliable results within typical engineering accuracy.

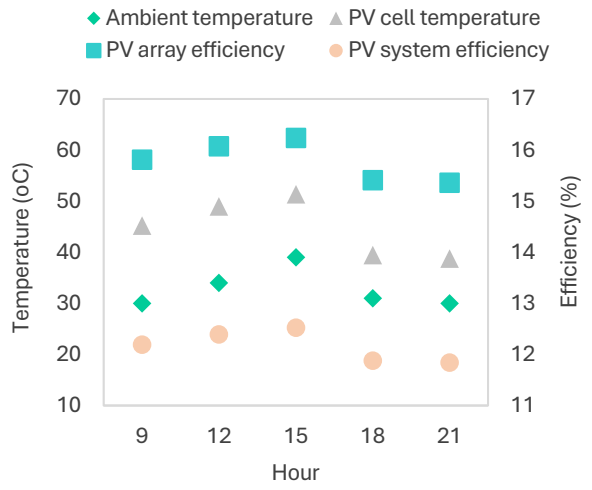

(a) June 19

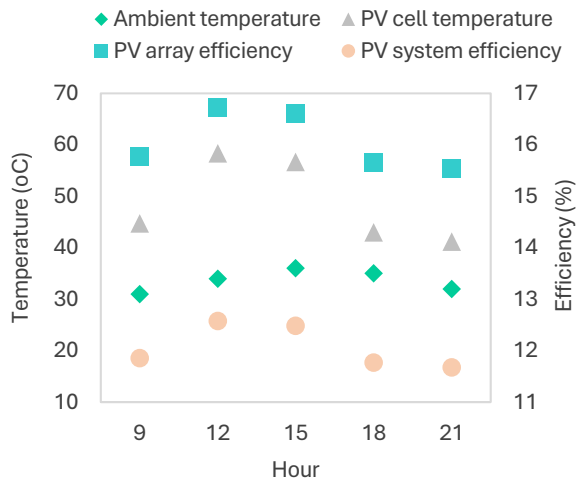

(b) July 24

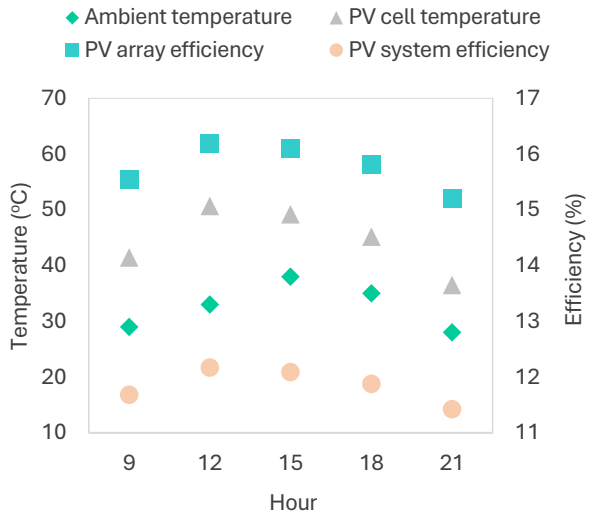

(c) August 2

Figure 17 Hourly ambient and cell operating temperatures, as well as array and system efficiency of the 9.87 kW_p PV system

4.1.3.3 Life cycle impact assessment

The environmental impacts associated with the entire life cycle of the PV systems investigated, specifically regarding GHG emissions and fossil and nuclear energy use, are summarized in Table 10. For small-scale poly-Si, grid-connected PV systems ranging from 2.59 to 9.87 kW_p, both GHG emissions and fossil and nuclear energy use decrease as the CF increases. This improvement can be attributed to the more efficient allocation of embodied impacts across a greater volume of electricity generated over the system's lifetime. Because most environmental impact are associated with the fabrication stage rather than the operation phase, higher-capacity systems effectively distribute these fixed, manufacturing-related burdens over a

larger energy output, resulting in lower impact intensity per kilowatt-hour. Quantitatively, the total GHG emissions decrease from 37.96 gCO_{2eq}/kWh for the 2.59 kW_p PV system to 30.02 gCO_{2eq}/kwh for the 9.87 kW_p PV system, thus representing a notable 21% reduction across the capacity range. A similar trend is observed for fossil energy use figure, which declines from 0.652 MJ/kWh to 0.531 MJ kWh, corresponding to a considerable 19% decrease. Across all system sizes, the PV module assembly contributes the majority of life cycle impacts, whereas the inverter contribution is comparatively lower but exhibits a more pronounced decline with increasing system capacity, further improving the environmental performance of larger systems.

These trends are directly supported by the EPBT analysis of the systems. Calculated EPBT figures range from 3.25 years for smaller systems (2.59 kW_p) to 2.72 years for larger systems (9.87 kW_p). While larger systems require higher total energy investment, their proportionally greater annual electricity generation allows them to recover the energy invested more quickly. This faster energy payback aligns with the decreasing environmental impacts per kilowatt-hour, underscoring g that higher-capacity systems not only achieve energy neutrality sooner but also reduce life cycle GHG emissions and fossil energy use via more efficient utilization of the embodied energy. Together, the EPBT and life cycle impact results highlight the dual benefit of scaling PV system capacity: improved energy efficiency and lower environmental impact intensity.

Table 10 Environmental impacts for the whole life cycle of the different PV power systems

Capacity	GHG emissions (g CO_{2eq} / kWh)			Fossil Energy (MJ / kWh)			EPBT
(kW)	PV assembly	Inverter	Total	PV assembly	Inverter	Total	(years)
2.59	27.343	10.617	37.960	0.497	0.154	0.652	3.25
4.94	26.080	8.500	34.580	0.474	0.124	0.598	3.10
7.05	26.202	7.397	33.600	0.476	0.108	0.584	2.75
8.93	26.148	5.525	31.672	0.475	0.080	0.556	2.74
9.87	25.946	4.077	30.024	0.472	0.059	0.531	2.72

Regarding the manufacturing phase of the PV module assembly, the poly-Si silicon production through the Siemens process constitutes the largest contributor to GHG emissions, representing 31.89% of the total climate change impact, and 37.15% of the fossil and nuclear energy use, as depicted in Figure 18 and Figure 19, respectively. This dominance is directly related to the energy - intensive production of high-purity silicon, as this stage involves chemical purification and crystallization of metallurgical-grade silicon. These processes require significant thermal energy, which is supplied by natural gas and light fuel oil. The poly-Si silicon wafer production stage presents the second-largest environmental hotspot, contributing 24.65% of the system's climate change impacts (see Figure 18). Its contribution to fossil and nuclear energy use is similarly significant, accounting for about 26.5% (refer to Figure 19). This stage covers the casting of silicon ingots, wafer slicing, and surface preparation for solar cell fabrication, with impacts largely driven by energy-intensive mechanical processing, the utilization of cutting fluids, and the silicon kerf loss management during wafering operations. The subsequent cell manufacturing accounts for 14.14% of the GWP and 12.83% of fossil and nuclear energy use. potential. This phase entails intricate metallization processes, encompassing the application of front and back contact metallization pastes, as well as the utilization of

silver, organic chemicals and glass materials. Aluminium back-surface field metallization further contributes to the adverse environmental impacts, requiring significant amount of aluminium and copper. Additional impacts stem from organic chemicals and solvents employed in surface preparation and the deposition of anti-reflective coatings. Finaly, the PV module assembly contributes 29.32% of climate change impacts and 23.56% of fossil and nuclear energy use, reflecting the complexity of integrating multiple material systems into weather-resistant packages designed for 25-year operational lifetimes This poor environmental performance can be attributed to utilizing aluminium for framing, ethylene vinyl acetate encapsulants, polyvinyl fluoride back sheet materials, and tempered glass substrates, as well as diverse chemical inputs, including ammonia, various acids, hydrogen fluoride, and organic solvent, along with fossil fuel-based electricity required for lamination, testing, and quality assurance procedures.

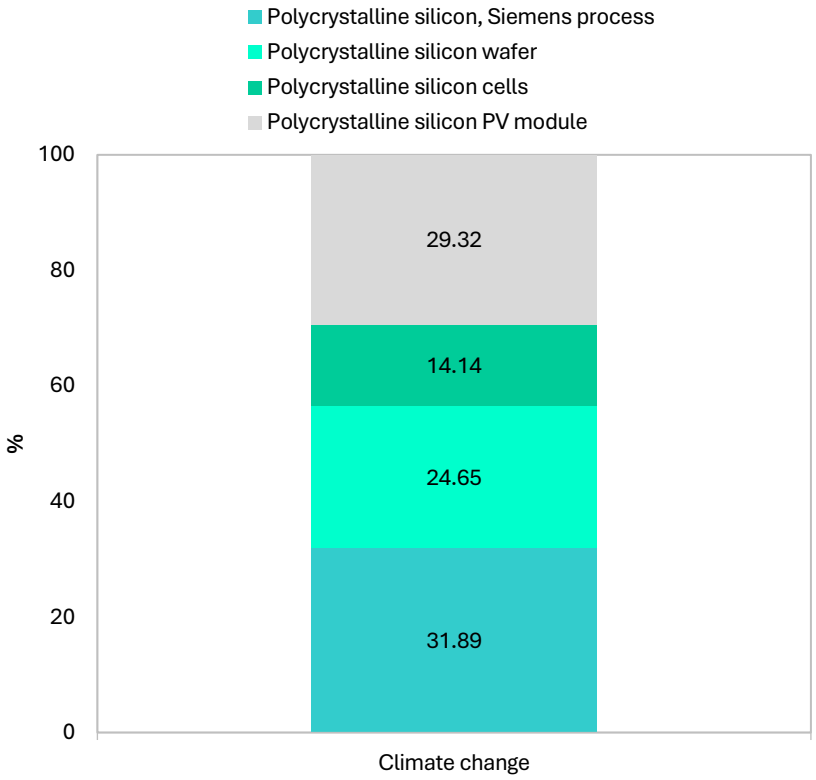

Figure 18 Percentage share of PV module assembly in overall climate change impact

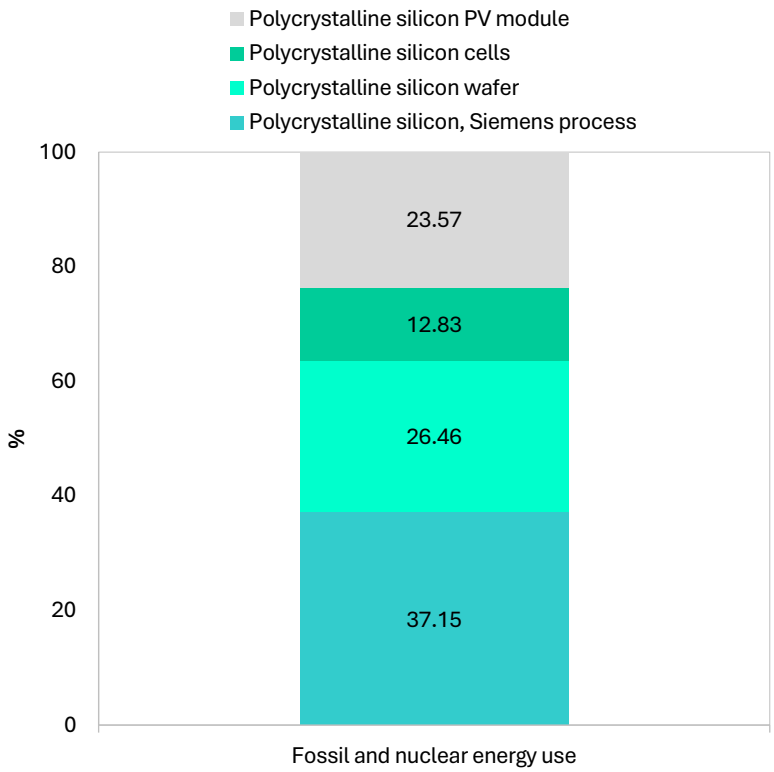

Figure 19 Percentage share of PV module assembly in overall fossil energy use

Overall, the distribution of GHG emissions indicates that silicon processing stages (Siemens process and wafer production) collectively account for 56.54% of total climate change impact, whereas downstream manufacturing operations (cell production and module assembly) contribute 43.46%. A similar pattern is observed for fossil and nuclear energy use, with silicon processing representing 63.61% and downstream manufacturing 43.46% of the total fossil and nuclear energy consumption. Material intensity analysis underscores substantial requirements for high-purity chemicals. Furthermore, across all stages, high energy consumption reflects both the precision demands of semiconductor processing and the energy-intensive nature of achieving the material purity levels required for efficient PV energy conversion.

For the inverter with a 9.87 kW_p capacity, printed board assemblies are the dominant contributors to its environmental impacts, accounting for 51.33% of climate change and 50.49% of fossil and nuclear energy use. This adverse impact stems from the complex, multi-stage manufacturing processes required for the electronic components, including semiconductor fabrication, surface-mount technology assembly, and precision manufacturing operations. Compared with structural materials, these components exhibit higher environmental intensity, mainly due to the energy demands of cleanroom operations, chemical processing, and high-temperature manufacturing steps involved in producing integrated circuits, memory devices, and logic components. Electronic compounds account for 32.23% of GHG emissions and 33.11% of fossil energy use, representing the second most important contribution category. Their poor performance arises from the high mass of inductors and ferrite materials, combined with the energy- and resource-intensive fabrication of integrated circuits and connectors. Main materials also contribute notable to environmental

impacts, accounting for about 10% of total climate change potential and 8% of non-renewable energy use, since their production involves substantial energy demand and process emissions, further amplifying the overall environmental footprint. Specifically, aluminium cast alloy contributes substantially due to the high energy demands of primary production, while copper components add significantly via energy-intensive mining, concentration, and refining operations. On the other hand, capacitors, despite their smaller mass relative to printed board assemblies and structural materials, still contribute meaningfully to the overall environmental impacts of inverters (about 5% of climate change and fossil and nuclear energy use), due to the energy- and resource-intensive nature of their production. Furthermore, the energy consumption during inverter manufacturing contributes modestly (<2%) to climate change impacts and fossil energy depletion. Grid electricity is primarily used for machining, welding, and assembly operations, while processing energy from natural gas supports metal forming, heat treatment, and curing processes essential to production. The remaining components, namely, plastics, resistors, and other minor compounds, have a relatively small impact on climate change and fossil energy use, demonstrating that comprehensive LCAs must account for all system components. It should be noted that these findings are consistent across inverters of different capacities, indicating that the relative contributions of printed board assemblies, structural materials, capacitors, energy use, and minor components remain largely unchanged regardless of system size.

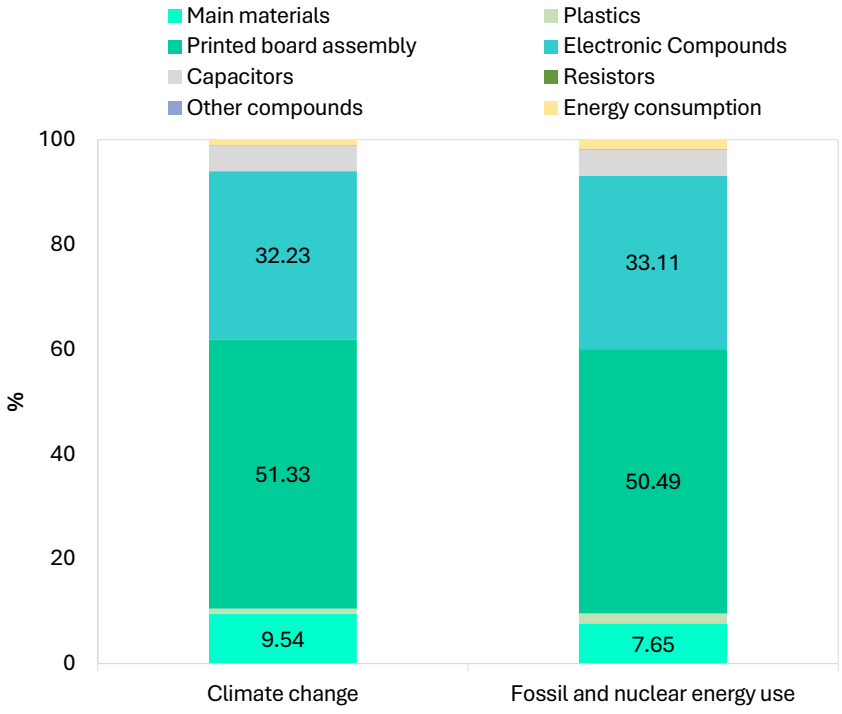

Figure 20 Percentage share of inverter with a 9.87 kW_p capacity in overall climate change impact and fossil energy use

The environmental benefits of deploying the largest PV system (9.87 kW_p) for electricity generation are clearly demonstrated in Figure 21, where the computed GHG emission metric/indicator of the PV system is compared with those of the conventional fossil fuel–powered energy systems/scenarios considered in this case study. The PV installation achieves emission reductions of approximately 90-91% relative to these alternatives. Both the electricity grid mix, and diesel generators emit over 320 g CO_{2eq}/kWh, making them more than ten times as carbon intensive as the solar alternative. Even a relatively cleaner natural gas-fired turbine, estimated at 243 g CO_{2eq}/kWh, produces roughly eight times more emissions per unit of electricity generated. These findings highlight the fundamental role that distributed solar PV systems can play in Greece's decarbonization efforts. Although the national electricity grid has improved significantly, reducing average emissions from over 600 g CO_2/kWh before 2019 to about 243 g CO_2/kWh in 2024 individual PV installations can achieve even more substantial emission reductions. This performance gap underscores the potential for residential and commercial solar systems to accelerate the country's transition towards net-zero emissions.

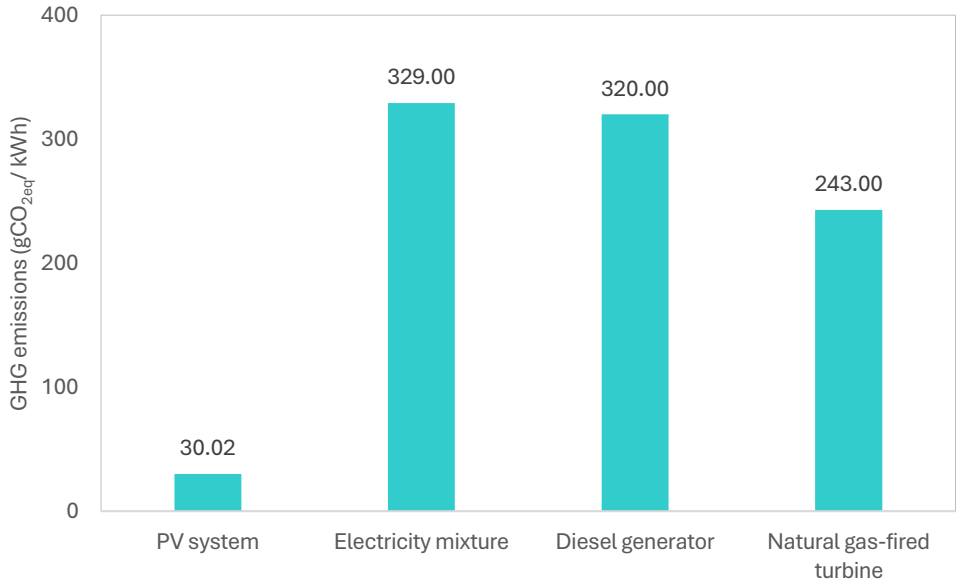

Figure 21 GHG emissions of the 9.87 kW_p PV system vs. conventional energy systems

4.1.3.4 TOPSIS ranking

Following the results of energy modelling, TEA and LCA, Figure 22 presents the TOPSIS evaluation of five grid-interconnected PV systems with installed capacities ranging from 2.59 to 9.87 kW_p. The analysis demonstrates that, although stakeholder priorities strongly effect system rankings, particularly under economically weighted scenarios, solar PV systems with higher rated power generally exhibit superior overall performance across environmental, economic, and technological criteria.

Under the "Environmental Priority" scenario (weights: 0.6 environmental, 0.2 economic, 0.2 technological), the 9.87 kW_p PV system achieves the highest closeness coefficient ($C^* = 0.761$), closely followed by the 8.93 kW_p system ($C^* = 0.733$). This outcome highlights the substantial GHG emissions mitigation potential associated with higher-capacity grid-connected PV installations, attributable to their increased electricity generation and displacement of grid-supplied energy. In contrast, smaller systems exhibit markedly inferior environmental performance; notably, the 2.59 kW_p system attains a closeness coefficient of only 0.239, underscoring the limited environmental benefits achievable at lower installed capacities. In the "Economic Priority" scenario (weights: 0.2 environmental, 0.6 economic, 0.2 technological), mid-sized PV systems are favoured, reflecting a trade-off between TCI and IRR. The 4.94 kW_p system represents the optimal option, performing slightly better than the 2.59 kWp system, with a closeness coefficient of 0.531 compared to 0.525. This result indicates an optimal balance between a moderate TCI (about 9,000 €) and a favourable IRR of 8.3%. Despite the fact that the 2.59 kW_p PV system requires a lower TCI (4,921 €), its comparatively lower IRR (6.7%) reduces its cost-effectiveness. Conversely, PV systems with higher rated capacity (> 5kW_p) achieve higher IRRs (up to approximately 10.1%, refer to Table 9); however, their substantial TCI (exceeding 16,000 €) result in lower overall rankings in the TOPSIS analysis, reflecting the trade-offs inherent in the economic decision-making. Under the "Technological Priority" scenario (weights: 0.2 environmental, 0.2 economic, 0.6 technological), the rated capacity of the PV system and the associated energy output dominate the evaluation. The 9.87 kW_p PV system ranks first with $C^* = 0.887$, followed by the 8.93 KW_p system ($C^* = 0.840$). These results reaffirm the advantages of larger PV systems in terms of operational efficiency and electricity production. Finally, when weights were distributed more evenly among economic, environmental and technological dimensions, the TOPSIS results indicate a consistent preference for higher - capacity PV systems. The 9.87 kW_p PV system achieves the highest score closeness value ($C^* = 0.737$), followed closely by the 8.93 kW_p system with $C^* = 0.725$, reflecting their robust performance across all evaluated dimensions. Mid-sized solar PV systems rank between the higher- and lower-capacity solutions, since their moderate investment costs partially offset lower energy yields and environmental benefits. In contrast, the smallest PV system with ranked capacity of 2.59 kW_p ranks lowest under this scenario, indicating that its limited electricity generation and the reduced environmental impact outweigh the advantages associated with lower capital expenditure and IRR when all criteria are considered simultaneously.

Overall, the TOPSIS analysis confirms that while stakeholder preferences can significantly affect PV system rankings, particularly when economic criteria are prioritized, grid-interconnected PV systems with higher capacities consistently demonstrate superior performance from both an environmental and a technological

perspective, whereas mid-sized systems offer a more balanced solution when economic considerations dominate.

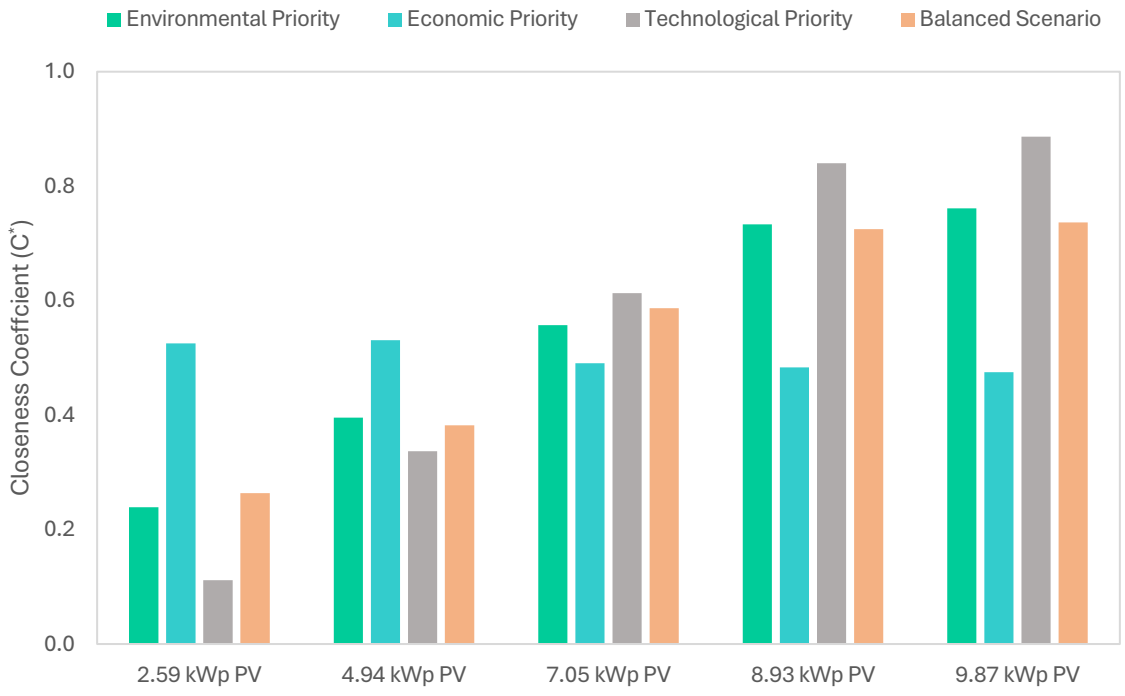

Figure 22 TOPSIS ranking of PV systems under different scenarios

4.2 Case study : RES-based hybrid electricity and heat system

Building on the insights from the analysis of urban grid-connected PV systems in Athens, which highlighted both the economic and environmental performance of building-integrated solar solutions, the focus now shifts to off-grid contexts with limited centralized energy access. The following case study investigates the design and optimization of an autonomous hybrid energy system for a remote household in Metsovo, in northwestern Greece, addressing both electricity and thermal energy demand under year-round autonomous operation. This case study allows for the investigation of renewable energy solutions in off-grid building applications, where technical robustness, economic viability, and environmental sustainability should be carefully balanced. By considering an integrated configuration of solar PV modules, wind turbines, diesel generator, battery storage, and biomass-based thermal systems, the Metsovo study extends the analysis of building-scale renewable energy strategies from urban, grid-connected contexts to remote, energy-isolated environments, thereby providing a broader perspective on sustainable building energy solutions in diverse geographic and climatic settings.

The specific case study has been published in a peer-reviewed scientific journal [199] *(Sagani A, Vrettakos G, Dedoussis V. Viability assessment of a combined hybrid electricity and heat system for remote household applications. Solar Energy 2017;151:33–47)*.

4.2.1 Case study overview

This case study is dedicated to the design, simulation, and evaluation of an autonomous hybrid energy system intended to meet both the electricity and thermal energy demand of a representative remote rural household located in the northwestern mainland Greece, namely the town of Metsovo. Owing to its geographic isolation and limited access to centralized energy infrastructure, Metsovo serves as a pertinent setting for exploring the feasibility and performance of off-grid renewable energy solutions for residential applications. The main objective of this study is to develop a technically robust, economically viable, and environmentally sustainable hybrid system capable of year-round autonomous operation. For electricity generation, the proposed configuration integrates both RES and conventional energy sources, specifically PV panels, wind turbines, diesel generators, and battery storage. The electric power supply system is designed and optimized using the Hybrid Optimization of Multiple Energy Resources (HOMER) software platform [200], which enables an integrated analysis of system performance under varying conditions of local solar irradiance, electrical load profiles, and diesel fuel prices. For thermal energy supply, the system combines a wood biomass-burning thermodynamic fireplace with a diesel oil burner to meet space heating and domestic hot water demands. The thermal subsystem is assessed employing the RETScreen Clean Energy Project Analysis Software version 4.0 [179], facilitating the evaluation of its energy efficiency, cost-effectiveness, and emissions reductions. The findings of this case study are expected to provide valuable insights into the potential of decentralized energy systems to improve sustainable deployment and promote energy independence in remote and rural communities, especially in regions with challenging geographic and climatic conditions.

4.2.1.1 Location and meteorological parameters

Metsovo is a remote rural town in the Epirus region of northwestern Greece, lying at an altitude of 1,250 m. It is located at 39°46.2' N latitude and 21°11.0' E longitude and has about 750 residential households [201]. Metsovo is characterized by a mountainous and rugged terrain, extensively faulted and folded, forming the southernmost extension of the European Alps. The region experiences a continental climate within the temperate zone. Summers tend to be hot with occasional local rainfall, whereas winters are long, cold, and marked by significant precipitation, including frequent snowfall. Its high-altitude climate alongside its mountainous landscape leads to substantial renewable energy potential in the area. Its high-altitude climate alongside its mountainous landscape leads to substantial renewable energy potential in the area.

Metsovo's renewable energy potential is primarily derived from solar and biomass resources, while wind energy remains relatively limited. The high solar radiation levels in the region, in conjunction with the clear atmosphere, make solar energy a promising option for sustainable energy development. Furthermore, the extensive forest resources and related biomass residues provide notable opportunities for bioenergy production. Although wind energy potential is modest, either small-scale wind energy systems or hybrid renewable energy solutions could be explored to enhance the energy security in the area. The strategic exploitation of Metsovo’s renewable energy resources could substantially support local economic development, promote energy autonomy, and advance environmental sustainability goals. The availability of RES the area is presented in detail in the following paragraphs.

Solar Energy Potential

Metsovo exhibits a high solar energy potential, mainly due to its clear atmosphere, which derives from the region's consistently low humidity levels. This characteristic enhances solar radiation availability, making it a promising location for solar energy applications. Relative meteorological data, encompassing monthly average solar global horizontal radiation and the monthly average clearness index, are depicted in Figure 23. The clearness index serves as an indicator of atmospheric transparency; it effects the amount of solar energy reaching the surface. These data are sourced from the NASA Surface Meteorology and Solar Energy Data Database [180]. The lowest level of solar irradiation occurs during the winter months, i.e., January, February, October, November, and December, whereas the highest figures are recorded from April to September, with a peak in June. The annual daily average of the solar global radiation is about 4.14 kWh/m^2/day, and the average clearness index is 0.511. These values point out that the region's potential for solar energy utilization, particularly during the extended summer period when solar availability is at its maximum.

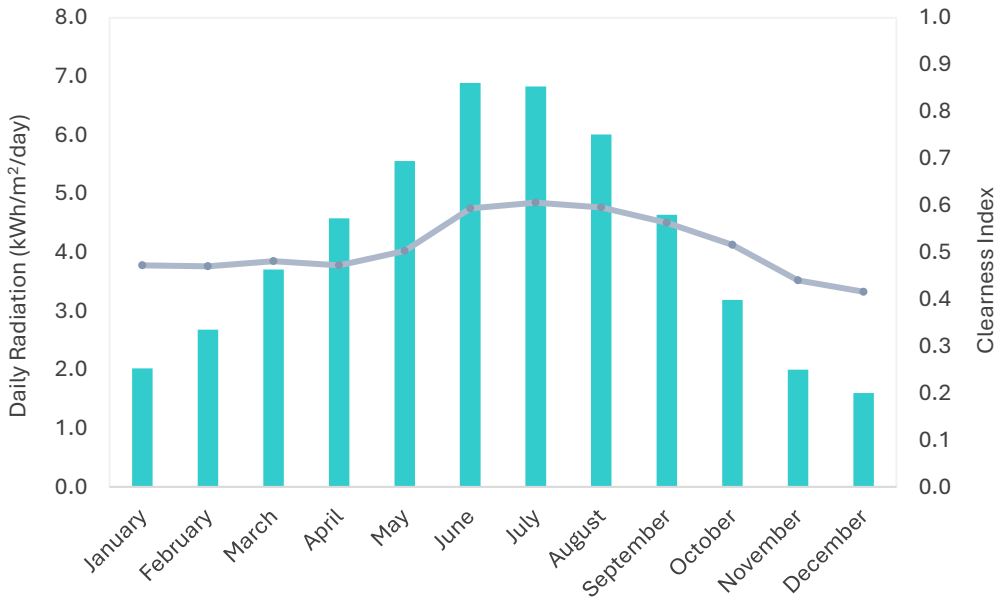

Figure 23 Monthly average solar global horizontal irradiation in Metsovo, Greece

Wind Energy Potential

On the other hand, Metsovo has limited wind energy potential, as demonstrated by wind speed data retrieved from [180]. Figure 24 illustrates the monthly average wind speed measurements recorded at 50 meters above the ground over a 10-year period. Wind speeds in the region vary between 3.7 m/s and 5.1 m/s. Seasonal variations reveal relatively higher wind speeds during the winter season, i.e., from January to December, with the peak value occurring in December. Nevertheless, the annual average wind speed is approximately 4.3 m/s, which is generally considered suboptimal for large-scale wind energy generation.

These conditions suggest that while wind energy may not be a primary renewable resource in the area, small-scale wind energy systems could still be explored to complement other renewable resources.

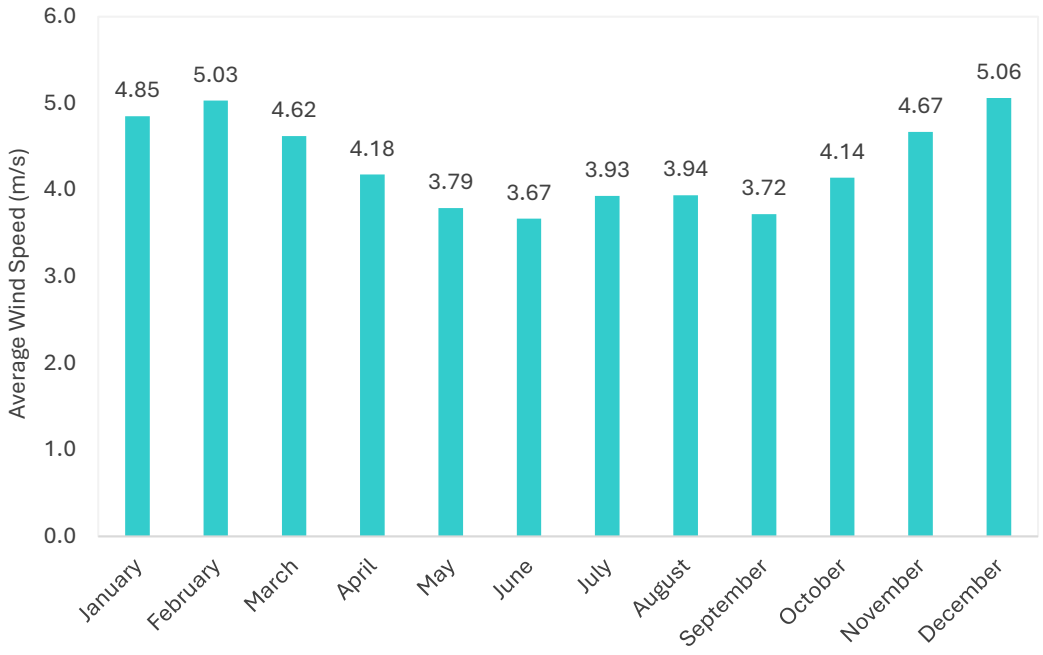

Figure 24 Monthly average wind speed data in Metsovo, Greece

Biomass Energy Potential

The vicinity of Metsovo is rich in forest resources, with about 28,500 hectares of forest systematically exploited. The dominant tree species in the region are black and pine beech [202]. Forest exploitation in Metsovo primarily yields three main products, i.e., firewood, technical timber, and posts for electricity and telecommunications networks. The estimation of biomass potential of Metsovo was based on forest production data recorded by the Local Forest Authorities [202]. These data span a ten-time period, from 2003-2012, which provides a reliable basis for evaluating the quantity of wood extracted from local forests. Table 11 presents the average annual production of forest-derives materials in Metsovo. In addition to direct forest production, wood residues are an important biomass source. The Forest Authorities estimate that residues from firewood production account for 10% of total firewood output, whilst residues from technical timber production constitute 20% of total timber production. Based on these estimates, wood residues amount to approximately 2,074 tons per year. Beyond forestry, additional biomass sources include agricultural residues and by-products from small-scale wood industries. Agricultural residues in the region are estimated at 810 tons per year, while wood industry residues contribute approximately 500 tons per year [202]. Therefore, the total theoretical wood biomass potential in Metsovo is estimated to be 15,815 tons per year. Given that the calorific value of wood biomass is approximately 4 kWh/kg [203], the total thermal energy potential from biomass resources in the region reaches about 63,260 MWh per year.

Table 11 Average annual quantities of forest products in Metsovo

Product	Mean annual production (tons/yr)
Firewood	4,112
Technical timber	6,180
Timber for posts	2,139
Total	12,431

4.2.1.2 Energy demand

Although Metsovo is endowed with high renewable energy resources, households face serious energy supply difficulties, a phenomenon known as energy poverty. The town also has high thermal energy loads due to harsh winters and poor insulation in older homes. Therefore, autonomous hybrid energy systems are required to meet both electrical and thermal energy needs. In this case study, a two-bedroom, 81 m^2 house for a four-member family was selected to investigate the feasibility of an autonomous hybrid system. The house is assumed to be located on the outskirts of Metsovo, beyond the reach of the electrical grid. A simple plan view is depicted in Figure 25.

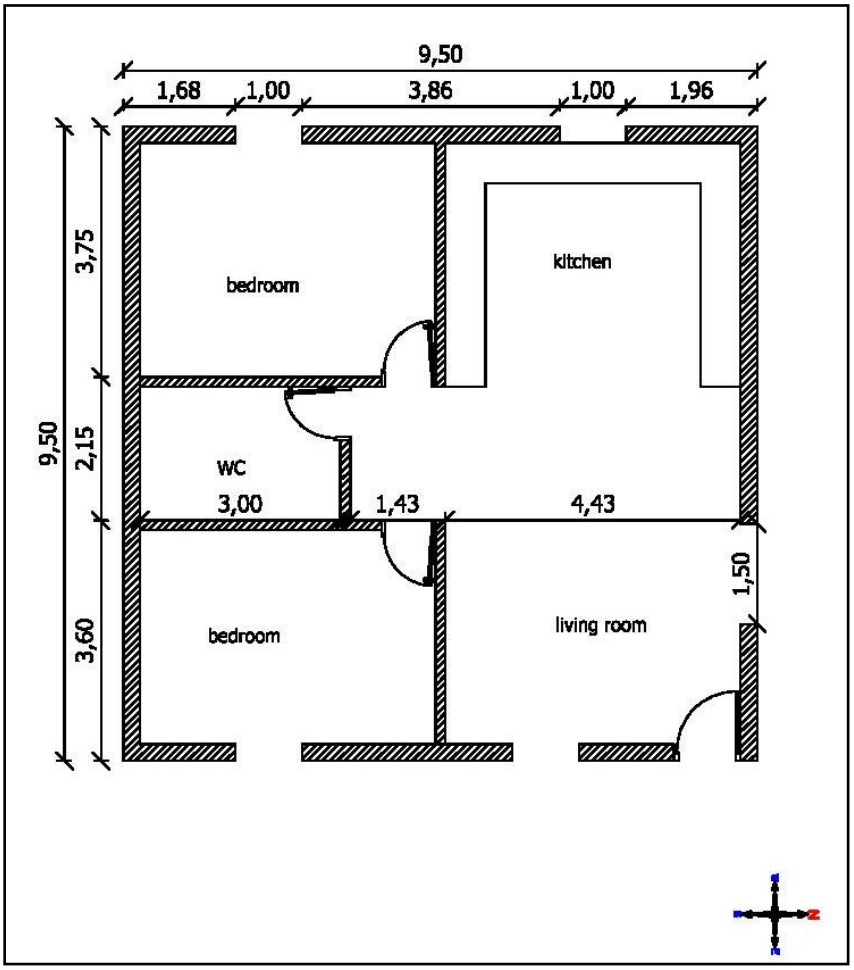

Figure 25 Typical household in Metsovo, Greece

The daily electrical load profile for a house in Metsovo is provided by HOMER [200]. Electricity loads fluctuate throughout the day; consumption is typically higher in the morning, afternoon, and early evening hours. The highest electricity consumption occurs in winter season (November to March) due to increased heating demands, whilst the lower loads occur during summer months (June to August), since air conditioning is rarely required. A random variability factor is applied in order to account for daily fluctuations, with day-to-day and time-step-to-time-step variability both estimated at 2% [204,205]. The total daily electricity demand for a typical residence in Metsovo, as simulated by HOMER, is about 11.25 kWh, with a peak demand of 1.57 kW.

On the other hand, the thermal load in residential buildings consists of space heating and hot water requirements. During summer, only hot water preparation is needed, and a solar water heating system is assumed to be in place, a common practice in Greece. Consequently, the performance of the existing solar water heating system is excluded from this analysis. Hot water demand is considered constant year-round, as consumption habits remain unchanged regardless of external temperatures. Space heating demand was assessed employing the German Standard DIN 4108-2 [206], in the absence of a Greek equivalent. This Standard, aligned with European energy performance guidelines, evaluates heating requirements based on heat loss through the building envelope and air leakage. The space heating demand for the household is estimated at 9,489 kcal/hr (11 kW), as shown in Table 12. According to Greek Directive 20701-1/2010 [207], hot water demand is estimated at 2.5 L/day/m^2. For an 81 m^2 residence, this corresponds to 202.5 L/day. Heating this volume from 4.2°C to 45°C requires about 9.6 kWh/day. The peak thermal power required for hot water preparation is 3.8 kW, assuming a daily heating duration of 2.5 hours. The combined space heating and hot water energy demand amounts to 14.8 kW (11 kW + 3.8 kW).

Table 12 Heat required for space heating in Metsovo household, Greece

Heat loss	Value (kcal/hr)
Building envelope	
Bedrooms	2,135
Bathroom	85
Living room	1,755
Kitchen	508
Floor	1,640
Roof	1,094
Ventilation heat loss	2,272
Total	9,489

4.2.2 Methodology application

4.2.2.1 Modelling of hybrid electricity power supply system

In the design of the hybrid electricity power supply system, a combination of PV, wind, battery storage, diesel generation, and power conversion was analysed to identify cost-effective configurations capable of reliably meeting the household electricity demand in Metsovo, while minimizing both diesel fuel consumption and

GHG emissions (refer to Figure 26). The PV subsystem was modelled with capacities ranging from 0 kW to 5 kW to determine the optimal sizing strategy for reducing diesel generator runtime. As expected, the PV subsystem primarily meets daytime loads, thereby reducing the operating hours of the diesel generator. The technical specifications and cost data associated with the PV units are presented in Table 13. Wind energy integration was achieved using the BWC XL1 (AC) wind turbine, whose power curve is depicted in Figure 27, and defines the turbine's electrical output as a function of hub-height wind speed. Three configurations were simulated: no turbine, one turbine, and two turbines, enabling assessment of the contribution of wind energy under different resource availability scenarios. Relevant technical and cost data for the wind energy conversion system are presented in Table 14.

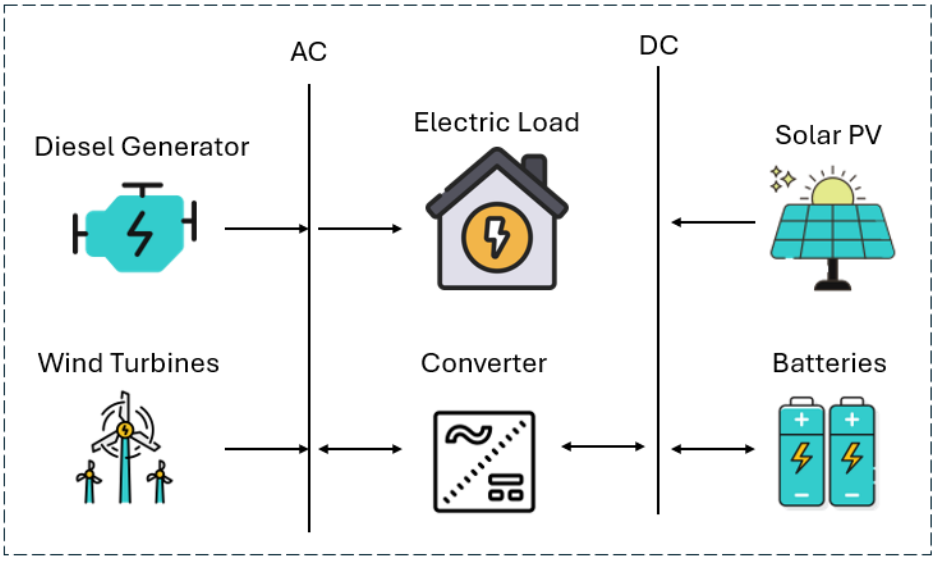

Figure 26 Configuration of hybrid PV/wind/diesel/battery system

Table 13 Technical specifications and cost data for the PV module [144,208]

PV module	Specifications
Technical Specifications	
Manufacturer	Generic
Panel Type	Flat Plate
Rated capacity	1 kW
Temperature Coefficient	-0.5 %/°C
Nominal operating cell temperature	47 °C
Efficiency in standard test condition	13 %
Lifetime	25 yrs
Economic Data	
Capital cost	2,500 €/kW
Replacement cost	2,500 €/kW
Operating and maintenance cost	12.5 €/kW/yr

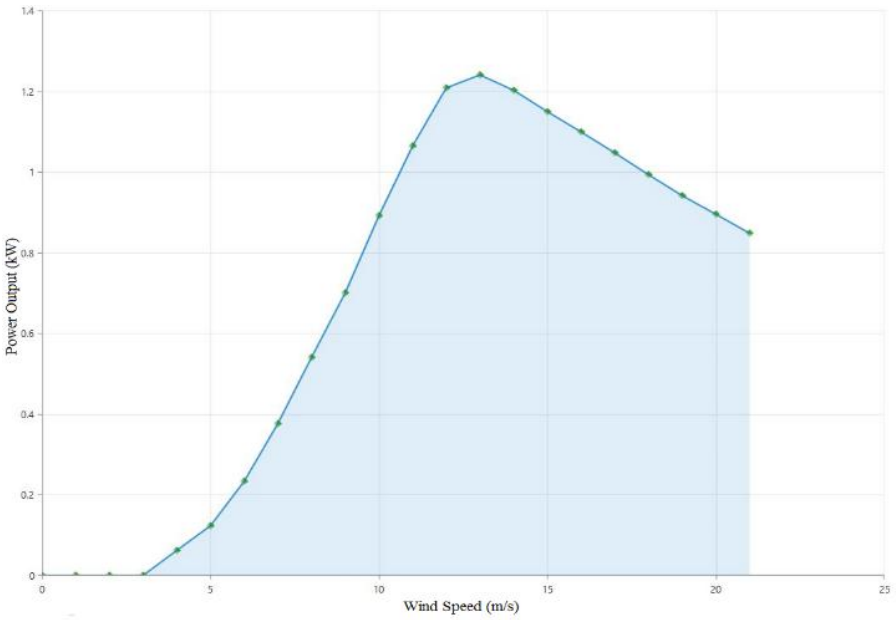

Figure 27 Wind power curve of BWC XL1 wind turbine

Table 14 Technical specifications and cost data for wind turbine [208]

Wind Turbine	Specifications
Technical Specifications	
Name	BWC XL1
Manufacturer	Bergey Windpower
Cut-in wind speed	4 m/s
Cut-out wind speed	21 m/s
Nominal wind speed	11 m/s
Rated power	1 kW
Lifetime	25 yrs
Economic Data	
Capital cost	6,000 €/kW
Replacement cost	6,000 €/kW
Operating and maintenance cost	120 €/kW/yr

To further enhance the hybrid system's autonomy and reduce dependence on fossil fuel backup, battery storage was incorporated as an energy buffer between fluctuating renewable generation and household demand. The Generic 1 kWh LA model was selected as the storage element, with batteries connected in series to achieve higher capacity. Simulations were conducted with battery quantities ranging from zero to ten units to determine the capacity that minimizes diesel generator operation without leading to excessive capital cost. Battery storage contributes substantially to reducing diesel generator runtime by storing

excess renewable (PV and wind) generation and discharging it during periods of low or no renewable output. The technical specifications and cost data of the selected battery model are presented in Table 15.

Table 15 Technical specifications and cost data for Generic 1 kWh LA [209,210].

Battery	Specifications
Technical Specifications	
Name	Generic
Manufacturer	Lead Acid
Nominal voltage	12.0 V
Nominal capacity	1.0 kWh
Maximum capacity	83.4 A
Round trip efficiency	80%
Minimum state of charge	40%
Maximum charge rate	1 A/Ah
Maximum charge current	16.7 A
Float life	10 yrs
Economic Data	
Capital cost	300 €/kW
Replacement cost	300 €/kW
Operating and maintenance cost	10 €/yr

Despite the integration of PV, wind, and energy (battery) storage, a dispatchable power source remains necessary in order to guarantee uninterrupted power supply during periods of prolonged renewable energy deficit. Accordingly, a diesel generator was incorporated and sized to meet peak electricity demand. Its operation follows the LF dispatch strategy analysed in the Chapter 3, ensuring that the diesel generator produces only the power required to meet the remaining demand after accounting for renewable energy generation and available battery discharge. Under this approach, the diesel generator output follows the net demand profile rather than operating at a fixed set point, thereby decreasing unnecessary fuel consumption and improving overall system efficiency [211,212]. The fuel consumption characteristics of the diesel generator were modelled using a load-dependent function expressed as follows [213].

$$F(t) = F_1 \cdot P_{DG}(t) + F_0 \cdot P_r \tag{44}$$

Where *F(t)* (expressed in L) denotes the (standby) fuel consumption of diesel generator at a specific time *t*, F_o (expressed in units/hr/kW) denotes the fuel curve intercept coefficient unit, F_1 (expressed in units/hr/kW) is the fuel curve slope (expressed in units/hr/kW), P_r (expressed in kW) represents the rated capacity of the diesel generator, and $P_{DG}(kW)$ is the electrical output of the diesel generator. It is worth mentioning that the coefficients in the fuel consumption curve are determined based on the operation parameters of the diesel generator, including load conditions, the generator's maximum power capacity, fuel efficiency and engine characteristics. To ensure safe and efficient operation, the generator output is constrained according to Equation 45 [214].

$$0 \leq P_{DG} \leq P_{DG,max} \quad (45)$$

where the power supply of the diesel generator, P_{DG}, cannot exceed its maximum power, $P_{DG,max}$, during its operation in the power system.

An auto-sizing generator model was used in the simulation to ensure that load requirements are always met under all operational scenarios. The fuel consumption and efficiency curves employed in this study are illustrated in respectively, while the technical specifications and cost data are summarized in Figure 28 and Figure 29, respectively, while the technical specifications and cost data are summarized in Table 16.

Table 16 Technical specifications and cost data for auto-sizing diesel generator [215]

Auto-sizing diesel generator	Specifications
Technical Specifications	
Name	Autosize Genset
Manufacturer	Generic
Capacity	Auto-sizing
Fuel curve slope	0.251 L/hr/kW
Minimum load ratio	25%
Lifetime	15,000 hrs
Economic Data	
Capital cost	500 €/kW
Replacement cost	500 €/kW
Operating and maintenance cost	0.030 €/hr

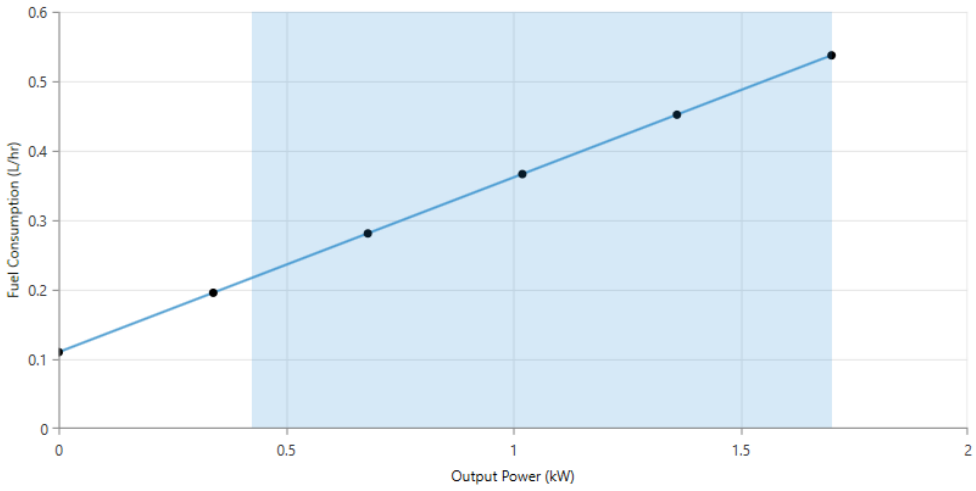

Figure 28 Typical fuel consumption curve of auto-sizing diesel generator

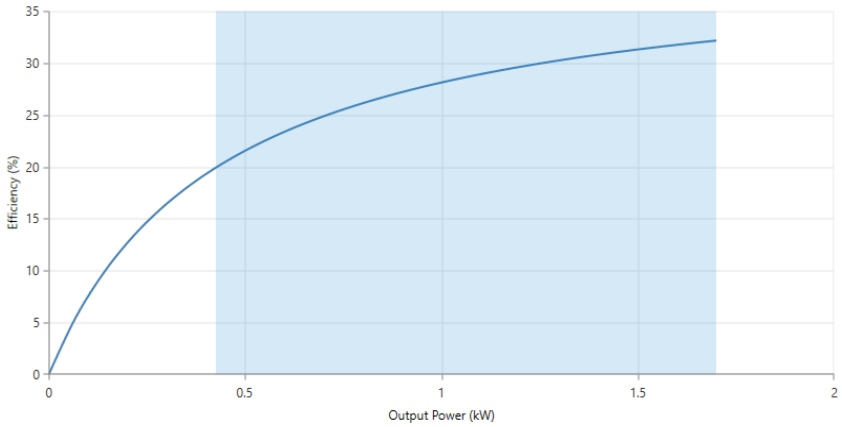

Figure 29 Typical efficiency curve of the auto-sizing diesel generator across varying load levels

Finally, since the hybrid system includes both AC and DC components, a power converter was incorporated to enable bidirectional power flow. The converter operates as both an inverter, i.e., converting DC power from the PV array or battery to serve AC loads, and a rectifier, i.e., converting AC power to charge the battery or serve DC loads. The efficiency of this converter reads [216]:

$$\eta_{cnv} = \frac{P_{output}}{P_{input}} \tag{46}$$

Where P_{output} (kW) and P_{input} (kW) denote the output and the input power from or to the converter. For this analysis, a converter efficiency of 96% and a lifetime of 10 years were assumed, as summarized in Table 17. Converter sizes ranging from 0 kW to 5 kW were evaluated to determine the optimal capacity that minimizes energy losses while meeting load requirements.

Table 17 Technical specifications and cost data for power converter

Power Converter	Specifications
Technical Specifications	
Name	Leonics S219CPH 5 kW 48 V_{dc}
Manufacturer	Leonics
Rated capacity	5 kW
Efficiency	96%
Lifetime	10 yrs
Economic Data	
Capital cost	600 €/kW
Replacement cost	600 €/kW
Operating and maintenance cost	10 €/yr

The entire hybrid electricity supply system was simulated and optimized using the HOMER software platform [200], enabling detailed hourly modelling over a full year. The software identified the optimal operation of PV, wind, battery storage, and diesel generator, while at the same time considering load variability, resource availability, operational constraints, and cost of components. Diesel generator fuel consumption was evaluated using its load-dependent fuel curve, with operation constrained within rated capacity to ensure efficiency and reliability. Battery performance accounted for depth-of-discharge and round-trip efficiency, and converter losses were included to reflect realistic energy transfer between DC and AC buses. Through this integrated simulation, HOMER determined the least-cost configuration capable of meeting the household's electricity demand with minimal diesel operation and maximal renewable energy utilization.

4.2.2.2 Modelling of biomass heating system

In parallel with the electricity supply system, the thermal energy demand of the Metsovo household is met via a forest biomass heating system, specifically a pine wood-burning "thermodynamic" fireplace. Forest pine wood was selected as the primary fuel because of its availability in the surrounding region, making it a sustainable and cost-effective option. The so-called "thermodynamic" fireplace features a combustion chamber where the wood/biomass is burned, in conjunction with a water heat exchanger, providing space heating and domestic hot water. The advantages of using natural resources instead of diesel oil-fired burners for producing the required heat are almost self-evident: lower household heating bills, reduced environmental footprint, and enhanced forest sustainability, among others [202].

A diesel oil burner is also considered as a backup system alongside the thermodynamic fireplace. The diesel oil burner could serve as a provider of high thermal peak loads. The assessment tool RETScreen® Clean [179] was employed to assess the technical and economic performance of the proposed heating system. During the winter season, the biomass-burning thermodynamic fireplace, combined with an auxiliary / backup diesel oil burner, meets the space heating and hot water load requirements. In the summer, when there is no need for space heating, the wood-burning fireplace is not in operation, and hot water demand is fully covered by solar water heaters. The biomass-burning thermodynamic fireplace (base load heating system) should have a capacity of 14.8 kW. Such a biomass combustion system will require 7 tons of wood annually. The power of the auxiliary diesel oil burner (backup and peak load heating system) should also be 14.8 kW, consuming 239 L of oil annually. An overall efficiency of 65% is assumed for both heating systems.

The economic assessment, based on studies of the Greek energy market [208], estimates the capital costs at 5,000 € for the biomass fireplace and 4,000€ for the diesel burner, totalling 9,000 €, while annual operation and maintenance costs are set at 2% of capital cost (180 €), covering insurance, labor, and routine maintenance. Fuel costs are calculated at 133 €/ton for pine wood and 0.8 €/L for diesel, resulting in a total annual fuel expense of 1,993 €, with 995 € for wood and 198 € for diesel oil.

By integrating a hybrid PV/wind/diesel/battery electricity power supply system with a locally sourced biomass heating system and supplementary solar water heating, the household achieves a comprehensive energy solution that maximizes the use of renewable resources, reduces reliance on fossil fuels, and provides both electrical and thermal energy in a cost-effective and environmentally responsible manner.

4.2.3 Simulation results and discussion

4.2.3.1 Hybrid electricity power supply system

4.2.3.1.1 Energy modelling & economic optimization results

A system simulation was conducted, assuming an annual interest rate of 12%, an inflation rate of 1.5%, and a project lifetime of 25 years. The categorized optimization outcomes are presented in Table 18, in ascending order. According to the NPC and LCOE metrics, whose calculation methodology is detailed in Chapter 3, the most economically viable configuration for the household under analysis is a hybrid PV/diesel/battery system. This optimal setup includes 1 kW_p of PV capacity, a 1.8 kW diesel generator, two battery units with a storage capacity of 1 kWh each, and a 1 kW power converter. In contrast, the PV/wind/diesel hybrid system is identified as the least cost-effective solution. The optimal configuration incurs a capital expenditure of 4,600 €, an annual operating cost of 1,750 €, a total NPC of 20,075 €, and a LCOE of 0.553 €/kWh. These findings indicate that wind-based hybrid systems are not as economically competitive as either diesel-only or PV-based hybrid alternatives within the given context. While the cost of wind energy has seen substantial reductions in recent years, the technology still demands a comparatively higher initial investment than either fossil-fuelled generators or PV generation units.

Table 18 Comparison among the optimized hybrid systems for the Metsovo household, Greece

Options	PV (kW)	XL1	Auto (kW)	1 kWh LA	BDI 1P (kW)	Initial Cost (€)	Operating Cost (€)	NPC (€)	COE (€/kWh)	REF (%)
PV/diesel/battery	1.00	-	1.80	2	1.00	4,600	1,750	20,075	0.553	30.0
Diesel/battery	-	-	1.80	2	1.00	2,100	2,427	23,556	0.649	0.0
PV/wind/diesel/battery	1.00	1	1.80	2	1.00	10,600	1,621	24,931	0.687	42.0
Diesel	-	-	1.80	-	-	900	2,769	25,381	0.699	0.0
PV/diesel	2.00	-	1.80	-	1.00	6,500	2,197	25,929	0.714	8.3
Wind/diesel/battery	-	1	1.80	2	1.00	8,100	2,288	28,327	0,780	13.0
Wind/diesel	-	1	1.80	-	-	6,900	2,825	31,874	0.878	0.0
PV/wind/diesel	2.00	1	1.80	-	1.00	12,500	2,240	32,309	0.890	13.0

The total annual electricity generated by the optimal hybrid power system is 4,410 kWh. The system can meet the electricity demand of the Metsovo household with a 30% Renewable Energy Fraction (REF) integrated into the current diesel-only power system. The relevant contribution of electricity from each component of the proposed hybrid PV/diesel/battery power system is presented in Table 19. According to this table, the diesel generator operates for 4,801 hours annually, consuming 1,280 L of diesel oil and generating 2,883 kWh of electrical energy, which accounts for approximately 65.4% of the system's total annual electricity production. The remaining 34.6% is supplied by the solar PV system, which has an annual energy output of 1,527 kWh. This high contribution from solar PV is particularly significant for rural areas in Greece, such as Metsovo, which have abundant solar energy potential and face high diesel fuel costs. The storage/battery system provides 475 kWh of electrical energy per year. The surplus electricity produced is reduced to 2.8%, amounting to 122 kWh annually. In general, this surplus electricity can be utilized to satisfy the household's dump load (e.g., heating or cooling) [217]. Since the batteries are exclusively charged by the PV system, it is noteworthy that the combined energy supply from the solar PV array and battery storage

accounts for approximately 30% of the total electricity generated by the system, aligning with the previously mentioned REF of 30%.

Table 19 Energy contribution of different energy sources of the optimal hybrid power system proposed

Item description	Value
Solar PV	
Rated capacity	1 kW
Percent contribution	34.6%
CF	17.43%
Mean output power	4.18 kWh/d
Annual energy output	1,527 kWh/yr
Annual hours of operation	4,382 hrs/yr
Battery	
Nominal capacity	2 kWh
Usable nominal capacity	1.2 kWh
Autonomy	3 hrs
Energy in	530 kWh/yr
Energy out	425 kWh/yr
Losses	104 kWh/yr
Annual throughput	475 kWh/yr
Expected life	3 yrs
Auto-sizing diesel generator	
Annual hours of operation	4,801 hrs
Number of starts	1,387 starts/yr
Operational life	3 yrs
Mean electrical output	0.6 kW
Annual electrical production	2,883 kWh/yr
Fuel consumption	1,280 L/yr
Average electrical efficiency	23%
Converter	
Inverter	
Rated Capacity	1 kW
CF	17%
Mean output	0.17 kW
Energy in	1,535 kWh/yr
Energy out	1,473 kWh/yr
Losses	61%
Annual hours of operation	5,610 hrs/yr
Rectifier	
Rated Capacity	1 kW
CF	3%
Mean output	0.03 kW
Energy in	250 kWh/yr
Energy output	235 kWh/yr
Losses	15%
Annual hours of operation	1,549 hrs

The monthly average electricity generated by the optimal hybrid PV/diesel/battery power system is illustrated in Figure 30. As depicted in this figure, the auto-sizing diesel generator serves as the primary base load provider from September to May due to the relatively lower solar radiation during this period. The solar PV system operates at its highest capacity during the summer months (June, July, and August), when solar radiation reaches its peak.

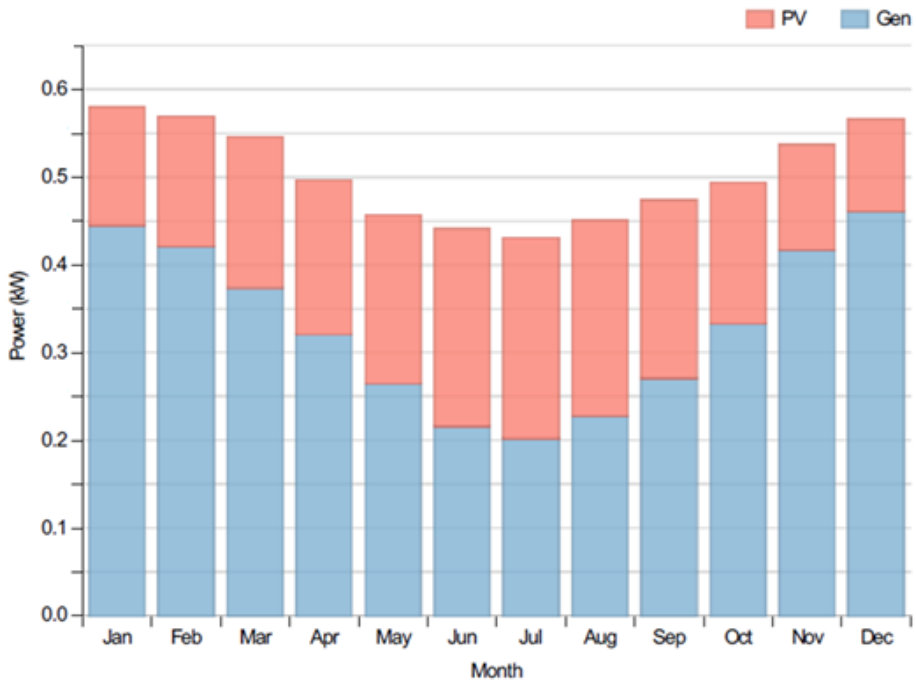

Figure 30 Monthly average electric production for the optimal hybrid PV/diesel/battery power system

Figure 31 illustrates the cash flow summary associated with each component of the proposed hybrid PV/diesel/battery power system. Detailed information on both actual and annualized costs, including capital investment, replacement, O&M, fuel consumption, and salvage value, is presented in Table 20. The total NPC of the system is estimated at 20,075 €. A substantial share of this cost, approximately 72%, is attributed to the auto-sizing diesel generator, primarily due to its elevated fuel consumption and O&M expenses.

The system's initial capital investment reaches 4,600 €, corresponding to an annualized cost of 520 €. Within this capital cost, the PV array constitutes 54% of the total, with the remaining 46% distributed among the diesel generator, battery storage units, and power converter. The relatively high capital cost of the PV array remains a significant barrier to the widespread adoption of building-integrated PV technologies in the residential sector. Consequently, targeted financial incentives and supportive policy frameworks from national and local governments are critical to offset upfront costs, particularly for consumers in rural or off-grid regions. Nevertheless, the PV array offers a distinct operational advantage: it incurs neither fuel costs nor substantial operating expenses, with minimal maintenance requirements when compared to the diesel generator. This long-term cost efficiency underscores the strategic value of incorporating renewable energy components within hybrid systems aimed at enhancing energy access and sustainability.

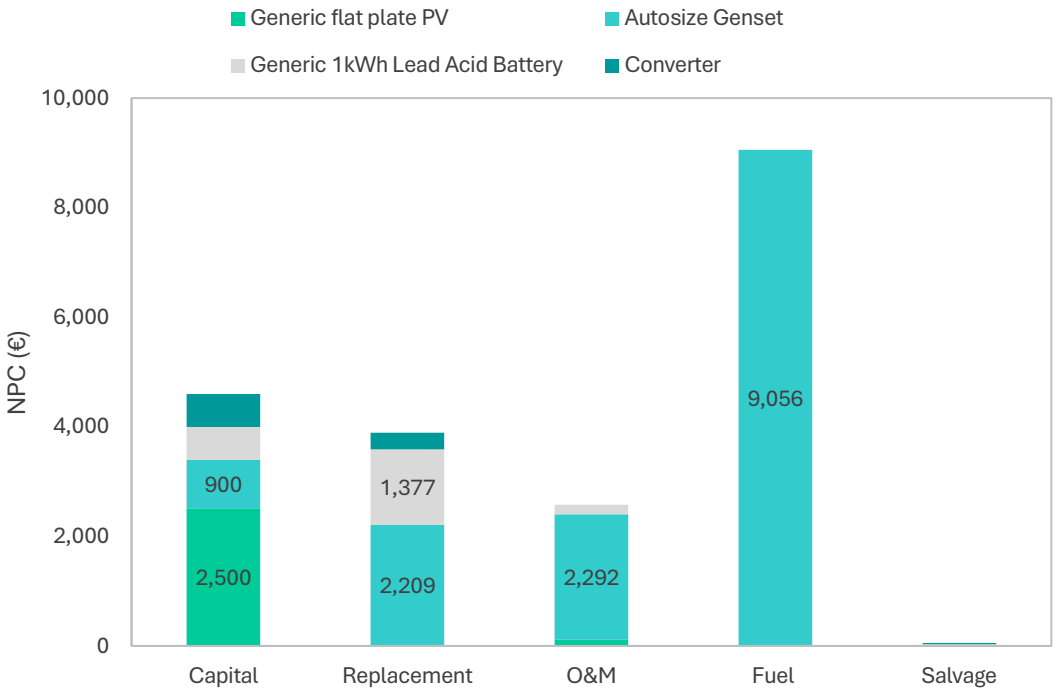

Figure 31 Cash flow summary of various components of the hybrid PV/diesel/battery power system proposed

Table 20 Summary of various absolute/annualized costs of the hybrid power system proposed

Component	Capital (€)	Replacement (€)	O&M (€)	Fuel (€)	Salvage (€)	Total (€)
Generic flat plate PV	2,500/283	0/0	111/13	0/0	0/0	2,611/295
Autosize Genset	900/102	2,209/250	2,292/259	9,056/1,024	0/0	14,457/1,635
Generic 1 kWh LA Battery	600/68	1,377/156	177/20	0/0	-29/-3	2,215/240
Converter	600/68	308/35	0/0	0/0	-26/-3	882/100
Whole System	4,600/520	3,894/440	2,580/292	9,056/1,024	-55/-6	20,075/2,270

4.2.3.1.2 Sensitivity analysis results

Following the economic assessment of the hybrid energy system, a comprehensive sensitivity analysis was conducted to evaluate the hybrid system's performance under varying input parameters. The key sensitivity variables included global solar radiation (**4.14**, 4.64, 5.14, and 5.64 kWh/m^2/day), diesel fuel price **(0.8**, 1.0, 1.2, and 1.4 €/L), daily electrical energy demand (9.25, **11.25**, 13.25, and 15.25 kWh/day), and peak load (**1.57**, 1.85, 2.13, 2.41, and 2.69 kW). Nominal system values are indicated in bold within the corresponding data tables and figures.

The performance of the proposed optimal PV/diesel/battery hybrid power system at different levels of global solar radiation is presented in Table 21. As expected, a linear correlation exists between global solar radiation and the annual energy output of the PV array. Specifically, as the solar radiation increases from

4.14 to 5.64 kWh/m^2/day, the annual PV generation grows from 1,527 kWh to 1,947 kWh, while the PV contribution to total system energy increases from 34.6% to 42.4%. This rise in generation also results in a corresponding increase in excess electricity, which ranges from 122 kWh (2.8%) to 297 kWh (6.5%). Accordingly, at the nominal radiation level of 4.14 kWh/m^2/day, diesel fuel consumption decreases with increasing solar availability, demonstrating the complementary nature of the hybrid configuration.

Table 21 Summary of various absolute/annualized costs of the hybrid power system proposed

Global solar radiation	Generic flat plate PV		Excess Energy		REF	Diesel	NPC	COE
(kWh/m^2/day)	(kWh/yr)	%	(kWh/yr)	%	(%)	(L)	(€)	(€/kWh)
4.14	1,527	34.6	122	2.8	30	1,280	20,075	0.553
4.64	1,735	38.5	221	4.9	32	1,228	19,487	0.537
5.14	1,881	41.1	256	6.2	34	1,190	19,062	0.525
5.64	1,947	42.4	297	6.5	36	1,164	18,759	0.517

The effect of diesel oil price and electricity demand on the NPC and LCOE at the nominal solar radiation level is depicted in Figure 32 and Figure 33, respectively. Both NPC and LCOE increase as the diesel oil price rises. For instance, as the diesel price escalates from its nominal value of 0.8 €/L to 1.4 €/L, the NPC rises from 20,075 € to 24,965 € (a 24% increase), while the LCOE increases from 0.553 €/kWh to 0.688 €/kWh. In contrast, when daily electricity demand increases while the peak load remains constant, NPC rises but LCOE declines. For example, increasing demand from 11.25 kWh/day to 13.25 kWh/day under a fixed peak load of 1.57 kW leads to a rise in the load factor (average load divided by peak load) from 30% to 35%. As a result, NPC increases moderately by 10% (from 20,075 € to 22,228 €), whereas LCOE decreases by 6% (from 0.553 €/kWh to 0.520 €/kWh). This outcome suggests that higher load factors can enhance cost-effectiveness by distributing fixed system costs over a larger volume of electricity consumption. However, when the peak load increases for the same daily energy demand, both NPC and LCOE experience notable increases. This is due to the requirement for larger generation and storage components to meet the higher instantaneous power demand. For example, at a constant daily demand of 11.25 kWh/day, increasing peak load from 1.57 kW to 2.69 kW results in an NPC increase from 20,075 € to 23,471 € and a 17% increase in LCOE (from 0.553 €/kWh to 0.647 €/kWh). Similarly, for a daily demand of 13.25 kWh/day, raising the peak load over the same range increases NPC from 22,228 € to 26,228 €, and LCOE from 0.520 €/kWh to 0.613 €/kWh - an 18% increase. These findings underscore the importance of peak load management in minimizing system costs. The implementation of peak shaving strategies, such as demand-side load control and/or integration of battery energy storage, could effectively smooth load profiles, reduce component oversizing, and lower the overall cost of energy generation.

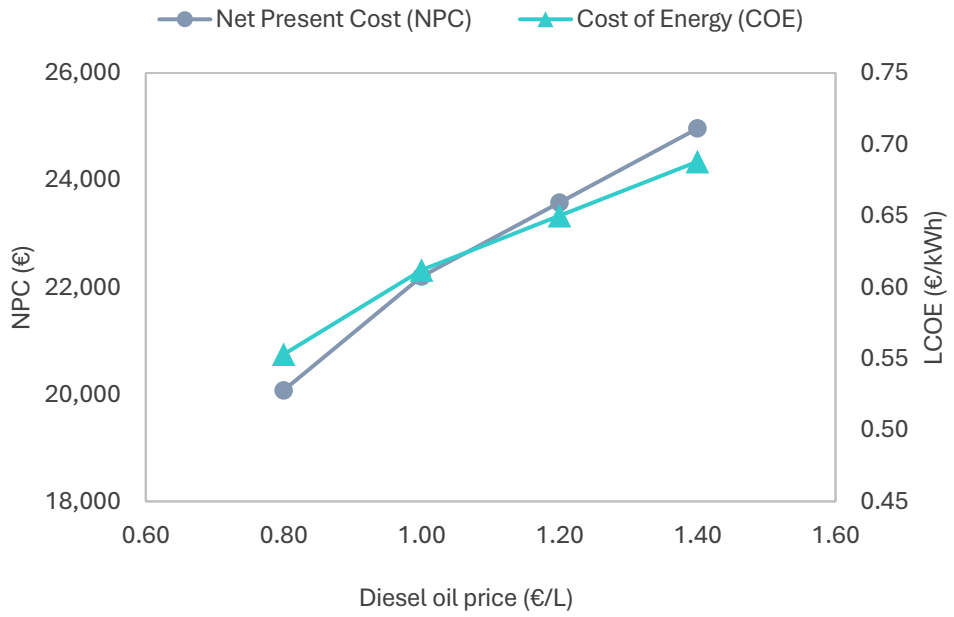

Figure 32 Effect of diesel oil price on NPC and LCOE of the hybrid PV/diesel/battery power system proposed

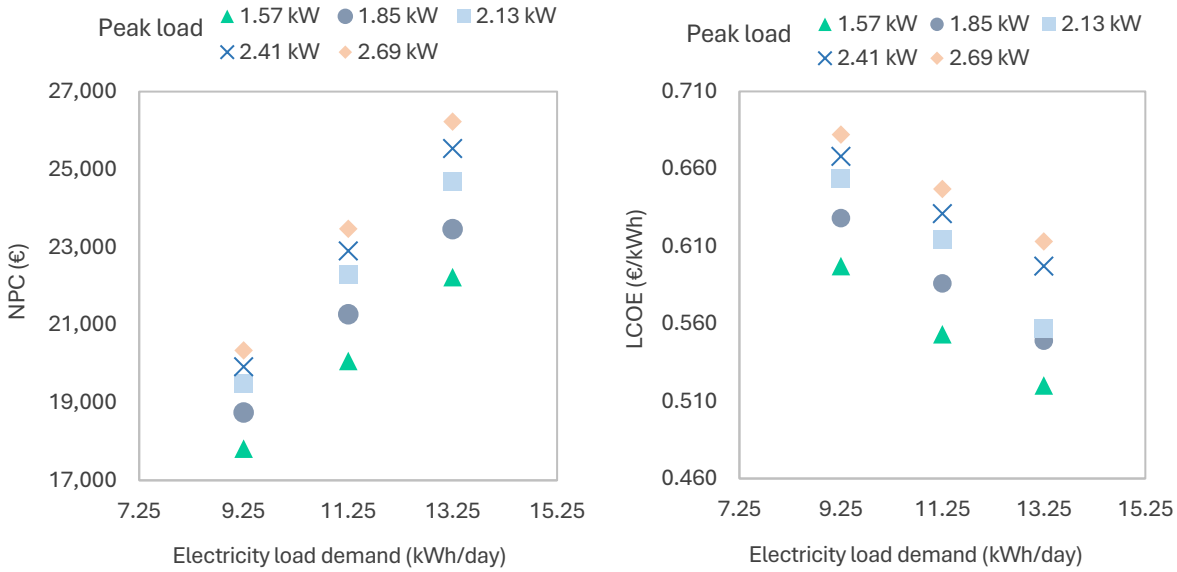

(a) NPC

(b) LCOE

Figure 33 Effect of electricity load demand and peak load on NPC and LCOE of the hybrid PV/diesel/battery power system proposed

4.2.3.1.3 Optimal break-even grid extension distance

The economic viability of the proposed autonomous hybrid energy system was evaluated in comparison to the cost of extending the national electricity grid. Based on the data provided by the Hellenic Electricity Distribution Network Operator (HEDNO) [218], the cost associated with grid extension is estimated at 40 €/m. Utilizing this figure, a break-even analysis was performed to determine the threshold distance at which the hybrid system becomes more cost-effective than grid extension. As illustrated in Figure 34, the break-even distance, which is defined as the point where the total cost of the hybrid system equals that of grid extension, is calculated at approximately 502 m. Beyond this threshold, the autonomous PV/diesel/battery hybrid system offers a more economically viable solution. Therefore, for off-grid locations such as those found in the mountainous region of Metsovo, where the distance to the nearest grid connection point exceeds 502 m, investment in a stand-alone hybrid energy system is justified both economically and logistically.

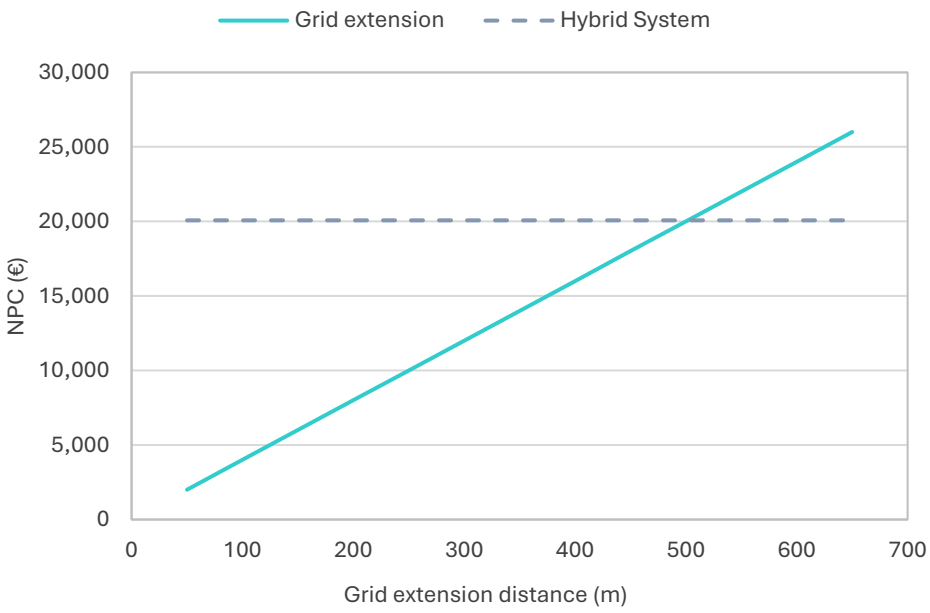

Figure 34 Electrification cost compared to the cost of an autonomous hybrid system

4.2.3.1.4 Greenhouse Gas emissions reduction

The environmental advantages of deploying the proposed hybrid power system for household electrification in Metsovo are quantified by evaluating the annual reduction in GHG emissions, in comparison to a conventional diesel-only generation system. The analysis indicates that the optimized PV/diesel/battery configuration, characterized by a REF of about 30%, yields a significant decrease in GHG emissions. Specifically, the hybrid system is projected to reduce CO_2-equivalent emissions by about 2,614 kg annually. This reduction is directly related to the substantial emissions produced by diesel generators, which are partially offset through the integration of solar PV energy. Over the 25-year lifespan of the hybrid system, a total of 65,350 tons of GHG emissions could be prevented from entering the local atmosphere of Metsovo.

The net annual GHG emissions reduction attributed to the proposed hybrid system is detailed in Table 22. A substantial decrease of approximately 43% in each pollutant is observed with a 30% renewable energy penetration in the existing diesel-only power system.

Table 22 Electricity system net annual GHG emissions reduction

Pollutant	Annual Emissions (kg/yr)		Net annual emission reduction (kg/yr)
	Diesel only	30% REF penetration	
Carbon dioxide	5,916	3,371	2,545
Carbon monoxide	15	8	7
Unburned hydrocarbons	2	1	1
Particulate matter	1	1	0
Sulphur dioxide	12	7	5
Nitrogen oxides	130	74	56
Total GHG	6,076	3,462	2,614

4.2.3.2 Biomass heating system

4.2.3.2.1 Energy modelling & economic analysis results

Energy modelling simulations indicate that the proposed heating system, consisting of a pine wood-burning thermodynamic fireplace and a diesel oil burner, will supply 29 MWh of thermal energy annually to the Metsovo household. The system design graph is depicted in Figure 35. Calculated results show that the thermodynamic fireplace, which meets the household's base heating load, provides 94.5% of the total required thermal energy. The diesel oil burner, serving as a backup and peak-load heating system, supplies the remaining 5.5% of the total annual thermal load, equivalent to 2 MWh.

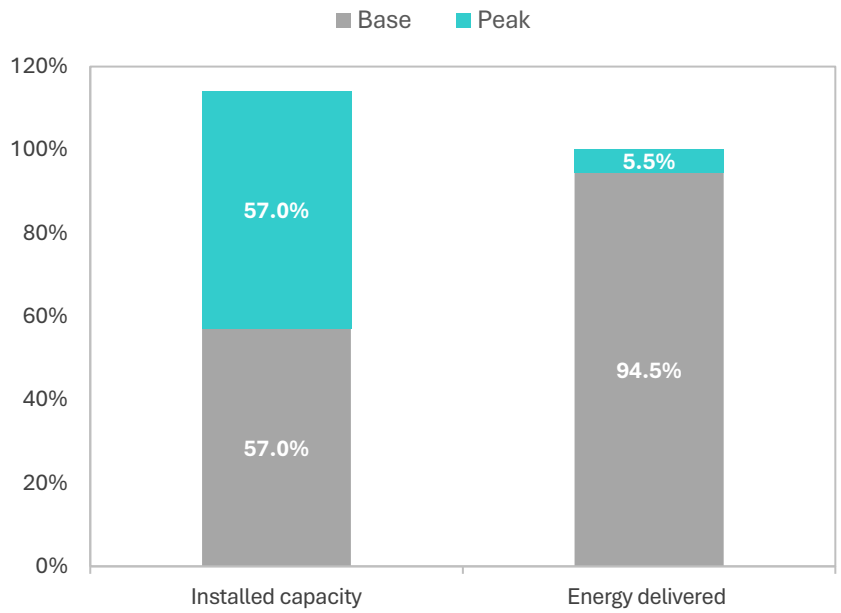

Figure 35 Proposed heating system design graph

Assuming a 12% discount rate, a 25-year investment lifetime, and no subsidy incentives, the computed NPV of the proposed biomass-based heating system is 8,500 €, with an IRR of 24.8%. It should be noted that the 12% discount rate reflects the higher risk profile of biomass projects, including uncertainty in long-term feedstock supply, price volatility and operational complexity. Additional risks arise from seasonality, storage requirements, and reliance on regulatory support frameworks subject to policy changes. The rate therefore incorporates an appropriate risk premium and provides a conservative basis for economic evaluation. The cumulative cash flow of the system over time is illustrated in Figure 36. The system achieves payback within about four years, as the cumulative cash flow turns positive at that point. This suggests that the proposed heating project is financially attractive, potentially encouraging off-grid consumers to adopt biomass combustion systems for their thermal energy needs.

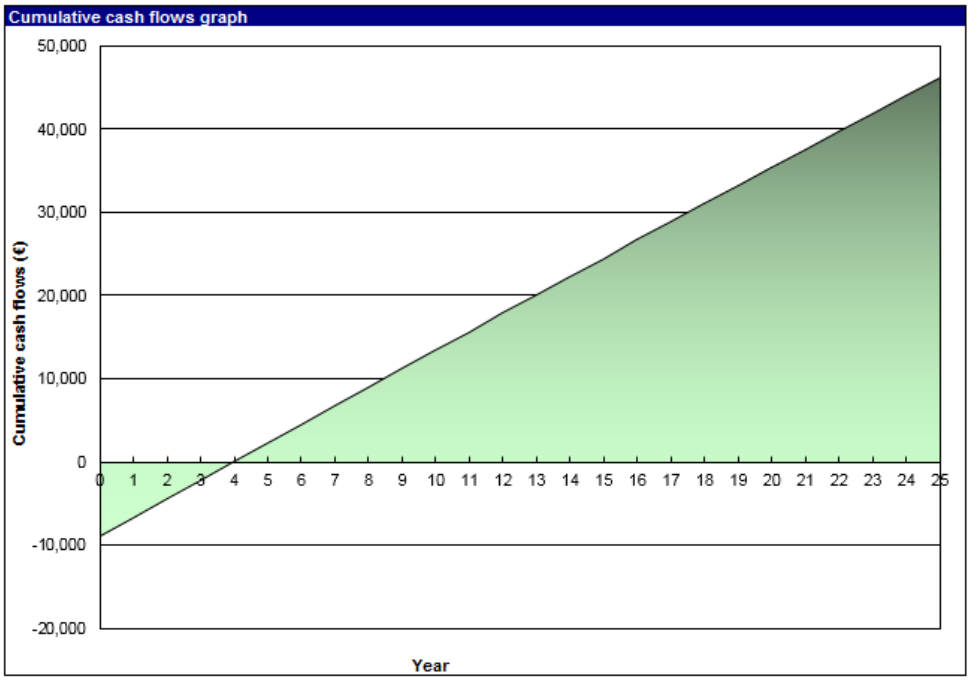

Figure 36 Cumulative cash flow for the proposed heating system

4.2.3.2.2 Sensitivity analysis results

Two critical factors influence the implementation of this biomass-based heating project in the residential sector: the total capital cost of the system and fuel costs (diesel oil and pine wood). A sensitivity analysis was conducted to assess their impact, considering both high (+15%, +30%) and low (-15%, -30%) cost scenarios relative to the nominal/reference case. The computed results for NPV and IRR are presented in Figure 37 and Figure 38, respectively. Even under the most unfavourable scenario, where both the total capital cost and fuel costs increase by 30%, the NPV remains positive at 2,993 €, and the IRR decreases to 15.6%, which is still higher than the assumed 12% discount rate. This indicates that the project remains profitable even in adverse conditions.

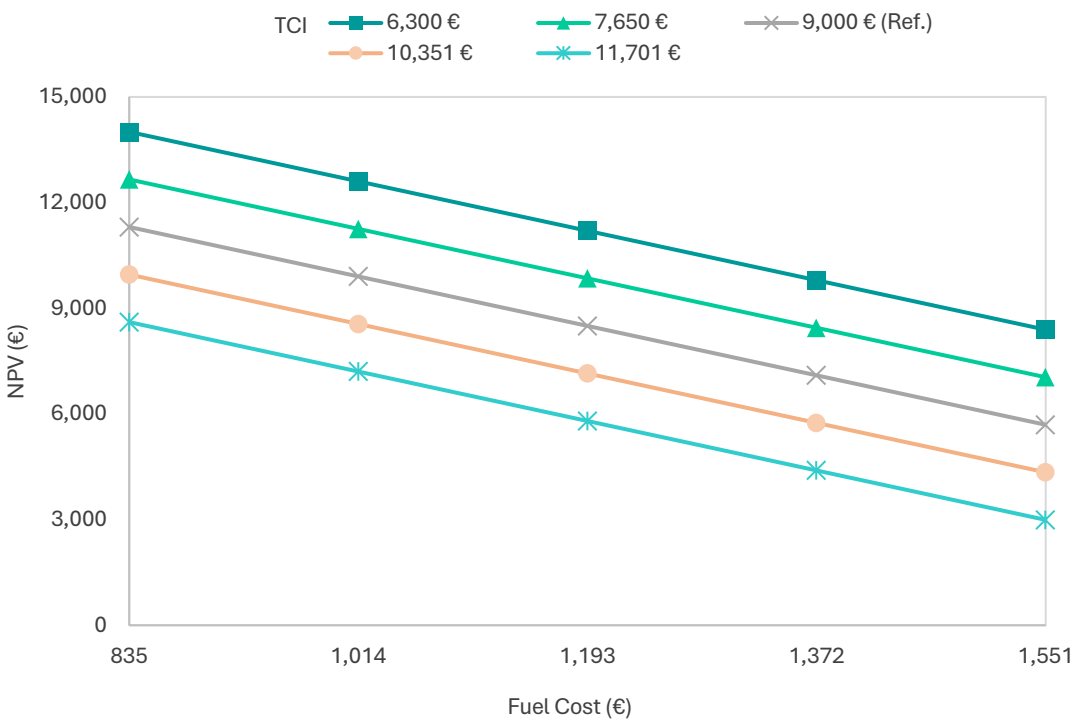

Figure 37 Sensitivity analysis of NPV with respect to fuel cost

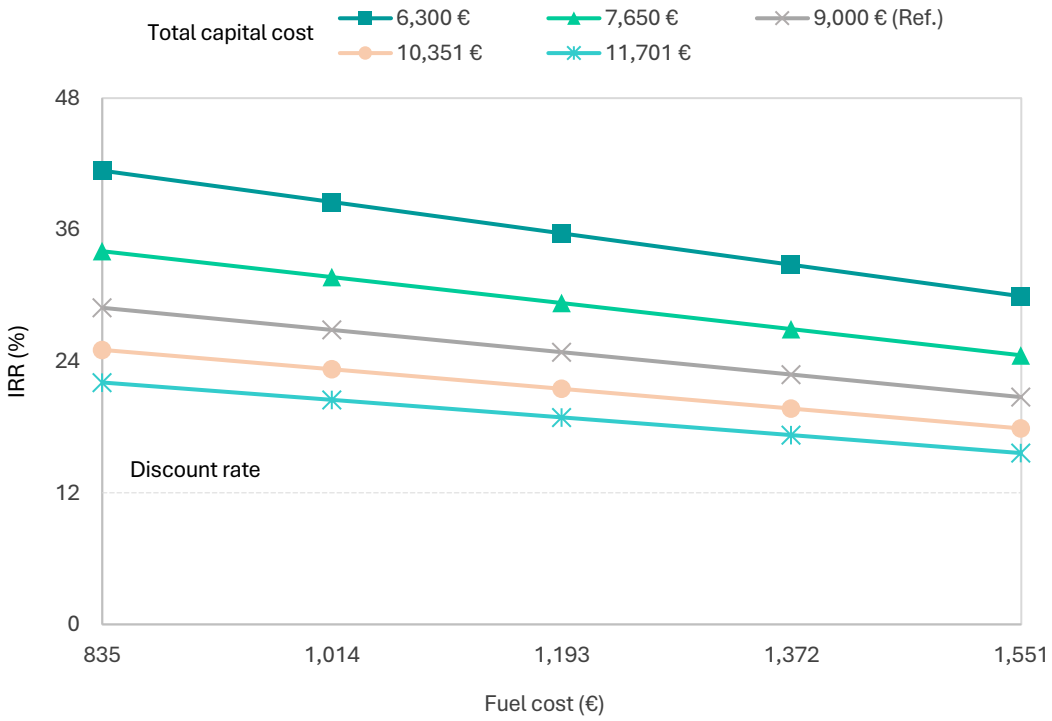

Figure 38 Sensitivity analysis of IRR with respect to fuel cost

4.3 Summary and conclusions

The investigated case studies collectively demonstrate the operational, environmental, and economic potential of renewable energy solutions for building applications, highlighting the necessity of adopting an integrated life cycle perspective. A comprehensive analysis of grid-connected PV systems reveals that increasing system capacities not only improves energy efficiency but also reduces GHG emissions and non-renewable energy consumption, with most of environmental impacts stemming from both energy-intensive silicon processing and module assembly. The rigorous economic evaluation indicates that investments in solar PV installations with rated power between 5 kW_p and 10 kW_p are generally cost effective. In contrast, smaller systems face substantial limitations, primarily because of high upfront costs and low electricity selling prices. Therefore, except in certain remote areas, such as the Greek islands or isolated mountainous villages, urban grid-connected consumers have little incentive to install solar PV systems below 5 kW_p. Nevertheless, potential increases in electricity selling prices or reductions in initial costs could stimulate the adoption of small-scale residential PV systems. Cost reduction efforts should mainly focus on module manufacturing and the production of BoS components, which constitute the largest portion of total expenses. The absence of financial incentives from the Greek government represents a significant barrier to the wider deployment of PV systems in both the domestic and commercial sectors. Currently, there is no National Energy Policy Scheme to support the integration of PV or other renewable energy technologies in buildings. To effectively promote PV as an alternative energy source, it is essential to establish a supportive policy framework that offsets the price barrier for selling renewable electricity to the national grid. Such a framework could include targeted investment incentives, well-designed feed-in tariff mechanisms, and pricing structures based on either the cost of generation or the electricity selling price. Moreover, a sustainable action plan could incorporate trading systems that provide credits to producers for fossil fuel displacement and GHG emissions reductions, further fostering the adoption of solar energy for electricity generation.

In the context of viable, fully autonomous off-grid solutions for electricity and thermal energy supply to remote rural buildings, the integration of PV arrays with diesel generators, battery storage, and biomass-based heating systems can reliably satisfy both electricity and thermal energy demand, while substantially improving the environmental footprint. The economic analysis indicates that the majority of the NPC of the system is associated with the PV modules, whereas the converter contributes the least. Sensitivity analysis further demonstrates that both the NPC and the LCOE increase with rising diesel fuel prices. Potential variations in the load profile also have a notable impact: increasing electricity demand while maintaining constant peak load elevates the NPC but reduces the LCOE, whereas increasing peak load for a constant electricity demand raises both metrics. These findings highlight the significance of load rescheduling or shifting to reduce peak demand and optimize energy generation costs. The initial investment for a combined hybrid electricity and heat autonomous system is relatively high. However, recent years have witnessed substantial cost reductions and technological advancements in autonomous hybrid power systems. To promote wider deployment of this emerging technology, financial support and incentives, such as construction subsidies, might be necessary. It is also important to mention that the costs of renewable systems are steadily declining as their deployment expands and manufacturing processes become more efficient and cost-effective. It seems that the time when the cost of energy generation via renewable energy

technologies is going to be similar to that of conventional, i.e. fossil fuel, energy systems is not too far away. Beyond economic considerations, the environmental benefits of implementing autonomous hybrid power systems, in terms of GHG emissions mitigation, are also considerable.

Collectively, these studies underscore that fully understanding the environmental and economic potential of renewable energy in building applications requires the integrated consideration of technical, operational, environmental and economic aspects. The implementation of such a holistic approach not only facilitates the design and deployment of low-carbon, sustainable, and economically viable building energy systems, but also offers actionable guidance for policymakers, industry stakeholders, and researchers. By fostering the development of efficient, resilient, and circular energy solutions, this perspective supports the transition towards sustainable urban and rural energy infrastructures. It also outlines the necessity of complementary policy frameworks, technological optimization, and life cycle-informed decision-making in achieving long-term energy and environmental targets.

Chapter 5

Community - Level Application

Building upon the techno-economic assessment and the life cycle environmental performance evaluation of renewable energy systems at the building scale presented in the previous chapter, this chapter extends the analytical framework to the community- level, focusing on the large-scale implementation of renewable energy technologies in autonomous/off-grid islands. In alignment with the national decarbonization targets and long-term sustainability objectives, the chapter addresses the design and performance evaluation of hybrid electricity supply systems that combine wind turbines, solar PVs, battery storage, and diesel backup generation for isolated applications. The proposed methodology, which bridges technical and economic optimization with life cycle environmental assessment, is demonstrated through real-world case studies on three isolated islands, particularly Lesvos, Karpathos and Astypalaia, in the Aegean Sea, Greece. These islands represent large-, medium-, and small-scale non-interconnected islands, characterized by abundant renewable energy potential and a strong dependence on thermal power plants of heavy oil fuel for electricity generation. Overall, Chapter 5 provides decision-makers with a structured and transparent methodological approach to support strategic planning and the transition of isolated island power systems towards reliable, cost-effective, and deeply decarbonized electricity generation pathways.

5.1 Case study overview

Part of his work has been published in the proceedings of the following International Conference [219] *(Sagani, A., Dedoussis V. An integrated analysis of Hybrid Energy Systems for decarbonization of off-grid Islands based on life cycle thinking. Striving for Stability in a Highly Uncertain Energy World, Maroussi Plaza Centre, Athens: HAEE Energy Transition Symposium: 2024)*.

5.1.1 Location and meteorological parameters

Lesvos is located in the north-eastern Aegean Sea (39°10'0" N, 26°20'0" E), with an area of 1,636 km^2 and a population of 85,330 habitants [220]. The current energy system of the island relies highly on existing autonomous power stations based on internal combustion engines (running on heavy oil fuel) and gas turbines (running on light diesel oil), which are owned by the PPC of Greece. Despite the high potential of powering the Island with renewables, the share of RES, mainly solar and wind power, in the electricity consumption reached 27.48 % in April 2024 [221]. Considering that Lesvos is a popular tourist destination, its population, and, consequently, the electricity demand, rises in summer (from June to August, in particular). The continuation of the operation of the existing thermal power system in the island will significantly increase the contribution to air pollution associated with fossil fuel-based power generation.

Karpathos is the second largest of the Greek Dodecanese islands located in the south-eastern Aegean Sea. It covers an area of 324 km^2 including the surrounding inlets, with a coastline of 160 km [222]. The permanent population of the island is 6,226 inhabitants; however, during the summer period, with the addition of both tourists and Karpathians visiting their homeland, the population of the island surpasses 20,000 residents [223]. The existing electricity production system in the island is based on diesel engines and a small wind park [224]. The share of the renewable energy in the electricity consumption reached 24.68% in April 2023 [221].

Lastly, Astypalaia, belonging also to the Dodecanese complex of islands, is a representative case study for investigating future perspectives of small, autonomous electricity generation systems, whose connection to other, greater electrical systems, or to interconnected electricity grid of mainland Greece, is rather difficult. The island covers an area of 96.9 km^2, and its permanent population is approximately 1,300 inhabitants (census 2011) [225]. The current energy system of the island of Astypalaia relies heavily on thermal power plants for electricity generation. In 2015, the diesel oil fuel consumption for meeting the electricity demand of the Island was about 2,300,000 Liters, indicating the necessity of its reduction from both an environmental and an economic perspective [225]. The share of renewable energies (wind and solar power) in the electricity consumption reached 16.11% in April 2023.

Solar energy potential across the selected islands

All three Aegean islands exhibit strong solar energy potential, supported by their characteristically clear atmospheric conditions, which enhance overall solar radiation levels. PV yields for the Aegean region are estimated between 1,230 and 1,530 kWh/kW_p, highlighting the suitability of the islands for solar energy deployment [226]. Relevant meteorological indicators for Lesvos, Karpathos, and Astypalaia, including the monthly average global horizontal solar radiation and the monthly average clearness index, are presented in Figure 39. These data are sourced from the NASA Surface Meteorology and Solar Energy Data Database [180]. For all three islands, solar irradiation is lowest during the winter months, namely, January, February, October, November, and December, and highest from April to September, with a peak in July. The annual average daily global horizontal irradiation is 4.62 kWh/m^2/day for Lesvos, 5.50 kWh/m^2/day for Karpathos, and 5.29 kWh/m^2/day for Astypalaia. The corresponding average clearness index values are 0.55, 0.64, and 0.62, reflecting generally clear atmospheric conditions. These metrics underscore the islands' substantial potential for solar energy utilization, especially during the extended summer period when solar availability is at its maximum.

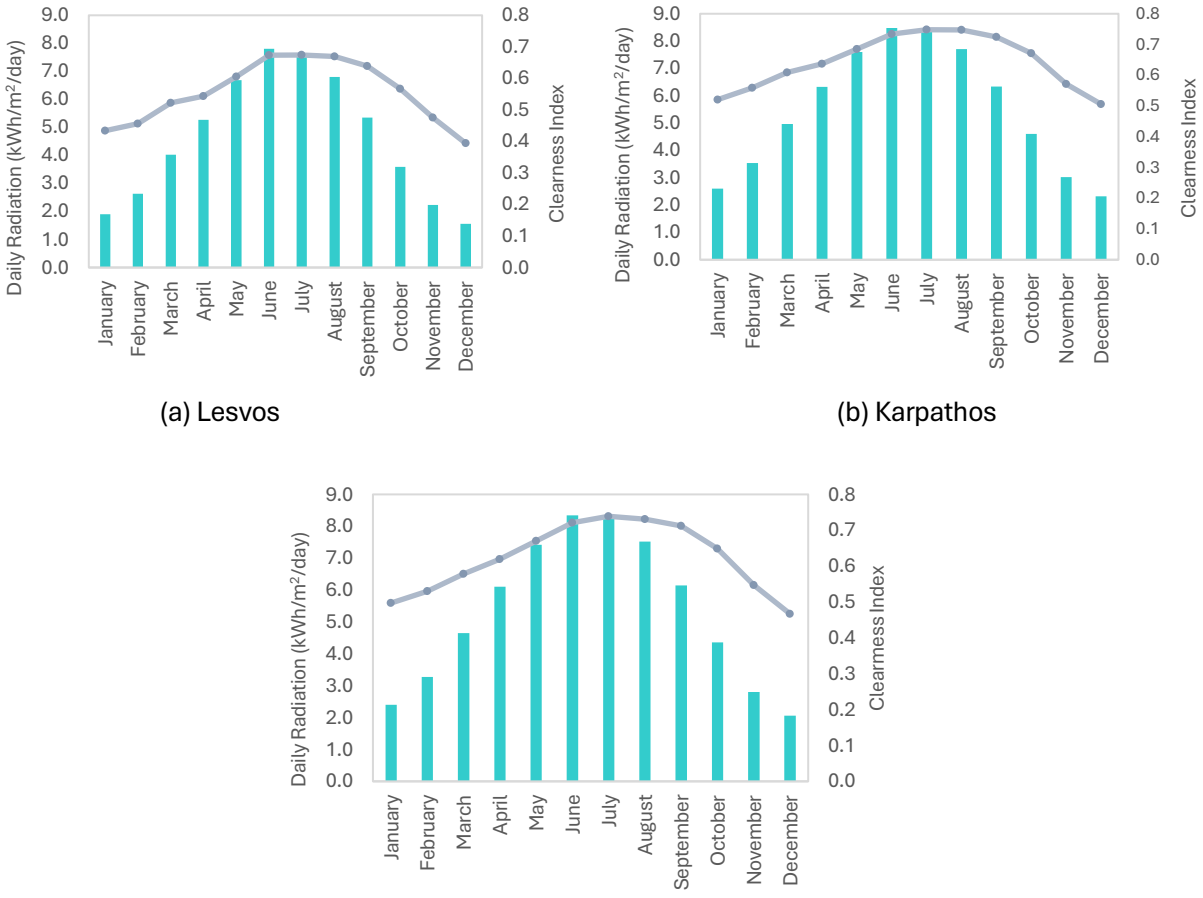

Figure 39 Monthly average solar global horizontal irradiation for all three Aegean islands

Wind energy potential across the selected islands

Wind speed data for all three islands were retrieved from [180], and correspond to the most recent available 10-year period. Figure 40 depicts the monthly average wind speeds measured at a height of 50 m over this period. It can be seen that all three Aegean islands present favourable wind energy potential throughout the year, with distinct seasonal patterns typical of the Mediterranean climate. Astypalaia exhibits the highest annual average wind speed, estimated at 7.56 m/s, with a peak value of 9.12 m/s occurring in July. Karpathos displays similar behaviour, with maximum wind speed values of 8.65 m/s in July and 8.04 m/s in August, and an annual mean of approximately 7.26 m/s. Although Lesvos records slightly lower speeds, it still presents substantial wind potential, with its peak at 7.55 m/s in February and 7.48 m/s in December, and an annual average of about 6.69 m/s. Overall, monthly wind speeds across the three islands range from 5.46 m/s to 9.12 m/s, corresponding to favourable wind power classes suitable for commercial wind turbine installations. These findings confirm that all three islands are exceptionally suitable for wind energy development and agree well with the trends reported in the literature.

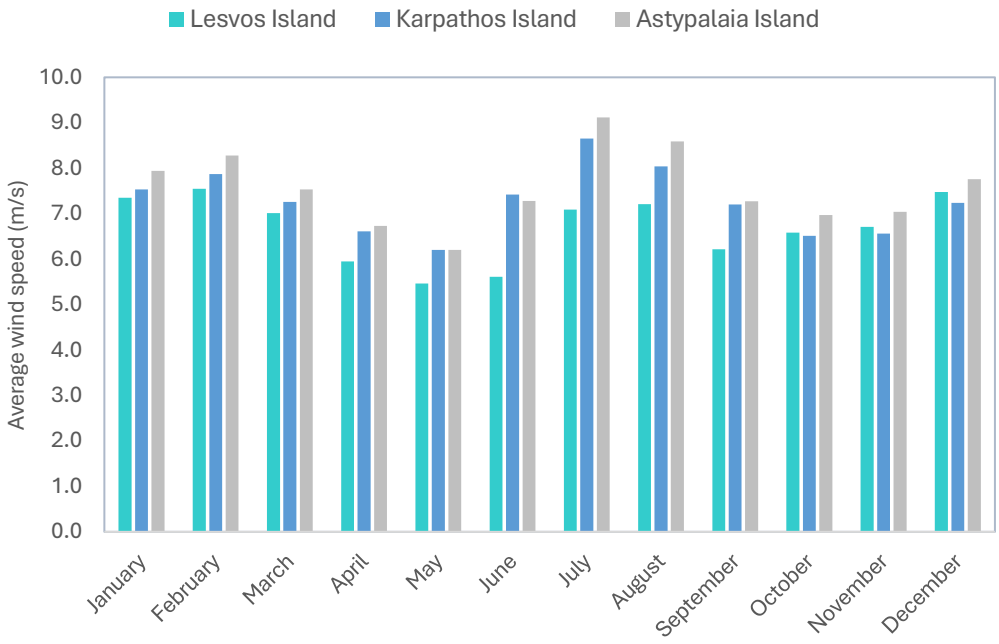

Figure 40 Monthly average wind speed data for all three Aegean islands

5.1.2 Electric load data

Electric load data for these islands indicate distinctive patterns that the literature links to their isolated power systems, strong dependence on tourism, and limited local generation. Studies consistently report pronounced seasonal variability, with electricity requirements rising substantially in summer months due to tourists inflows, increased cooling demand, and intensified commercial activity, whereas winter load remains comparatively low. The limited presence of stabilizing industrial loads further accentuates these fluctuations, making load forecasting and system planning more challenging for the Aegean region [227]. According to the data published by HEDNO [221] for the year 2024, the average monthly electrical energy production of Lesvos, Karpathos, and Astypalaia is shown in Table 23, Table 24, and Table 25, respectively. The total annual average electricity production is 278.36 GWh in Lesvos, 43.89 GWh in Karpathos, and 7.17 GWh in Astypalaia.

The hourly electricity production data for the entire year were generated based on the monthly average values. To account for daily fluctuations, an hourly profile for a specific day, provided by HOMER, was used as a reference and scaled appropriately for each month. This approach ensures that the generated hourly data reflect both the seasonal variations in monthly averages and the typical intra-day variations observed in electricity production. The daily electric load profiles for Lesvos, Karpathos, and Astypalaia are presented in Figure 41, with the corresponding seasonal profiles illustrated in Figure 42.

Table 23 Electricity generation data in Lesvos – Year 2024

Month	Thermal Stations			RES Technologies	
	Capacity (MW)	Generation (MWh)	Peak (MW)	Generation (MWh)	Share (%)
January	102.56	19,866.13	63.00	5,260.30	20.94
February	102.56	17,483,89	63,00	4,713.74	21.24
March	102.56	16,829.71	63.00	4,071.60	19.48
April	102.56	12,644.06	63,00	4,790.12	27.48
May	102.56	15,489.17	63.00	3,634.62	19.01
June	102.56	20,483.68	63,00	4,756.71	18.85
July	102.56	25,503.69	63.00	6,003.45	19.05
August	102.56	25,933.05	63,00	4,919.88	15.95
September	102.56	18,228.83	63.00	3,801.54	17.26
October	102.56	13,822.08	63,00	4,433.21	24.28
November	102.56	17,143.37	63.00	3,881.80	18.46
December	102.56	20,307.11	63,00	4,357.35	17.67
Total	-	223,734.77	-	54,624.32	-

Table 24 Electricity generation data in Karpathos – Year 2024

Month	Thermal Stations			RES Technologies	
	Capacity (MW)	Generation (MWh)	Peak (MW)	Generation (MWh)	Share (%)
January	25.35	2,095.26	13.43	479.50	18.62
February	25.35	1,906.12	13.43	514.37	21.25
March	25.35	1,844.92	13.43	475,04	20.48
April	25.35	1,659.84	13.43	543.92	24.68
May	25.35	2,624.40	13.43	640.87	19.63
June	25.35	4,421.59	13.43	664.75	13.07
July	25.35	5,623.34	13.43	760.53	11.91
August	25.35	6,121.44	13.43	738.08	10.66
September	25.35	4,301.52	13.43	629.77	12.77
October	25.35	2,394.50	13.43	545.43	18.58
November	25.35	1,886.62	13.43	415.13	18.04
December	25.35	2,168.17	13.43	434.09	16.68
Total	-	37,047.72	-	6,841.48	-

Table 25 Electricity generation data in Astypalaia – Year 2024

Month	Thermal Stations			RES Technologies	
	Capacity (MW)	Generation (MWh)	Peak (MW)	Generation (MWh)	Share (%)
January	5.10	390.27	2.53	27.93	6.68
February	5.10	346.25	2.53	43.34	11.13
March	5.10	319.60	2.53	55.93	14.89
April	5.10	304.26	2.53	58.45	16.11
May	5.10	414.25	2.53	63.19	13.23
June	5.10	724.78	2.53	63.19	8.02
July	5.10	1,075.89	2.53	64.24	5.63
August	5.10	1,197.05	2.53	62.77	4.98
September	5.10	694.22	2.53	56.43	7.52
October	5.10	368.79	2.53	56.43	12.73
November	5.10	331.80	2.53	39.56	10.65
December	5.10	389.19	2.53	26.65	6.41
Total	-	6,556.35	-	618.11	-

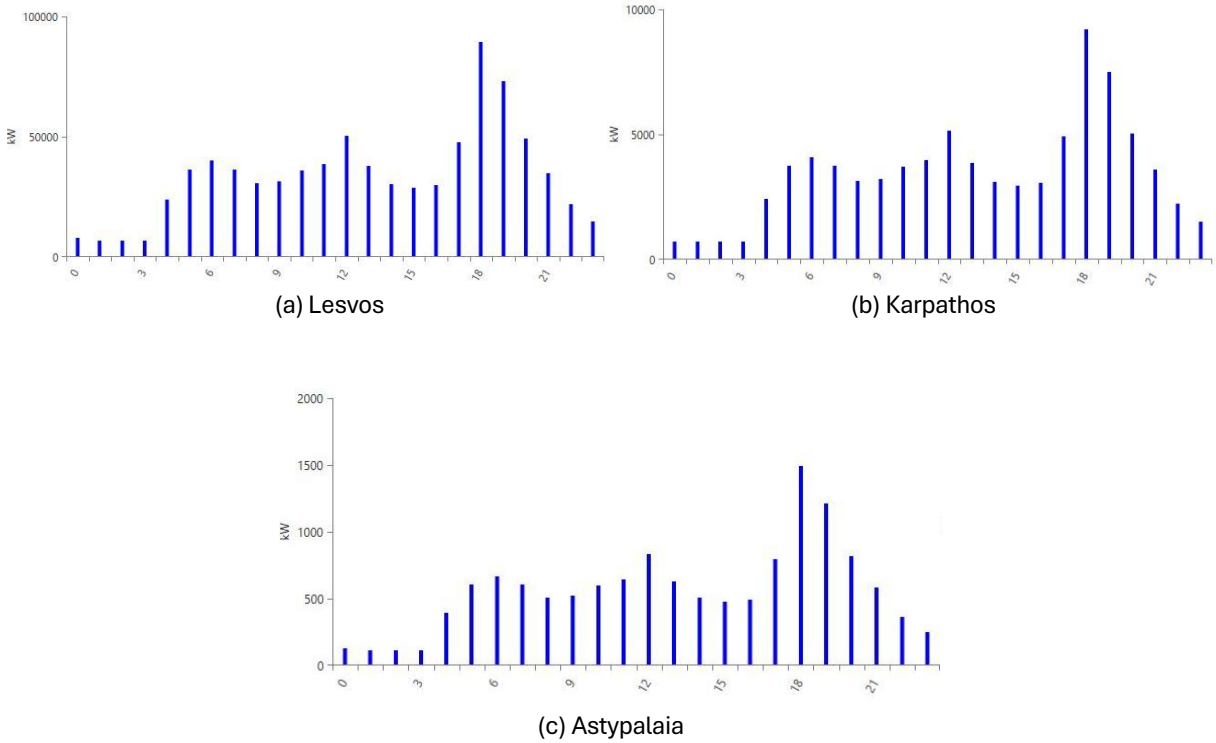

(a) Lesvos

(b) Karpathos

(c) Astypalaia

Figure 41 Daily electric load profiles for selected Aegean islands

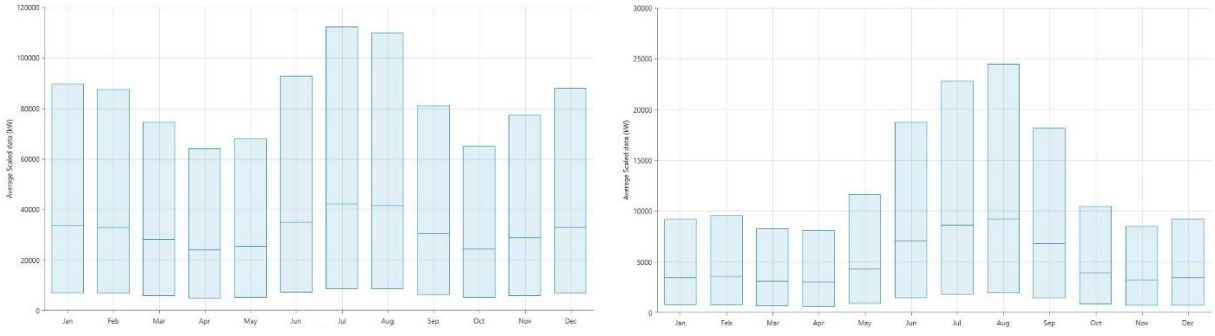

(a) Lesvos

(b) Karpathos

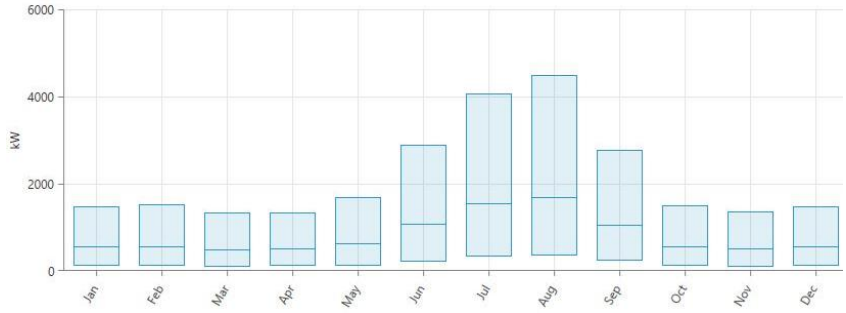

(c) Astypalaia

Figure 42 Seasonal electric load profiles for selected Aegean islands

According to the Python-based simulation, the total daily electricity demand for Lesvos amounts to 751.64 MWh/day, while the relevant values for Karpathos and Astypalaia are 120.24 MWh/day, and 19.66 MWh/day. Furthermore, the peak demand for Lesvos reaches 112.33 MW, whilst the corresponding values for Karpathos and Astypalaia are evaluated at 25 MW and 4.49 MW, respectively, based on their relevant load factors. It can be observed from Figure 41 that electricity requirements vary throughout the day. More specifically, all three islands follow a similar pattern: electricity generation gradually increases after the early morning hours, reaches a first peak about midday, and then rises again towards a higher evening peak between 18:00-19:00. Electricity generation levels are lowest during the night, reflecting decreased night-time consumption. A smooth increment starts in the early morning hours, as daily activities resume across households and businesses. The overall magnitude of each island's profile aligns with its population size and electricity demand, with Lesvos showing the highest values, followed by Karpathos and Astypalaia. Regarding the seasonal profile (see Figure 42), the highest electricity loads for all islands are expected to occur in the summer months (June to August), primarily due to the high temperatures, which result in substantial electricity demand for air-conditioning and cooling systems.

5.1.3 Energy cost data

One of key characteristics of the autonomous energy systems on the Aegean islands is the high cost of generating electricity, mainly because the islands rely almost entirely on imported oil and diesel electric generators, which are expensive and inefficient. In addition, substantial fluctuations in electricity demand further contribute to elevated costs, since they require either a higher installed generation capacity or the frequent redeployment of generators to meet peak electricity demand periods [227]. The total cost of energy production varies among the three islands under investigation. This is expected, considering the notable differences in electricity consumption across the energy systems of the islands. The energy producers that provide electricity to the off-grid/isolated islands are compensated for the total energy production cost, expressed in €/MWh, which is defined by Equation 47 [227,228].

$$Production\ Cost_{m,s} = \frac{VC_{m,s} + C_{GHG_{m,s}} + RAV_{m,s} \cdot r + D_{m,s} + OC_{m,s} + IC_{m,s} + AC_{m,s}}{Q_{m,s}} \quad (47)$$

$VC_{m,s}$ refers to the variable cost of electricity, particularly the cost of fuel of electricity production including excise duty, $C_{GHG_{m,s}}$ denotes the cost of GHG emissions, $RAV_{m,s}$ is the sum of the non-depreciated value of fixed assets plus the working capital (also called "Regular asset base"), r is the reasonable return on the value of the regulated asset base, $D_{m,s}$ is the depreciation of fixed assets, $OC_{m,s}$ represents the operational expenses, encompassing payroll costs, maintenance and replacement costs, insurance costs, third-parties remuneration, costs of electricity consumed by the energy units, taxes and levies, $IC_{m,s}$ denotes the expenses for renting, transferring and installing electrical generators for meeting seasonal energy demand, and $AC_{m,s}$ reflects the shared administrative costs. Additionally, $Q_{m,s}$ represents the sum of net electricity produced and supplied to the grid from all thermal stations of each autonomous system (s) per month (m) in MWh.

The total monthly production cost for the selected islands is depicted in Figure 43, based on official cost data provided by HEDNO for the year 2024 [221]. Lesvos records the lowest average cost, estimated at 264.38 €/MWh, with relatively stable monthly figures lying in the range 229.29 (in July) to 382.05 €/MWh (in January). On the other hand, Karpathos has a higher average cost of 362.16 €/MWh, with a notable peak in November (736.09 €/MWh), accounting for seasonal demand fluctuations. Last, but not least, Astypalaia exhibits the highest average cost at 573.40 €/MWh, reaching up to 786.09 €/MWh in November, while the lowest figure occurs in June (446.46 €/MWh). These differences demonstrate the effect of island-specific load demand patterns and generation constraints on overall electricity production costs.

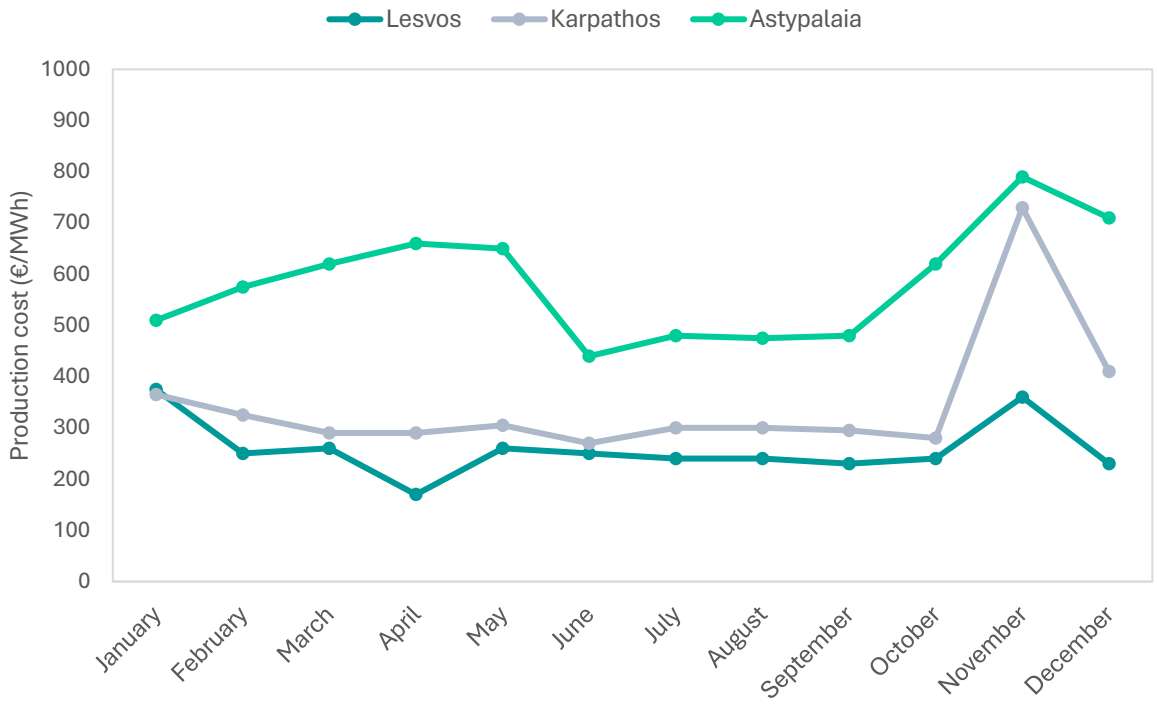

Figure 43 Monthly production cost or the selected Aegean islands (Ref. Year 2024)

5.2.Modelling of hybrid electricity power supply systems

System components

In the design of the hybrid electricity power supply systems, a combination of solar PV, wind, battery storage, electric diesel generation, and power conversion was analysed to identify cost-effective configurations capable of reliably meeting the electricity demand in the selected islands, while minimizing both diesel fuel consumption and the climate change impact, in terms of GHG emissions.

The first step is to define the renewable energy components to be added to the system. For solar power, a generic flat-plate PV system was employed in all cases, as it is the commonly applied type of PV technology. The specific capital investment cost of the utility-scale PV system was set at 650 €/kW, with an O&M cost of 19.5 €/kW/year, equivalent to 3% of the initial cost. The solar PV system operates with a derating factor of 80% and is expected to have a lifetime of 25 years. Based on the electric load requirements of each island, different wind turbine models were selected For Lesvos, the Leitwind E-101 wind turbine with a capacity of 2.5 MW was chosen, while for Karpathos and Astypalaia, the Leitwind 77 model with a capacity of 1 MW was selected. All wind turbines are expected to have a lifetime of 20 years. It should be noted that the hub height of each wind turbine was selected according to the manufacturer's recommendations; namely, 93.50 m for the Leitwind E-101 model, and 80m for the Leitwind 77 model. The initial capital cost of the wind turbine is 1.300 €/kW, while the relevant O&M cost is 39 €/kW/year, also representing 3% of the capital cost, as in the case of the solar PV system [229,230].

The next step is to incorporate energy storage (batteries) into the hybrid power systems, aiming at increasing the penetration of renewable energy technologies, namely, solar PV and wind, enhance network stability, as well as support the transition of each Island towards more autonomous and resilient energy systems. Storage batteries play a fundamental role in addressing the fluctuating/intermittent nature of solar and wind energy by absorbing excess electricity generation during periods of low demand and releasing it when demand exceeds the renewable energy supply. By integrating storage, the autonomous/off-grid islands can better manage peak loads, minimize curtailment of renewable energy, and achieve more sustainable and self-sufficient energy systems. In the present analysis, Lithium-Ion (Li-Ion) batteries with 1 MWh of energy storage were selected, with a roundtrip efficiency of 90%, a minimum state of charge of 40%, and a lifetime of 15 years. It is worth mentioning that the cost of storage batteries notably decreased in recent years; this is attributed to technological advancements and large-scale deployment. Based on the relevant literature, the initial capital cost of Li-Ion batteries is assumed to be 160 €/MWh, while the relevant O&M cost is set at 3.2 €/MWh/year, representing only 2% of the capital investment [229,230].

Subsequently, a diesel generator is sized in such a way so as to be able to meet the peak load demand of electricity, especially when both the generator and the loads are connected to the same AC bus. On the other hand, it should run at very low loads during ‘‘off-peak” hours [211]. An auto-sizing diesel generator is considered in the present work in order to meet the electric load requirements. According to official data provided by HEDNO for the year 2023, the diesel fuel price in Lesvos, Karpathos, and Astypalaia reached 0.839, 0.925 and 0.924, respectively [230]. The diesel generator is assumed not to be purchased, as it is already operational in the current islands’ system. The minimum load factor is 25%, the lifetime is estimated at 150,000 hours, and the O&M cost is 0.030 € per operating hour.

Since the hybrid systems encompass both AC and DC components, power converters are also required. The converter functions as both an inverter, in which DC components serve an AC load, and a rectifier, in which AC components serve a DC load. In the system considered in this work, the efficiency of the converter is assumed to be 95% and its lifetime 15 years. From an economic perspective, the initial capital cost of the system converter is set at 300€/kW and the O&M cost at 9 €/kW/year, which is equivalent to 3% of the capital cost [230].

At this point, it should be noted that for all the islands under investigation, the discount rate was set at 8%, and the inflation rate was assumed to be 2%, based on historical average data from the Hellenic Statistical Authority (ELSTAT) over the past ten year [231]. The project lifetime is 25 years.

Operating strategies and system control parameters

The proposed hybrid electricity power systems are assumed to operate according to the LF dispatch strategy, thoroughly presented in Chapter 3. Under this strategy, the diesel generator is called upon to produce just the amount of power that is required to meet excessive load demands. Lower-priority tasks, in particular, such as charging battery storage elements are left to RES - wind turbines and PV modules. The LF dispatch strategy is particularly well suited for off-grid or isolated systems with high renewable energy potential. Adopting this strategy can lead to a reduction in the total NPC of the system, as well as a decrease

in associated emissions. The surplus electricity produced may be also reduced, since it is only utilized just to charge the storage batteries.

The following analysis constraints are also applied:

i. Maximum annual capacity shortage*:*
The maximum annual capacity shortage represents the highest allowable value of the capacity shortage fraction, defined as the total capacity shortage divided by the total electricity load [232]. In this analysis, it is set to zero, so as to ensure that the system is designed to cover even the highest peak loads without any capacity shortage.

ii. Minimum renewable fraction*:*
The minimum REF denotes the lowest acceptable percentage of annual electricity generation that should be derived from renewable resources. It defines the threshold below which the contribution of renewables to the overall electricity mix cannot drop. For this case study, the minimum renewable fraction was set at 35% [233].

iii. Operating Reserve:
The OpRe is the surplus operating capacity that ensures reliable electricity supply in unexpected and perhaps random situations where the load demand suddenly increases, or renewable power output suddenly decreases or fails. In the current analysis, OpRe is set to be 10%, 25% and 50%, as a percentage of hourly load, solar power output and wind power output, respectively. It is evaluated, as follows [15]:

$$OpRe = (0.10 \times E_L) + (0.25 \times E_{PV}) + (0.50 \times E_{WT}) \quad (48)$$

E_L is the energy required by the load, E_{PV} is the energy generated by the PV system, and E_{WT} is the energy generated by the wind turbines.

The entire hybrid electricity supply systems are simulated and optimized employing the HOMER software platform [200], enabling detailed hourly modelling over a full year. Specifically, following the load dispatch strategy described in Chapter 3, the simulation aims at optimizing the operation of solar PV, wind, battery storage, and diesel generation, while considering load variability, resource availability, operational constraints, and component costs. Diesel consumption is modelled employing load-dependent fuel curves within rated capacity, and battery behavior included depth -of-discharge limits, round-trip efficiency, and converter losses. HOMER then identifies the least-cost configuration that meets the islands' electricity requirements with minimal diesel use and maximum renewable energy contribution. The energy flow diagram of the proposed hybrid wind/PV/diesel/battery electricity supply system for the different islands considered, as simulated by HOMER Software, is presented in Figure 44.

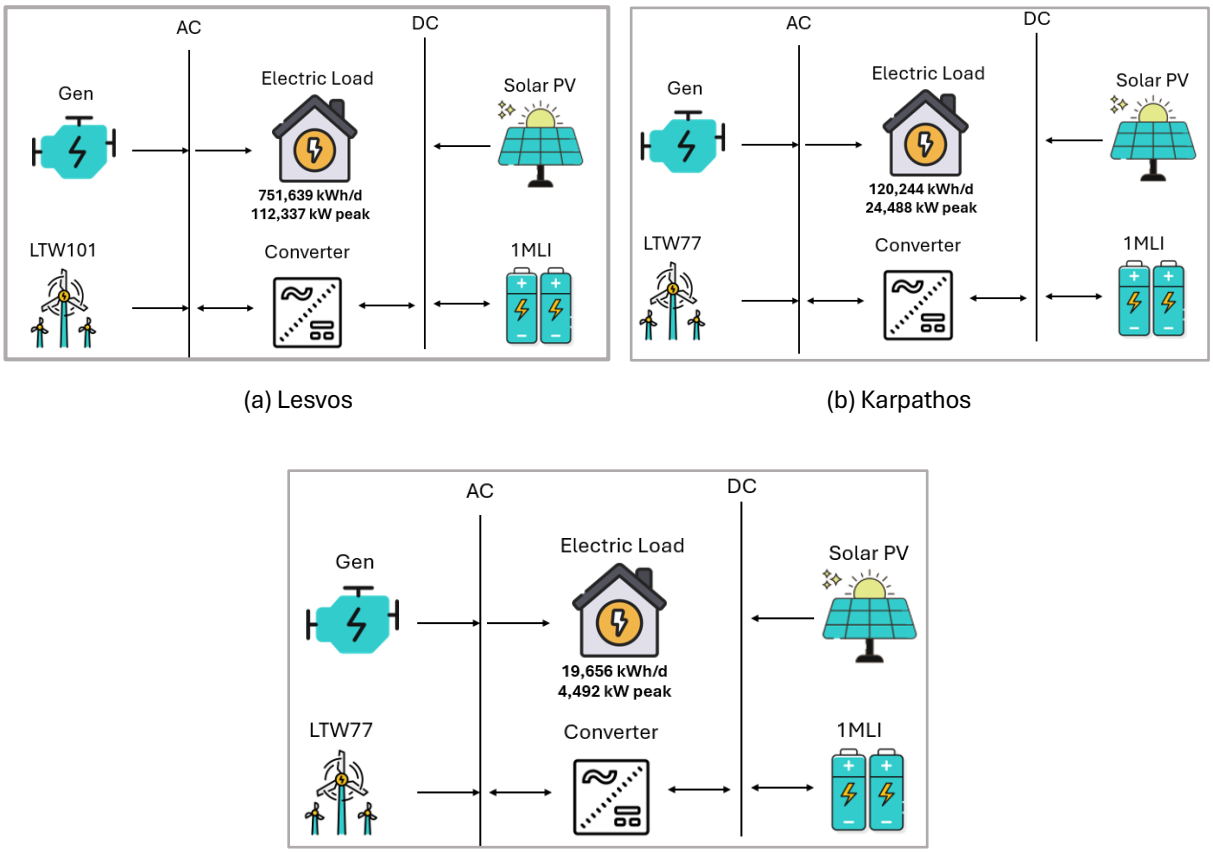

(a) Lesvos

(b) Karpathos

(c) Astypalaia

Figure 44 Configuration of hybrid PV/wind/diesel/battery systems in the selected islands

5.3 Simulation results and discussion

5.3.1 Energy modelling and economic optimization results

Big island Analysis - The case of Lesvos

According to the NPC and LCOE metrics described in Chapter 3, the most cost-effective configuration for the Lesvos island is a hybrid PV/diesel/battery system. This optimal setup consists of 60 MW of PV capacity, 35 wind turbines of 2.5 MW, a 130 MW diesel generator, and 350 batteries of 1 MWh storage each. The optimal configuration incurs a capital expenditure of 227 M€, an annual operating cost of 16.60 M€, an NPC of 441 M€, and a LCOE of 0.124 €/kWh.

The total annual electricity generated by the optimal hybrid power system is approximately 513.20 GWh. This system can meet the electricity demand of the Lesvos island, while integrating an 92.7% REF into the existing, almost entirely diesel-based power system. Specifically, the electric diesel generator produces 19,920 MWh/year of electricity, which accounts for 3.88% of the system's total annual electricity generation, and consumes 5,812,272 L fuel. A substantial percentage of the order of 78.6 % of the electricity

is supplied by the wind power systems, while the remaining 17.5% comes from the PV array. The corresponding annual energy output of the wind and solar PV power systems are about 403,528 MWh and 89,752 MWh, respectively. The high contribution from RES are important for isolated / off-grid islands in the country, such as Lesvos, which possess abundant wind and energy potential and face high diesel fuel costs. Furthermore, the cost of both solar energy conversion units and wind turbines has decreased notably in recent decades, further enhancing their economic viability in these green technologies.

In support of the high wind and solar power penetration of the hybrid electricity supply system, the batteries play a fundamental role in balancing supply and demand. The system's battery bank has a total nominal capacity of 350 MWh, allowing it to absorb excess wind and solar electricity and release it during periods of low renewable generation. The annual energy throughput of the storage system is about 46,800 MWh/year, indicating frequent cycling and effective utilization for load-shifting and grid stabilization. With an autonomy of 8.94 hours, the battery bank can supply the island's average electrical load for nearly nine hours without support from renewable systems or diesel generators. The system also produces a substantial amount of surplus renewable energy, about 44.6% of total annual generation (226,061 MWh/year), which occurs during the periods when the wind and solar output exceed both the instantaneous demand and the battery bank's charging capability. Despite the fact that the excess energy cannot be fully exploited under the current conditions, its strategic utilization not only maximizes renewable penetration but also reduces dependence on diesel generator, enhancing both the economic and environmental performance of the system. This highlights the strong renewable resource potential of Lesvos and emphasizes the need for expanded storage capacity, flexible loads, or alternative uses for surplus generation. Overall, the battery bank is essential for maintaining high REF levels, reducing curtailment, minimizing the operation of the diesel generator, and ensuring stable energy supply for isolated island grids, such as Lesvos. The power output of solar PV, wind turbines, and diesel generator is illustrated in Figure 45, Figure 46, and Figure 47, respectively.

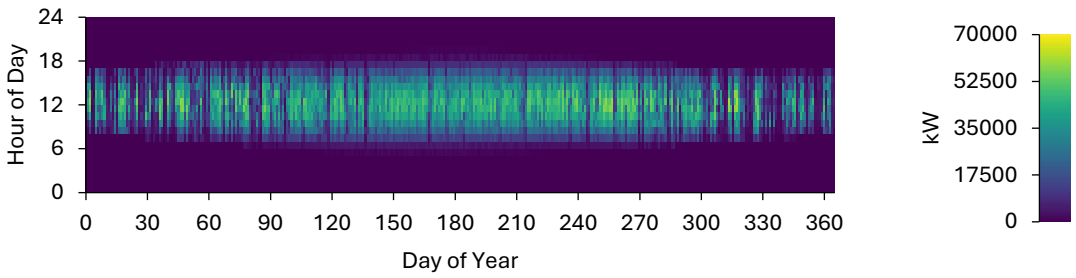

Figure 45 PV power output (Lesvos island)

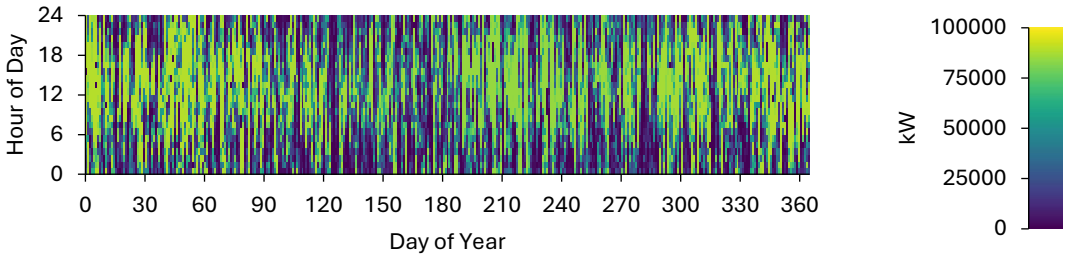

Figure 46 Wind power output (Lesvos island)

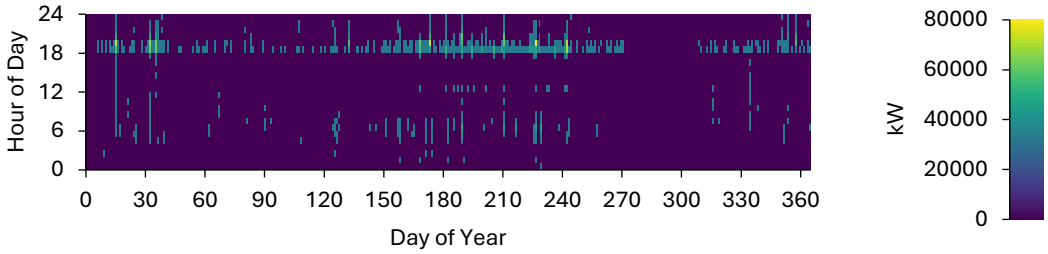

Figure 47 Diesel generator power output (Lesvos island)

The monthly average electricity generated by the optimal hybrid wind/PV/diesel/battery power system is depicted in Figure 48. The wind energy is the dominant source of electricity throughout the year, accounting for the highest share in every month. On the other hand, solar PV generation varies seasonably, with higher contributions during the summer months, i.e., June, July, and August, due to increased solar irradiance. The contribution of the electric diesel generator is relatively small, indicating that it is mainly used as a backup source when renewable generation is insufficient.

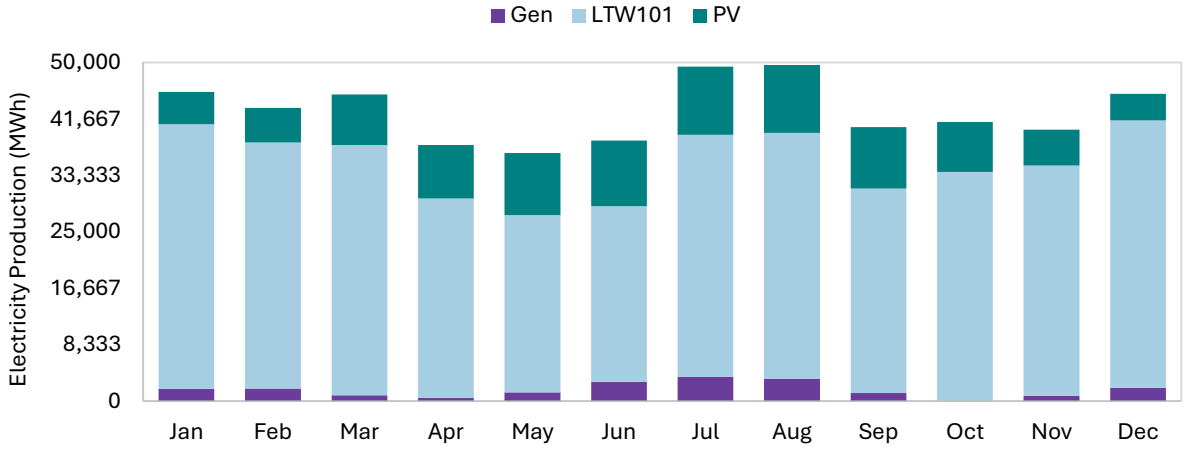

Figure 48 Monthly average electric production for the optimal hybrid PV/diesel/battery power system in Lesvos

Figure 49 presents the cash flow summary of the proposed hybrid wind/PV/diesel/battery energy system in Lesvos, expressed in terms of NPC for the main cost components over the project life-time. Detailed information on the annualized costs, including capital investment, replacement, O&M, fuel consumption, and salvage value, is provided in Figure 50. The results indicate that capital costs constitute the largest share of the total NPC; they amount to approximately 225.75 M€, corresponding to an annualized cost of 17.54 M€. Within the capital cost, the wind turbines contribute about 58% of the total, which corresponds to 113.75 M€. On the other hand, the solar PV array constitutes 17% of the total, corresponding to 39 M€. The remaining 25% is distributed among the battery storage units (56 M€) and power converter (18 M€). The high capital costs of renewable energy technologies reflect the substantial initial investment required for their installation. Therefore, targeted financial incentives and supportive policies are essential to offset the high initial costs of wind turbines and solar PV arrays on non-interconnected islands, such as Lesvos. However, despite these costs, renewable energy technologies offer long-term advantages with no fuel expenses and minimal maintenance, underscoring their strategic value in sustainable energy systems.

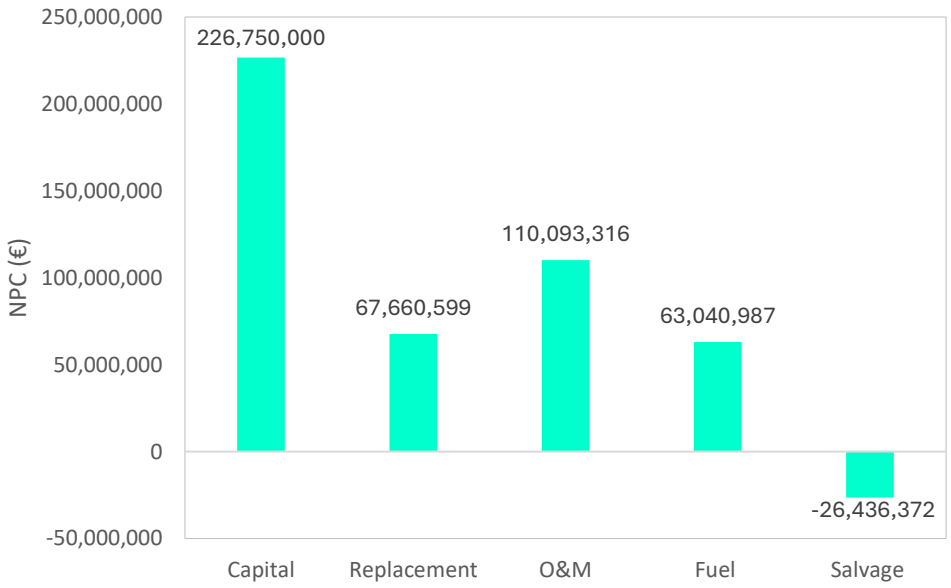

Figure 49 Cash flow summary associated with each component of the proposed hybrid system in Lesvos

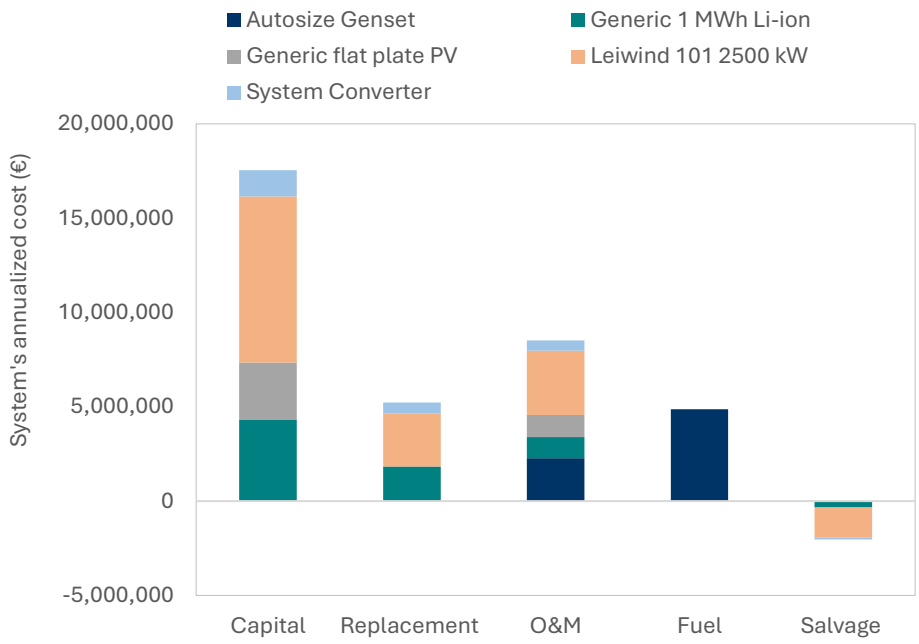

Figure 50 Annualized cost of the various components of the proposed hybrid system in Lesvos

Medium island Analysis - The case of Karpathos

The most cost-effective configuration for the Karpathos Island is a hybrid PV/diesel/battery system. This optimal setup consists of 10 MW of PV capacity, 27 wind turbines of 1.0 MW, a 27 MW electric diesel generator, and 50 batteries of 1 MWh storage each. The optimal configuration incurs a capital expenditure of 34.6 M€, an annual operating cost of 2.55 M€, an NPC of 67.5 M€, and a LCOE of 0.119 €/kWh.

The total annual electricity generated by the optimal hybrid power system is about 86.89 GWh. The proposed system can cover the electricity requirements of the Karpathos island, while integrating a 92.0% REF into its current power system. In detail, the diesel generator produces 3,507 MWh of electricity annually and consumes 1,017,307 L fuel. A 75.4% of the electricity comes from the wind turbines, and a 20.5% is supplied from the solar PV array. Lower penetration of solar is expected because solar PV only generates electricity during daylight hours. The annual overall energy output of wind and solar PV are estimated at about 65.53 MWh and 17.86 MWh. High renewable penetration is important for ensuring the sustainability of Karpathos' autonomous energy system. The battery storage, with an overall nominal capacity of 50 MWh, and an annual throughput of approximately 6.26 MWh, contributes significantly to maintaining the balance between supply and demand, and, thereby, ensuring the reliability of the system. The 5.99-hour autonomy allows the battery bank to meet the Island's average load for nearly six hours without any contribution from diesel generators. However, by prioritizing renewable output, the system results in notable excess energy, reaching 47.9% of annual production during periods of high wind and solar availability. As in the case of Lesvos, the surplus energy cannot be fully utilized under the current conditions; nonetheless, developing appropriate strategies for its exploitation would enable higher renewable penetration and a reduced need for diesel operation, yielding sustainability benefits. The power output of the solar PV array, wind turbines, and diesel generator is shown in depicted in Figure 51, Figure 52, and Figure 53, respectively.

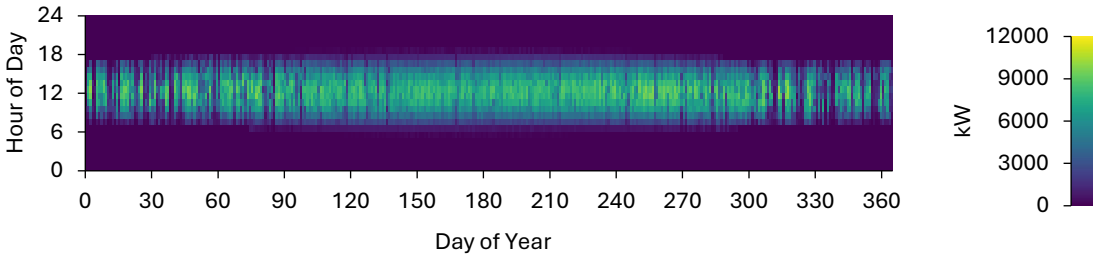

Figure 51 PV power output (Karpathos island)

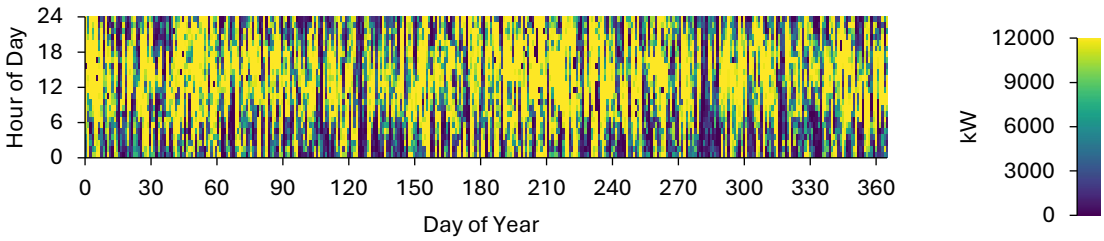

Figure 52 Wind turbine power output (Karpathos island)

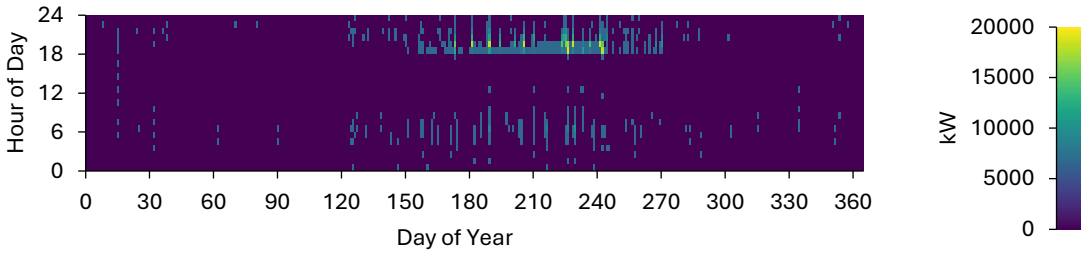

Figure 53 Diesel generator power output (Karpathos island)

The monthly average electricity generated by the optimal hybrid wind/PV/diesel/battery power system is depicted in Figure 54. It is seen that wind energy represents the primary source of electricity throughout the year, contributing the largest share in all months. On the other hand, solar PV output exhibits a clear seasonal pattern, with increased generation during the summer period, as a result of higher solar irradiance. The contribution of the diesel generator remains limited, suggesting that it is primarily utilized as a backup source during periods of insufficient renewable energy production.

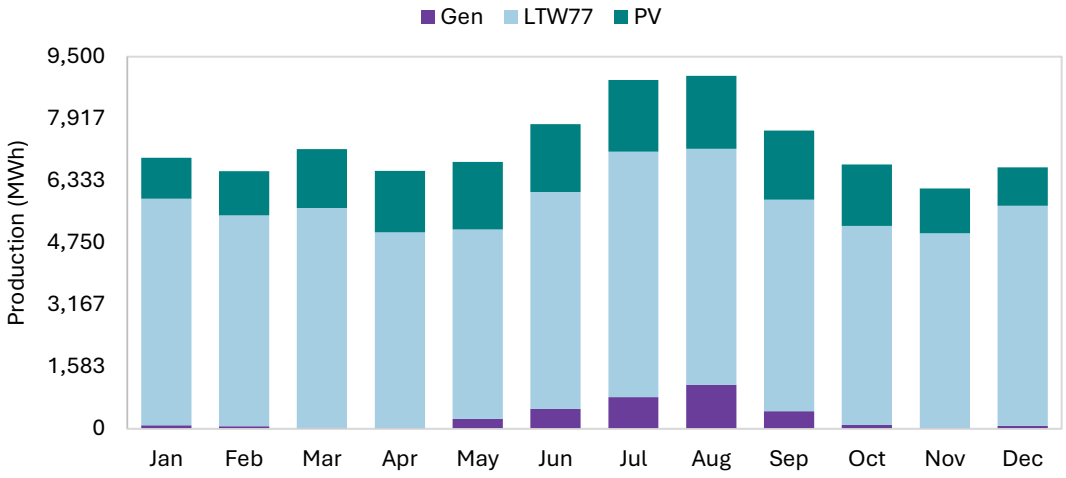

Figure 54 Monthly average electric production for the optimal hybrid PV/diesel/battery power system in Karpathos

From an economic standpoint, the initial capital cost of the proposed hybrid system is evaluated at 34 M€ (refer to Figure 55), which corresponds to an annualized cost of 2.67M€. Among all the system components, wind turbines exhibit the highest cost contribution, with a capital cost of 15.60 M€, representing 45% of the total system cost, followed by the battery storage units with a capital cost of 8 M€ (23%), and the solar PV array with 6.50 M€ (19%). The remaining 13% of the total capital cost is attributed to the power converter (4.50 M€). Detailed information on the annualized costs, including capital investment, replacement, O&M, fuel consumption, and salvage value, is shown in Figure 56. As expected, the wind turbines have the highest annualized replacement cost, estimated at 387,713 €, followed by the system converter with 147,687 €. In terms of annualized O&M costs, wind turbines represent the highest contribution (468.000 €), followed by the autosizing diesel generator (387,990 €), and the solar PV system (195,000 €). Fuel costs are associated exclusively with the diesel generator while wind and solar systems do not incur any fuel-related expenses.

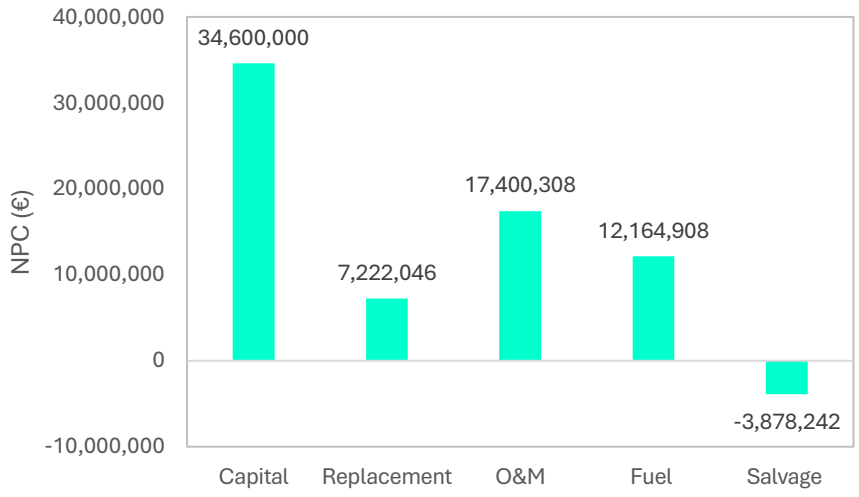

Figure 55 Cash flow summary associated with each component of the proposed hybrid system in Karpathos

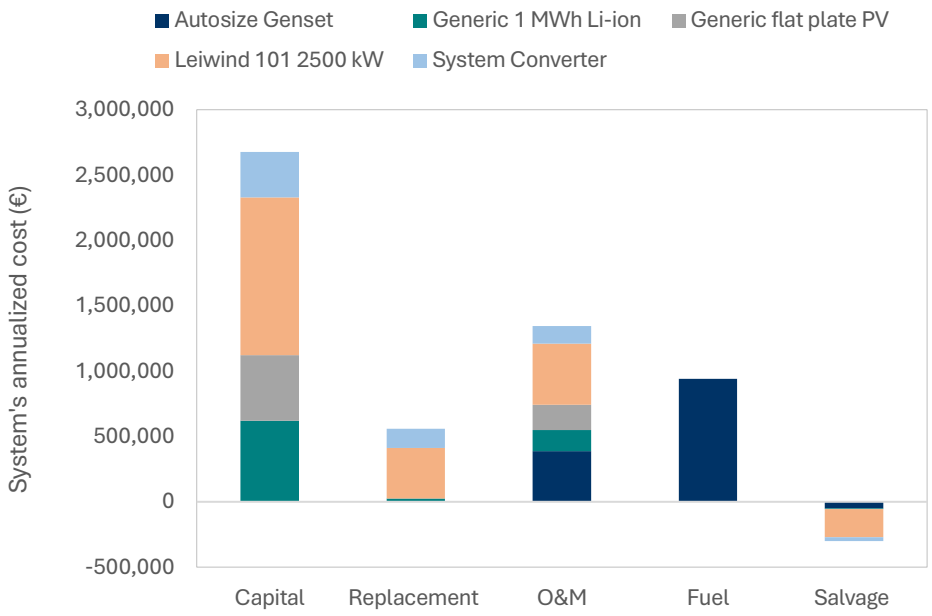

Figure 56 Annualized cost of the various components of the proposed hybrid system in Karpathos

Small island Analysis – The case of Astypalaia

The most cost-effective configuration for the Astypalaia Island is a hybrid PV/diesel/battery system. This optimal setup consists of 1.5 MW of PV capacity, 2 wind turbines of 1 MW, a 5 MW diesel generator, and 8 batteries of 1 MWh storage each. The optimal configuration incurs an NPC of 8.90 M€, and a LCOE of 0.096 €/kWh.

The total annual electricity generated by the optimal hybrid power system is approximately 14.35 GWh. This system can meet the electricity demand of the Astypalaia island, while integrating an 90.3% REF into the existing, almost entirely diesel-based power system. In detail, the autosizing diesel generator produces 698,231 kW/year of electricity, which accounts for 4.86% of the system's total annual electricity generation, and consumes 203,124 L. An important percentage of 77.2% of the electricity is supplied by the wind power systems, whilst the remaining 17.9% comes from the solar energy conversion units. The corresponding annual energy output of the wind and solar PV power systems are about 11,085 MWh, and 2,571 MWh, respectively. To balance supply and demand, 8 batteries, with total power capacity of 8 MWh, are implemented. The annual energy throughput of the storage system is about 963,535 kWh, indicating frequent cycling and effective utilization for load-shifting and grid stabilization. With an autonomy of 5.86 hours, the battery bank can supply the island's average electrical load for nearly six hours without support from renewable systems or diesel generators. A notable amount of surplus energy is also produced, reaching 6,975 MWh/year. The surplus energy occurs during the periods when the wind and solar output exceed both the instantaneous demand and the battery bank's charging capability. The power output of solar PV, wind turbines, and diesel generator is illustrated in Figure 57, Figure 58, and Figure 59, respectively.

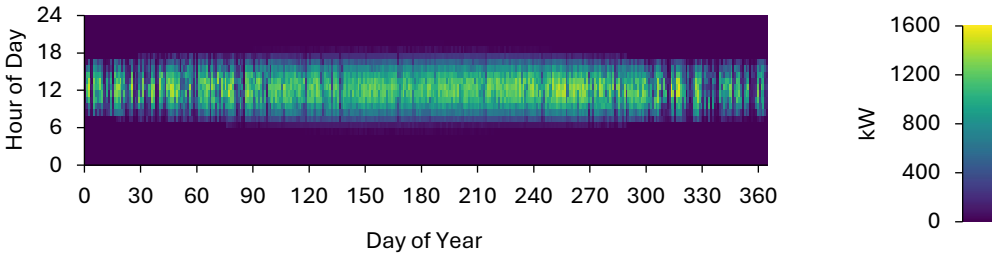

Figure 57 PV power output (Astypalaia island)

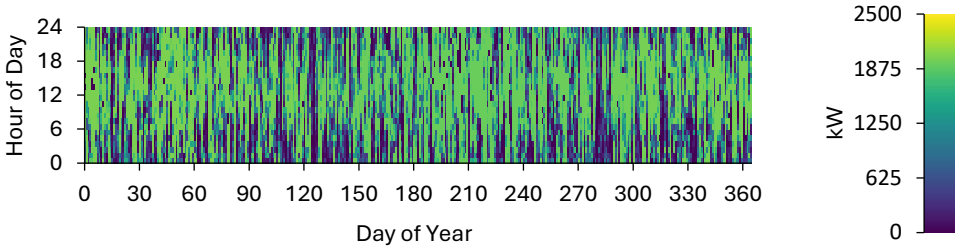

Figure 58 Wind turbine power output (Astypalaia island)

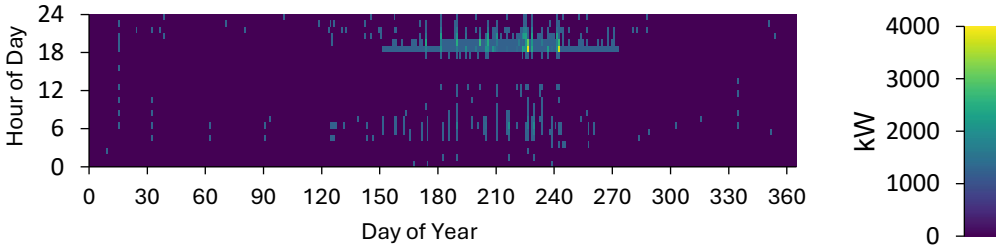

Figure 59 Diesel generator power output (Astypalaia island)

The monthly average electricity generated by the optimal hybrid wind/PV/diesel/battery power system is presented in Figure 60. It is seen that wind energy represents the primary source of electricity throughout the year, contributing the largest share in all months. On the other hand, solar PV output exhibits a clear seasonal pattern, with increased generation during the summer period, due to higher solar irradiance. The contribution of the diesel generator remains limited, suggesting that it is primarily utilized as a backup source during periods of insufficient renewable energy production.

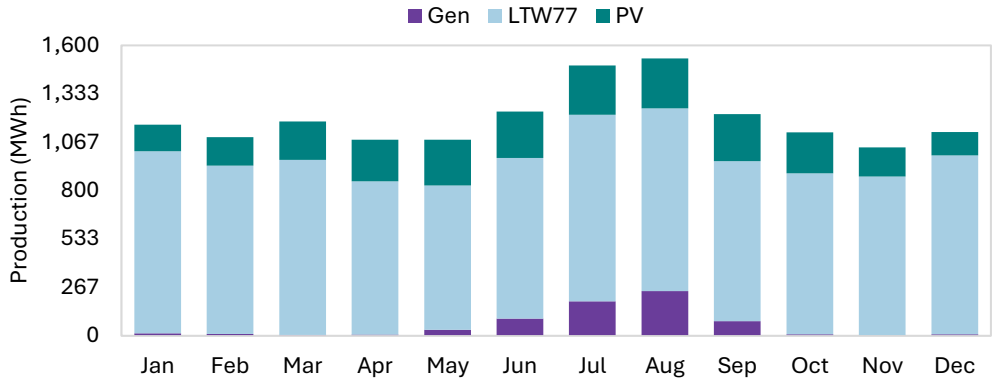

Figure 60 Monthly average electric production for the optimal hybrid PV/diesel/battery power system in Astypalaia

Figure 61 presents the cash flow summary of the proposed hybrid energy system in Astypalaia. Calculated results indicate that the capital expenditure is the dominant cost component, reaching 5.45 M€. This value highlights the substantial upfront investment for the hybrid power system. The capital cost is followed by the O&M cost at about 2.96 M€ and the fuel (diesel) cost at about 2.43 M€, demonstrating that long-term operational expenses also contribute notably to the overall l cost. Replacement costs are comparatively lower, at about 1.63 M€, suggesting that component substitution, when necessary, is not the primary cost driver. In contrast, the salvage value is negative, estimated at about -0.62 €M, reflecting a residual value at the end of the project life that partially offsets the overall life cycle cost. The annualized cost breakdown, depicted in Figure 62, that annualized capital-related costs, with a total of 421,968 €/year, are driven by the wind turbine, the solar PV array and the battery storage. Replacement costs amount to about 126,000 € annually, reflecting periodic component renewals, particularly for the wind system, battery, and power converter. Annualized O&M costs are also significant at roughly 229,300 €/year, with notable contributions of the autosizing diesel generator, and the renewable energy technologies. The fuel costs, totalling about 187,687 € annually, are exclusively associated with the diesel generator, underscoring its operational dependency on fuel compared to the renewable components.

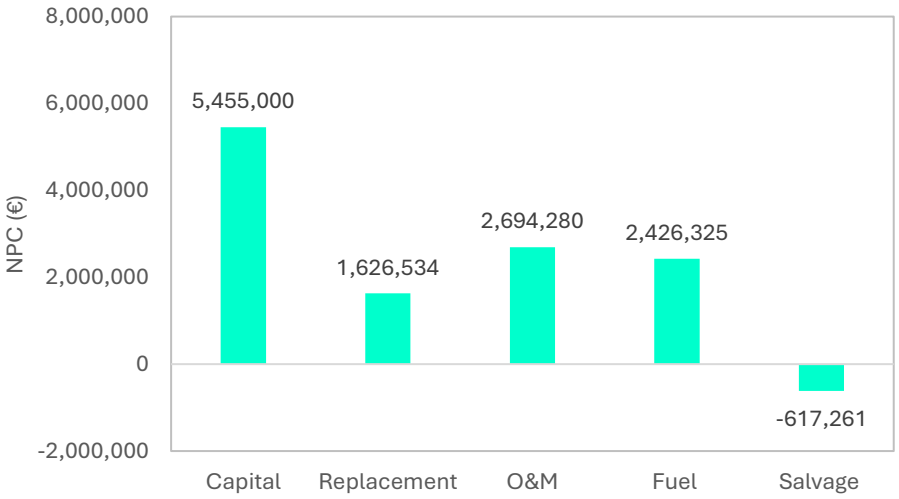

Figure 61 Cash flow summary associated with each component of the proposed hybrid system in Astypalaia

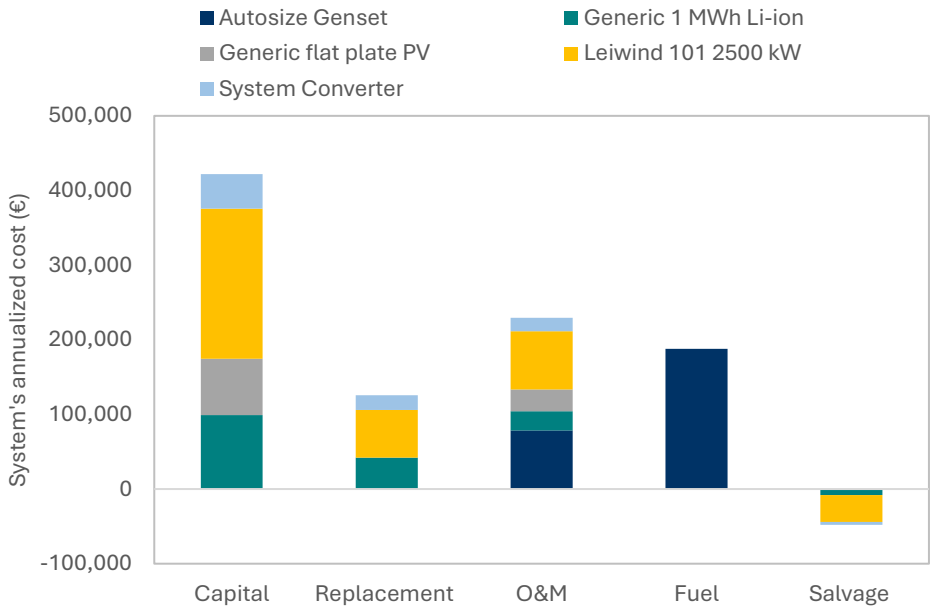

Figure 62 Annualized cost of the various components of the proposed hybrid system in Astypalaia

Comparative analysis of the results

The optimization results for all islands are summarized in Table 26. Clear differences are observed in systems sizing and economic performance across small-, medium-, and large-scale islands. Particularly, Lesvos, representing a large-scale Island, requires substantially higher installed capacities of renewable energy technologies, electric diesel generators, and battery storage to cover the energy requirements, resulting to an NPC of 441 million €. Despite the high overall cost, Lesvos achieves a substantial REF of 92.7%, although this leads to an important surplus energy share of 44.6%. On the other hand, Karpathos, as a medium-scale island, shows a more balanced system configuration, with moderate capacities pf wind, solar PV, diesel generators, and batteries. Its NPC, evaluated at 0.119 €/kWh, is notably lower than that of Lesvos, while it achieves the lowest LCOE among the three Aegean islands, evaluated at 0.119 €/kWh. The REF remains high at 92.0%, with excess energy is slightly higher than Lesvos, reaching 47.9%. Finally, Astypalaia, representing a small-scale island, requires much smaller installed power capacities, compared to Lesvos and Karpathos islands. Although the absolute NPC is the lowest, the LCOE is the highest at 0.128 €/kWh, indicating higher unit energy costs for smaller electricity supply systems. The renewable energy penetration drops to 90.3%, and excess energy reaches the highest value (48.6%), thereby, suggesting reduced flexibility and economies of scale compared to larger islands.

Table 26 Comparison of results across small-, medium-, and large-scale islands

Off-grid Island)	Wind turbines (MW)	PV (MW)	Diesel Generator (MW)	Battery (MWh)	NPC (M€)	LCOE (€/kWh)	REF (%)	Excess Energy (%)
Lesvos	87.5	60.0	130.0	350.0	441.0	0.124	92.7	44.6
Karpathos	12.0	10.0	27.0	50.0	67.5	0.119	92.0	47.9
Astypalaia	2.0	1.5	5.0	8.0	11.9	0.128	90.3	48.6

A comparison between the LCOE figures of the proposed optimized systems and the ones of the existing electricity supply systems on Aegean islands, presented in Figure 63, clearly demonstrates the economic advantages of deploying renewable energy-based hybrid power systems in isolated/off-grid islands. In case of the Lesvos island, the LCOE of the optimized hybrid system is significantly lower (above 50%) than the corresponding one of the current energy system, which relies highly on existing autonomous power stations based on internal combustion engines (running on heavy fuel oil) and gas turbines (running on light diesel oil). Similarly, in Karpathos, the optimized system achieves an LCOE of 0.119 €/kWh compared to the existing fossil fuel-dependent cost of 0.362 €/kWh, highlighting an even larger relative cost reduction. The contrast is most pronounced in Astypalaia, where the optimized LCOE figure of 0.128 €/kWh is substantially lower than the current diesel/heavy fuel oil-based value of 0.573€/kWh, indicating a substantial decrease of more than 75%. Overall, this comparison underscores the strong economic advantage of transitioning from diesel-reliant power systems to high-renewable-penetration hybrid configurations, particularly for smaller islands where electric diesel generators lead to exceptionally high electricity costs.

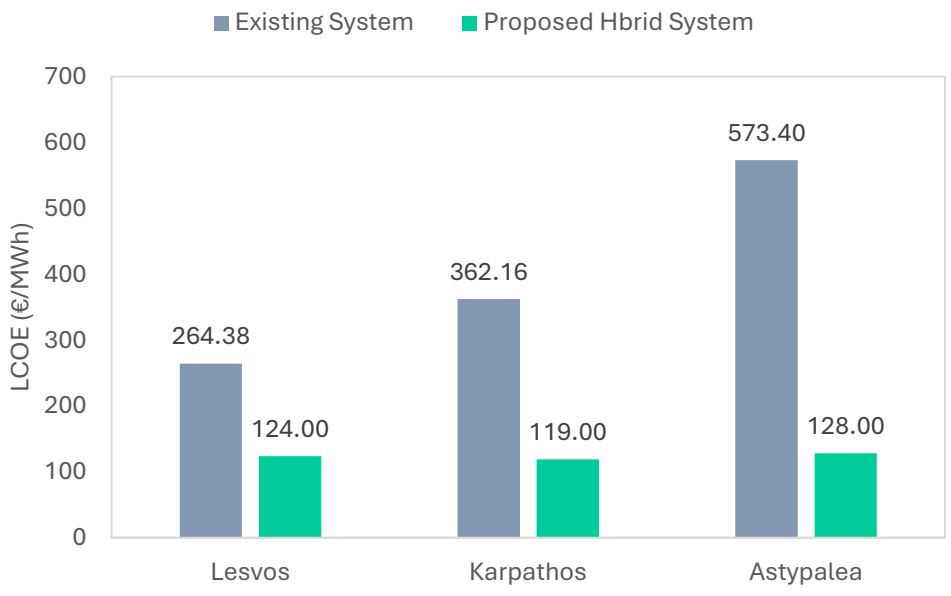

Figure 63 Comparison of LCOE for proposed optimized systems and existing electricity supply systems on Aegean islands

5.3.2 Environmental performance evaluation results

Figure 64 presents a comparative assessment of GHG emissions between the existing fossil fuel-based electricity systems and proposed hybrid renewable energy systems across the three Aegean islands under analysis. It should be mentioned that for both the diesel generator and the RES technologies the Ecoinvent database [234] was employed to model the operation/power generation stage of the power systems. Calculated results demonstrate the substantial environmental benefits that could be achieved through energy system transformation in the three islands considered of, namely, Lesvos, Karpathos, and Astypalaia. It can be seen from Figure 64 that the current power systems exhibit significant GHG emissions, with Astypalaia showing the highest emissions, evaluated at 921 gCO_{2eq}/kWh, followed by Karpathos with 854 gCO_{2eq}/kWh, and Lesvos with 810 gCO_{2eq}/kWh. These elevated emission levels are characteristic of diesel-dependent islands' electricity generation, reflecting the carbon-intensive nature of the autonomous thermal power plants operating on isolated grids. In contrast, the deployment of the proposed hybrid wind/PV/diesel/ battery electricity generations systems demonstrate enhanced carbon footprint, achieving only 70.7 gCO_{2eq}/kWh (about 92.3% reduction), in case of Astypalaia, 63.8 gCO_{2eq}/kWh (92.5% reduction), in case of Karpathos, and 60.8 gCO_{2eq}/kWh (92.5% reduction), in case of Lesvos. These remarkably consistent mitigation rates, all exceeding 92%, point out the transformative potential of hybrid electricity supply systems combining solar, wind, and energy storage technologies in replacing fossil fuel generation.

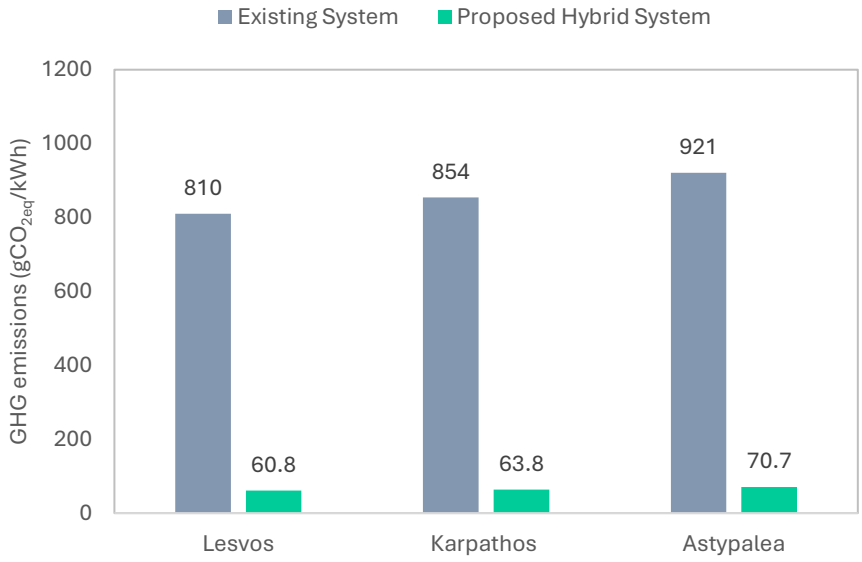

Figure 64 Comparison of GHG emissions for proposed optimized systems and existing electricity supply systems on Aegean islands

5.4 Summary and conclusions

The proposed hybrid power systems, combining wind energy, solar energy conversion units, battery storage, and diesel backup, could represent robust, cost-effective and sustainable solutions/alternatives for isolated/non-interconnected Aegean islands. Through the joint exploitation of the complementary nature of wind and solar resources, and, at the same, time the utilization of battery storage, the hybrid systems could cater for the local electricity requirements, which reaching very high levels of renewable energy penetration. In all three islands investigated, namely Lesvos, Karpathos, and Astypalaia, renewable generation forms the core of electricity supply, with a substantial contribution more than 90%, whilst the electric diesel generators assume a secondary, supportive role that ensures security of supply during periods of low renewable availability. The battery bank is a key component of the hybrid system, since it enables the alignment of the fluctuating renewable electricity generation with the demand through load shifting and grid stabilization. The presence of surplus renewable energy further confirms the abundant renewable resource potential of the islands, and, at the same time, underscores the notable opportunities for future systems enhancement via additional storage capacity, flexible demand, or alternative energy uses. From an economic perspective, the analysed hybrid power systems proved to be highly cost-effective for the isolated islands, achieving competitive electricity generation costs (of the order of 0.12-0.15 €/kWh), despite higher upfront capital investments, thereby highlighting that large-scale REF can be economically sustainable across off-grid/ isolated power systems. Last, but not least, from the environmental point of view, the substitution of the diesel-based electricity generation with hybrid wind/PV/diesel/battery systems on Aegean islands, can lead to a significant decrease in climate change impact, lowering GHG emissions from the very high diesel-dominated levels to less than 71 gCO_{2eq}/kWh across all islands, and achieving emission reductions exceeding 92%. Consequently, the integrated renewable energy systems provide a highly effective, circular economy-driven pathway towards the deep decarbonization of non-interconnected islands in the country.

Chapter 6
Grid-Level Application

Following the completion of earlier case studies on environmental performance evaluation at both the building- and community- levels, this chapter extends the analysis to the electricity-grid level, addressing a key gap identified in the technical literature. At the building-level, the environmental impacts associated with the construction materials and operational energy use, were quantified. The subsequent community-level study broadened this analysis by evaluating the environmental performance of isolated island communities, encompassing the integration of renewable energy technologies with storage systems, power converters, and electric diesel generators. However, the previous case studies investigated the environmental impacts of electricity supply without fully considering the generation and transmission systems underpinning power delivery. Chapter 6 addresses this limitation by evaluating the performance of a broader suite of electricity-generation technologies, encompassing renewable sources such as biomass, small hydro, wind, and solar PV, as well as large hydroelectric systems, and conventional fossil fuel options, such as lignite, oil and natural gas. The environmental profile of the transmission system is also examined, accounting for infrastructure, operational losses, and the efficiency of electricity delivery across the grid. By incorporating both generation and transmission impacts and considering a wide range of renewable and conventional technologies, this chapter offers a thorough understanding of the environmental footprint of the electricity sector in Greece. It also serves as a basis for policy development aimed at meeting future electricity demands with minimized environmental impacts, linking end-use consumption to primary energy sources across the entire energy supply chain.

6.1 Literature review of LCA of electricity sector

A review of the literature shows that most LCA studies of the electricity sector are devoted to individual electricity generation technologies, either conventional or renewable ones. Odeh and Cockerill [235] examined fossil fuel-based power plants, namely, supercritical pulverized coal, natural gas combined cycle and integrated gasification combined cycle, with or without carbon capture and storage (CCS), showing that CCS can reduce GHG emissions by 75-84%.Similarly, Cui et al. [236] demonstrated lower impacts for ultra-supercritical coal plants compared to sub-critical and super-critical designs, while Riva et al. [237] highlighted the environmental advantages of natural gas-fired thermal power plants over conventional ones, considering the entire lifecycle of the fuels used, from production to final consumption. Other studies, including Yang et al. [238] and Song et al. [239] explored the adverse environmental impacts across various fuels, consistently demonstrating that fossil fuel-based power generation technologies are the most substantial contributors to the GHG impact. Comparisons between conventional and renewable energy technologies indicate that solar PV, wind, hydroelectric, and nuclear technologies generally exhibit lower life cycle impacts, with offshore wind and solar PV systems resulting notable GHG reductions relative to fossil fuel-based generation [28,240–246].

Nevertheless, very few LCA studies take into consideration the environmental impacts of transmission and distribution of electricity, which can be significant because of infrastructure, material intensity, and energy losses [247–253]. Blackett et al. [247] compared the environmental impacts associated with current and alternative materials used in high-voltage transmission towers, conductors, and insulators across the UK power grid. Their study also examined how local climate conditions, including coastal, rural, urban, and industrial environments, affect the environmental performance of these materials. The authors concluded that the overall environmental impacts of steel and aluminium towers are broadly similar. The same applies to conductors. Of the three components assessed, insulators exhibited the most favourable environmental performance. Harrison et al. [254] found that grid power losses represent most of the life cycle impacts. Jorge and Hertwich [249], who evaluated the environmental impacts of the Norwegian transmission grid, showed that the total climate change impacts in Norway are evaluated between 1.3 and 1.5 gCO_{2eq}/kWh_e of electricity transmitted and are equally divided between the infrastructure activities linked to construction, materials processing, components manufacturing, etc., and transmission lines power losses. Arvesen et al. [250], Jones and McManus [251], Bumby et al. [252], and Turconi et al. [253] further demonstrated that distribution impacts often exceed transmission impacts, mainly due to higher losses and material intensity. They also pointed out that these impacts are expected to increase with higher penetration of renewable energy in the electricity mix.

Comprehensive life cycle analyses associated with a country's electricity mix, including studies on Greece, remain limited. Santoyo-Castelazo et al. [255] reported that electricity generation in Mexico, estimated at 225 TWh per year, results in 129 million tons of CO_{2eq}, largely driven by the combustion of fossil fuels. In contrast, nuclear power and renewable energy technologies together contribute only about 1.1% of the country's total GHG emissions. Brizmohun et al. [256] conducted a similar study for Mauritius, assessing total GHG emissions at 868 kg CO_{2eq}/MWh of electricity generated. Their analysis highlighted that oil- and coal-fired power plants are the dominant contributors to overall life cycle impacts, accounting for about 88-99% of overall emissions. Rakotoson and Praene [257] reported that French Guyana shows the lowest GHG impact, estimated at 373 gCO_{2eq}/kWh_e, among the islands examined, mainly because of its high share of renewable energy in the electricity mix. In Nigeria, Somorin et al. [258] pointed out that the substitution of diesel fuel with Jatropha biodiesel for self-generated electricity could reduce the GHG emissions by up to 76%. From a broader sustainability perspective, Atigun and Azapagic [259] performed an integrated LCA of Turkey's electricity sector using multiple environmental, economic, and social indicators. Their findings indicate that the main environmental impacts are related to the combustion of conventional fossil fuels, whereas hydropower, followed by geothermal and wind, emerges as the most sustainable set of options. In addition, García-Gusano et al. [260] carried out environmental performance evaluations under a Business-as-Usual (BaU) scenario and an ambitious CO_2 reduction pathway (−80% vs. 2005). Both scenarios lead to long-term reductions across most impact categories, ranging from 21–85% (BaU) and 56–87% (low-carbon scenario), demonstrating the benefits of deep decarbonization. For Singapore, Quek et al. [261] investigated the 2015-2050 transition towards renewable electricity. While GHG emissions and eutrophication decrease, human toxicity and acidification potentials increase, mainly due to material- and energy-intensive solar PV manufacturing processes. This confirms that renewable energy technologies, particularly solar PV, might shift environmental burdens upstream even as they reduce operational emissions. LCA studies

focused on Greece, including Kaldellis [262], Georgakellos [263], and Theodosiou et al. [264], concluded that lignite-fired power plants have the worst environmental performance in mainland Greece, followed by natural gas-fired units, whilst renewable energy technologies exhibit relatively small impacts. Notably, these studies focus on the generation stage alone of the electricity, omitting the transmission one, which is increasingly important for accurate LCA results.

6.2 Case study overview

The research presented in this section has been published in a peer-reviewed scientific journal [265] (*Orfanos N, Mitzelos D, Sagani A, Dedoussis V. Life cycle environmental performance assessment of electricity generation and transmission systems in Greece. Renewable Energy 2019;139:1447–62)*.

6.2.1 Electricity generation in Greece

The Greek electricity generation sector continues to be a substantial source of GHG emissions. Although it has historically accounted for the highest share of national emissions, recent years have seen a marked decline in lignite consumption, alongside a substantial expansion of renewable energy deployment. The adoption of an updated National Energy and Climate Plan, featuring more ambitious decarbonization goals, further reflects this positive trajectory. Nevertheless, sustained and robust emission-reduction strategies and measures are needed to ensure that Greece, as an EU Member State, fully complies with European directives and international climate policy frameworks [264].

The major electricity supplier in Greece is the PPC [266], which is mainly a state owned enterprise. The private sector contributes to electricity power generation via natural gas-fired power plants and renewable energy technologies. The electricity grid of Greece is divided into two main parts; (i) the national mainland grid, and (ii) the so called “non-interconnected islands grid”, i.e. islands which have autonomous systems that are not connected to the mainland grid. PPC's power generation units consist of thermal and hydroelectric power plants, as well as renewable energy facilities [267]. Corresponding data on electricity generation for both the mainland Greece grid and the non-interconnected islands grid for the period 2010–2016 are summarized in Table 27, reflecting the period examined in the case study carried out in 2026. These data are provided by the Greek Independent Power Transmission Operator (IPTO) [268], the Operator of the Greek Electricity Market and Guarantees of Origin (DAPEEP) [269], and the HEDNO [221].

Table 27 Total electricity generation in Greece in the period 2010-2016

	Electricity generation (GWh)							Annual change (%)					
	2010	2011	2012	2013	2014	2015	2016	11/10	12/11	13/12	14/13	15/14	16/15
Electrical system of mainland Greece													
Thermal power plants													
Lignite	27,439	27,570	27,554	23,231	22,709	19,418	14,898	0.5	-0.1	-16.0	-2.3	-14.5	-23.3
Heavy fuel oil	113	8	78	0	1	1	1	-92.9	875	-100	-	0	0
Natural gas	10,365	14,850	14,135	12,150	6,339	7,267	12,512	43.2	-4.8	-15.3	-47.8	14.6	72.2
Total thermal	37,917	42,428	41,767	35,381	29,049	26,686	27,411	14.1	-1.6	-15.1	-18.1	-8.1	2.7
CHP power plants	114	141	148	118	158	188	185	23.7	5	-20.3	33.9	19	-1.6
Large hydro power plants (>10MW)	6,702	3,675	3,891	5,640	3,906	5,391	4,843	-45.2	5.9	45	-30.7	38	-10.2
RES power plants													
Solar PV	132	441	1,231	2,928	3,087	3,171	3,175	234	179.1	137.9	5.4	2.7	0.1
Wind	2,061	2,595	3,160	3,391	3,009	3,856	4,330	25.9	21.8	7.3	-11.3	28.2	12.3
Biomass	193	199	196	209	207	222	252	3.1	-1.5	6.6	-1	7.3	13.5
Small hydro (1-10 MW)	753	580	669	771	701	707	721	-23	15.3	15.3	-9.1	0.9	2
Total RES	3,139	3,815	5,256	7,299	7,004	7,956	8,478	21.5	37.8	38.9	-4	13.6	5.8
Imports/Exports	5,706	3,232	1,784	2,103	8,819	9,609	8,796	-43.4	-44.8	17.9	319.3	9	-8.5
Total	53,578	53,291	52,846	50,541	48,936	49,830	49,713	1.1	-2.4	-4.4	-3.4	1.8	-0.2
Electrical System of non-interconnected islands													
Thermal power plants													
Lignite	-	-	-	-	-	-		-	-	-	-	-	-
Heavy fuel oil	4,954	4,758	4,707	4,369	4,799	4,571	4,628	-4	-1.1	-7.2	9.8	-4.8	1.2
Natural gas	-	-	-	-	-	-	-	-	-	-	-	-	-
Total thermal	4,954	4,758	4,707	4,369	4,799	4,571	4,628	-4	-1.1	-7.2	9.8	-4.8	1.2
CHP power plants	-	-	-	-	-	-	-	-	-	-	-	-	-
Large hydro power plants (>10MW)	-	-	-	-	-	-	-	-	-	-	-	-	-
RES power plants													
Solar PV	25	114	183	239	235	235	243	356	60.5	30.6	-2.1	0	3.4
Wind	652	719	689	747	679	765	815	20.2	-4.2	8.2	-9.1	12.7	6.5
Biomass	-	-	-	-	-	-	-	-	-	-	-	-	-
Small hydro (1-10 MW)	0.4	0.8	0.9	0.5	0.03	0.4	0.4	100	12.5	-44.4	-94	1,233	0
Total RES	677.4	833.8	872.9	986.5	914.03	1,000.4	1,058.4	24.9	4.7	14.5	-4.5	-2.5	5.8
Imports/Exports	-	-	-	-	-	-	-	-	-	-	-	-	-
Total	5,631.4	5,591.8	5,579.9	5,355.5	5,713.03	5,571.4	5,686.4	-0.5	-0.2	-4	6.7	-2.5	2.1
Total of mainland Greece and non-interconnected islands grid													
Thermal power plants	42,871	47,186	46,474	39,750	33,848	31,257	32,039	10.1	-1.5	-14.3	-14.5	-7.7	2.5
CHP power plants	114	141	148	118	158	188	185	23.9	5	-20.3	33.9	19	-1.6
Hydro power plants	6,702	3,675	3,891	5,640	3,906	5,391	4,843	-45.2	5.9	45	-30.7	38	-10.2
RES power plants	3,816.4	4,648.8	6,128.9	8,282.5	7,918.03	8,956.4	9,536.4	21.8	31.8	35.1	-4.4	13.1	6.5
Imports/Exports	5,706	3,232	1,784	2,103	8,819	9,609	8,796	-43.4	-44.8	17.9	319.3	9	-8.5
Total	59,209.4	58,882.8	58,425.9	55,893.5	54,649.0	55,401.4	55,399.4	-0.6	-0.8	-4.3	-2.4	1.4	0

In 2016, the annual electric power generation reached 55.4 TWh, representing a 6.4% decline compared to 2010, which is in line with the economic recession of this period. About 90% of the electricity was generated by mainland power facilities, while the remaining 10% derived from the non-interconnected islands. During 2010-2016, electricity generation from thermal power plants declined by 25%, primarily due to the decommissioning of most heavy oil-fired facilities. In contrast, RES expanded substantially over the same period, increasing their share in the electricity mix by 150% compared to 2010 levels. By 2016, renewables accounted for 17.2% of Greece's electricity generation, coming close to the 2020 target of 18% [270]. Moving towards 2024, the transition continues, but with notable adjustments. In 2024, renewable energy covered about 50.8% of the total electricity production, while fossil fuels, mainly natural gas, accounted for nearly half (~47%) of the generation. Electricity generation in the non-interconnected island grids, however, is still carried out, almost exclusively, via diesel electric generators and relies heavily on heavy fuel oil imports [269]. Overall, Greece has made significant progress, particularly in reducing lignite utilization, expanding renewable energy resources, and reaching the highest share of clean energy in over a decade. However, the 2024 data indicate that the transition is still ongoing and has not yet been fully achieved.

6.2.2 Electricity transmission in Greece

As electricity generation increasingly depends on dispersed renewable resources, the transmission system becomes an important component in the overall electricity supply chain. The Greek electricity transmission system is part of the interconnected electricity power system, which is managed, operated and maintained by IPTO [268]. It consists primarily of high voltage transmission lines and transformer substations. Most of these transmission lines are overhead, with only a limited number of underwater cables connecting certain islands to the mainland grid, and they extend over approximately 11,650 km in total length [271]. Single- and double-circuit lines, operating at voltage levels of 150 kV and 400 kV, respectively, account for all lines in the transmission system. The 400 kV double-circuit lines transfer electricity to major electricity demand centres of central and southern Greece, which together represent about 65% of the country's electricity demand.

Key components and technical characteristics of the Greek transmission system for the two voltage levels, i.e. 150 kV and 400 kV, are summarized in Table 28 and Table 29. Six types of high voltage transmission lines are utilized: E, B, and 2B for the 150 kV lines, and B'B', 2B'B' and B'B'B' for the 400 kV lines [268]. Overhead transmission power lines are supported by pylons. The conductive material of transmission lines is aluminium with steel reinforcement, whereas pylons are made out of galvanized mild steel. In three-phase lines, conductors are characterized by electric resistance, inductive and capacitance reactance [271]. Substations include transformers, which are employed for transforming the voltage levels, either between high voltage transmission lines and lower voltage distribution ones, or at the interconnection of transmission lines with different voltages. Concrete is used for the construction of substation structures housing the transformer equipment and other electrical devices, whereas steel, aluminium alloy and copper are used for the fabrication of the actual transformers themselves. In December 2013, 331 substations, including all the relevant transformer and auxiliary electrical hardware, were installed in the Greek inter-connected electricity transmission system, see Table 29.

Table 28 Transmission lines types and components

Transmission line type	Transmission line voltage (kV)	Overhead cables		Pylons (tons)	Insulators (tons)
		(km)	(tons)		
E	150	2,483	5,213	24,826	1,887
B	150	2,070	8,074	26,913	1,573
2B	150	6,819	53,186	122,737	10,501
B'B'	400	239	2,648	7,158	515
2B'B'	400	3,768	83,656	207,257	14,470
B'B'B'	400	379	6,307	17,046	1,045

Table 29 Transformers and substations characteristic

Grid voltage level (kV)	Weights (kg)			Number of substations and transformer type		
	Steel	Aluminium alloy	Copper	Steel	Aluminium alloy	Copper
150	656,708	27,126	25,448	166	166	165
400	288,982	22,220	25,448	167	167	166

6.3 Life Cycle Assessment methodology

This case study employs LCA to evaluate the environmental impacts associated with electricity generation and transmission in Greece, with the aim of providing a rigorous framework to inform policymaking for the sustainable development of the Greek electricity sector. It is noted that the system boundaries are confined to generation and transmission processes, while the stages of electricity distribution and end-use are excluded from the present analysis. As already mentioned, and in alignment with ISO 14040 and 14044 Standards [30,31], the LCA process consists of four interconnected phases: (i) system boundaries identification, (ii) inventory analysis, (iii) impact assessment, and (iv) interpretation of results. These phases are discussed in detail in the following sections.

Phase 1 System boundary and description

The system boundaries and the individual components of the Greek electricity grid model are presented in Figure 65. The model comprises the following stages: (1) fuel extraction, (2) fuel processing and transport, (3) construction of electricity generation plants, (4) plant operation and electricity generation, and (5) electricity transmission. Power plant decommissioning and waste management are excluded. The dismantling stage of power plants, associated machinery, and infrastructure is omitted, as its overall contribution to life cycle impacts is generally negligible relative to the total lifetime of the system [264].

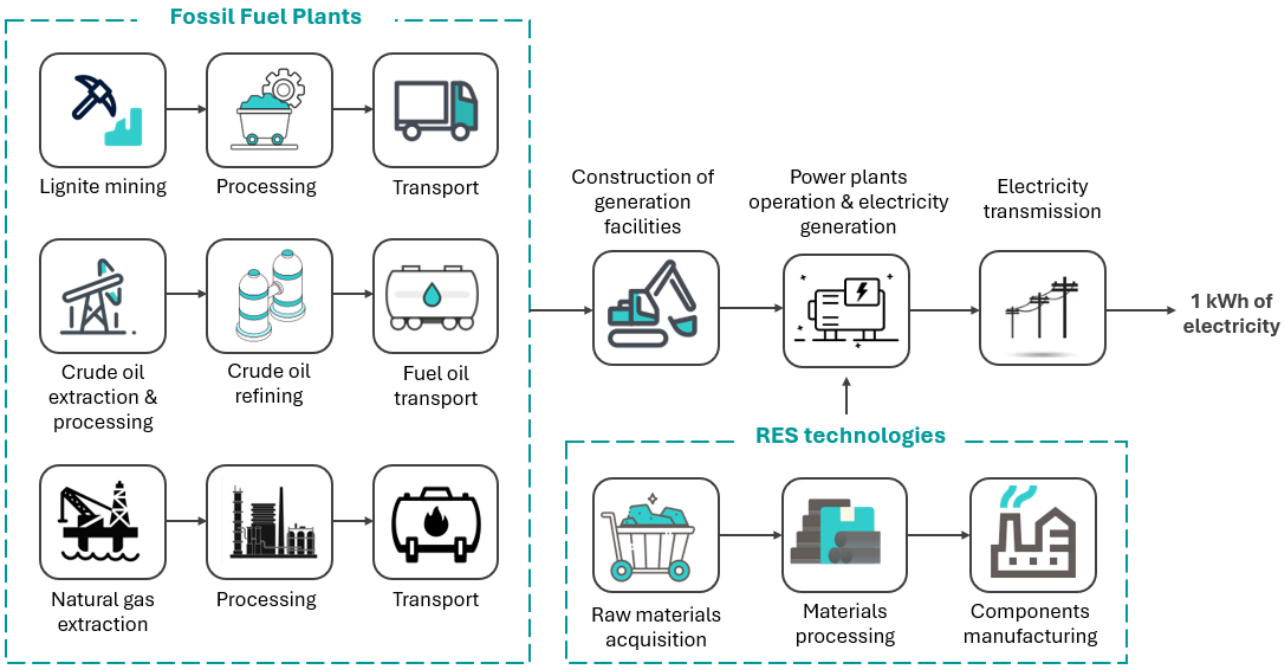

Figure 65 Flow diagram of the life cycle stages of fossil fuels plants and renewables of the Greek electricity generation sector

It is worth noting that the life cycle stages of conventional thermal power plants are more complicated than the ones of renewable energy technologies, due to the fact the LCA system of the fossil fuel plants includes the fuel preparation stage as well. Each of the different power generation technologies currently employed in Greece is modelled as a separate subsystem. On the other hand, the Greek interconnected electrical transmission system is analysed as a combination of the transmission grid infrastructure construction / preparation processes and transmission lines power losses. The individual stages of construction, installation, and maintenance of transmission lines and transformers are considered in the environmental performance evaluation, while the decommissioning stage is excluded, consistent with the assumptions made for power generation systems [254]. It is worth noting that the effect of energy imports / exports was also not investigated. The Greek electricity grid was assumed to be manufactured and assembled using currently available technologies, despite individual components having lifetimes of up to 40 years. The FU chosen for this case study, to enable comparison across different electricity generation options, is 1 kWh of electricity produced.

Phase 2 Data Sources of Life Cycle Inventory

The LCI analysis phase of the LCA includes data compilation of materials, energy flows and environmental releases involved in the entire life cycle of the electricity generation sector and the interconnected electrical transmission system. The collection of these data is both critical and challenging, since the use of outdated or inconsistent data can lead to misleading findings and potentially misinform practitioners and decision-makers relying on LCA outcomes.

To create the inventory, primary (foreground) data for all power generation technologies were obtained from the IPTO [268], the DAPEEP [269], and the HEDNO [221]. The base year for this case study was 2016; however, results are also provided for the year 2024 to account for updates in the electricity market. The background LCI required data for the construction and operation stage of all power generation technologies included in the system boundaries were taken from the Ecoinvent Database, which has been created using European industrial data. In particular, it includes power generation datasets for the following energy sources: lignite, hard coal, industrial gases, natural gas (conventional or combined cycle with or without combined heat and power-CHP), oil, nuclear, hydropower (reservoir plants, run-of-river plants and pumped storage plants), PVs (building integrated and open ground), wind (on- and off-shore), geothermal, biomass (biogas, wood) and waste [187]. Data and key assumptions for the different power generation technologies considered in the present case study are summarized in Table 30.

It should be noted that for lignite-fired power plants, the Ecoinvent database was employed to model lignite mining and processing, as well as plant operation/power generation. The operational stage was evaluated assuming a typical Greek lignite-fired power plant with 35% thermal efficiency. The construction stage was excluded due to its negligible influence on life cycle impacts [246,272]. Similarly, no life cycle impacts were assumed for lignite transportation, as these plants are generally located close to the mines to minimize transport costs. Regarding oil-fired power plants, although the extraction, transportation, and refining of crude oil are associated with environmental impacts [28,246,273], these stages were excluded from the present analysis due to the lack of sufficiently reliable data. Similarly, the construction phase of diesel electric generators was not considered, mainly because its environmental impact is relatively minor compared to other life cycle stages [28,246,273]. For natural gas-fired power plants, only the operational phase was investigated, assuming an average net efficiency of 45%, based on data from ten European countries, including Greece [274]. The construction stage of the power plants, as well as the extraction, processing, and transportation of natural gas, were omitted due to the unavailability of consistent data for these processes. Nevertheless, several LCA studies indicate that approximately 1-2% of high-pressure natural gas might leak into the atmosphere during the extraction phase, and up to 10% of the extracted gas may be consumed for processing and transportation purposes [275,276]. These contributions are relatively minor in the context of the overall assessment, thus justifying their exclusion from this analysis. Finally, for renewable energy technologies, life cycle data were obtained from the Ecoinvent database, covering material manufacturing and processing, transportation, assembly, and installation under average European conditions. The operational phase of renewable systems was assumed to have negligible life cycle impacts

Table 30 Data and key assumptions of electricity generation technologies included in the Ecoinvent Database

Technology	Electricity generation in 2016 (GWh)		Notes for Ecoinvent Database
	Mainland Greece	Non-interconnected islands	
Lignite-fired power plant	14,898	-	A typical Greek lignite-fired power plant with 35% thermal efficiency is assumed. The total annual full load operation of the plant is estimated to be 4,354 hours/year. The lifespan of such a plant is about 45 years. In order to evaluate the main characteristics (stoichiometric chemical composition of coal, Lower Heating Value-LHV properties, and efficiency of the plant) and emissions inventories (e.g. SO_x, NO_x, CO_2, etc.) a bottom-up approach has been employed.
Oil-fired power plant	1	4,628	A typical Greek diesel electric generator, for the case of the non-interconnected islands, and a typical Greek heavy oil-fired station, for the case of the mainland Greece, are assumed. The net efficiency of oil-fired electricity generation in Greece is 36%.
Natural-gas power plant	12,512	-	A typical European natural gas-fired power plant is assumed. Included processes: fuel input from high pressure network, infrastructure, emissions, and materials required for operation. The module uses the average net efficiency of natural gas power plants in UCTE (estimated from IEA 2001, including countries AT, BE, DE, ES, FR, IT, LU, NL, GR, PT).
Large hydro power plant	4,843	-	A typical large (>10 MW) Greek hydroelectric power plant with pumped storage is assumed. Electricity generation shares are determined on annual average and on the level of net production.
CHP power plant	185	-	A natural gas-fuelled CHP power plant with 360 kW_{th} thermal capacity and 160 kW_e electrical capacity is assumed. It consists of a gas motor, a heat pump, two peak load oil boilers, a hot water storage and an electric generator. The annual average total efficiency of the plant is 76% and 86% excluding and including heat pump contribution to heat supply, respectively. Small CHP production describes the production of electricity and heat with a gas-fired spark ignition engine.
Solar PV power plant	3,175	243	Annual output of grid-connected PV power plants differentiated for roof-top and façade plants. Included process: production mix of electricity in Greece. The average annual specific electricity generation of Greek grid-connected roof-top and façade PV power plants is 117 kWh/kW_p and 712 kWh/kW_p, respectively. Waste heat emission due to electrical losses is also included.
Wind power plant	4,330	815	A wind power plant installed in Grenchenberg, Germany, is assumed. The rotor has 3 blades with a total diameter of 23.8 m. The blades are made of fiber glass reinforced epoxide resin. The tower is 23.8 m tall and is made out of zinc coated steel. The lifetime of moving and non-moving parts is 20 and 50 years, respectively.
Biomass power plant	252	-	The use of biogas in a cogeneration unit is assumed. Included processes: biogas consumption, use and disposal of operational supplements and infrastructure expenditures, as well as emissions to air. Electrical and thermal efficiency are 33% and 67%, respectively. In this plant, only half of the heat is used or sold.
Small hydro power plant	721	0.4	A run-of-river power plant installed in Greece is assumed. Run-of-river power plants use the fall of rivers to produce electricity. There is only little, or no storage and electricity is produced in a continuous base.

Primary data on the actual quantities and technical characteristics of conductors, components, equipment, etc. constituting the Greek interconnected electrical transmission system were obtained from official materials and equipment catalogues of the IPTO [268]. Transmission line specifications are provided in Table 28 and Table 29. Based on these data, six types of high-voltage transmission lines were defined in the model: three for 150 kV (E, B, and 2B) and three for 400 kV (B'B', 2B'B', and B'B'B). Background LCI data linked to the material production of transmission grid infrastructure, including aluminium conductors, galvanized mild steel pylons, glass insulators, and transformers composed of steel, aluminium alloy, or copper, were sourced from average European production processes in the Ecoinvent database. Grid power losses were modelled based on the configuration of the Greek electrical system in 2016 (excluding imports and exports). Losses in the transmission and distribution network were assumed to represent about 7% of the total electricity fed into the grid, corresponding to 3,262 GWh [277].

Phase 3 Life Cycle Impact Assessment

The data collection phase for each component (LCI) was followed by the LCA. The stages of the electricity generation model, depicted in Figure 65, were incorporated in SimaPro PhD 9.5 [190], according to the share of each power generation technology in the total electricity mix for the base year 2016 (refer to Table 30). Similarly, the stages of the transmission grid infrastructure were introduced in the software, with relevant quantities referring to the transmission lines and transformers listed in Table 28 and Table 29. As previously mentioned, power losses were modelled as approximately 7% of the electricity fed into the grid [277].

Environmental impact assessment methodology

The potential environmental impacts of electricity generation and transmission in Greece were evaluated using the Impact World+ methodology [39]. Seventeen categories included in this specific methodology were investigated to carry out life cycle impact, namely, climate change, fossil and nuclear energy use, mineral resources use, photochemical oxidant formation, ozone layer depletion, freshwater ecotoxicity, human toxicity cancer, human toxicity non-cancer, freshwater acidification, terrestrial acidification, freshwater eutrophication, marine eutrophication, particulate matter formation, ionizing radiation, land transformation (biodiversity), land occupation (biodiversity), and water scarcity.

Energy and emission savings calculation - Scenarios selection

To assess the environmental benefits from the penetration of renewables in the Greek electricity generation mix, different scenarios were developed, each corresponding to a distinct combination of feedstocks for electricity production. The analysis covers a 20-year period from 2010 to 2030, accounting for both the relatively long investment payback period horizon in the energy sector and the slow response time typically associated with changes in energy policy. "*Scenarios 2010-2016*" reflect the historical evolution of the share of renewables in the Greek electricity mix during the six-year period prior to the study, which was carried out in 2016, On the other hand, *"Scenarios 2024–2030"* were configured in line with the European and national binding targets for renewable energy penetration in the milestone year 2030. It is noting that since this research was initially conducted in 2016, the analysis has been updated to include the year 2024, reflecting the most recent data available and intermediate progress towards the 2030 targets.

"*Scenario 30*", which describes the projected evolution of the Greek electricity sector in the near future, is based on the findings of the final report by Moirasgentis and colleagues from the National Observatory of Athens [278]. This scenarios was constructed using a set of assumptions and time-dependent projections reflecting the demographic, economic, and technological development of the country. Specifically, the following parameters were considered: (i) future population and household estimates provided by the Hellenic Statistical Authority, (ii) the projected annual electricity output for each generation technology available in Greece, (iii) economic growth forecasts from the European Commission and the International Monetary Fund up to 2030, (iv) anticipated variations in CO_2 emissions allowance prices, (v) investment and operational costs of various electricity generation and energy storage technologies, (vi) investment and operational costs associated with anti-pollution technologies, primarily those required to retrofit existing lignite-fired power plants in compliance with future emission standards, and (vii) expected future inter-connections of the electricity grid of mainland Greece with those of neighbouring countries and the Greek islands. It should be noted that "*Scenarios 2024-2030*" refer exclusively to the electricity system of mainland Greece, as data for electricity demand and generation in the autonomous island systems for the 2024-2030 period are unavailable. Furthermore, it is assumed that the total annual full-load operating hours of all power generation technologies remain constant throughout the 2010-2030 timespan.

Percentage shares of electricity generation technologies operating in mainland Greece from 2010 to 2030 are depicted in Figure 66 [221,268,269,278]. In 2016 (reference mix), fossil fuels represented the dominant share of electricity generation, though lignite's contribution had decreased compared to earlier years. Over the period 2010-2016, renewables experienced significant growth, largely driven by the financial incentives introduced by the Greek government. Based on current national energy policies and regulatory frameworks, the share of renewables in electricity generation rose further, in particular, from 22% in 2016 to 46% in 2024. The "Scenario 2024" reflects the current electricity generation mix: 6% lignite, 37% natural gas, 11% hydropower, 1% CHP, and 46% RES (including wind, PV, and biomass). The "Scenario 2030" incorporates recent developments in the Greek energy sector, including accelerated renewable energy deployment and the progressive phase-out of lignite, in alignment with updated national energy plans and the EU Green Deal objectives. Building on these trends, RES are expected to supply approximately 80% of the electricity fed into the mainland grid by 2030, with wind power exhibiting the most significant growth, from 22% in 2020 to 42% in 2030.

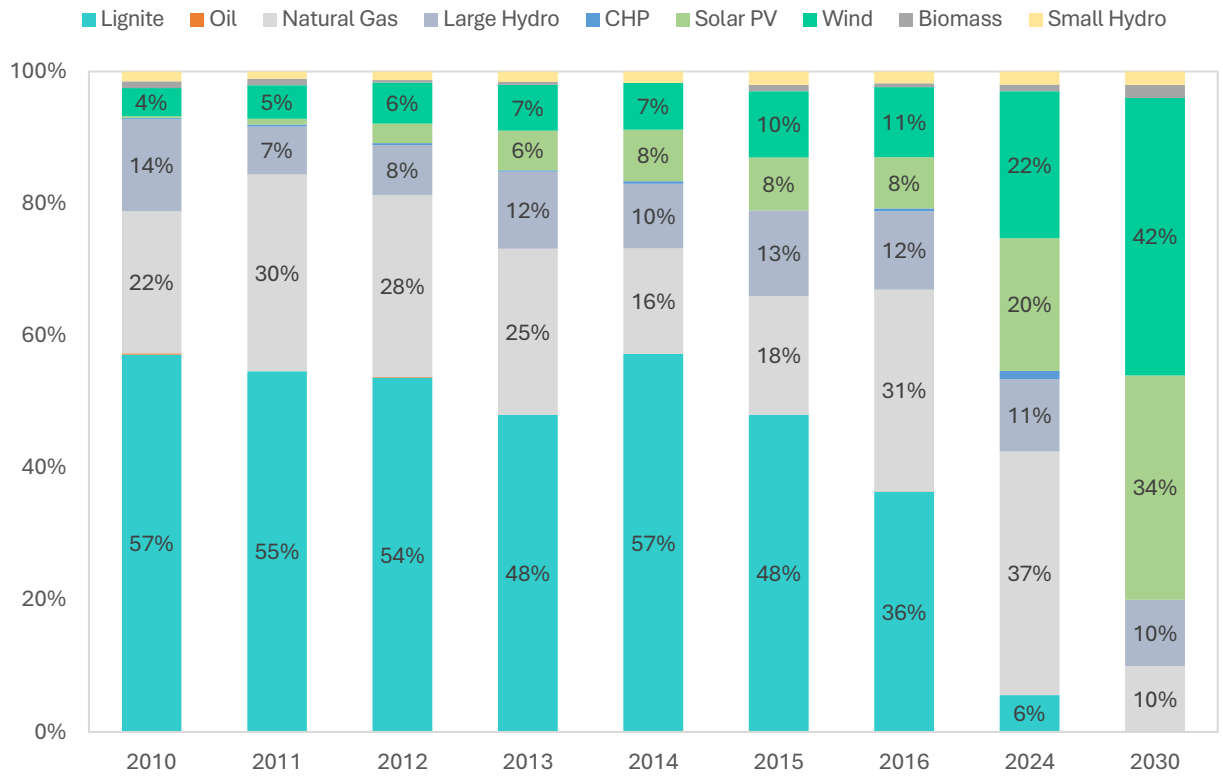

Figure 66 Shares of electricity generation technologies operating in mainland Greece within the timespan 2010-2030

6.4 Results and discussion

6.4.1 Electricity generation system

Reference electricity generation mix (2016)

The environmental impacts for the entire life cycle of the Greek electricity generation sector for the reference year 2016 are summarized in Table 31. it is noted that imported/exported electricity is not taken into account.

Table 31 Life cycle GHG emissions and fossil energy use of the Greek electricity generation sector in 2016

Electricity generation technology	Mainland Greece		Non-interconnected islands	
	GHG emissions (gCO_{2eq}/kWh_e)	Fossil energy use (MJ/kWh_e)	GHG emissions (gCO_{2eq}/kWh_e)	Fossil energy use (MJ/kWh_e)
Thermal power plants				
Lignite	496.26	7.32		-
Heavy fuel oil	-	-	76.9	9.94
Natural gas	162.52	3.13		-
Large hydro (>10 MW)	5.60	0.01		-
CHP power plants	7.70	0.12		-
RES power plants				
Solar PV	4.95	0.07	2.17	0.04
Wind	1.44	0.02	1.94	0.03
Biomass	0.98	0.01	<0.01	-
Small hydro	0.07	<0.01	<0.01	<0.01

Climate change impact

The GHG emissions for 1 kWh of electricity generated in Greece was evaluated at about 653 gCO_{2eq},for the reference year 2016. The majority of these emissions originate from the operation phase of thermal power plants due to fuel combustion. Thermal power plants account for about 98% of the total climate change impact associated with electricity generation. Within this category, lignite-fired power plants are the major source, contributing about 62% of total GHG emissions. Oil-fired and natural gas-fired plants contribute roughly 15% and 21%, respectively. In contrast, emissions from low-carbon sources are minimal. Specifically, renewable energy technologies and CHP power plants together are responsible for about 1.3% of the total GHG emissions, whilst large hydroelectric power plants contribute only 0.7%._Within the electricity system of mainland Greece, lignite-fired power plants exhibit the highest climate change impact, evaluated at approximately 1,300 gCO_{2eq}/kWh_e. Given that these units contribute about 36% of total mainland electricity generation, their resulting weighted contribution to the system's overall GHG intensity is 469 gCO_{2eq}/kWh_e. The poor GHG performance of lignite-fired electricity generation in not only because of the high carbon content and low calorific value of lignite, but also due to its notable penetration in the generation mix; the latter in absolute terms. Natural gas-fired power plants, in contrast, have lower per-unit GHG emissions than lignite, estimated at 533 gCO_{2eq}/kWhe. However, their 30.6% share in mainland electricity generation limits their weighted contribution to 163 gCO_{2eq}/kWh_e. For the aforementioned fossil fuel-based electricity generation options, the estimated GHG emission values are in agreement with those reported in the relevant literature; the overall range of reported values being: 800-1700 gCO_{2eq}/kWh_e for lignite-fired power plants [246,253], and 440-780 gCO_{2eq}/kWh_e for natural gas-fired power plants [28,246], with relatively higher and lower combustion process efficiency, respectively. Large hydroelectric power plants have relatively small GHG emissions (47.5 gCO_{2eq}/kWh_e), even when the entire life cycle is taken into account. Considering their contribution of about 11.8% to mainland electricity generation, their corresponding weighted impact on the system's overall GWP is comparatively minor (~6 gCO_{2eq}/kWh_e). This

figure is in agreement with the corresponding values reported of 2–9 gCO_{2eq}/kWh_e for the construction and operation stage of hydroelectric power plants, reported in the technical literature [272]. Considering the various renewable technologies options, the GHG impact of biomass, solar PV, and wind power systems across their life cycles is estimated at 164 gCO_{2eq}/kWh_e, 63.5 gCO_{2eq}/kWh_e, and 13.6 63.5 gCO_{2eq}/kWh_e. For biomass-based systems, the literature reports a wide range of GHG emission values: 9 -118 gCO_{2eq}/kWh_e for direct combustion, 25-307 gCO_{2eq}/kWh_e for co-combustion with a fossil fuel, and 17–117 gCO_{2eq}/kWh_e for biomass gasification [272,279]. These figures strongly depend on the energy intensity of the fuel-cycle, the biofuel properties, as well as the plant technology and its specific thermal energy conversion efficiency. The estimated GHG emission values for solar PV and wind power generation are also consistent with those reported in other studies; namely 30–130 gCO_{2eq}/kWh_e [272], and 10-124 gCO_{2eq}/kWh_e [28] for solar PV and wind power systems, respectively. As already discussed in Chapter 2, the GHG emissions from various solar PV systems depend mainly on the type of the PV module employed, i.e. mono-Si or poly-Si, whereas the GHG emissions from wind turbines re site-dependant and quite sensitive to wind speed conditions. Last, but not least, Last, but not least, small hydroelectric plants exhibit the lowest GWP among the aforementioned renewable technologies, with only 4 gCO_{2eq}/kWh_e, a value that is almost entirely attributable to the construction stage. Again, this figure is in agreement with the corresponding values reported of 2–5 gCO_{2eq}/kWh_e in technical literature [272]. At this point, it should be noted that, owing to the relatively small share of biomass, solar PV, wind, and small hydro power plants in the mainland electricity grid, their overall weighted contribution to the system's GHG intensity remains minimal, namely, below 5 gCO_{2eq}/kWh_e for solar PV, below gCO_{2eq}/kWh_e for wind power, and below 1 gCO_{2eq}/kWh_e for both biomass and small hydroelectric systems. Regarding the electricity system of the non-interconnected islands, diesel electric generators have the highest environmental impacts, with an estimated GHG emissions figure of 823 gCO_{2eq}/kWh_e. This is mainly attributed to the fact that the primary energy supply of autonomous/isolated Greek islands relies almost exclusively (about 81%) on heavy and light fuel oil. As expected, the climate change impact from renewables is several orders of magnitude lower than that of diesel-fired electric generators.

Fossil energy use

Results for fossil energy use are analogous. The estimated fossil energy use for generating 1 kWh in 2016 is approximately 10.60 MJ. Regarding the electricity system of mainland Greece, lignite-fired power plants exhibit the highest non-renewable energy use, evaluated at 7.32 MJ/kWh_e, followed by natural gas with 3.13 MJ/kWh_e. Large hydroelectric power plants and CHP power plants are good option with fossil energy use of 0.12 MJ/kWh_e and 0.01 MJ/kWh_e, respectively. Their good environmental performance is largely due to the small contribution (below 1% and 12%, respectively) to mainland electricity generation. The fossil energy use figure for solar PV systems is 0.07 MJ/kWh_e, ranking it as the least favourable renewable option. This is directly related to the electricity-intensive nature of the PV module fabrication, with the required electricity supplied mainly by fossil-fuelled power plants. Wind turbines perform better, with a non-renewable energy use value of 0.02 MJ/kWh_e, whereas biomass and small hydro power plants present the best options, each accounting for below 0.01 MJ/kWh_e. In the autonomous/isolated Greek islands, electricity supplied through diesel generators is the least sustainable, with a fossil energy figure of 9.94 MJ/kWh_e. The corresponding

figures for renewables are approximately ten orders of magnitude lower than the ones of diesel electric generators.

Life cycle impact contribution of the Greek electricity generation mix

The life cycle contribution of the Greek electricity generation mix to each of the environmental impact categories considered in this study is depicted in Figure 67. Lignite-fired electricity generation is found to exhibit the highest adverse environmental impacts, accounting for more than 55% in ten out the eighteen categories, namely, climate change (long and short term), fossil and nuclear energy use, mineral resources use, freshwater ecotoxicity, human toxicity (cancer and non-cancer), freshwater acidification, terrestrial acidification, freshwater eutrophication, particulate matter formation, and ionizing radiation. This poor environmental performance is attributed to the low calorific value and high carbon content of lignite, as well as to the impacts associated with its mining and combustion stages. The operation of oil-fired power plants contributes significantly (above 45%) to marine eutrophication impacts, largely as a result of nitrogen oxide emissions generated during combustion [280]. Freshwater eutrophication impacts are also notable (~ 34%) but arise mainly from upstream processes. Natural gas-fired power plants account for high contribution in the categories of ozone layer depletion (~84%) and freshwater eutrophication (~43%), mainly because of nitrogen oxide emissions during combustion, and small amounts of chemicals used in fuel processing or equipment [281,282]. Mineral resource impacts (~48%) are also important and are largely associated with the extraction and processing of natural gas, as well as the materials required for plant construction and operation, encompassing metals and concrete, which demand significant mining and processing of mineral resources. On the other hand, large hydroelectric power plants is the dominant contributor (>70%) to water scarcity through the evaporative losses from their reservoirs, which account for the largest portion of fresh-water consumption relative to the river's natural pre-dam flow [283]. CHP power plants and renewables are nearly free of environmental burdens, even from an entire life cycle perspective. Among renewables, wind power accounts for a considerable contribution in the category of mineral resources use (~13%). This is probably due to metallic and other raw materials that are utilized for the fabrication of wind turbines, especially steel, iron, copper, aluminium, and alloy components.

Overall, immediate reduction in adverse environmental impacts can be achieved through energy efficiency enhancements, along with stricter enforcement of pollution control measures at existing conventional fossil fuel power plants. Nevertheless, a sustainable long-term strategy for the Greek electricity generation sector should focus on expanding renewable electricity generation, such as wind and solar, while also investigating the potential role of carbon capture and storage in the country's future energy mix.

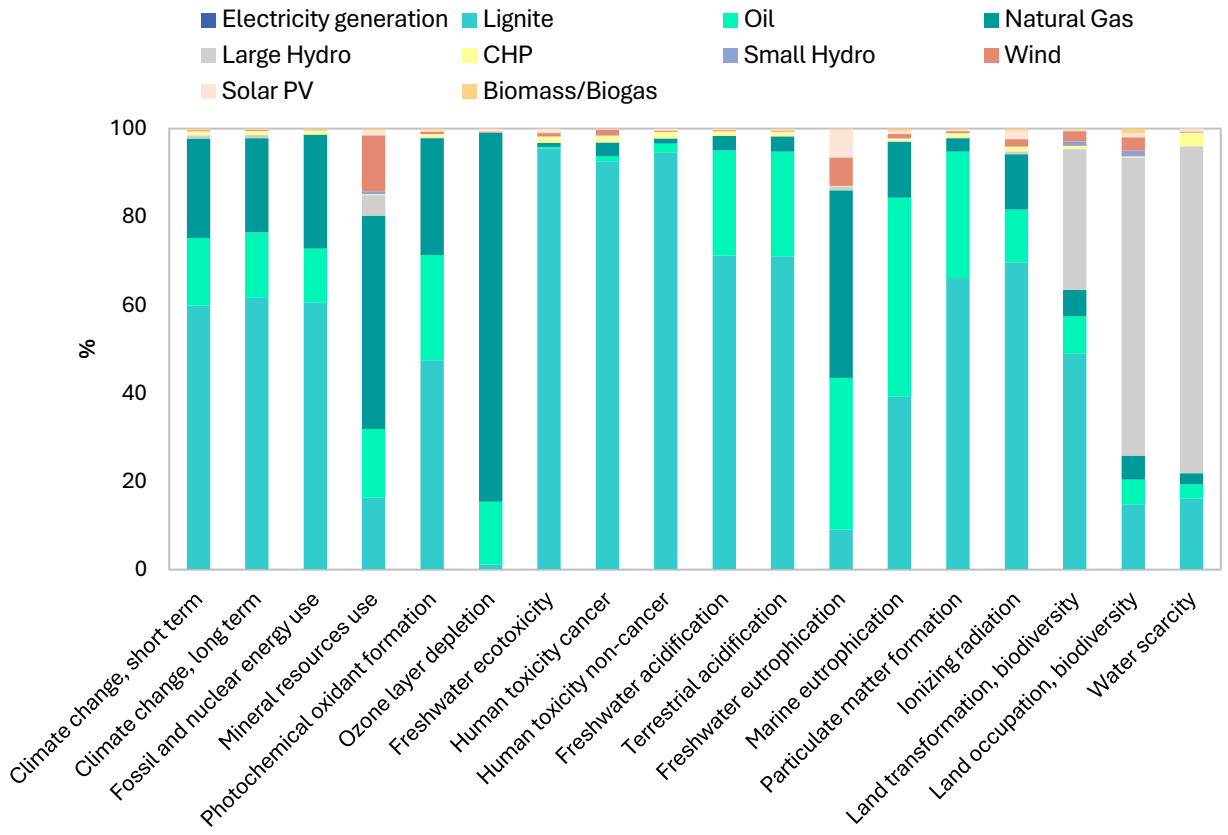

Figure 67 Life cycle impact categories of the electricity generation sector (mainland Greece and non-interconnected islands) in 2016 (IMPACT World+ Midpoint methodology)

Current and future electricity generation mix

The trends of GHG emissions and fossil energy use in the Greek electricity sector for the period 2010–2030 (see Figure 66) are illustrated in Figure 68 and Figure 69, respectively. In terms of climate change impact, the highest GHG emissions are exhibited within the time period 2010 to 2012, primarily because of the substantial share (>70%) of thermal power plants to the electricity generation mix. In 2016, the GHG emissions experienced a considerable reduction, accounting for approximately 24%, compared to 2012 levels. This is attributed to decommissioning of the majority of oil-fired power plants. In 2024, the GHG emissions figure is evaluated at 337.09 gCO_{2eq}/kWh_e. which is significantly lower (by 48%) than the relevant figure of 2016. This is directly related to the increased penetration of renewable energies, mainly solar and wind power, into the electricity generation mix. As anticipated, future electricity generation scenarios with greater renewable energy integration is likely to contribute to a further reduction in climate change impacts. Specifically, in 2030 the GWP decreases further, reaching 175.67 gCO_{2eq}/kWh_e. The fossil energy use results display a comparable trend; electricity generation mix of 2024 with 46% share of renewables has the lowest non-renewable energy use value of 5.94 MJ/kWh_e, compared to the period 2010-2016. The 2030 mix scenario has a fossil energy use value of 3.19 MJ/KWh_e, which is notable lower than the corresponding one of 2024 scenario.

The analysis demonstrates that higher integration of renewable energy in the Greek electricity sector significantly mitigates climate change impacts and reduces dependence on non-renewable energy resources. Expanding the penetration of renewables and associated technologies is projected to further strengthen the sustainability of electricity generation in the coming decades.

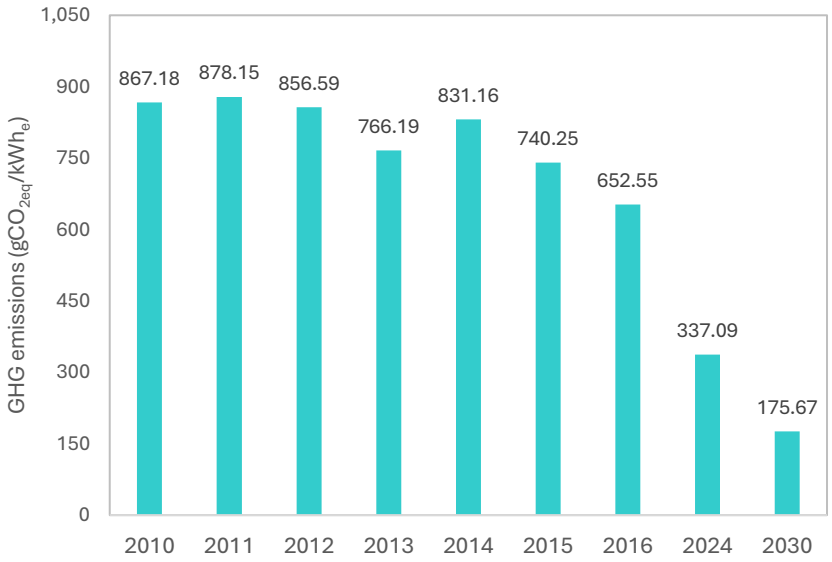

Figure 68 GHG emissions of electricity generation mix in mainland Greece within the timespan 2010-2030

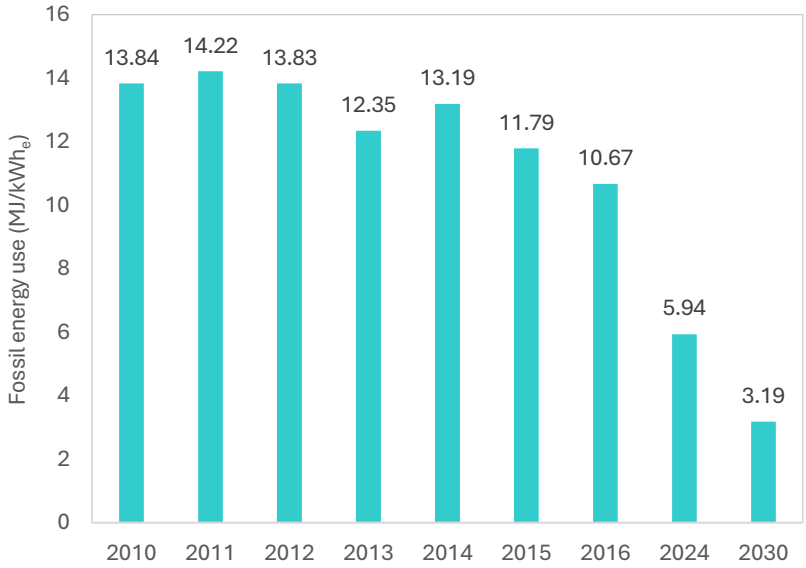

Figure 69 Fossil energy use of electricity generation mix in mainland Greece within the timespan 2010-2030

Electricity generation sector of other countries

For the shake of completeness, the results for the Greek electricity generation sector are compared with those of Portugal, Italy, and Mexico for the year 2024. These countries were selected as they represent a wide spectrum of electricity generation mixes [284], as shown in Figure 70. The electricity system of Mexico is dominated by natural gas, accounting for about 60% of its generation, supplemented by smaller shares of oil and coal. In contrast, Italy exhibits a more diversified portfolio, with substantial penetrations from natural gas (36%), solar (14%), hydropower (15%), and modest levels of wind (8%) energy. Portugal presents a markedly different profile, which is characterized by a high presence of renewable energy source, namely, hydropower (28%), wind (22%), and solar (14%), while fossil fuels consumption remains limited. These distinct configurations serve as a broad basis for contextualizing and comparing the environmental profile of the Greek electricity sector.

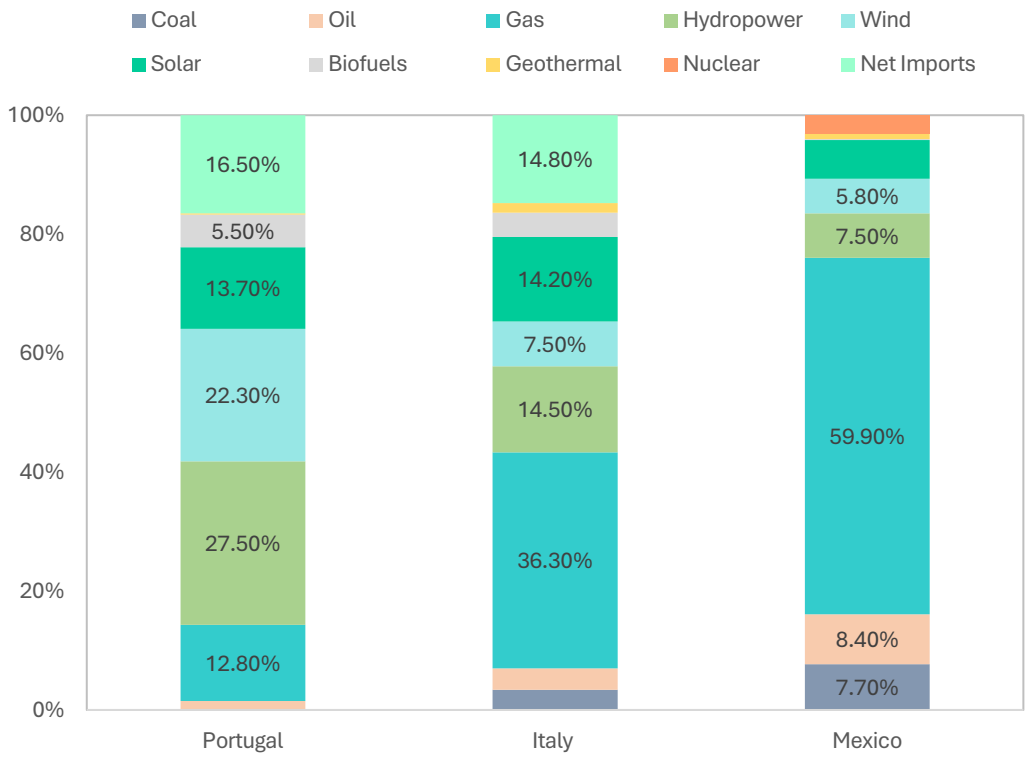

Figure 70 Electricity generation mix for Portugal, Italy and Mexico in 2024

Comparison results are presented in Figure 71, where notable variations in GHG emissions are noticed. The electricity generation sector of Mexico exhibits the highest life cycle climate change impact, with estimated GHG emissions of 445 gCO_{2eq}/kWh_e. This is primarily due to the sector's strong dependence on fossil fuels, especially natural gas, which accounts for 60% of the mix, whist low-carbon sources represent only about 24% of the total electricity generation. The next major contributor to GHG emissions is Greece, with 337 gCO_{2eq}/kWh_e, followed by Italy with 307 gCO_{2eq}/kWh_e. Currently, in Italy, low-carbon energy sources supply approximately 42% of electricity generation, with hydropower, solar, and wind collectively contributing

more than 35% of the total. Both Greece's and Italy's efforts in expanding green energy are evident; however, there remains substantial potential for further reducing dependence on fossil fuels and increasing the share of renewable energies. The Portugal has the lowest GHG emissions (131 gCO_{2eq}/kWh_e), as compared to other countries. The good performance can be attributed to the substantial share of RES, approximately 69%, in Portugal's electricity generation mix. On the contrary, fossil-fuel-based electricity represents just over 14%, with natural gas being the dominant contributor at about 13% and oil providing a negligible share of approximately 1%.

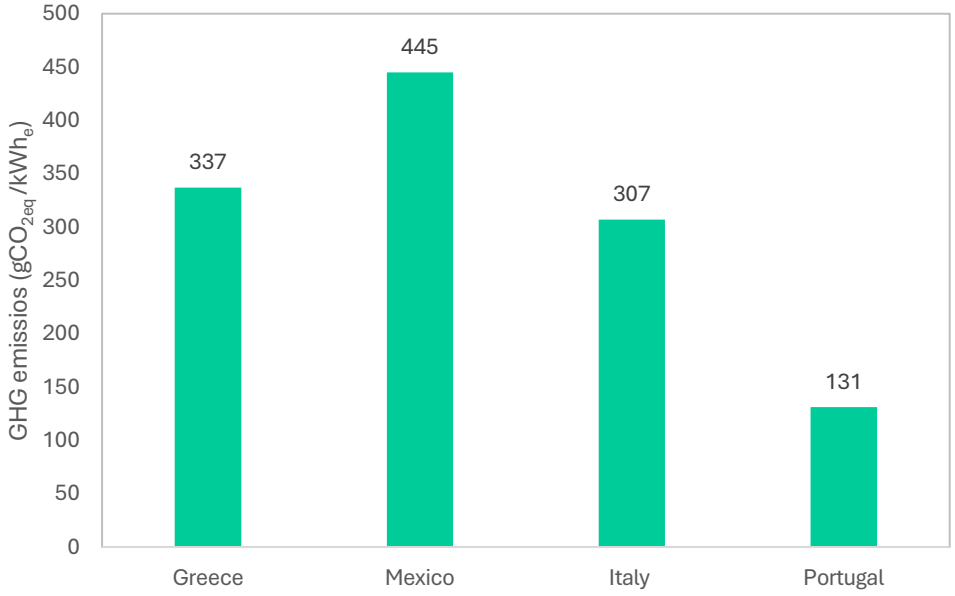

Figure 71 Electricity generation sector life cycle GHG emissions; Greece: present work, other countries (Imports/exports are excluded)

6.4.2 Interconnected electricity transmission system

The environmental impacts, in terms of GHG emissions and fossil energy use, for the entire life cycle of the Greek interconnected electricity transmission system are presented in Figure 72. For 1 kWh of electricity transmitted in mainland Greece, the total GHG emissions figure is estimated to be 153.19 gCO_{2eq}. The relevant fossil energy use figure is evaluated at approximately 1,753 MJ/kWh_e. Infrastructure processes for the transmission lines are the most impact intensive ones, accounting for about 60% and 52% of the total GHG emissions and non-renewable energy use, respectively. Most of these impacts are linked to the energy consumed for the production of raw materials, mainly aluminium and steel, required for the fabrication of transmission lines conductors. Power losses are responsible for 34.3% and 42.5% of the total climate change impact and fossil energy demand, respectively. These figures are in agreement with those of other studies [253,272]. Their poor performance is attributed to the fact that the extra capacity required to make up for the power that is lost is supplied by conventional thermal power plants. Transformers contribute only 5.8% and 5.3% of the total GHG emissions and the fossil energy use, respectively. Mostly, these figures are

related to the production processes of materials, namely, steel, aluminium and copper, utilized in fabricating transformers and other auxiliary electrical equipment and components. Obviously, there is an additional contribution from the preparation of concrete, which is used for the construction of substation structures.

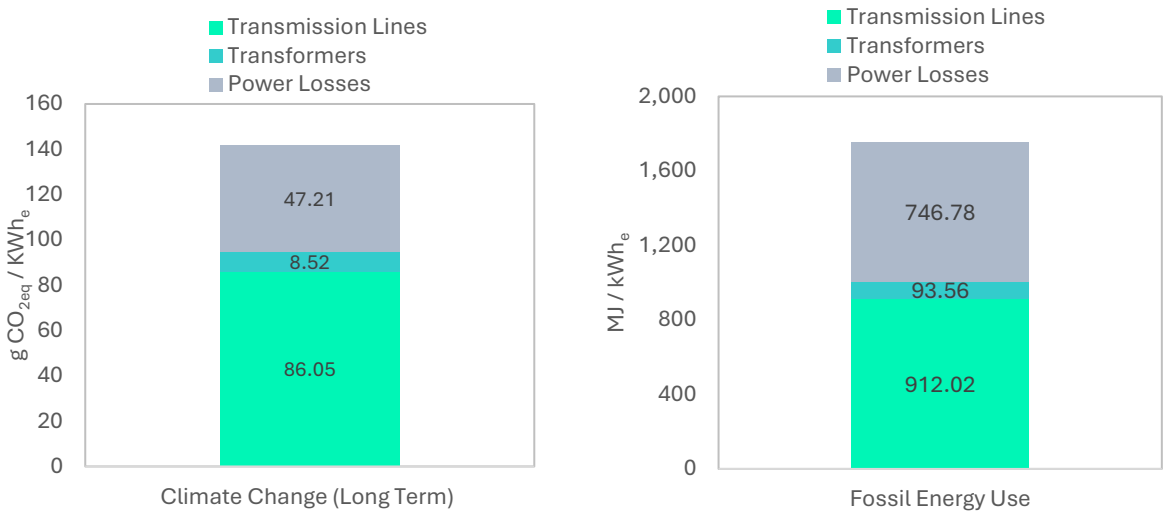

Figure 72 Life cycle GHG emissions and fossil energy use of the Greek interconnected electricity transmission system in 2016

Figure 73 presents the relative contributions from both infrastructure activities and power losses in the Greek interconnected transmission system. It is evident from this figure that, for most impact categories, the majority of the adverse environmental impacts are associated with the construction and installation of transmission lines. In detail, transmission lines account for approximately 60–85% of environmental impacts in the categories of climate change (~61%), fossil and nuclear energy use (~52%), mineral resource depletion (~70%), photochemical oxidant formation (~73%), human toxicity cancer (~79%), freshwater acidification (~65%), terrestrial acidification (~66%), freshwater eutrophication (~84%), marine eutrophication (~79%), particulate matter formation (~71%), ionizing radiation (~84%), land transformation (~58%), and land occupation (~66%). These high contributions could be attributed to the highly electricity intensive production stage of aluminium, which is the main raw material for manufacturing transmission lines conductors. Conversely, grid power losses have a greater influence on the categories of water scarcity (~51%), and ozone layer depletion (~47%). The poor environmental performance in these categories can be justified considering the additional electricity required in order to compensate for wasted energy, which proportionally increases water consumption in cooling-intensive thermal power plants, and amplifies emissions of ozone-depleting substances from power generation equipment and refrigerants. Lastly, processes related to the fabrication of transformer equipment and substation construction have relatively small life cycle impacts in all categories, but for the mineral resources use (~29%), freshwater ecotoxicity (~28%), human toxicity non-cancer (~25%), and water scarcity (~23%). These adverse effects are associated again with the production stage of the relevant raw materials utilized for their fabrication.

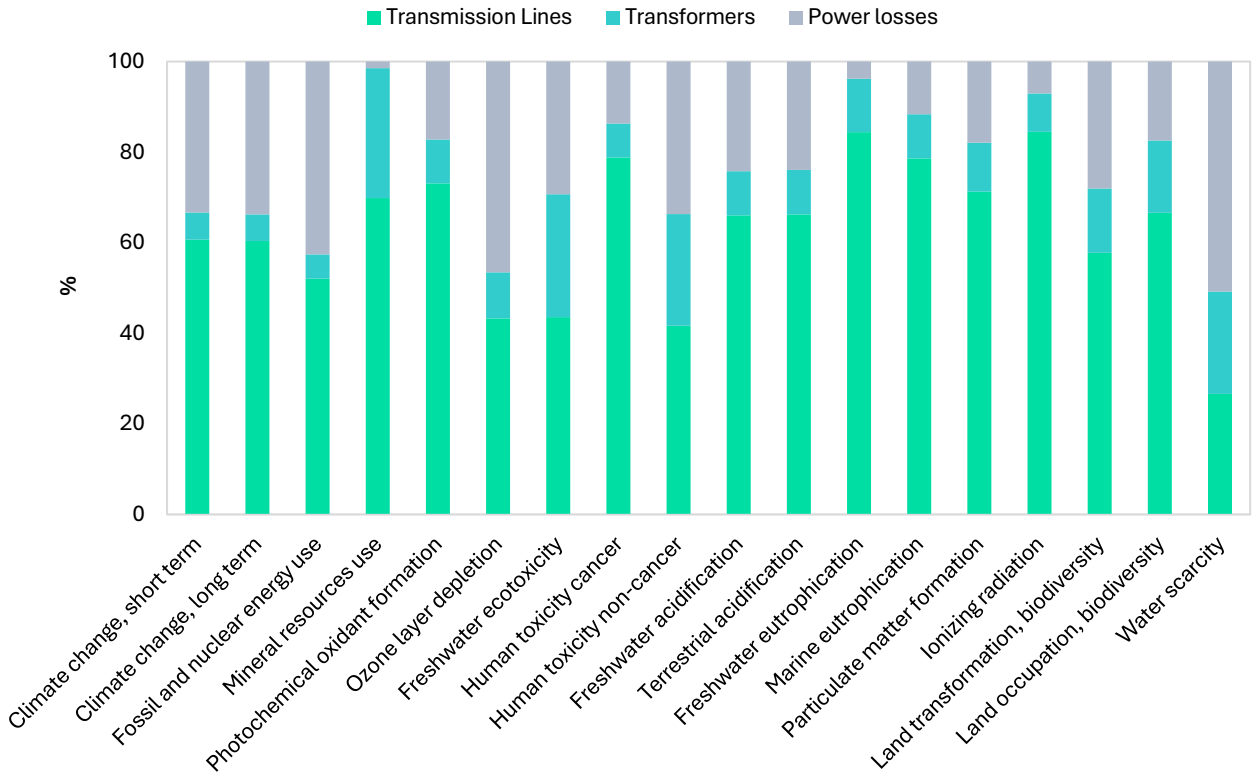

Figure 73 Life cycle impact categories of the Greek interconnected electricity transmission system in 2016.

6.4.3 Combined electricity generation and interconnected transmission systems

The life cycle contribution of the entire electricity sector, including both the generation and transmission of electricity, on each one of the individual impact categories, is presented in Figure 74. It is clearly observed that most GHG emissions and fossil energy consumption come from the electricity generation sector, accounting for more than 90% of the total climate change impact and non-renewable energy demand. The electricity generation system of mainland Greece, which depends heavily on local lignite resources and imported natural gas, is the major contributor to the categories of freshwater ecotoxicity (~77%), human toxicity (cancer, ~62%, and non-cancer, ~73%), water scarcity (~72%), as well as land occupation and transformation (>50%). A markedly different pattern emerges for the categories of climate change, fossil energy use, photochemical oxidant formation, ozone layer depletion, freshwater acidification, terrestrial acidification, freshwater eutrophication, marine eutrophication, and particulate matter formation. In these impact categories, the contribution of the mainland electrical distribution system decreases substantially, accounting for about 23-40%, whilst the electrical systems of the non-interconnected islands contribute significantly (more than 50%). As it has already been noted, electricity generation in isolated/autonomous Greek islands is carried out, almost exclusively, employing diesel electric generators. The low efficiency of diesel generators, as well as, the high CO_2, particulate matter, SO_2 and NO_x emissions, are responsible for the high contribution of the islands grid in these specific categories. Last, but not least, the interconnected

electricity transmission system exhibits relatively small impacts in all categories, accounting for up to 30% of total impacts when compared with the electricity generation sector. The sole notable exception is the mineral resource use impact category, in which the transmission system contributes a substantially higher share (approximately 65%), primarily because of the extensive use of aluminium and steel in transmission line conductors and supporting infrastructure.

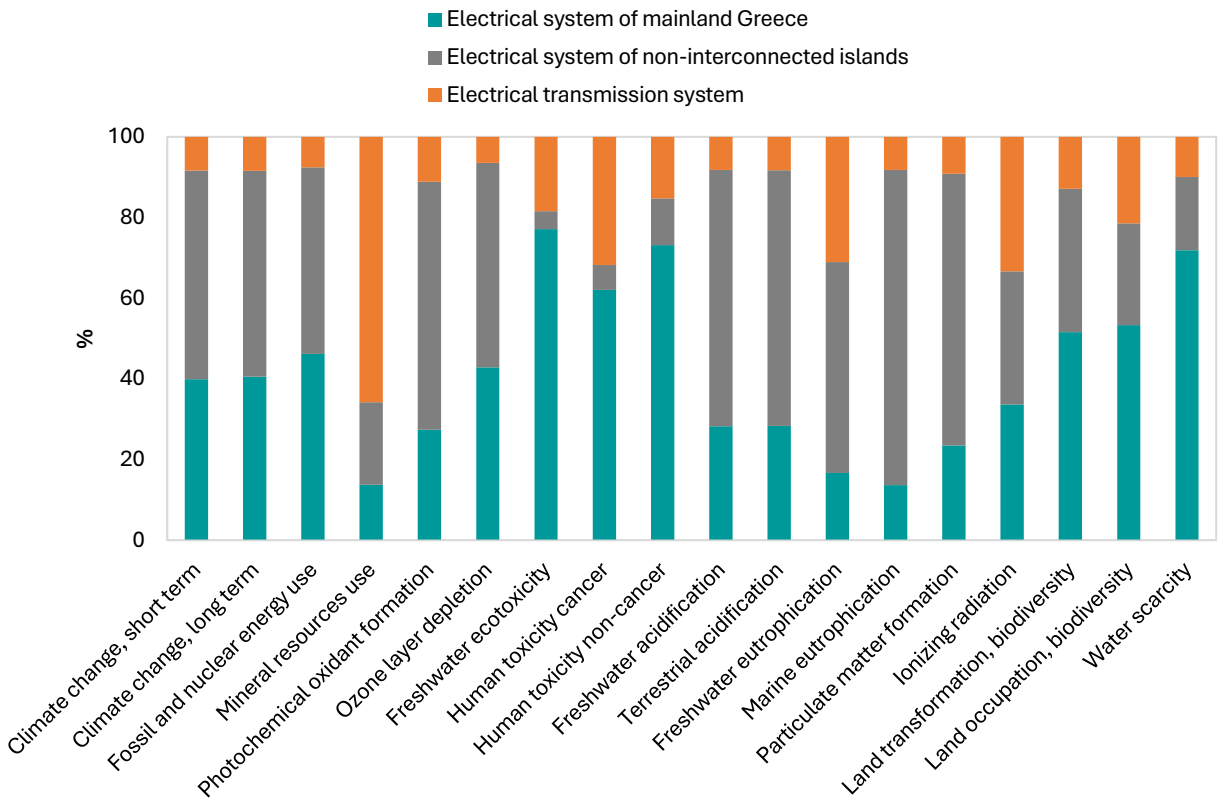

Figure 74 Life cycle impact categories of the electricity generation sector (mainland Greece and non-interconnected islands), and the interconnected transmission system in 2016

6.5 Summary and conclusions

This case study investigated the environmental performance of the Greek electricity sector as a whole, by considering the various power generation technologies currently operating in Greece, and the inter-connected electricity transmission system of mainland Greece. The detailed results included show that the main, environment-wise, adverse impacts are associated with the electricity generation system, which is dominated by centralized thermal power plants and relies heavily on lignite resources. The estimated GHG emissions figure from electricity generation in the country amounts to 653 gCO_{2eq}/kWh_e, whilst the relevant non-renewable energy use value reaches at 7.32 MJ/kWh_e. These figures reflect the electricity generated in Greece in 2016, and do not account for the contribution of electricity imports and exports in the national

supply mix. Consequently, the total environmental impacts associated with power generation are expected to be somewhat higher.

Having addressed the entire life of the energy sources used in the Greek electricity sector, lignite-fired electricity generation emerges as the dominant contributor to life cycle environmental impacts across most of the impact categories examined. This predominance is driven not only by the high share of lignite in the national generation mix, but also by its intrinsically high carbon content and low calorific value, which result in elevated fuel consumption and emissions per unit of electricity produced. The next significant, environment-wise, adverse contribution comes from natural gas-fired electricity generation, followed by oil-fired generation. Large hydro, CHP plants, and renewable energy technologies are associated with much lower environmental impacts. For fossil fuel-based electricity generation technologies, most life cycle impacts come from the plants operation and generation stage (combustion process). On the other hand, renewables impacts are linked to raw materials processing, as well as components and/or equipment fabrication and facilities construction. From an environmental perspective, results included in the present work indicate clearly that the composition of the generation mix of the country cannot be decided by referring only to GHG emissions and non-renewable energy demand figures associated with each one of the various power generation options involved. Significant environmental impacts in categories related to mineral resources use, human toxicity, freshwater acidification, marine eutrophication, water scarcity, etc., should be also taken into consideration as the relevant environmental scores of different electricity generation options vary considerably.

Recent national energy policies promote electricity generation mixes with a substantially higher penetration of renewable energies. As a result, GHG emissions decline markedly, reaching 337.09 gCO_{2eq}/kWh_e in 2024, which represents a 48% reduction compared to 2016 levels. This decrease is related to the increased contribution of solar and wind power in the electricity mix. Looking ahead, scenarios with further renewable integration are expected to deliver additional climate benefits. By 2030, the GHG emissions are projected to fall to 175.67 gCO_{2eq}/kWh_e. A similar trend is observed for fossil energy use, which declines to 5.94 MJ/kWh_e in the 2024 mix (with a 46% renewable share) and further to 3.19 MJ/kWhe in the 2030 scenario. Overall, these results highlight the effectiveness of renewable energy expansion in reducing substantially both climate change impacts and reliance on non-renewable energy resources. Nonetheless, the transition to more sustainable energy technologies should be carefully managed through the introduction of appropriate policies which take into account factors associated with the adverse impacts of the early stages in the life cycle of renewables. Furthermore, the electricity transmission system of mainland Greece was found to have relatively small environmental impacts, as compared to the generation one. Transmission lines infrastructure is the most significant source of GHG emissions and fossil energy use, accounting for 61% and 54% of the total GHG impact and primary energy demand, respectively. Important contribution comes also from the grid power losses, whereas transformers impacts are considerably lower.

The results of this case study are expected to provide useful insights to policy makers for developing / proposing appropriate energy and environmental policies that will encourage the implementation of both energy efficient practices and clean energy technologies in the country, so as to minimize the environmental footprint of the electricity sector in general.

Chapter 7
Wind Turbine End-of-Life Options

The previous chapters of this thesis examined the energy, economic, and environmental impacts of wind turbines, solar PV systems, and hybrid fossil–renewable power systems across key life cycle stages, with a focus on construction, operation, and system integration at both community and grid levels. While these analyses provided a comprehensive assessment of renewable energy performance during their active lifetime, the EoL phase was not explicitly addressed. Given the rapid expansion of wind energy deployment and the approaching decommissioning of early-generation turbines, EoL management has emerged as a critical factor influencing the overall sustainability of wind power systems. Wind turbines comprise complex material assemblies, including composite components that pose significant challenges for conventional waste treatment, while simultaneously offering opportunities for resource recovery within a circular economy framework. To address this gap, this chapter advances the methodological framework by focusing on the EoL phase of wind turbines. An integrated application of LCA and DEA, complemented by TOPSIS, is employed to evaluate the efficiency of alternative EoL treatment options from technological, economic, and environmental perspectives. Eleven scenarios are developed for the material waste management of a representative wind turbine operating in Greece, covering mechanical recycling, landfill disposal, and advanced chemical recycling technologies, including conventional and microwave pyrolysis. The proposed approach supports evidence-based decision-making and informs circular economy-oriented policies for more sustainable wind turbine waste management in the built environment.

7.1 Case study overview

Part of this work has been published in a peer-reviewed scientific journal [285] *(Gennitsaris S, Sagani A, Sofianopoulou S, Dedoussis V. Integrated LCA and DEA approach for circular economy-driven performance evaluation of wind turbine end-of-life treatment options. Applied Energy 2023;339:120951)*.

7.1.1 Key components and material composition of an onshore wind turbine

This case study aims to identify the most sustainable EoL treatment option for decommissioning a Vestas V52 onshore wind turbine operating in Greece. The Vestas V52 model was selected as one of the most commonly deployed wind turbine types in the country, accounting for approximately 45% of the installed onshore capacity [286].

The principal subsystems of a standard onshore wind turbine are: (a) the rotor assembly, which typically consists of three aerodynamically optimized blades mounted on a central hub; this hub interfaces with the main shaft and frequently incorporates either hydraulic or electromechanical mechanisms to adjust blade angles for load and performance optimization, (b) the nacelle, housing shafts, a gearbox, and a generator, as well as auxiliary systems, encompassing lubrication units, cooling systems, and a yaw drive mechanism

to adjust the nacelle's orientation, (c) a tower and foundation to support the rotor and the nacelle, and (d) the electrical and control infrastructure, including power converters, transformers, monitoring sensors, internal cabling, and a centralized control unit for performance tracking, fault detection, and operational coordination [287].

The tower, which is the largest structural element of a wind turbine, is constructed from steel due to its strength and ability to withstand dynamic loads associated with high wind speeds. The nacelle is commonly fabricated from a combination of steel and iron materials, owing to their durability under the mechanical and thermal stresses encountered during the wind turbine operation. Small amounts of copper and silica are also present within the nacelle because of including electronic components. The nacelle cover generally consists of composite materials, such as fiberglass reinforced with resin, in order to provide a lightweight yet robust enclosure. Regarding rotor materials, iron or cast iron is typically utilized for the blade hub, while glass-reinforced plastic (GRP) and resin are used for the nose cone and blades, mainly due to their favourable strength-to-weight ratio and resistance to environmental degradation. The foundation is mainly made from concrete, reinforced with steel and iron to ensure structural stability and load distribution [288,289]. The detailed material composition of the wind turbine evaluated in this study is presented in derived from the data reported in Table 32 [289].

Table 32 Material composition of an onshore wind turbine

Material	w/w
Steel	71-79%
Fiberglass, resin, or plastic	11-16%
Iron or cast iron	5-17%
Copper	1%
Aluminium	0-2%

7.1.2 End-of-life scenarios for onshore wind turbine materials

Considering the existing waste treatment practices, the material composition of wind turbine systems (see Table 32), the waste hierarchy highlighted in the EU Waste Framework [290], as well as the technological readiness of available waste treatment methods, eleven distinct EoL management scenarios have been defined. These scenarios, summarized in Table 33, aim to identify the most effective strategies for managing wind turbine waste by comparing the potential benefits of mechanical recycling, thermal recycling, and material repurposing within the context of a circular economy. The scenarios focus on three primary waste streams, as illustrated in Figure 75: (1) landfill disposal or mechanical recycling of metals, with a recovery rate of approximately 95%, (2) landfill disposal or mechanical recycling of concrete from the foundation (as concrete aggregates), and (3) landfill disposal or recycling of turbine blades, either via mechanical grinding or thermal processes such as pyrolysis or microwave pyrolysis. It is worth mentioning that while mechanical recycling remains the predominant waste treatment practice in Greece, and advanced thermal recycling technologies are still in the early stages of adoption across much of Europe, their inclusion in this analysis

underscores the necessity for future investments in high-efficiency, innovative waste processing infrastructure.

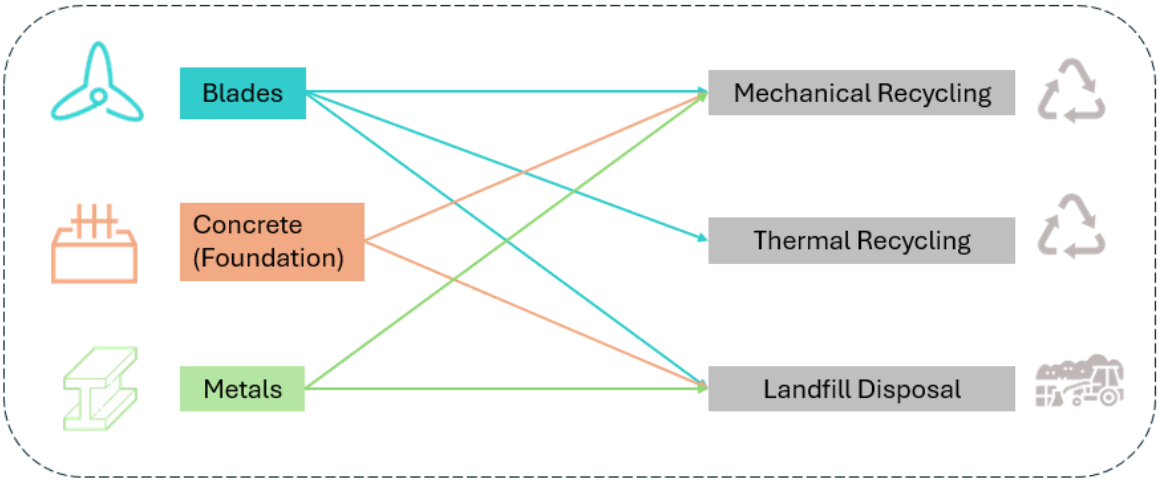

Figure 75 EoL treatment methods for key wind turbine components

Table 33 Scenarios for waste management of materials of onshore wind turbines

	EoL waste management		
Scenario	Metals	Foundation Concrete	Wind Turbine Blades
1	Landfill Disposal	Landfill Disposal	Landfill Disposal
2	Mechanical Recycling	Mechanical Recycling	Landfill Disposal
3	Mechanical Recycling	Mechanical Recycling	Repurposing
4	Mechanical Recycling	Landfill Disposal	Landfill Disposal
5	Mechanical Recycling	Landfill Disposal	Repurposing
6	Mechanical Recycling	Mechanical Recycling	Chemical Recycling / Pyrolysis
7	Mechanical Recycling	Mechanical Recycling	Chemical Recycling / Microwave Pyrolysis
8	Mechanical Recycling	Mechanical Recycling	Recycling / Mechanical Grinding
9	Mechanical Recycling	Landfill Disposal	Chemical Recycling / Pyrolysis
10	Mechanical Recycling	Landfill Disposal	Chemical Recycling / Microwave Pyrolysis
11	Mechanical Recycling	Landfill Disposal	Recycling / Mechanical Grinding

7.2 Methodology application

7.2.1 Comparative analysis via Life Cycle Assessment

This section provides a holistic environmental evaluation of the different EoL material management scenarios considered for the decommissioning of a typical wind turbine. The analysis is conducted using LCA, following the methodological framework established by the with ISO 14040 and ISO 14044 Standards [30,31].

Phase 1 System boundaries and description

The system boundaries of this case study encompass (Figure 76): (i) the decommissioned wind turbine, disaggregated into its major assemblies, subcomponents, and material constituents, (ii) the transportation of these subcomponents/materials from the installation site to either landfill facilities or recycling centres, and (iii) the EoL treatment alternatives available, namely disposal or recycling, of the principal wind turbine waste materials. This life cycle environmental assessment is limited to the decommissioning stage, and explicitly excludes the upstream stages of infrastructure development, such as the fabrication and assembly of turbine components. Furthermore, the effect of the construction, installation and maintenance of supporting infrastructure, including transformers, substations, and auxiliary systems integral to wind energy operations, is also not investigated. This exclusion is justified on the basis that such infrastructure often continues to function beyond the turbine's operational life, for instance, in repowering scenarios or integration within hybrid renewable energy and storage systems. The FU is defined as one wind turbine, providing a standardized reference point for systematic comparisons with existing LCA studies. This enhances the consistency and reliability of the environmental impact assessment outcomes.

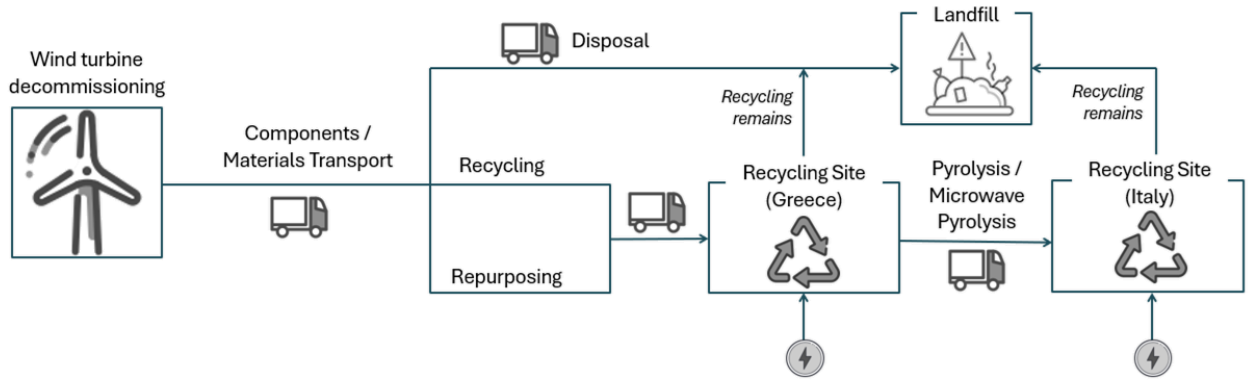

Figure 76 System boundaries of EoL treatment of decommissioned wind turbine material

Phase 2 Life Cycle Inventory

As previously noted, the LCI phase is widely regarded as the most complex and resource-intensive stage of the LCA process. This phase involves the systematic compilation of data related to material flows associated with wind turbine components and their EoL treatment. It also entails energy flows, for instance the energy consumed during the transportation and decommissioning activities, as well as emissions generated throughout the EoL processes, specifically those arising from the transportation, recycling, repurposing, or landfilling of decommissioned materials. The wind turbine is assumed to have an operational lifespan of approximately 25 years.

Table 34 presents the required data for all unit processes involved in the system boundaries. The LCI data for wind turbine decommissioning is based on material flows provided by the work of Andersen [291]. It is significant to note that the total weight of the wind turbine comprises the tower, nacelle and rotor (including its hub), with all weight estimations based on a rotor diameter of 52 m. Additional material data concerning the wind turbine foundation correspond to the ones reported in [292]. Landfill disposal and the recycling processes for metals and concrete were modelled using secondary data from relevant literature sources and the Ecoinvent Database version 3.9.1 [293]. The Ecoinvent Database is a widely accepted, consistent, and transparent resource commonly used for sustainability assessments in the context of wind turbines.

Table 34 Material data for the examined onshore wind turbine

Part	Steel (ton)	Iron (ton)	Aluminium (ton)	Copper (ton)	Composite material (ton)	Concrete (ton)
Wind turbine	76	11.0	1.2	1.2	8.0	-
Foundation	30.7	-	-	0.025	0.025	570.9
Total	106.7	11.0	1.2	1.225	8.025	570.9

In the waste management of wind turbines, metals and concrete represent two of the most fundamental recyclable materials, with estimated recyclability rates of about 95% and 80%, respectively. As reported in [294], conventional pyrolysis is an energy intensive process, with an energy consumption figure of 30 MJ/kg, while microwave-assisted pyrolysis reduces energy demand to 10 MJ/kg. Mechanical grinding, in contrast, is the most energy-efficient method, consuming only 0.27 MJ/kg. It should be noted that both conventional and microwave pyrolysis can offer considerable energy savings by eliminating the need to produce virgin glass fiber-reinforced materials, which require about 22.5 MJ/kg. As demonstrated in [295], pyrolysis has high material and energy recovery potential, particularly through the use of syngas and pyrolytic oil generated during the process to partially or fully fuel the reaction itself. Since pyrolysis is an endothermic process, i.e., requires heat to sustain the reaction, the ability to reuse its own by-products (oil and gas) can substantially reduce the need for external energy inputs. Notably, pyrolytic oil and pyrolytic gas have high heating values, with pyrolytic oil ranging between 33.6 and 37 MJ/kg, and pyrolytic gas ranging from 13.9 to 37.7 MJ/m^3, making them promising options for heat applications. However, in this case study only the avoided energy demand has been considered in the evaluation. The positive effects of material and energy recovery were not investigated, as the high heating values of pyrolysis by-products are strongly dependent on process conditions (e.g., temperature, pressure, residence time) and the type of the reactor employed.

In addition, high-efficiency pyrolysis of wind turbine blades, capable of maximizing energy and material recovery, can only be conducted in specially designed facilities [296].

Regarding the transportation stage data (refer to Table 35), it is assumed that the decommissioned wind turbine originates from a wind farm located in Xirolivado, in Northern Greece, at latitude 40.99° N and longitude 24.37° E. Mavroraxi Waste Landfill Site, located in Thessaloniki, in Northern Greece, is identified as the most appropriate site for the disposal of wind turbine waste material. Moreover, the primary mechanical recycling facility in Greece is located in the city of Kavala, also in Northern Greece. For advanced recycling methods, such as conventional and microwave pyrolysis, the most suitable facility is located in Northern Italy, at latitude 46.01° N and longitude 9.57° E.

Table 35 Input data related to transportation stages

Route	Transportation Distance (km)
Disposal	
Wind Farm (Xirolivado) – Landfill (Mavroraxi)	120
Recycling	
Wind Farm (Xirolivado) – Main Recycling Facility (Kavala)	250
Main Recycling Facility (Kavala) – Landfill (Mavroraxi)	160
Main Recycling Facility (Kavala) – Recycling Facility (Italy)	1750

Phase 3: Life Cycle Impact Assessment

Following the data collection phase, the LCA was carried out. The various stages of the EoL management of the wind turbine sub-components and relevant materials, as depicted in Figure 76, were modelled using the SimaPro PhD 9.4 software . Following a comprehensive literature review on the existing Standardized LCIA Methodologies, distinguished either as single-issue ones or typical European ones, the IMPACT World+ Midpoint methodology was selected to assess the potential environmental impacts of the different EoL scenarios under consideration (refer to Table 33). This assessment approach was chosen due to its robust framework and its compatibility with the specific impact categories investigated in this study, namely climate change, land occupation, and fossil and nuclear energy use. A detailed documentation of the IMPACT World+ methodology is available in the technical literature, for example, in the work of Bulle et al. [39].

7.2.2 DEA-TOPSIS scenario selection for end-of-life management

Having evaluated the environmental performance of the different EoL management scenarios employing the LCA methodology, the assessment is further extended to a multi-criteria perspective by applying DEA-TOPSIS. Specifically, the DEA is utilized to assess the relative efficiency of each scenario, incorporating both economic and environmental indicators, with the latter derived from the LCA findings. Following the DEA assessment, TOPSIS is implemented to rank the scenarios and provide a comprehensive decision-making framework that integrates both efficiency and preference-based evaluation. The under-lying analytical equations and detailed methodology for the hybrid DEA-TOPSIS have been presented in Chapter

3. For computational implementation, the relevant algorithms have been developed in Python, ensuring a consistent and reproducible framework for scenario evaluation.

Input and Output Parameters

The DEA analysis was performed employing real-world data for the decommissioning of the Vestas V52 wind turbine. Specific input and output parameters were selected to capture both the environmental and economic dimensions of each scenario. Input parameters encompass: (a) total cost (€), representing the overall expenditure for disposing construction material associated with all wind turbine components, (b) material transport demand (tkm), reflecting the transport effort required for each scenario. It should be noted that, for consistency, the cost of metal landfill disposal is assumed to be equivalent to that of concrete disposal. On the other hand, output parameters include: (a) land occupation (m^2), which refers to the land area, particularly landfill, required for implementing each waste material management scenario, (b) climate change (ton CO_{2eq}), which represents the total GHG emissions associated with each scenario, reflecting the environmental impact of the different waste treatment processes, and (c) fossil and nuclear energy use (MJ), which denotes the primary energy consumption linked to each EoL management scenario. Primary energy is defined as the energy directly related to the amount of natural resources (in most cases fossil fuels, such as coal, crude oil, natural gas, etc.) that has not undergone any anthropogenic conversion and has to be converted and transported in order to become useful energy. Relevant input (cost) data for the different scenarios considered are summarized in Table 36. Data for the aforementioned output parameters were obtained through LCA using SimaPro PhD 9.5 software. The corresponding DEA matrix, incorporating both the input and output parameters used in this study, is presented in Table 37.

Table 36 Cost of EoL treatment of wind turbine materials [297–300]

Waste material	Cost (€/ton)
Mechanical Recycling	
Aluminium	45.5
Copper	181.8
Steel	181.8
Iron	30.5
Concrete (as aggregate)	
Mechanical Grinding	
Composite Material	85.6
Landfill Disposal	
Aluminium	35.0
Copper	35.0
Steel	35.0
Iron	35.0
Concrete	35.0
Composite Material	88.2
Pyrolysis	225.6
Microwave Pyrolysis	182.6

Table 37 Original DEA matrix (Input – Output Parameters)

DMU	Input values		Output values		
	Cost (€)	Transport (tkm)	Land occupation, biodiversity (m^2)	Climate change (ton CO_{2eq})	Fossil and nuclear energy use (GJ)
1	24,893.12	83,886.00	958.24	66.29	1,032.39
2	39,323.19	192,949.05	-10.79	31.80	1,336.96
3	38,615.77	193,992.30	248.80	10.58	970.30
4	41,383.18	100,463.25	-286.87	-49.68	162.73
5	40,675.76	101,506.50	-29.29	-71.04	-203.99
6	40,666.56	208,036.05	190.75	41.46	1,488.35
7	40,080.93	208,036.05	-385.20	18.47	1,128.71
8	39,302.77	208,036.05	-21.82	20.64	922.48
9	42,726.54	115,550.25	-87.34	-40.16	314.06
10	42,140.92	115,550.25	-663.29	-63.15	-45.62
11	41,362.76	115,550.25	-299.91	-60.98	-251.82

The DEA model applied in this case study follows the assumptions involved in classical DEA models, where inputs are minimized and outputs are maximized, and all input and output parameters are required to take positive values. Nevertheless, considering that some output parameters reflect undesirable environmental impacts, their numerical values should be minimized. The original output parameters, derived through the LCA methodology and summarized in Table 37, encompass both positive and negative values. To address this, an appropriate numerical transformation [301] has been applied the original output values so as not only to make them positive, but also to convert them to desirable output measures, i.e., as the transformed output value is maximized by the DEA method, the original/actual output value is decreased [302]. The appropriately transformed output parameter data used in the analysis are shown in Table 38.

Table 38 Appropriately transformed output parameters data

DMU	Land occupation, biodiversity (m^2)	Climate change (ton CO_{2eq})	Fossil and nuclear energy use (GJ)
1	95.82	6.63	604.80
2	1,064.85	41.12	300.23
3	805.27	62.34	666.88
4	1,340.94	122.59	1,474.46
5	1,083.36	143.96	1,841.18
6	863.32	31.46	148.84
7	1,439.27	54.45	508.48
8	1,075.89	52.28	714.71
9	1,141.41	113.08	1,323.13
10	1,717.36	136.07	1,682.81
11	1,353.98	133.90	1,889.01

Building on the DEA results, TOPSIS was employed to derive a comprehensive ranking of the EoL scenarios and to test the robustness of the DEA-based efficiency scores under different weighting visions. To capture potential stakeholder priorities, three weighting visions were taken into consideration. The first vision, "*Environmental Priority"*, places dominant emphasis on climate change impact (weight 0.40), land occupation (0.20) and fossil and nuclear energy use (0.20), reflecting a focus on reducing GHG emissions and minimizing landfill use and primary energy demand. Lower weights are given to cost and transport demand (0.10 each). The second vision, "*Cost Efficiency",* assigns the highest weight to decommissioning costs (0.60), followed by transport demand (0.15), which is treated as a hybrid criterion due to its dual economic (logistics costs) and environmental (transport emissions) implications. Lower weights are given to GHG emissions and fossil and nuclear energy use (0.10 each), and land occupation (0.05). Finally, the "Balanced Circular Economy" vision distributes the weights more evenly, allocating 0.25 to cost, 0.15 to transport, and 0.20 to each of the three environmental indicators, thus promoting a compromise between economic feasibility and environmental performance consistent with circular economy principles. All weights satisfy the normalization constraints, summing to unity in accordance, ensuring consistency in the multi-criteria evaluation. The aforementioned, summarized in Table 39, were combined with the DEA efficiency scores and used as inputs to the TOPSIS method, enabling an integrated multi-criteria ranking of EoL scenarios.

Table 39 Decision visions and associated criterion weights for DEA-TOPSIS

Stakeholder Preferences / Vision	Weighting of performance indicators					Description
	Climate change	Land occupation	Fossil and nuclear energy use	Cost	Transport	
Environmental Priority	40%	20%	20%	10%	10%	Strong focus on GHG mitigation, landfill and primary energy demand minimization, with minimal weight given to cost and transport
Cost efficiency	10%	5%	10%	60%	15%	Dominant emphasis on minimizing decommissioning costs, with limited consideration of environmental impacts
Balanced Circular Economy	18%	10%	12%	40%	20%	Seeks compromise between economic feasibility and environmental performance, aligning with circular economy principles

7.3 Simulation results and discussion

7.3.1 LCA results

The results of the environmental evaluation are depicted in Figure 77, Figure 79 and Figure 81, which present the impacts in terms of climate change, land use, and fossil and nuclear energy use, respectively.

7.3.1.1 Climate change impact

The comparative analysis of climate change impacts across the scenarios examined reveals substantial variation in GHG emissions performance (refer to Figure 77). Scenario 1 shows the highest GHG emissions, estimated at 66.29 ton CO_{2eq}/wind turbine, mainly because of the transportation activities, which account for approximately 94 % of total emissions (see Figure 78). The notable contribution from transportation results from the utilization of diesel-powered trucks for transporting the wind turbine materials from the wind park to landfill facilities. Conversely, mechanical recycling of metals is highly beneficial, avoiding more than 41% of GHG emissions in all scenarios, except the Scenario 1, where metals are landfilled. Concerning composite blade management, repurposing (Scenarios 3 and 5), microwave pyrolysis (Scenarios 7 and 10), and mechanical recycling (Scenarios 8 and 11) lead to moderate benefits, with avoided emissions ranging between 4% and 19%. On the other hand, conventional pyrolysis (Scenarios 6 and 9) is associated with significant GHG emissions due to its energy-intensive nature, with the required energy being generated via fossil fuels. Scenarios 2, 3, 7, and 8 also display elevated GHG emissions due to the increased transport needs for mechanical recovery of foundation concrete. Specifically, Scenario 2 reaches 31.8 ton CO_{2eq}/ wind turbine, because of landfill disposal of blade composite materials. Scenarios 8 (20.64 ton CO_{2eq}/wind turbine), 7 (18.47 ton CO_{2eq}/wind turbine), and 3 (10.58 ton CO_{2eq}/wind turbine) follow with progressively lower impacts. The most favourable outcome is observed in Scenario 5, which demonstrates net negative emissions of 71.04 ton CO_{2eq}/wind turbine via the combined effect of metal recycling, blade repurposing, and concrete disposal. Scenarios 10 and 11 also exhibit strong environmental performance, both achieving -63.15 ton $CO_{2εq}$/wind turbine due to a mix of metal recycling, concrete disposal, and advanced blade recycling techniques(microwave-assisted pyrolysis or mechanical recycling). It is worth mentioning that negative GHG emission values represent overall avoided impacts and indicate a net environmental benefit. Overall, blade repurposing consistently improves environmental performance, as indicated by Scenarios 3 and 5, with Scenario 5 clearly outperforming landfill-intensive scenarios such as 1 and 2 (see Figure 77).

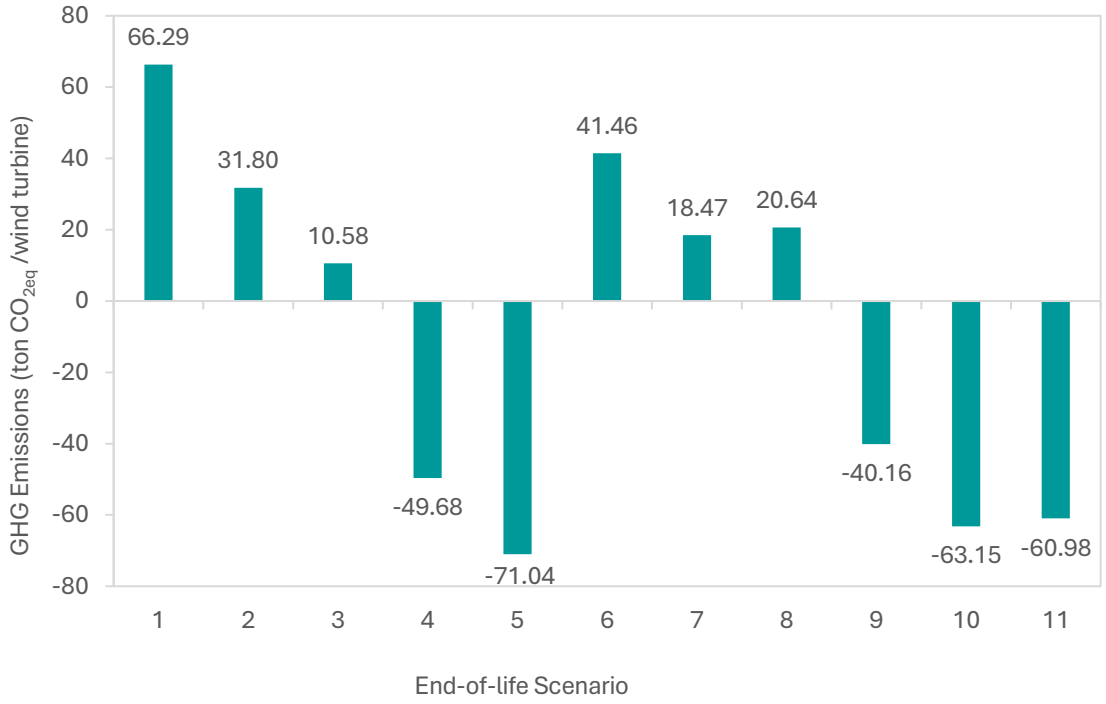

Figure 77 GHG emissions of different EoL scenarios investigated (IMPACT World+ Midpoint methodology)

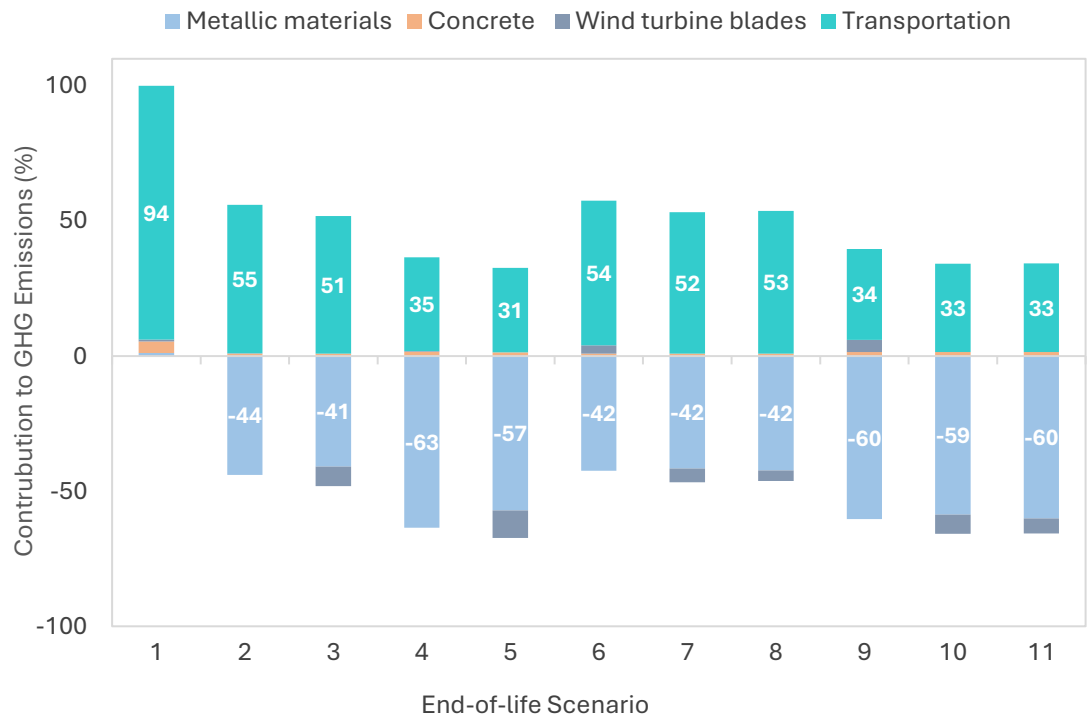

Figure 78 Percentage share of the different treatment methods in overall GHG emissions for the examined EoL scenarios (IMPACT World+ Midpoint methodology)

7.3.1.2 Land occupation impact

The impact of different waste management options on land occupation for wind turbine materials and components at the end of their life is depicted in Figure 79. Scenario 10 is the most sustainable EoL treatment solution with an estimated land occupation indicator of -663.29 m^2/wind turbine, due to landfill disposal of concrete and microwave-assisted pyrolysis of composite materials. Scenario 7 ranks second, with -385.20 m^2/wind turbine, due to mechanical recycling of concrete and microwave-assisted pyrolysis of composite materials. Scenarios 11 and 4 also present important land use benefits, with -299.99 m^2/wind turbine and -286.87 m^2/wind turbine, respectively. On the other hand, Scenario 1 has the highest land occupation impact; this is attributed to the fact that all materials (metals, concrete and composites) are disposed of in landfills. It is important to note that microwave-assisted pyrolysis of composite materials significantly improves the land use impact indicator by almost 131%, when compared to landfill disposal (Scenario 10 vs. Scenario 4, in Figure 79). As illustrated in Figure 80, metallic materials recycling has the strongest positive effect on land occupation, showing the highest negative land use values (indicating environmental benefits).

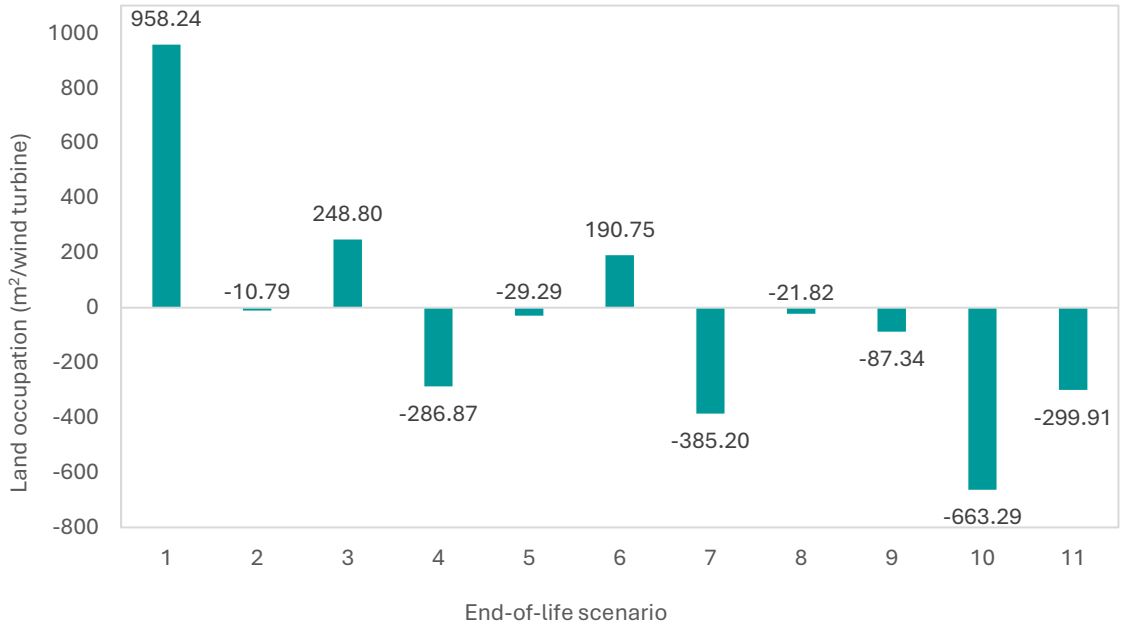

Figure 79 Land occupation of different EoL scenarios investigated (IMPACT World+ Midpoint methodology)

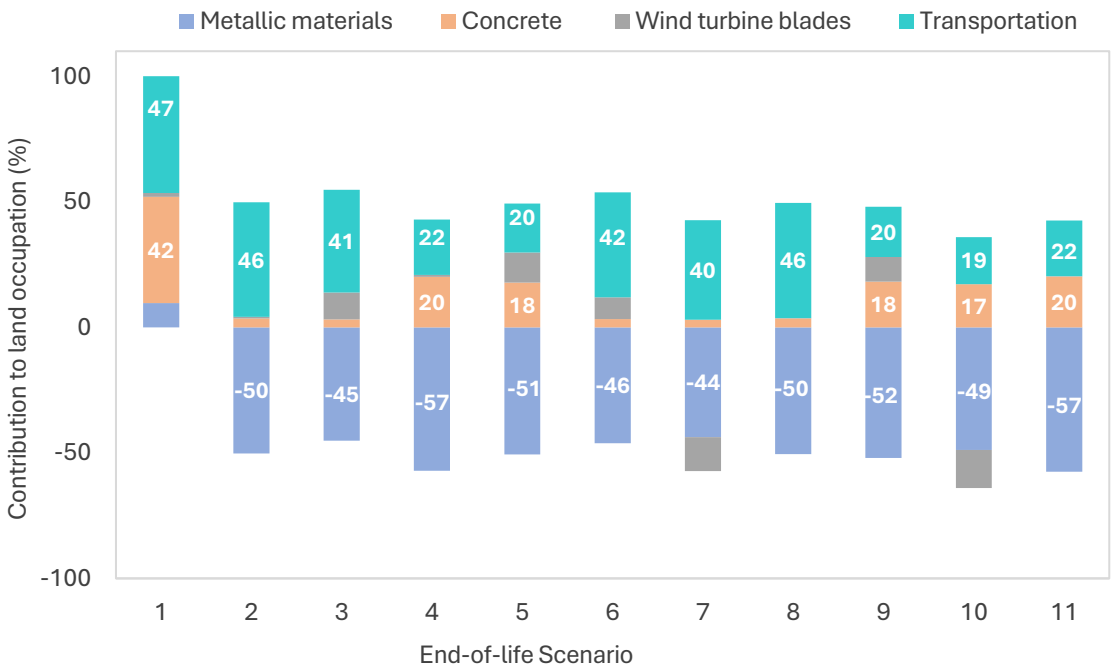

Figure 80 Percentage share of the different treatment methods in land occupation for the EoL scenarios investigated (IMPACT World+ Midpoint methodology)

7.3.1.2 Fossil and nuclear energy use

Calculated results, illustrated in Figure 81, reveal that Scenario 6, related to mechanical recycling of both metals and foundation concrete, along with conventional pyrolysis of blades composite material, has the highest non-renewable energy consumption, evaluated at about 1,488 GJ/wind turbine. This can be attributed to high transportation demands, and fossil-based energy-intensive conventional pyrolysis. In particular, pyrolysis relies on thermal power generation, whereas diesel trucks transport composite materials. Therefore, both transportation distances and energy needs for pyrolysis should be carefully considered when selecting EoL strategies. Scenarios 2, 7, 1, 3 and 8 are also high-impact ones, with 1,136.96, 1,128.71, 1,032.29, 970.3 and 922.48 GJ/wind turbine, respectively. These scenarios are largely impacted by transport demands for mechanical recycling of concrete and waste management of composites. On the other hand, Scenarios 11, 5 and 10 are linked to the lowest fossil & nuclear energy consumption, mainly due to landfill disposal of the concrete foundation rather than energy intensive chemical recycling processes. It is worth noting that mechanical recycling has positive effect by decreasing the need for primary metal extraction (refer to Figure 82). Moreover, as shown in Figure 81, substituting chemical recycling/microwave pyrolysis with composite material repurposing (i.e., consider Scenario 3 instead of Scenario 7) reduces significantly fossil and nuclear energy use by 15%.

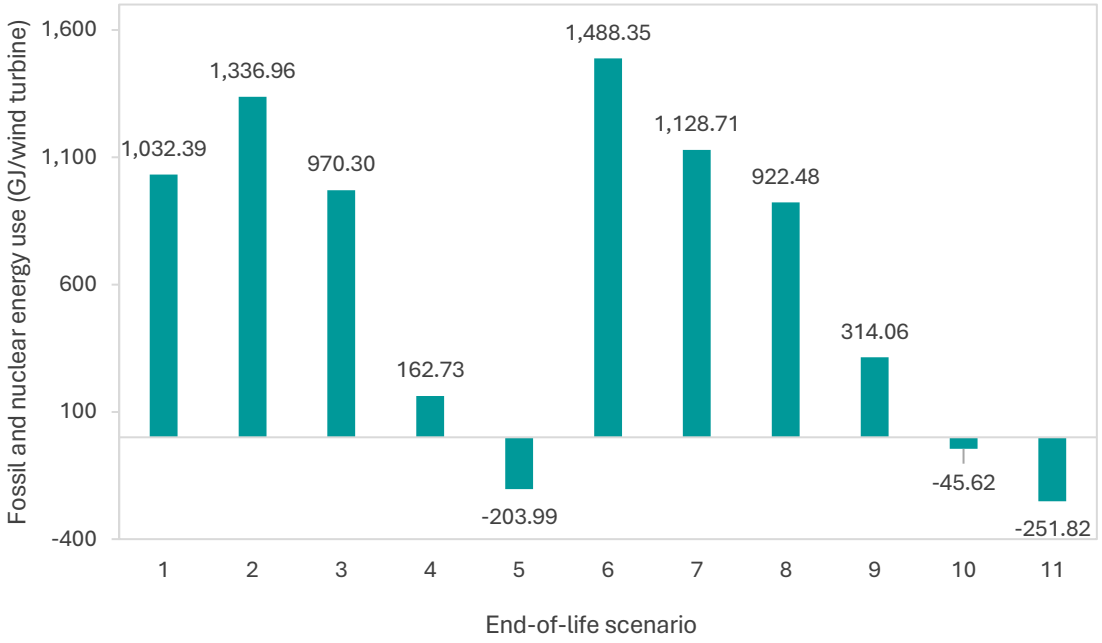

Figure 81 Fossil and nuclear energy use of different EoL scenarios investigated (IMPACT World+ Midpoint methodology)

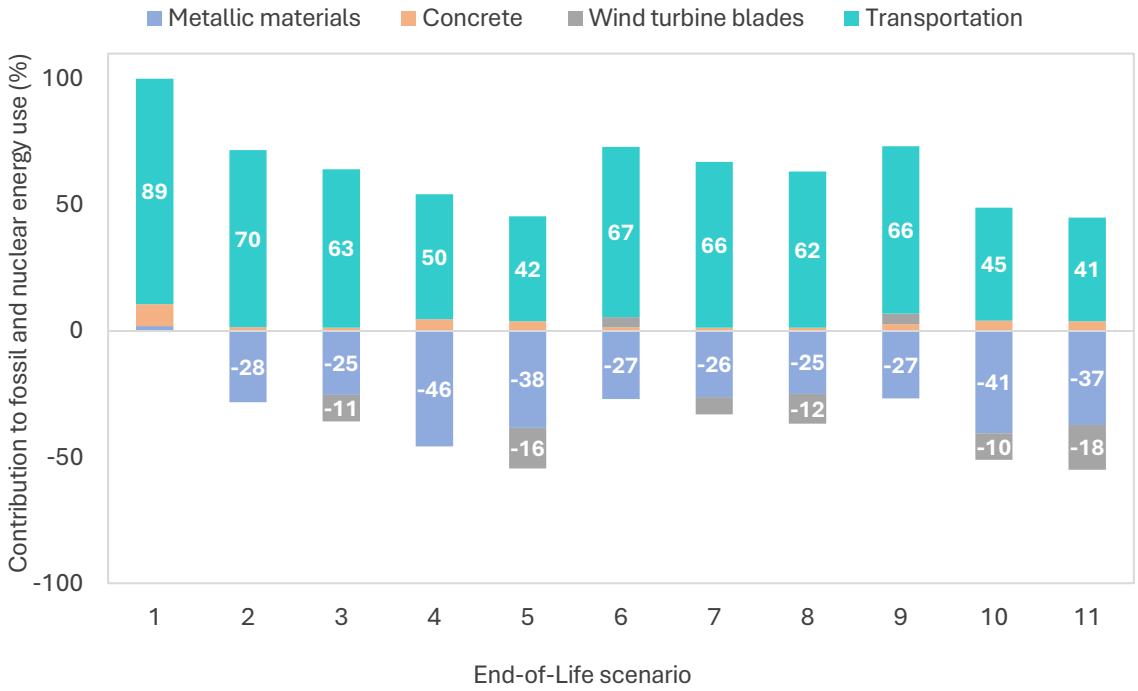

Figure 82 Percentage share of the different treatment methods in overall fossil and nuclear energy use impact category for the EoL scenarios investigated (IMPACT World+ Midpoint methodology)

7.3.2 DEA-TOPSIS results

7.3.2.1 DEA efficiency analysis

The DEA methodology was implemented to distinguish efficient EoL treatment processes/scenarios from inefficient ones, considering both economic and environmental aspects. Furthermore, DEA provides performance targets and benchmarks for the inefficient EoL scenarios. The DEA efficiency scores (ϕ) for the different scenarios (DMUs) investigated in this case study are illustrated in Figure 83. These results have been obtained with the DEA approach carried out "in terms of the inputs", i.e., by minimizing the cost of waste management treatment and transportation demand (inputs) of each one of the different EoL scenarios, while keeping environmental indicators (outputs) constant. Scenarios 1, 4, 5, 10 and 11 are identified as technically efficient, with $\phi = 1$, whereas Scenarios 2, 3, 6, 7, 8, and 9 are inefficient, exhibiting efficiency scores ranging between 0.81 and 0.98 ($\phi < 1$).

Figure 84 and Figure 85 demonstrate the original input values and the estimated target values of the virtual DMUs for treatment cost and transportation demand, respectively. The reduction targets indicate potential input savings that inefficient scenarios could achieve if they operated under DEA efficiency conditions. Reductions of 2.2-18.7% in treatment costs and 10.6-52.5% in transportation demand could be realized, with the largest savings associated with the most inefficient scenarios, i.e., scenarios 6, 3, 9, 2, 8, and 7. These findings demonstrate that scenarios with relatively adverse environmental impacts may still be considered economically efficient when only cost and transportation are evaluated. Scenarios 1, 4, 5, 10, and 11 thus emerge as efficient EoL options from both an economic and environmental perspective, with treatment costs ranging from 24,893 € to 42,141€ and transportation distances from 83,886 to 155,550 tkm.

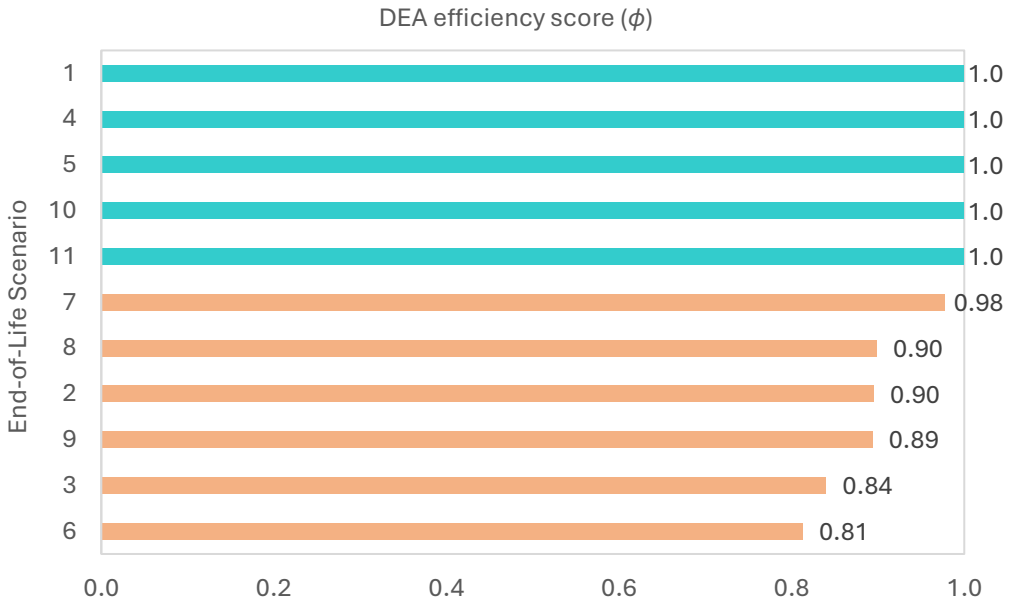

Figure 83 DEA efficiency score for the EoL scenarios/DMUs under investigation

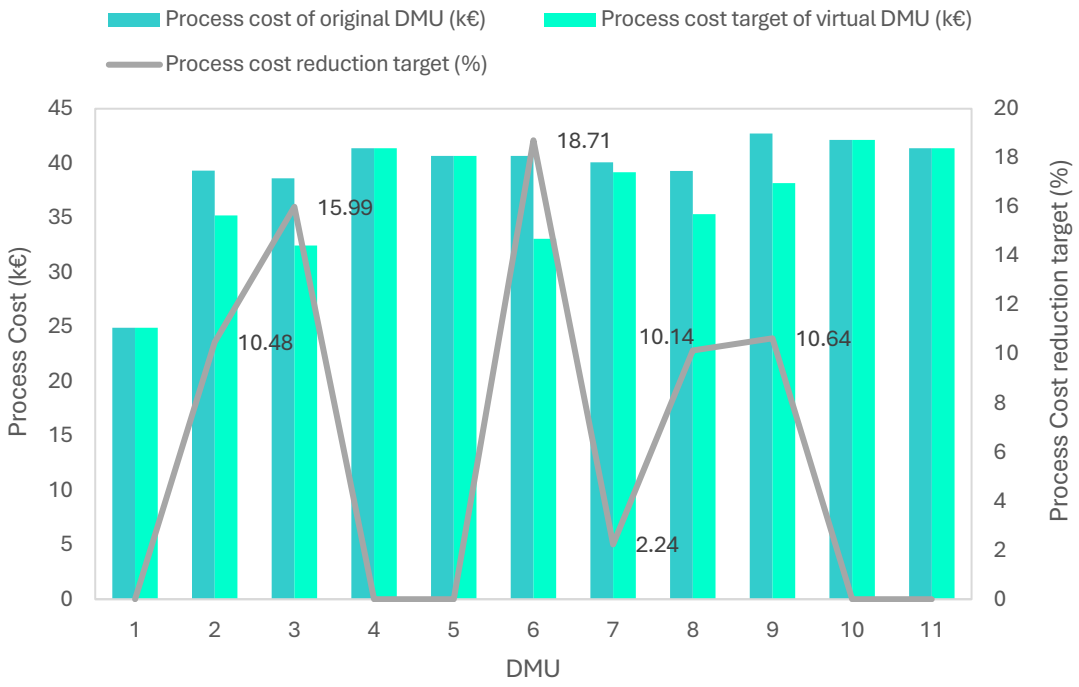

Figure 84 Cost of EoL treatment for the original and virtual DMUs and the corresponding cost reduction target

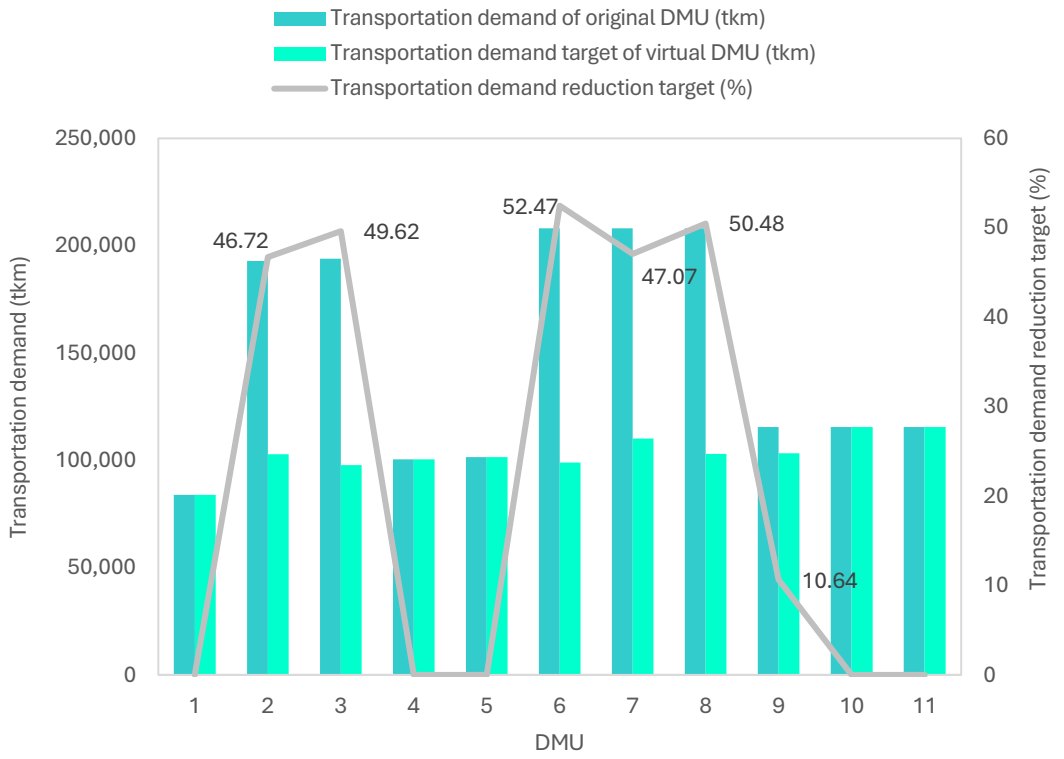

Figure 85 Transportation demand for the original and virtual DMUs and the corresponding transportation reduction target

DEA outputs derived from LCA findings highlight that the environmental performance of waste management processes strongly influences the overall efficiency. Conventional chemical recycling (pyrolysis) of blade composites demonstrates adverse environmental impacts due to the high fossil-fuel energy demand of the process, whereas microwave pyrolysis exhibits greater efficiency because of its lower energy requirements, as reflected in the scores of Scenarios 10 and 9. Similarly, EoL scenarios encompassing landfill disposal instead of mechanical recycling of wind turbine foundation concrete are found to be technically efficient because of the high transportation impacts linked to mechanical recycling. Comparing Scenarios 2, 3, 7, and 8 with Scenarios 4, 5, 10, and 11 reveals that mechanical recycling of foundation concrete introduces significant environmental impacts, and a potential decrease in transportation demand of 46.7 - 52.5% could substantially improve its efficiency. This underlines the significance of establishing dedicated concrete recycling facilities near wind farm clusters to minimize transport distances and promote material circularity.

Interestingly, Scenario 1, accounting for landfill disposal of all wind turbine materials, was found to be technically efficient, primarily due to its low cost and transport demand. However, this option is the least sustainable [106] and increasingly incompatible with EU regulatory frameworks banning composite waste landfilling in countries such as Germany, Austria, the Netherlands, and Finland. This further supports the need for solutions that go beyond landfill and focus on recycling, reuse, and circular economy strategies [303]. Reuse and repurposing of composite materials from decommissioned wind turbines are generally regarded as preferred options, although the low price of virgin glass fibers remains a barrier to wider adoption. DEA findings indicate that mechanical recycling or grinding of composites can be efficient when combined with landfill disposal of concrete (Scenario 11). Comparison across environmental impact categories (Figure 77, Figure 79, Figure 81) confirms that grinding composites has a favourable effect and recent studies [186] support mechanical recycling as the only currently profitable recycling option for decommissioned blades. However, challenges remain, comprising the low quality of recycled composites due to contamination and the high proportion (about 40%) of material waste generated during grinding and sieving [191].

The high cost of recycling processes remains a significant barrier to their implementation. Increasing landfill gate fees for composite materials could make disposal less attractive, while investment in research and development could enhance the energy efficiency and cost-effectiveness of chemical recycling - particularly conventional pyrolysis. DEA results suggest that subsidies in the range of 10.6-18.7% could make pyrolysis more competitive. Beyond cost, structural issues in markets and supply chains also limit recycling adoption. New business models and value chains are needed to address the lack of demand for recovered materials and the limited expertise in integrating recycled composites into new products. Facilitating cross-border movement of waste and recycled materials is also essential to minimize costs and enhance competitiveness.

Finally, the absence of chemical recycling facilities in Greece represents a critical barrier to implementing pyrolysis as a viable alternative to landfill disposal. This study assumes that pyrolysis plants are located in Italy, but DEA results indicate that reducing transportation distances by 10.6–52.5% would significantly improve efficiency. Policymakers should therefore prioritize establishing chemical recycling facilities domestically and support the industrial-scale deployment of microwave pyrolysis. A cross-sectoral

approach, processing composite waste not only from wind farms but also from manufacturing, automotive, and aerospace industries, could improve economies of scale and viability. Future research should explore the economic feasibility, material flows, and value chains required to implement this integrated recycling strategy effectively.

7.3.2.2 TOPSIS ranking

To further discriminate among the efficient alternatives, the TOPSIS method was applied exclusively to the five DMUs identified as technically efficient in the DEA stage (DMUs 1, 4, 5, 10, and 11, refer to Figure 83). This ensured that the multi-criteria ranking was restricted to DEA-efficient solutions, i.e., those located on the efficiency frontier and not dominated by any other alternative in terms of input-output performance.

TOPSIS ranking with environmental priority

Under the environmentally oriented weighting scheme, which allocates 80% of the overall weight to the key environmental performance indicators, namely, climate change, land occupation and fossil and nuclear energy use, the analysis provided a clear hierarchy among the efficient alternatives (see Figure 86). DMU 10 ranked first (C^* = 0.886), mainly due to its significant land use benefits alongside the comparative results across climate change and fossil and nuclear energy use. The employment of microwave pyrolysis further enhances its environmental profile, fully aligning with circular economy targets. DMU 11 followed closely in second place (C^* = 0.854), owing to its low primary energy demand and the small and occupation impact. Its reliance on mechanical grinding for blade recycling presents a viable, though less advanced, circular strategy. DMU ranked third (C^* = 0.821), driven by the substantial GHG emissions mitigation and the low non-renewable energy consumption. DMU 4 place fourth (C^* = 0.794), reflecting moderate performance across all environmental dimensions. Nevertheless, its strong dependence on landfill for both concrete and blades limits its contribution to circular material flows, thus explaining its weaker relative standing. By contrast, DMU 1 (C^* = 0.089) ranks last; although it achieves the lowest cost, it relies exclusively on landfill disposal for metals, concrete and blades. This conventional EoL treatment strategy, combined with adverse impacts in terms of climate change, land use occupation and non-renewable energy use, under-scores its weakness under environmentally weighted scenarios.

Overall, DMUs integrating advanced or semi-advanced recycling technologies (DMUs 10, 11 and 5) resulted in higher TOPSIS rankings, whereas landfill-dependent strategies (DMUs 1 and 4) systematically weakened environmental performance.

TOPSIS ranking with cost efficiency

When economic criteria were given higher weight the ranking of DEA-efficient alternatives shifted markedly (refer to Figure 86). DMU 1 (C^* = 0.637), emerged as the optimal option, capitalizing on its lowest cost and transport requirements. This highlights its substantial competitiveness in purely economic terms, despite its poor environmental profile. The remaining DMUs clustered closely together, with only marginal differences in performance: DMU 5 (C^* = 0.373) and DMU 11 (C^* = 0.355) retained modest advantages due to their stronger environmental contributions, while DMU 10 (C^* = 0.345) and DMU (C^* = 0.324) followed with slightly lower scores. Unlike the environmental-priority scenario, where DMU 10 dominated, this cost

efficiency vision outlines how heavily the balance of weights can reshape the ranking order, shifting emphasis from advanced recycling strategies (DMUs 10, 11, 5) to cost-effective but environmentally weak landfill-based management (DMU 1).

TOPSIS ranking with balanced circular economy

When weights were distributed more evenly among economic and environmental dimensions, the rankings shifted towards compromise solutions that balance economic viability with sustainability outcomes (refer to Figure 86) DMU 5 (C^* = 0.595) achieved the highest score, indicating its substantial climate change mitigation benefits and competitive non-renewable energy consumption, supporting by its repurposing strategy for blades. DMU 10 (C^* = 0.579) and DMU (C^* = 0.585) followed closely, demonstrating their consistently good environmental performance, notably in land Occupation and fossil and nuclear energy use, in conjunction with acceptable economic characteristics. DMU 4 (C^* = 0.555) also ranked competitively under this balanced circular economy perspective, outlining that moderate but steady outcomes across all indicators allow it to gain relevance when neither economic nor environmental criteria dominate. On the other hand, DMU 1 (C^* = 0.406) was found to be the least competitive, since its cost-effectiveness was inefficient to offset its persistent environmental weaknesses under a weighting structure that values both domains equally.

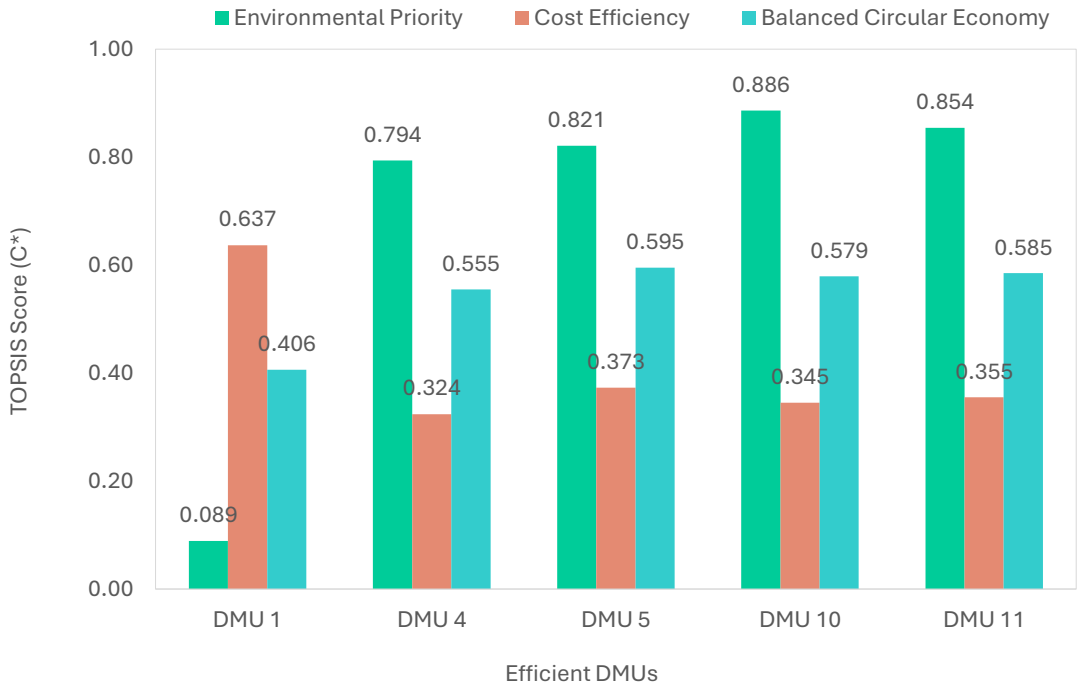

Figure 86 TOPSIS ranking of efficient alternatives under different visions

7.3.2.3 Sensitivity analysis

A comprehensive sensitivity analysis was conducted across 8,960 feasible weight combinations (5% step size, weights summing to unity to investigate the robustness of rankings (Figure 87). It is noting that only DEA-efficient DMUs were encompassed, ensuring that non-dominated solutions defined the ranking space. Computed results demonstrated that DMU 10 was the most robust EoL option, ranking first in 3,988 scenarios (44.5%), driven by the environmental advantages of advanced microwave-assisted pyrolysis for blade recycling. DMU 5 followed closely, achieving top rank in 3,173 combinations (35.4%) when climate change and non-renewable energy indicators linked to higher weights, underscoring the benefits of its repurposing strategy. Moreover, DMU 11 ranked first in 903 scenarios (10.1%), primarily under configurations prioritizing primary energy requirements, reflecting the effectiveness of its mechanical grinding-based treatment. On the other hand, DMU 1 was optimal in only 649 scenarios (7.2%), exclusively when economic criteria dominated the weighting structure (exceeding 60% of the total weight). This outcome shows its cost and transport efficiency yet revealing the environmental limitations of its landfill-based strategy. Last, but not least, DMU 4 was found to be optimal in just 247 scenarios (2.8%), underscoring its marginal role across most sustainability prioritizations. Overall, the sensitivity analysis highlights the distinct strengths and weaknesses of each DMU under varying circular economy-based criteria, providing fundamental insights into the trade-offs between environmental sustainability and economic viability.

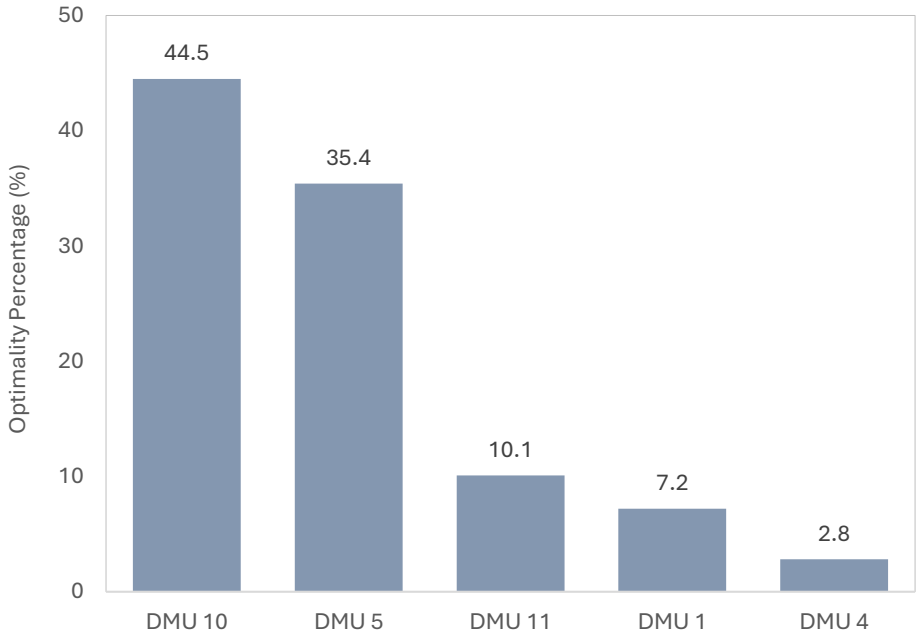

Figure 87 Frequency of optimality across weight combinations

7.4 Summary and conclusions

This chapter presented an integrated framework combining environmental LCA with DEA-TOPSIS in order to evaluate the environmental, technical and economic efficiency of EoL management options for materials from decommissioned wind turbines. The methodology is applied to a representative Vestas V52 wind turbine located in northern Greece, investigating alternative treatment scenarios including landfill disposal, mechanical recycling, advanced thermal recycling (i.e. conventional and microwave-assisted pyrolysis), and repurposing.

The LCA results indicate that the transportation associated with concrete waste from turbine foundations is the most important contributor to GHG emissions and non-renewable energy consumption, while the recycling of metallic components yields clear environmental benefits in terms of GHG emissions, land occupation, and fossil and nuclear energy consumption. Conventional pyrolysis of blade composite materials is identified as environmentally inefficient, mainly due to its high energy intensity and the long-distance transportation of materials to facilities in Italy using diesel-powered trucks. On the contrary, repurposing of composite materials can reduce fossil and nuclear energy use by 15%, while thermal recycling or microwave pyrolysis of composite materials instead of landfill disposal significantly improves the land occupation indicator (up to 131%). The combined application of LCA and DEA-TOPSIS identified the relationships between overall technical efficiency scores and various environmental performance indicators (GHG emissions, fossil and nuclear energy use and land occupation), as well as cost parameters (cost of waste management procedures). It was demonstrated that mechanical recycling of foundation concrete and novel handling or repurposing of composite blade materials emerge as the most effective pathways. In contrast, energy-intensive chemical recycling processes, particularly those involving long-distance transport, are less efficient and costlier. Integrating these strategies with remanufacturing, design-for-recycling, and waste prevention measures can facilitate a transition from a linear to a circular economy framework. Furthermore, targeted financial incentives from government authorities could help offset the cost disadvantages of advanced recycling technologies, further enhancing their adoption. Taken together, these approaches offer a robust framework for sustainable wind turbine decommissioning, providing guidance for policymakers, industry stakeholders, and researchers aiming to minimize environmental impacts while optimizing economic and operational efficiency.

Chapter 8
Conclusions and Future Work

8.1 Concluding remarks

The current Ph.D. thesis demonstrates the development and application of a comprehensive, multi-dimensional methodological framework for assessing and optimizing energy systems, from building-scale solutions to island microgrids and the national electricity sector. Through the incorporation of energy system design, modelling and optimization, life cycle performance evaluation and multi-criteria decision analysis, this dissertation serves as a foundation for the rigorous and holistic assessment of thermal power systems and renewable energy technologies, their operation performance under real-world conditions, economic viability and environmental impacts based on life cycle principles. Based on the key findings presented in detail in the previous chapters, the following conclusions can be drawn:

- LCAs of renewable energy technologies, particularly solar PV and wind power, are free of emissions during their operation phase; however, significant environmental impacts occur during the stages of fabrication, installation and EoL management. The energy- and material- intensive processes, including e.g., silicon purification, for PV systems, and steel and concrete production, for wind turbines, contribute significantly to climate change impact and non-renewable energy use. Shifting manufacturing processes to renewable energy, along with enhancing energy efficiency and adopting circular economy-driven strategies, including recycling, repurposing, and design-for-recycling, can substantially mitigate the adverse environmental impacts. Region-specific datasets, economic viability indicators, like net present value, levelized cost of energy and cost-benefit ratios can improve the reliability of sustainability evaluations and inform policy and technological optimization.
- At the building level, grid-connected solar PV systems and autonomous hybrid solutions incorporating PV, wind, diesel, battery storage, and biomass, demonstrate the ability to meet electricity and thermal energy demand efficiently, while minimizing environmental burdens. Energy (battery) storage is essential for balancing supply and demand, optimizing load management, and reducing curtailment. Economic analyses reveal that system sizing, technological efficiency, and operational strategies are critical for cost-effectiveness.
- Focusing on Greece, grid-connected solar PV systems with rated power between 5 kW_p and 10 kW_p are generally financially attractive. Smaller systems, with capacities below 5 kW_p, are currently not viable. This is mainly due to high investment costs and low electricity selling prices, with the exception perhaps of remote locations such as islands or isolated mountainous villages. However, reductions in initial costs, particularly in module manufacturing and balance of system component production or increases in electricity selling prices could enhance the feasibility of small-scale residential PV installations. In general, the absence of financial incentives represents a significant barrier to the wider deployment of

PV systems in both the domestic and commercial sectors. To effectively promote solar PV as an alternative energy source, it is essential to establish a supportive policy framework that offsets the price barrier for selling renewable electricity to the national grid. Such a framework could include targeted investment incentives, well-designed feed-in tariff mechanisms, and pricing structures based on either the cost of generation or the electricity selling price. Moreover, a sustainable action plan could incorporate trading systems that provide credits to producers for fossil fuel displacement and GHG emissions reductions, fostering further the adoption of solar energy for electricity generation. From an environmental perspective, the deployment of solar PV technology presents important environmental benefits compared to fossil fuel-powered electricity systems.

- In the context of viable, fully autonomous off-grid solutions for electricity and thermal energy supply to remote rural buildings, the integration of PV arrays with diesel generators, battery storage, and biomass-based heating systems can reliably satisfy both electricity and thermal energy requirements, while substantially improving the environmental footprint. The economic analysis revealed that the majority of the NPC of the system is associated with the PV modules, whereas the converter contributes the least. Sensitivity analysis further indicates that both the net present cost and the levelized cost of energy increase with rising diesel fuel prices. The significance of load rescheduling or shifting to decrease peak demand and optimize electricity generation costs was also demonstrated. The initial investment for a combined hybrid electricity and heat autonomous system was found to be relatively high. Nonetheless, recent years have witnessed important initial cost reductions and technological advancements in off-grid/autonomous hybrid power systems. Although the costs of renewable systems are steadily declining as their deployment expands and manufacturing processes become more efficient and cost-effective, financial support and incentives are fundamental to support the wider deployment of these autonomous solutions. Beyond economic considerations, the environmental benefits, in terms of GHG emissions mitigation, of implementing autonomous hybrid power systems are considerable.
- Island-scale hybrid electricity supply systems, combining PV, wind, diesel, and battery storage, could achieve high renewable energy penetration (>90%) and significantly reduce diesel dependency and the associated GHG emissions. Larger isolated/off-grid islands benefit from economies of scale and more efficient storage utilization, while smaller islands face higher unit energy costs and larger proportions of surplus energy. Batteries play an important role in load shifting, grid stabilization, and enabling high renewable penetration. Surplus renewable energy, if strategically exploited, can further enhance system flexibility, reduce curtailment, and maximize environmental and economic benefits. Across all island scales, hybrid power systems achieve substantial GHG emission reductions exceeding 90%, underscoring their transformative potential for isolated grids.
- At the national level, fossil fuel-based electricity generation remains the major contributor to GHG emissions, whereas renewable sources have a small contribution, offering a clear mitigation potential. Nevertheless, the composition of the generation mix of the country cannot be decided by referring only to GHG emissions. Significant environmental impacts related to mineral resources use, human toxicity, freshwater acidification, marine eutrophication, water scarcity, etc., should be also taken into account as the relevant environmental scores of different electricity generation options vary considerably. Future

scenarios with higher renewable penetration suggest significant reductions in the GWP by 2030, highlighting the importance of systemic planning and life cycle-informed strategies for decarbonization. Furthermore, the transmission system was found to have relatively small environmental impacts, as compared to the generation one. Transmission lines infrastructure is the most significant source of GWP and non-renewable energy consumption, accounting for 61% and 54% of the total GHG emissions and primary energy demand, respectively. Important contribution comes also from the grid power losses, whereas transformers impacts are considerably lower.

- EoL management of wind turbine components further highlights the substantial role of circular economy-driven strategies in promoting both environmental and economic sustainability. The combined application of LCA and DEA-TOPSIS shows that recycling, repurposing, and circular design approaches can substantially reduce GHG emissions, fossil energy consumption, land occupation, and total waste management costs. It was pointed out that mechanical recycling of foundation concrete and innovative processing or repurposing of composite blade materials emerge as the most efficient solutions, whereas energy-intensive chemical recycling processes, particularly those involving long-distance transport, are less efficient and costlier. Integrating these strategies with remanufacturing, design-for-recycling, and waste prevention measures can facilitate a transition from linear to circular economy frameworks. In addition, targeted financial incentives could contribute towards offsetting the cost disadvantages of advanced recycling technologies, thus, further enhancing their adoption.
- Achieving sustainable energy transitions requires more than deploying renewable energy technologies; it depends on the combination of technological optimization, circular economy integration, storage management, policy incentives, and life cycle-informed decision-making. This holistic perspective facilitates the deployment of reliable, cost-effective, and sustainable energy systems at multiple scales, from urban buildings to island microgrids and national grids.

8.2 Future work

Future research should prioritize several critical areas to enable and accelerate the large-scale integration of renewable energy systems, ensuring reliability, efficiency, and sustainability in the transition toward a low - carbon energy future. In the field of solar energy conversion units, further investigation is required into advanced PV technologies, including perovskite solar cells and tandem configurations, which exhibit higher theoretical and experimentally demonstrated power conversion efficiencies compared to conventional silicon-based modules. Nevertheless, despite their rapid efficiency improvements, significant technical barriers remain. These encompass limited long-term operational stability under thermal cycling, concerns regarding lead content and potential environmental toxicity, as well as challenges related to scalable, high-throughput fabrication techniques. Addressing these constraints requires a rigorous evaluation through integrated techno-economic modelling and comprehensive life cycle assessment frameworks to determine their commercial viability and overall environmental performance under real-world operating conditions. Regarding wind energy systems, future work should focus on offshore wind farms with floating platforms, as they enable the exploitation of high wind potential in deep-water regions where fixed-bottom structures

are not feasible. Their large-scale deployment requires further investigation of structural stability, supply chain logistics, grid integration, environmental sustainability, and long-term economic competitiveness. The incorporation of advanced energy storage technologies, including flow batteries and hydrogen-based storage systems, should be also investigated as complementary mechanisms to mitigate intermittency, and, therefore, improve the reliability and stability of the power output from both wind and PV systems, as well as enhance grid flexibility. Equally important is the integration of demand response strategies capable of adjusting electricity consumption patterns in response to supply conditions. Demand-side flexibility can not only significantly reduce peak loads and enhance grid stability but also maximize the renewable energy utilization. The combined implementation of storage technologies and demand response mechanisms can provide a flexible and cost-effective pathway for balancing supply and demand in large-scale renewable systems, especially under high variability conditions.

A second key research direction involves the simultaneous control and optimization of electricity and heating power supply systems within an integrated framework. The aim of such an optimization would be to design entirely autonomous systems capable of ensuring reliable energy supply with the lowest possible capital investment. Advanced computational intelligence techniques, such as genetic algorithms, artificial neural networks, and hybrid metaheuristic optimization approaches, could be employed to identify optimal system configurations. These techniques could simultaneously optimize equipment sizing, technology selection, storage capacity, and operational strategies. Importantly, optimization should move beyond purely economic objectives. A multi-objective optimization framework is recommended, incorporating economic indicators (e.g., NPV and LCOE), environmental impact categories (e.g., GHG emissions, fossil energy use and resource depletion), technical performance metrics (such as system reliability, unmet load, and resilience under dynamic operating conditions), and social indicators (e.g., energy security, job creation, and human health). Such a holistic optimization approach would strengthen decision-making process and guide resilient, low-carbon energy system planning.

A significant research gap exists in the expansion and refinement of LCI datasets for renewable energy technologies. Existing datasets often lack comprehensive coverage of upstream processes, supply chain variability, and especially waste treatment. Future research should prioritize the development of integrated inventory data capturing decommissioning procedures, disposal routes, material recovery rates, recycling efficiencies, and secondary material markets. The absence of EoL inventory data limits the accuracy of the sustainability assessments and constraints the design of effective circular economy strategies. Addressing these data gaps would enable more precise environmental impact assessments, while facilitating the development of practical circular solutions. For example, the establishment of dedicated facilities for mechanical recycling of wind turbine foundation concrete materials near wind farm clusters could notably enhance material circularity. In the context of this thesis, the techno-economic evaluation of composite material recycling facilities at national level represents a promising future research direction, with the potential to further strengthen the long-term sustainability and resource efficiency of the wind power industry.

While high-voltage transmission systems are often the primary focus of grid-level analyses, medium- and low-voltage distribution networks constitute an important share of the grid infrastructure and associated

environmental impacts. Distribution systems, comprising control systems, distribution lines, transformers, substations, and smart metering equipment, play a significant role in enabling decentralized renewable integration, electric vehicle charging, and demand-side flexibility. Although this dissertation does not model the distribution system due to scope limitations, spatial heterogeneity and limited availability of detailed LCI data, its strategic importance for overall grid sustainability is acknowledged. Future work should therefore extend the analytical framework to incorporate distribution-level modelling, covering infrastructure material inventories, losses and efficiency parameters, smart grid technologies and digital monitoring systems, and environmental and economic assessment at local scales. The integration of distribution infrastructure modelling into life cycle environmental and economic assessment frameworks would provide a more comprehensive evaluation of energy system sustainability and support evidence-based grid optimization strategies.

Finally, the methodological framework forms the foundation for future development into a digital twin-based platform, enabling real-time monitoring, advanced analytics, and intelligent optimization of energy systems. In compliance with the strategic priorities of the European Union, particularly those devoted to digitalization and smart infrastructures, the next stage of research will focus on evolving the proposed framework from static modelling towards a real-time, data-driven digital twin architecture, integrating high-resolution data from smart meters, IoT devices, SCADA systems, and interoperable platforms. The modular digital twin will support multi-scale applications across smart grids, microgrids, buildings, and industrial energy systems, enhancing their operational efficiency and resilience while facilitating the integration of higher shares of renewable energy sources. Advanced artificial intelligence and optimization techniques will be incorporated to enable predictive maintenance, demand response, dynamic load management, and resilience assessment under high renewable energy penetration. The platform will integrate multi-criteria performance evaluation, covering technical, economic, environmental, and social dimensions, within a unified decision-support environment, enhancing transferability and supporting evidence-based policy and investment decisions for the digital and green transition.

Collectively, the aforementioned future research directions aim to advance the methodological framework towards an interoperable and scalable digital platform dedicated to the electricity sector, capable of integrating decentralized generation and demand-side resources, while incorporating comprehensive electricity system data across multiple voltage levels. By combining next-generation renewable energy technologies, advanced optimization methods, expanded life cycle datasets, circular economy principles, and distribution-level modelling, the research will contribute to the development of resilient, efficient, and sustainable electricity systems aligned with long-term decarbonization targets.

References

[1] Ram M, Bogdanov D, Aghahosseini A, Gulagi A, Oyewo AS, Odai Mensah TN, et al. Global energy transition to 100% renewables by 2050: Not fiction, but much needed impetus for developing economies to leapfrog into a sustainable future. Energy 2022;246:123419. https://doi.org/10.1016/j.energy.2022.123419.

[2] Sachs JD, Schmidt-Traub G, Mazzucato M, Messner D, Nakicenovic N, Rockström J. Six Transformations to achieve the Sustainable Development Goals. Nat Sustain 2019;2:805–14. https://doi.org/10.1038/s41893-019-0352-9.

[3] European Commission. European Climate Law. Off J Eur Union 2021;2021:17.

[4] Law 4936/2022. National Climate Law - Transition to climate neutrality and adaptation to climate change, urgent provisions to address the energy crisis and protect the environment. Gov Gaz 105/A/27-05-2022 2022:3561–92.

[5] Zahid H, Zulfiqar A, Adnan M, Iqbal MS, Shah A, Mohamed SEG. Global renewable energy transition: A multidisciplinary analysis of emerging computing technologies, socio-economic impacts, and policy imperatives. Results Eng 2025;26:105258. https://doi.org/10.1016/j.rineng.2025.105258.

[6] Kaldellis JK, Kapsali M, Katsanou E. Renewable energy applications in Greece—What is the public attitude? Energy Policy 2012;42:37–48. https://doi.org/10.1016/j.enpol.2011.11.017.

[7] Kaldellis JK. The wind potential impact on the maximum wind energy penetration in autonomous electrical grids. Renew Energy 2008;33:1665–77. https://doi.org/10.1016/j.renene.2007.09.011.

[8] Kaldellis JK. Integrated electrification solution for autonomous electrical networks on the basis of RES and energy storage configurations. Energy Convers Manag 2008;49:3708–20. https://doi.org/10.1016/j.enconman.2008.06.034.

[9] Voumvoulakis E, Asimakopoulou G, Danchev S, Maniatis G, Tsakanikas A. Large scale integration of intermittent renewable energy sources in the Greek power sector. Energy Policy 2012;50:161–73. https://doi.org/10.1016/j.enpol.2012.05.056.

[10] Ramachandra T V. Integrated Renewable Energy System - Perspectives and Issues 2014.

[11] Wolsink M. Wind power implementation: The nature of public attitudes: Equity and fairness instead of 'backyard motives.' Renew Sustain Energy Rev 2007;11:1188–207. https://doi.org/10.1016/j.rser.2005.10.005.

[12] Simoglou CK, Biskas PN, Vagropoulos SI, Bakirtzis AG. Electricity market models and RES integration: The Greek case. Energy Policy 2014;67:531–42. https://doi.org/10.1016/j.enpol.2013.11.065.

[13] Merei G, Berger C, Sauer DU. Optimization of an off-grid hybrid PV–Wind–Diesel system with different battery technologies using genetic algorithm. Sol Energy 2013;97:460–73. https://doi.org/10.1016/j.solener.2013.08.016.

[14] Li C, Ge X, Zheng Y, Xu C, Ren Y, Song C, et al. Techno-economic feasibility study of autonomous hybrid wind/PV/battery power system for a household in Urumqi, China. Energy 2013;55:263–72. https://doi.org/10.1016/j.energy.2013.03.084.

[15] Lau KY, Yousof MFM, Arshad SNM, Anwari M, Yatim AHM. Performance analysis of hybrid photovoltaic/diesel energy system under Malaysian conditions. Energy 2010;35:3245–55. https://doi.org/10.1016/j.energy.2010.04.008.

[16] Sen R, Bhattacharyya SC. Off-grid electricity generation with renewable energy technologies in India: An application of HOMER. Renew Energy 2014;62:388–98. https://doi.org/10.1016/j.renene.2013.07.028.

[17] Mezilis L, Lavidas G. Future scenarios for 100% renewables in Greece, untapped potential of marine renewable energies. Energy Convers Manag X 2025;27:101085. https://doi.org/10.1016/j.ecmx.2025.101085.

[18] Rehman S, Mahbub Alam M, Meyer JP, Al-Hadhrami LM. Feasibility study of a wind–pv–diesel hybrid power system for a village. Renew Energy 2012;38:258–68. https://doi.org/10.1016/j.renene.2011.06.028.

[19] Kalampalikas NG, Pilavachi PA. A model for the development of a power production system in Greece, Part I: Where RES do not meet EU targets. Energy Policy 2010;38:6499–513. https://doi.org/10.1016/j.enpol.2010.05.038.

[20] Kalampalikas NG, Pilavachi PA. A model for the development of a power production system in Greece, Part II: Where RES meet EU targets. Energy Policy 2010;38:6514–28. https://doi.org/10.1016/j.enpol.2010.05.037.

[21] Koltsaklis NE, Dagoumas AS, Kopanos GM, Pistikopoulos EN, Georgiadis MC. A spatial multi-period long-term energy planning model: A case study of the Greek power system. Appl Energy 2014;115:456–82. https://doi.org/10.1016/j.apenergy.2013.10.042.

[22] Caputo, A.C., Federici, A., Pelagagge, P.M., Salini P. Offshore wind power system economic evaluation framework under aleatory and epistemic uncertainty. Appl Energy 2023;350:121585. https://doi.org/10.1016/j.apenergy.2023.121585.

[23] Wang J, Chen X, Zhuang M, Li Y, Ruan Z, Wang Y, et al. Accelerating exploitation and integration of global renewable energy. Innov 2025:100873. https://doi.org/10.1016/j.xinn.2025.100873.

[24] Ćorović, N., Urošević, B.G., Katić N. Decarbonization: Challenges for the electricity market development — Serbian market case. Energy Reports 2022;8:2200–9. https://doi.org/10.1016/j.egyr.2022.01.054.

[25] Dijkgraaf, E., Van Dorp, T.P., Maasland E. On the effectiveness of feed-in tariffs in the development of solar photovoltaics. Energy J 2018;39. https://doi.org/10.5547/01956574.39.1.edij.

[26] Marques AC, Fuinhas JA, Pereira DS. The dynamics of the short and long-run effects of public policies supporting renewable energy: A comparative study of installed capacity and electricity generation. Econ Anal Policy 2019;63:188–206. https://doi.org/10.1016/j.eap.2019.06.004.

[27] Faia R, Lezama F, Soares J, Pinto T, Vale Z. Local electricity markets: A review on benefits, barriers, current trends and future perspectives. Renew Sustain Energy Rev 2024;190:114006. https://doi.org/10.1016/j.rser.2023.114006.

[28] Varun, Bhat IK, Prakash R. LCA of renewable energy for electricity generation systems—A review. Renew Sustain Energy Rev 2009;13:1067–73. https://doi.org/10.1016/j.rser.2008.08.004.

[29] Fthenakis V, Kim HC. Energy Use and Greenhouse Gas Emissions in the Life Cycle of CdTe Photovoltaics. MRS Proc 2005;895:0895-G03-06. https://doi.org/10.1557/PROC-0895-G03-06.

[30] International Organization for Standardization (ISO). ISO 14040 - environmental management - life cycle assessment - principles and framework (ISO 14040:2006). Geneva, Switzerland.: 2006.
[31] ISO 14044. ISO 14044:2006 Environmental management — Life cycle assessment — Requirements and guidelines. 2007.
[32] Guinee, J.B., Gorre´e, M., Heijungs, R., Huppes, G., Kleijn, R., de Koning, A., van Oers, L. W, Sleeswijk, A., Suh, S., Udo de Haes, H.A., de Bruijn, H., van Duin, R. and Huijbregts MAJ. Handbook on Life Cycle Assessment. Operational Guide to the ISO Standards. Dordrecht, The Netherlands: Kluwer; 2002. https://doi.org/10.1007/BF02978897.
[33] Petrillo A, De Felice F, Jannelli E, Autorino C, Minutillo M, Lavadera AL. Life cycle assessment (LCA) and life cycle cost (LCC) analysis model for a stand-alone hybrid renewable energy system. Renew Energy 2016;95:337–55. https://doi.org/10.1016/j.renene.2016.04.027.
[34] Cellura M, Luu LQ, Guarino F, Longo S. A review on life cycle environmental impacts of emerging solar cells. Sci Total Environ 2024;908:168019. https://doi.org/10.1016/j.scitotenv.2023.168019.
[35] Gerbinet S, Belboom S, Léonard A. Life Cycle Analysis (LCA) of photovoltaic panels: A review. Renew Sustain Energy Rev 2014;38:747–53. https://doi.org/10.1016/j.rser.2014.07.043.
[36] Muteri V, Cellura M, Curto D, Franzitta V, Longo S, Mistretta M, et al. Review on Life Cycle Assessment of Solar Photovoltaic Panels. Energies 2020;13:252. https://doi.org/10.3390/en13010252.
[37] Boretti A, Castelletto S. Annual relative performance degradation in photovoltaic solar plants. Sol Energy Adv 2024;4:100074. https://doi.org/10.1016/j.seja.2024.100074.
[38] Impact Assessment Categories (CML, TRACI and PEF) n.d.
[39] Bulle C, Margni M, Patouillard L, Boulay AM, Bourgault G, De Bruille V, et al. IMPACT World+: a globally regionalized life cycle impact assessment method. Int J Life Cycle Assess 2019;24:1653–74. https://doi.org/10.1007/s11367-019-01583-0.
[40] Huijbregts MAJ, Steinmann ZJN, Elshout PMF, Stam G, Verones F, Vieira M, et al. ReCiPe2016: a harmonised life cycle impact assessment method at midpoint and endpoint level. Int J Life Cycle Assess 2017;22:138–47. https://doi.org/10.1007/s11367-016-1246-y.
[41] Rigon MR, Zortea R, Moraes CAM, Modolo RCE, Rigon MR, Zortea R, et al. Suggestion of Life Cycle Impact Assessment Methodology: Selection Criteria for Environmental Impact Categories. In: Petrillo A, De Felice F, editors. New Front. Life Cycle Assess. - Theory Appl., IntechOpen; 2019. https://doi.org/10.5772/INTECHOPEN.83454.
[42] Soonmin H, Hardani, Nandi P, Mwankemwa BS, Malevu TD, Malik MI. Overview on Different Types of Solar Cells: An Update. Appl Sci 2023;13:2051. https://doi.org/10.3390/app13042051.
[43] Mdallal A, Yasin A, Mahmoud M, Abdelkareem MA, Alami AH, Olabi AG. A comprehensive review on solar photovoltaics: Navigating generational shifts, innovations, and sustainability. Sustain Horizons 2025;13:100137. https://doi.org/10.1016/j.horiz.2025.100137.
[44] Allouhi A, Rehman S, Buker MS, Said Z. Up-to-date literature review on Solar PV systems: Technology progress, market status and R&D. J Clean Prod 2022;362:132339. https://doi.org/10.1016/j.jclepro.2022.132339.
[45] Cowern NEB. Silicon-based photovoltaic solar cells. Woodhead Publishing Limited; 2012. https://doi.org/10.1016/9780857096371.1.1.

[46] Seigneur H, Mohajeri N, Brooker RP, Davis KO, Schneller EJ, Dhere NG, et al. Manufacturing metrology for c-Si photovoltaic module reliability and durability , Part I : Feedstock , crystallization and wafering. Renew Sustain Energy Rev 2016;59:84–106. https://doi.org/10.1016/j.rser.2015.12.343.

[47] Méndez L, Forniés E, Garrain D, Pérez A, Souto A, Vlasenko T. Science of the Total Environment Upgraded metallurgical grade silicon and polysilicon for solar electricity production : A comparative life cycle assessment 2021;789. https://doi.org/10.1016/j.scitotenv.2021.147969.

[48] Fan M, Yu Z, Ma W, Li L. Life Cycle Assessment of Crystalline Silicon Wafers for Photovoltaic Power Generation 2021:3177–89.

[49] Hsu DD, Donoughue PO, Fthenakis V, Heath GA, Kim HC, Sawyer P, et al. Life Cycle Greenhouse Gas Emissions of Crystalline Silicon Photovoltaic Systematic Review and Harmonization 2012;16. https://doi.org/10.1111/j.1530-9290.2011.00439.x.

[50] Fu Y, Liu X, Yuan Z. Life-cycle assessment of multi-crystalline photovoltaic (PV) systems in China. J Clean Prod 2015;86:180–90. https://doi.org/10.1016/j.jclepro.2014.07.057.

[51] Sheng X, Chen L, Liu M, Yuan X, Wang Q, Ma Q. Resources , Conservation & Recycling Environmental impact of monocrystalline silicon photovoltaic modules. Resour Conserv Recycl 2025;220:108373. https://doi.org/10.1016/j.resconrec.2025.108373.

[52] Vega-de-lille MI, Sacramento-rivero JC. Life cycle assessment of photovoltaic panels including transportation and two end-of-life scenarios : Shaping a sustainable future for renewable energy 2024;51.

[53] Duan Y, Guo F, Gardy J, Xu G, Li X, Jiang X. Life cycle assessment of polysilicon photovoltaic modules with green recycling based on the ReCiPe method. Renew Energy 2024;236:121407. https://doi.org/10.1016/j.renene.2024.121407.

[54] Stylos N, Koroneos C. Carbon footprint of polycrystalline photovoltaic systems. J Clean Prod 2014;64:639–45. https://doi.org/10.1016/j.jclepro.2013.10.014.

[55] Fukurozaki SH, Zilles R, Sauer IL. Energy Payback Time and CO2 Emissions of 1.2 kWp Photovoltaic Roof-Top System in Brazil. Int J Smart Grid Clean Energy 2013;2:164–9. https://doi.org/10.12720/sgce.2.2.164-169.

[56] Kannan R, Leong KC, Osman R, Ho HK, Tso CP. Life cycle assessment study of solar PV systems: An example of a 2.7 kWp distributed solar PV system in Singapore. Sol Energy 2006;80:555–63. https://doi.org/10.1016/j.solener.2005.04.008.

[57] Muneer T, Younes S, Lambert N, Kubie J. Life cycle assessment of a medium-sized photovoltaic facility at a high latitude location. Proc Inst Mech Eng Part A J Power Energy 2006;220:517–24. https://doi.org/10.1243/09576509JPE253.

[58] Jungbluth, .N, Bauer, C., Dones, R., Frischknecht R. Life cycle assessment for emerging technologies: case studies for photovoltaic and wind power. Int J Life Cycle Assess 2005;10:24–34.

[59] Jungbluth N. Life cycle inventory databases used for our consultancy projects 2019.

[60] Lee TD, Ebong AU. A review of thin film solar cell technologies and challenges. Renew Sustain Energy Rev 2017;70:1286–97. https://doi.org/10.1016/j.rser.2016.12.028.

[61] Shah N, Shah AA, Leung PK, Khan S, Sun K, Zhu X, et al. A Review of Third Generation Solar Cells. Processes 2023;11:1852. https://doi.org/10.3390/pr11061852.

[62] Al-Ali S, Olabi AG, Mahmoud M. A review of solar photovoltaic technologies: developments, challenges, and future perspectives. Energy Convers Manag X 2025;27:101057. https://doi.org/10.1016/j.ecmx.2025.101057.

[63] Ali AO, Elgohr AT, El-Mahdy MH, Zohir HM, Emam AZ, Mostafa MG, et al. Advancements in photovoltaic technology: A comprehensive review of recent advances and future prospects. Energy Convers Manag X 2025;26:100952. https://doi.org/10.1016/j.ecmx.2025.100952.

[64] Hondo H. Life cycle GHG emission analysis of power generation systems: Japanese case. Energy 2005;30:2042–56. https://doi.org/10.1016/j.energy.2004.07.020.

[65] Pacca S, Sivaraman D, Keoleian GA. Parameters affecting the life cycle performance of PV technologies and systems. Energy Policy 2007;35:3316–26. https://doi.org/10.1016/j.enpol.2006.10.003.

[66] Mohr NJ, Meijer A, Huijbregts MAJ, Reijnders L. Environmental life cycle assessment of roof-integrated flexible amorphous silicon/nanocrystalline silicon solar cell laminate. Prog Photovoltaics Res Appl 2013;21:802–15. https://doi.org/10.1002/pip.2157.

[67] Aleksandra A, Brian B, Sara BP, Davide P, Miguel C. Role of solar PV in net-zero growth : An analysis of international manufacturers and policies 2024:607–22. https://doi.org/10.1002/pip.3797.

[68] Alsema, De Wild-Scholten MJE. Reduction of the environmental impacts in crystalline silicon module manufacturing. 22nd Eur Photovolt Sol Energy Conf 2007:829–36.

[69] Kim B, Lee J, Kim K, Hur T. Evaluation of the environmental performance of sc-Si and mc-Si PV systems in Korea. Sol Energy 2014;99:100–14. https://doi.org/10.1016/j.solener.2013.10.038.

[70] Hong J, Chen W, Qi C, Ye L, Xu C. Life cycle assessment of multicrystalline silicon photovoltaic cell production in China. Sol Energy 2016;133:283–93. https://doi.org/10.1016/j.solener.2016.04.013.

[71] Huang J, Mao L. A Review on Perovskite / Silicon Tandem Solar Cells : Current Status and Future Challenges 2025.

[72] Hallam B, Kim M, Underwood R, Drury S, Wang L, Dias P. A Polysilicon Learning Curve and the Material Requirements for Broad Electri fi cation with Photovoltaics by 2050 2022;2200458:1–8. https://doi.org/10.1002/solr.202200458.

[73] Sumper A, Robledo-García M, Villafáfila-Robles R, Bergas-Jané J, Andrés-Peiró J. Life-cycle assessment of a photovoltaic system in Catalonia (Spain). Renew Sustain Energy Rev 2011;15:3888–96. https://doi.org/10.1016/j.rser.2011.07.023.

[74] Akinyele DO, Rayudu RK, Nair NKC. Life cycle impact assessment of photovoltaic power generation from crystalline silicon-based solar modules in Nigeria. Renew Energy 2017;101:537–49. https://doi.org/10.1016/j.renene.2016.09.017.

[75] Zhai P, Williams ED. Dynamic Hybrid Life Cycle Assessment of Energy and Carbon of Multicrystalline Silicon Photovoltaic Systems. Environ Sci Technol 2010;44:7950–5. https://doi.org/10.1021/es1026695.

[76] Latunussa CEL, Ardente F, Andrea G, Mancini L. Solar Energy Materials & Solar Cells Life Cycle Assessment of an innovative recycling process for crystalline silicon photovoltaic panels. Sol Energy Mater Sol Cells 2016;156:101–11. https://doi.org/10.1016/j.solmat.2016.03.020.

[77] Lombardi L, Mendecka B, Carnevale E, Stanek W. Environmental impacts of electricity production of micro wind turbines with vertical axis. Renew Energy 2018;128:553–64.

https://doi.org/10.1016/j.renene.2017.07.010.
[78] Matveev A, Shcheklein S. Life cycle analysis of low-speed multi-blade wind turbine. Int J Renew Energy Res 2015;5:991–7.
[79] Kouloumpis V, Sobolewski RA, Yan X. Performance and life cycle assessment of a small scale vertical axis wind turbine. J Clean Prod 2020;247:119520. https://doi.org/10.1016/j.jclepro.2019.119520.
[80] Arvesen A, Hertwich EG. Assessing the life cycle environmental impacts of wind power: A review of present knowledge and research needs. Renew Sustain Energy Rev 2012;16:5994–6006. https://doi.org/10.1016/j.rser.2012.06.023.
[81] Mello G, Ferreira Dias M, Robaina M. Evaluation of the environmental impacts related to the wind farms end-of-life. Energy Reports 2022;8:35–40. https://doi.org/10.1016/j.egyr.2022.01.024.
[82] Raadal HL, Vold BI, Myhr A, Nygaard TA. GHG emissions and energy performance of offshore wind power. Renew Energy 2014;66:314–24. https://doi.org/10.1016/j.renene.2013.11.075.
[83] Yang J, Chen B. Integrated evaluation of embodied energy, greenhouse gas emission and economic performance of a typical wind farm in China. Renew Sustain Energy Rev 2013;27:559–68. https://doi.org/10.1016/j.rser.2013.07.024.
[84] Turkmen BA, Babuna FG. Life Cycle Environmental Impacts of Wind Turbines: A Path to Sustainability with Challenges. Sustainability 2024;16:5365. https://doi.org/https://doi.org/10.3390/su16135365.
[85] Guillore A, Canet H, Bottasso CL. Life Cycle Environmental Impact of Wind Turbines: What are the Possible Improvement Pathways? J Phys Conf Ser 2022;2265. https://doi.org/10.1088/1742-6596/2265/4/042033.
[86] Morozovska K, Bragone F, Svensson AX, Shukla DA, Hellstenius E. Trade-offs of wind power production: A study on the environmental implications of raw materials mining in the life cycle of wind turbines. J Clean Prod 2024;460:142578. https://doi.org/10.1016/j.jclepro.2024.142578.
[87] van Oudheusden AA. Recycling of composite materials. Delft University of Technology, 2019. https://doi.org/10.1016/0924-0136(95)02037-3.
[88] Krauklis AE, Karl CW, Gagani AI, Jørgensen JK. Composite Material Recycling Technology—State-of-the-Art and Sustainable Development for the 2020s. J Compos Sci 2021;5:28. https://doi.org/10.3390/jcs5010028.
[89] Zhao Y, Wang M, Lin J, Liu W, Chen L, Wang Z, et al. Exploring recycling strategies for retired wind turbine blades: The impact of policy subsidies and technological investments using a game-theoretic approach. J Clean Prod 2025;490:144628. https://doi.org/10.1016/j.jclepro.2024.144628.
[90] Bonou A, Laurent A, Olsen SI. Life cycle assessment of onshore and offshore wind energy-from theory to application. Appl Energy 2016;180:327–37. https://doi.org/10.1016/j.apenergy.2016.07.058.
[91] Cooperman A, Eberle A, Lantz E. Wind turbine blade material in the United States: Quantities, costs, and end-of-life options. Resour Conserv Recycl 2021;168:105439. https://doi.org/10.1016/j.resconrec.2021.105439.
[92] Nagle AJ, Mullally G, Leahy PG, Dunphy NP. Life cycle assessment of the use of decommissioned

wind blades in second life applications. J Environ Manage 2022;302:113994. https://doi.org/10.1016/j.jenvman.2021.113994.

[93] Liu P, Barlow CY. Wind turbine blade waste in 2050. Waste Manag 2017;62:229–40. https://doi.org/10.1016/j.wasman.2017.02.007.

[94] Uddin MS, Kumar S. Energy, emissions and environmental impact analysis of wind turbine using life cycle assessment technique. J Clean Prod 2014;69:153–64. https://doi.org/10.1016/j.jclepro.2014.01.073.

[95] Gorman MR, Dzombak DA, Frischmann C. Potential global GHG emissions reduction from increased adoption of metals recycling. Resour Conserv Recycl 2022;184:106424. https://doi.org/10.1016/j.resconrec.2022.106424.

[96] Alavi Z, Khalilpour K, Florin N, Hadigheh A, Hoadley A. End-of-life wind turbine blade management across energy transition: A life cycle analysis. Resour Conserv Recycl 2025;213:108008. https://doi.org/10.1016/j.resconrec.2024.108008.

[97] Zhang W, Yu H, Yin B, Akbar A, Liew KM. Sustainable transformation of end-of-life wind turbine blades: Advancing clean energy solutions in civil engineering through recycling and upcycling. J Clean Prod 2023;426:139184. https://doi.org/10.1016/j.jclepro.2023.139184.

[98] Das Karmakar S, Chattopadhyay H. A comprehensive look into the sustainability of wind power. Renew Sustain Energy Rev 2025;217:115694. https://doi.org/10.1016/j.rser.2025.115694.

[99] Davidsson S, Höök M, Wall G. A review of life cycle assessments on wind energy systems. Int J Life Cycle Assess 2012;17:729–42. https://doi.org/10.1007/s11367-012-0397-8.

[100] Vestas. Life Cycle Assessment of Electricity Production from an offshore V236-15 MW Wind Plant. Denmark: 2024.

[101] Zajicek, L., Drapalik, M., Kral, I., Liebert W. Energy efficiency and environmental impacts of horizontal small wind turbines in Austria. Sustain Energy Technol Assessments 2023;59:103411. https://doi.org/10.1016/j.seta.2023.103411.

[102] Martínez E, Sanz F, Pellegrini S, Jiménez E, Blanco J. Life cycle assessment of a multi-megawatt wind turbine. Renew Energy 2009;34:667–73. https://doi.org/10.1016/j.renene.2008.05.020.

[103] Vargas A V., Zenón E, Oswald U, Islas JM, Güereca LP, Manzini FL. Life cycle assessment: A case study of two wind turbines used in Mexico. Appl Therm Eng 2015;75:1210–6. https://doi.org/10.1016/j.applthermaleng.2014.10.056.

[104] Laurent, A., Espinosa, N., Hauschild MZ. LCA of energy systems. Life Cycle Assess., Springer; 2018, p. 663–8. https://doi.org/10.1007/978-3-319-56475-3_26.

[105] Cong N, Song Y, Zhang M, Wu W. Life cycle assessment of carbon reduction potential of EoL wind turbine blades disposal scenarios in China. Environ Impact Assess Rev 2023;100:107072. https://doi.org/10.1016/j.eiar.2023.107072.

[106] Deeney P, Nagle AJ, Gough F, Lemmertz H, Delaney EL, McKinley JM, et al. End-of-Life alternatives for wind turbine blades: Sustainability Indices based on the UN sustainable development goals. Resour Conserv Recycl 2021;171:105642. https://doi.org/10.1016/j.resconrec.2021.105642.

[107] Intergovernmental Panel on Climate Change. Technology-specific Cost and Performance Parameters. Clim Chang 2014 Mitig Clim Chang 2015:1329–56. https://doi.org/10.1017/cbo9781107415416.025.

[108] Wang S, Wang S, Liu J. Life-cycle green-house gas emissions of onshore and offshore wind turbines. J Clean Prod 2019;210:804–10. https://doi.org/10.1016/j.jclepro.2018.11.031.
[109] Jungbluth N, Bauer C, Dones R, Frischknecht R. Life cycle assessment for emerging technologies: Case studies for photovoltaic and wind power. Int J Life Cycle Assess 2005;10:24–34. https://doi.org/10.1065/lca2004.11.181.3.
[110] Tremeac B, Meunier F. Life cycle analysis of 4.5MW and 250W wind turbines. Renew Sustain Energy Rev 2009;13:2104–10. https://doi.org/10.1016/j.rser.2009.01.001.
[111] Rathore N, Panwar NL. Environmental impact and waste recycling technologies for modern wind turbines: An overview. Waste Manag Res J a Sustain Circ Econ 2023;41:744–59. https://doi.org/10.1177/0734242X221135527.
[112] Demir N, Taşkin A. Life cycle assessment of wind turbines in PInarbaşI-Kayseri. J Clean Prod 2013;54:253–63. https://doi.org/10.1016/j.jclepro.2013.04.016.
[113] Crawford RH. Life cycle energy and greenhouse emissions analysis of wind turbines and the effect of size on energy yield. Elsevier Renew Sustain Energy Rev 2009;13:2653–60. https://doi.org/10.1016/j.rser.2009.07.008.
[114] Kabir MR, Rooke B, Dassanayake GDM, Fleck BA. Comparative life cycle energy, emission, and economic analysis of 100 kW nameplate wind power generation. Renew Energy 2012;37:133–41. https://doi.org/10.1016/j.renene.2011.06.003.
[115] Tremeac B, Meunier F. Life cycle analysis of 4.5 MW and 250 W wind turbines. Renew Sustain Energy Rev 2009;13:2104–10. https://doi.org/10.1016/j.rser.2009.01.001.
[116] Bhandari R, Kumar B, Mayer F. Life cycle greenhouse gas emission from wind farms in reference to turbine sizes and capacity factors. J Clean Prod 2020;277:123385. https://doi.org/10.1016/j.jclepro.2020.123385.
[117] Lenzen M, Munksgaard J. Energy and CO2 life-cycle analyses of wind turbines-review and applications. Renew Energy 2002;26:339–62. https://doi.org/10.1016/S0960-1481(01)00145-8.
[118] Mondal AH, Denich M. Hybrid systems for decentralized power generation in Bangladesh. Energy Sustain Dev 2010;14:48–55. https://doi.org/10.1016/j.esd.2010.01.001.
[119] Haidar AMA, John PN, Shawal M. Optimal configuration assessment of renewable energy in Malaysia. Renew Energy 2011;36:881–8. https://doi.org/10.1016/j.renene.2010.07.024.
[120] Bin L, Shahzad M, Farhan M, Ayoub M, Ali S, Bitew GT. Technoeconomic analysis of solar PV electrification to remote areas of Dera Ghazi Khan: A case study. Heliyon 2024;10:e36990. https://doi.org/10.1016/j.heliyon.2024.e36990.
[121] Office of Energy Efficiency & renewable energy. Modeling of Photovoltaic Systems: Basic Challenges and DOE-Funded Tools. 2022.
[122] Ingle A, Sangotra DI, Chadge RB, Thorat P. Module configurations in photovoltaic system: A review. Mater Today Proc 2017;4:12625–9. https://doi.org/10.1016/j.matpr.2017.10.072.
[123] Pavlovic T, Milosavljevic D, Pirsl D. Simulation of photovoltaic systems electricity generation using homer software in specific locations in Serbia. Therm Sci 2013;17:333–47. https://doi.org/10.2298/TSCI120727004P.
[124] Khanna R, Qinhao Zhang, Stanchina WE, Reed GF, Zhi-Hong Mao. Maximum Power Point Tracking Using Model Reference Adaptive Control. IEEE Trans Power Electron 2014;29:1490–9.

https://doi.org/10.1109/TPEL.2013.2263154.
[125] Skoplaki E, Palyvos JA. On the temperature dependence of photovoltaic module electrical performance: A review of efficiency/power correlations. Sol Energy 2009;83:614–24. https://doi.org/10.1016/j.solener.2008.10.008.
[126] Almonacid F, Rus C, Pérez-Higueras P, Hontoria L. Calculation of the energy provided by a PV generator. Comparative study: Conventional methods vs. artificial neural networks. Energy 2011;36:375–84. https://doi.org/10.1016/j.energy.2010.10.028.
[127] Kumar NM, Gupta RP, Mathew M, Jayakumar A, Singh NK. Performance, energy loss, and degradation prediction of roof-integrated crystalline solar PV system installed in Northern India. Case Stud Therm Eng 2019;13:100409. https://doi.org/10.1016/j.csite.2019.100409.
[128] El-Maaroufi A, Daoudi M, Ahl Laamara R. Techno-economic analysis of a PV/WT/biomass off-grid hybrid power system for rural electrification in northern Morocco using HOMER. Renew Energy 2024;231:120904. https://doi.org/10.1016/j.renene.2024.120904.
[129] Balat M. A Review of Modern Wind Turbine Technology. Energy Sources, Part A Recover Util Environ Eff 2009;31:1561–72. https://doi.org/10.1080/15567030802094045.
[130] Bhattacharjee S, Acharya S. PV–wind hybrid power option for a low wind topography. Energy Convers Manag 2015;89:942–54. https://doi.org/10.1016/j.enconman.2014.10.065.
[131] Yang H, Wei Z, Chengzhi L. Optimal design and techno-economic analysis of a hybrid solar–wind power generation system. Appl Energy 2009;86:163–9. https://doi.org/10.1016/j.apenergy.2008.03.008.
[132] Belmili H, Haddadi M, Bacha S, Almi MF, Bendib B. Sizing stand-alone photovoltaic–wind hybrid system: Techno-economic analysis and optimization. Renew Sustain Energy Rev 2014;30:821–32. https://doi.org/10.1016/j.rser.2013.11.011.
[133] Koholé YW, Wankouo Ngouleu CA, Fohagui FCV, Tchuen G. Optimization of an off-grid hybrid photovoltaic/wind/diesel/fuel cell system for residential applications power generation employing evolutionary algorithms. Renew Energy 2024;224:120131. https://doi.org/10.1016/j.renene.2024.120131.
[134] Allouhi A, Zamzoum O, Islam MR, Saidur R, Kousksou T, Jamil A, et al. Evaluation of wind energy potential in Morocco's coastal regions. Renew Sustain Energy Rev 2017;72:311–24. https://doi.org/10.1016/j.rser.2017.01.047.
[135] Hosseinalizadeh R, Shakouri G H, Amalnick MS, Taghipour P. Economic sizing of a hybrid (PV–WT–FC) renewable energy system (HRES) for stand-alone usages by an optimization-simulation model: Case study of Iran. Renew Sustain Energy Rev 2016;54:139–50. https://doi.org/10.1016/j.rser.2015.09.046.
[136] Mathur A, Prakash V, Singh J, Rawat T. Capacity planning of wind farm to simultaneously optimize hosting capacity and losses in distribution system with electric vehicles. Electr Power Syst Res 2024;229:110159. https://doi.org/10.1016/j.epsr.2024.110159.
[137] Misiç AS, Karatas M, Dasci A. Optimal sizing and location of energy storage systems for transmission grids connected to wind farms. Omega 2025;134:103301. https://doi.org/10.1016/j.omega.2025.103301.
[138] Yang Y, Bremner S, Menictas C, Kay M. Modelling and optimal energy management for battery energy

storage systems in renewable energy systems: A review. Renew Sustain Energy Rev 2022;167:112671. https://doi.org/10.1016/j.rser.2022.112671.

[139] Nguyen TA, Crow ML, Elmore AC. Optimal Sizing of a Vanadium Redox Battery System for Microgrid Systems. IEEE Trans Sustain Energy 2015;6:729–37. https://doi.org/10.1109/TSTE.2015.2404780.

[140] Zhou W, Zheng Y, Pan Z, Lu Q. Review on the Battery Model and SOC Estimation Method. Processes 2021;9:1685. https://doi.org/10.3390/pr9091685.

[141] Suryoatmojo H, Anam S, Rahmawan Z, Asfani DA, Faurahmansyah MA, Prabowo P. State of Charge (SOC) Estimation on Lead-Acid Batteries Using the Coulomb Counting Method. 2022 10th Int. Conf. Smart Grid Clean Energy Technol., IEEE; 2022, p. 78–84. https://doi.org/10.1109/ICSGCE55997.2022.9953693.

[142] Fatin Ishraque M, Shezan SA, Ali MM, Rashid MM. Optimization of load dispatch strategies for an islanded microgrid connected with renewable energy sources. Appl Energy 2021;292:116879. https://doi.org/10.1016/j.apenergy.2021.116879.

[143] Kabeyi MJB, Olanrewaju OA. The levelized cost of energy and modifications for use in electricity generation planning. Energy Reports 2023;9:495–534. https://doi.org/10.1016/j.egyr.2023.06.036.

[144] Kalfountzou E. Economic Evaluation of Photovoltaic Plants in Greece under the Recently Introduced De-Escalating Feed-in-Tariff Policy. SSRN Electron J 2012. https://doi.org/10.2139/ssrn.1810233.

[145] Huang B, Wang Y, Huang Y, Xu X, Chen X, Duan L, et al. Life cycle cost analysis of solar energy via environmental externality monetization. Sci Total Environ 2023;856:158910. https://doi.org/10.1016/j.scitotenv.2022.158910.

[146] Abu Qadourah J. Energy and economic potential for photovoltaic systems installed on the rooftop of apartment buildings in Jordan. Results Eng 2022;16:100642. https://doi.org/10.1016/j.rineng.2022.100642.

[147] Stehly T, Beiter P, Duffy P. 2020 Cost of Wind Energy Review. Nrel 2024:68.

[148] Shimura S, Herrero R, Zuffo MK, Baesso Grimoni JA. Production costs estimation in photovoltaic power plants using reliability. Sol Energy 2016;133:294–304. https://doi.org/10.1016/j.solener.2016.03.070.

[149] Summary report of the workshop on sustainable approaches to wind turbine decommissioning BIOWIND 2024.

[150] Suganthi D, Jamuna K. Optimizing campus microgrid energy systems: Economic, environmental, and sensitivity insights. Energy Convers Manag X 2025;27:101046. https://doi.org/10.1016/j.ecmx.2025.101046.

[151] Rifansyah M, Hakam DF. Techno economic study of floating solar photovoltaic project in Indonesia using RETscreen. Clean Energy Syst 2024;9:100155. https://doi.org/10.1016/j.cles.2024.100155.

[152] Gessinger GH. Financial Management of a Company. Mater. Innov. Prod. Dev., Elsevier; 2009, p. 139–80. https://doi.org/10.1016/B978-1-85617-559-3.00007-7.

[153] Roy D, Wang R, Roy S, Smallbone A, Roskilly AP. Hybrid renewable energy systems for sustainable power supply in remote location: Techno-economic and environmental assessment. Energy Convers Manag X 2024;24:100793. https://doi.org/10.1016/j.ecmx.2024.100793.

[154] Demiroren, A., Yilmaz U. Analysis of change in electric energy cost with using renewable energy sources in Gökceada, Turkey: An island example. Renew Sustain Energy Rev 2010;14:323–33.

https://doi.org/https://doi.org/10.1016/j.rser.2009.06.030.
[155] Razmjoo A, Gakenia Kaigutha L, Vaziri Rad MA, Marzband M, Davarpanah A, Denai M. A Technical analysis investigating energy sustainability utilizing reliable renewable energy sources to reduce <math altimg="si1.svg"> <mrow> <msub> <mtext>CO</mtext> <mn>2</mn> </msub> </mrow> </math> emissions in a high potential area. Renew Energy 2021;164:46–57. https://doi.org/10.1016/j.renene.2020.09.042.
[156] Al-Sharafi A, Al-Buraiki AS, Al-Sulaiman F, Antar MA. Hydrogen refueling stations powered by hybrid PV/wind renewable energy systems: Techno-socio-economic assessment. Energy Convers Manag X 2024;22:100584. https://doi.org/10.1016/j.ecmx.2024.100584.
[157] Samatar AM, Mekhilef S, Mokhlis H, Kermadi M, Alshammari O. Performance analysis of hybrid off-grid renewable energy systems for sustainable rural electrification. Energy Convers Manag X 2024;24:100780. https://doi.org/10.1016/j.ecmx.2024.100780.
[158] Hadwan M, Alkholidi A. Solar power energy solutions for Yemeni rural villages and desert communities. Renew Sustain Energy Rev 2016;57:838–49. https://doi.org/10.1016/j.rser.2015.12.125.
[159] Balasubramanian V, Haque N, Bhargava S, Madapusi S, Parthasarathy R. Techno-economic evaluation methodology for hydrogen energy systems. Bioenergy Resour. Technol., Elsevier; 2021, p. 195–218. https://doi.org/10.1016/B978-0-12-822525-7.00016-0.
[160] Olatayo KI, Wichers JH, Stoker PW. Energy and economic performance of small wind energy systems under different climatic conditions of South Africa. Renew Sustain Energy Rev 2018;98:376–92. https://doi.org/10.1016/j.rser.2018.09.037.
[161] Asamoah SS, Parbey J, Yankey IK, Awuah A. Techno-economic assessment of a central grid-connected wind farm in Ghana using RETScreen® Expert. Heliyon 2023;9:e12902. https://doi.org/10.1016/j.heliyon.2023.e12902.
[162] Mellichamp DA. Internal rate of return: Good and bad features, and a new way of interpreting the historic measure. Comput Chem Eng 2017;106:396–406. https://doi.org/10.1016/j.compchemeng.2017.06.005.
[163] Kreith F. PRINCIPLES OF ECONOMICS FOR SOLAR ENERGY INVESTMENTS. Sol. Energy Convers. II, Elsevier; 1981, p. 497–515. https://doi.org/10.1016/B978-0-08-025388-6.50071-4.
[164] Shouman ER, El Shenawy ET, Khattab NM. Market financial analysis and cost performance for photovoltaic technology through international and national perspective with case study for Egypt. Renew Sustain Energy Rev 2016;57:540–9. https://doi.org/10.1016/j.rser.2015.12.074.
[165] Cheremisinoff NP, Rosenfeld P, Davletshin AR. Environmental Economics. Responsible Care, Elsevier; 2008, p. 477–513. https://doi.org/10.1016/B978-1-933762-16-6.50012-8.
[166] Coker AK. COST ESTIMATION AND ECONOMIC EVALUATION. Ludwig's Appl. Process Des. Chem. Petrochemical Plants, Elsevier; 2007, p. 69–102. https://doi.org/10.1016/B978-075067766-0/50009-9.
[167] Frej EA, Ekel P, de Almeida AT. A benefit-to-cost ratio based approach for portfolio selection under multiple criteria with incomplete preference information. Inf Sci (Ny) 2021;545:487–98. https://doi.org/10.1016/j.ins.2020.08.119.
[168] Davidsdottir B, Ásgeirsson EI, Fazeli R, Gunnarsdottir I, Leaver J, Shafiei E, et al. Integrated Energy

Systems Modeling with Multi-Criteria Decision Analysis and Stakeholder Engagement for Identifying a Sustainable Energy Transition. Energies 2024;17:4266. https://doi.org/10.3390/en17174266.

[169] Das S, Dutta R, De S, De S. Review of multi-criteria decision-making for sustainable decentralized hybrid energy systems. Renew Sustain Energy Rev 2024;202:114676. https://doi.org/10.1016/j.rser.2024.114676.

[170] Charnes A, Cooper WW, Lewin AY, Seiford LM. Data Envelopment Analysis: Theory, Methodology, and Applications. Dordrecht: Springer Netherlands; 1994. https://doi.org/10.1007/978-94-011-0637-5.

[171] Hwang CL, Yoon K. Multiple Attribute Decision Making: Methods and Applications Springer-Verlag. New York, NY, USA 1981.

[172] Mergoni A, Emrouznejad A, De Witte K. Fifty years of Data Envelopment Analysis. Eur J Oper Res 2024. https://doi.org/10.1016/j.ejor.2024.12.049.

[173] Sofianopoulou S, Dedoussis V, Konstas K, Kassimis A. Efficiency evaluation of natural gas power plants using data envelopment analysis. IEEM 2009 - IEEE Int Conf Ind Eng Eng Manag 2009;2:315–9. https://doi.org/10.1109/IEEM.2009.5373352.

[174] Saati S, Marbini AH, Tavana M. Data envelopment analysis: an efficient duo linear programming approach. Int J Product Qual Manag 2011;7:90. https://doi.org/10.1504/IJPQM.2011.037733.

[175] Chakraborty S. TOPSIS and Modified TOPSIS : A comparative analysis. Decis Anal J 2022;2:100021. https://doi.org/10.1016/j.dajour.2021.100021.

[176] Zadeh Sarraf A, Mohaghar A, Bazargani H. Developing TOPSIS method using statistical normalization for selecting knowledge management strategies. J Ind Eng Manag 2013;6:860–75. https://doi.org/10.3926/jiem.573.

[177] Sagani A, Mihelis J, Dedoussis V. Techno-economic analysis and life-cycle environmental impacts of small-scale building-integrated PV systems in Greece. Energy Build 2017;139:277–90. https://doi.org/10.1016/j.enbuild.2017.01.022.

[178] Huld T, Müller R, Gambardella A. A new solar radiation database for estimating PV performance in Europe and Africa. Sol Energy 2012;86:1803–15. https://doi.org/10.1016/j.solener.2012.03.006.

[179] RETScreen® Clean Energy Management Software 2024. https://natural-resources.canada.ca/science-data/science-research/data-analysis/geospatial-data-portals-tools-services/retscreen.

[180] Surface Meteorology and Solar Energy. NASA Prediction Of Worldwide Energy Resources 2019. http://eosweb.larc.nasa.gov/sse.

[181] Christian Schill et. al. Task 13 Performance, Operation and Reliability of Photovoltaic Systems-Task 13 Report Template Task 13 Performance, Operation and Reliability of Photovoltaic Systems Soiling Losses-Impact on the Performance of Photovoltaic Power Plants 2022. 2022.

[182] SHARP (ND-235QCJ) 2017. http://www.wholesalesolar.com/products.folder/module-folder/sharp/ND-235QCJ.html.

[183] Solar Technology SA. SUNNY BOY 3000TL 2017. https://manuals.sma.de/SB30-50TL-21/en-US/822941067.html.

[184] Solar Technology SA. SUNNY TRIPOWER 5000TL - 12000TL - The Three-Phase Inverter – Not Only for Your Home... 2017. http://files.sma.de/dl/17781/STP12000TL-DEN1723-V10web.pdf.

[185] Islam MA, Ali MMN, Benitez IB, Sidi Habib S, Jamal T, Flah A, et al. A comprehensive evaluation of photovoltaic simulation software: A decision-making approach using Analytic Hierarchy Process and performance analysis. Energy Strateg Rev 2025;58:101663. https://doi.org/10.1016/j.esr.2025.101663.
[186] Febrian HG, Supriyanto A, Purwanto H. Calculating the energy capacity and capacity factor of floating photovoltaic (FPV) power plant in the cirata reservoir using different types of solar panels. J Phys Conf Ser 2023;2498. https://doi.org/10.1088/1742-6596/2498/1/012007.
[187] Frischknecht R, Jungbluth N, Althaus HJ, Doka G, Dones R, Heck T, et al. The ecoinvent database: Overview and methodological framework. Int J Life Cycle Assess 2005;10:3–9. https://doi.org/10.1065/lca2004.10.181.1.
[188] IEA PVPS. Life Cycle Inventories and Life Cycle Assessments of Photovoltaic Systems 2020. 2020.
[189] Tsiropoulos I, Nijs W, Tarvydas D, Ruiz Castello P. Towards net-zero emissions in the EU energy system by 2050. 2020. https://doi.org/10.2760/081488.
[190] PRé Sustainability. SimaPro. LCA software for informed change-makers 2022. https://simapro.com/.
[191] Herrmann IT, Moltesen A. Does it matter which Life Cycle Assessment (LCA) tool you choose? – a comparative assessment of SimaPro and GaBi. J Clean Prod 2015;86:163–9. https://doi.org/10.1016/j.jclepro.2014.08.004.
[192] DAPEEP. Energy mix 2024. 2025.
[193] Flavin C, Gonzalez M, Majano AM, Ochs A, Rocha M da, Tagwerker P. Study on the Development of the Renewable Energy Market in Latin America and the Caribbean. Inter-American Dev Bank 2014:1–67.
[194] Chumpolrat K, Sangsuwan V, Udomdachanut N, Kittisontirak S, Songtrai S, Chinnavornrungsee P, et al. Effect of Ambient Temperature on Performance of Grid-Connected Inverter Installed in Thailand. Int J Photoenergy 2014;2014:1–6. https://doi.org/10.1155/2014/502628.
[195] Kouremenos DA, Antonopoulos KA, Domazakis ES. Solar radiation correlations for the Athens, Greece, area. Sol Energy 1985;35:259–69. https://doi.org/10.1016/0038-092X(85)90105-7.
[196] Chandel SS, Aggarwal RK. Estimation of Hourly Solar Radiation on Horizontal and Inclined Surfaces in Western Himalayas. Smart Grid Renew Energy 2011;02:45–55. https://doi.org/10.4236/sgre.2011.21006.
[197] Hellenic National Meteorological Service. Hellenic National Meteorological Service 2025. https://www.emy.gr/.
[198] Kumar R, Umanand L. Estimation of global radiation using clearness index model for sizing photovoltaic system. Renew Energy 2005;30:2221–33. https://doi.org/10.1016/j.renene.2005.02.009.
[199] Sagani A, Vrettakos G, Dedoussis V. Viability assessment of a combined hybrid electricity and heat system for remote household applications. Sol Energy 2017;151:33–47. https://doi.org/10.1016/j.solener.2017.05.011.
[200] National Renewable Energy Laboratory. HOMER Pro Microgrid Analysis Software 2021. https://www.homerenergy.com/index.html.
[201] Soutsas K, Tsantopoulos G, Arabatzis G, Christopoulou O. Characteristics of tourism development

in mountainous regions using categorical regression. Int J Sustain Dev Plan 2006;1:32–45. https://doi.org/10.2495/SDP-V1-N1-32-45.

[202] Katsoulakos N. Is Forest Biomass Exploitation a Panacea To Deal With Energy Poverty in Mountainous Areas ? 2015.

[203] Gradziuk P, Development A. Wood fuels handbook: production, quality requirements, trading 2023.

[204] Li Z, Boyle F, Reynolds A. Domestic application of solar PV systems in Ireland: The reality of their economic viability. Energy 2011;36:5865–76. https://doi.org/10.1016/j.energy.2011.08.036.

[205] Kelleher J, Ringwood JV. A computational tool for evaluating the economics of solar and wind microgeneration of electricity. Energy 2009;34:401–9. https://doi.org/10.1016/j.energy.2008.10.009.

[206] German Institute for Standardisation. DIN 4108-2:2013-02. THERMAL PROTECTION AND ENERGY ECONOMY IN BUILDINGS - PART 2: MINIMUM REQUIREMENTS TO THERMAL INSULATION. 2013.

[207] Technical Chamber of Greece. TOTEE 20701-1 (2010), Technical Guideline of the Technical Chamber of Greece: Technical Guidelines on Buildings' Energy Performance. 2010.

[208] Tsalemis, D., Doulos, A., Perrakis. K., Tigkas, K., Vougiouklakis, G., Karalis, G., Vasilikos, C., Loumakis, S., Papastamatiou, P., Seimanidis, S., Siamidis, M., Psomas S. Redesign of the Market Support Mechanisms for Renewable Energy Sources in Greece, Hellenic Ministry for Energy and Climate Change. 2012.

[209] Arévalo P, Benavides D, Lata-García J, Jurado F. Energy control and size optimization of a hybrid system (photovoltaic-hidrokinetic) using various storage technologies. Sustain Cities Soc 2020;52:101773. https://doi.org/10.1016/j.scs.2019.101773.

[210] Babaei R, Ting DS-K, Carriveau R. Feasibility and optimal sizing analysis of stand-alone hybrid energy systems coupled with various battery technologies: A case study of Pelee Island. Energy Reports 2022;8:4747–62. https://doi.org/10.1016/j.egyr.2022.03.133.

[211] Nfah EM, Ngundam JM, Tchinda R. Modelling of solar/diesel/battery hybrid power systems for far-north Cameroon. Renew Energy 2007;32:832–44. https://doi.org/10.1016/j.renene.2006.03.010.

[212] Hidalgo-Leon R, Amoroso F, Urquizo J, Villavicencio V, Torres M, Singh P, et al. Feasibility Study for Off-Grid Hybrid Power Systems Considering an Energy Efficiency Initiative for an Island in Ecuador. Energies 2022;15:1776. https://doi.org/10.3390/en15051776.

[213] Hamanah WM, Abido MA, Alhems LM. Optimum Sizing of Hybrid PV, Wind, Battery and Diesel System Using Lightning Search Algorithm. Arab J Sci Eng 2020;45:1871–83. https://doi.org/10.1007/s13369-019-04292-w.

[214] Ghenai C, Bettayeb M. Modelling and performance analysis of a stand-alone hybrid solar PV/Fuel Cell/Diesel Generator power system for university building. Energy 2019;171:180–9. https://doi.org/10.1016/j.energy.2019.01.019.

[215] Aderemi BA, Chowdhury SD, Olwal TO, Abu-Mahfouz AM. Techno-Economic Feasibility of Hybrid Solar Photovoltaic and Battery Energy Storage Power System for a Soshanguve Mobile Cellular Base Station in South Africa 2018. https://doi.org/10.20944/preprints201804.0318.v1.

[216] Mokhtara C, Negrou B, Bouferrouk A, Yao Y, Settou N, Ramadan M. Integrated supply–demand energy management for optimal design of off-grid hybrid renewable energy systems for residential electrification in arid climates. Energy Convers Manag 2020;221:113192.

https://doi.org/10.1016/j.enconman.2020.113192.
[217] Beccali M, Brunone S, Cellura M, Franzitta V. Energy, economic and environmental analysis on RET-hydrogen systems in residential buildings. Renew Energy 2008;33:366–82. https://doi.org/10.1016/j.renene.2007.03.013.
[218] HEDNO. Hellenic Electricity Distribution Network Operator. Statistics reports and monthly reports on Non-Interconnected Islands released 2020. https://doi.org/https://deddie.gr/en/themata-tou-diaxeiristi-mi-diasundedemenwn-nisiwn/agora-mdn/stoixeia-ekkathariseon-kai-minaion-deltion-mdn/stoixeia-ekkathariseis-mdn/.
[219] Sagani, A., Dedoussis V. An integrated analysis of Hybrid Energy Systems for decarbonization of off-grid Islands based on life cycle thinking. Striving Stab. a Highly Uncertain Energy World, Maroussi Plaza Centre, Athens: HAEE Energy Transition Symposium; 2024.
[220] Strantzali E, Aravossis K, Livanos GA. Evaluation of future sustainable electricity generation alternatives: The case of a Greek island. Renew Sustain Energy Rev 2017;76:775–87. https://doi.org/10.1016/j.rser.2017.03.085.
[221] HEDNO. Hellenic Electricity Distribution Network Operator 2025. https://www.deddie.gr/en/ (accessed October 3, 2025).
[222] Skroufouta S, Baltas E. Investigation of hybrid renewable energy system (HRES) for covering energy and water needs on the Island of Karpathos in Aegean Sea. Renew Energy 2021;173:141–50. https://doi.org/10.1016/j.renene.2021.03.113.
[223] Giatrakos, G.P., Tsoutsos, T.D., Mouchtaropoulos, P.G., Naxakis, G.D., Stavrakakis G. Sustainable energy planning based on a stand-alone hybrid renewable energy/hydrogen power system: Application in Karpathos island, Greece. Renew Energy 2009;34:2562–70. https://doi.org/https://doi.org/10.1016/j.renene.2009.05.019.
[224] Katsaprakakis D Al, Christakis DG, Pavlopoylos K, Stamataki S, Dimitrelou I, Stefanakis I, et al. Introduction of a wind powered pumped storage system in the isolated insular power system of Karpathos-Kasos. Appl Energy 2012;97:38–48. https://doi.org/10.1016/j.apenergy.2011.11.069.
[225] Katsoulakos NM. An Overview of the Greek Islands' Autonomous Electrical Systems: Proposals for a Sustainable Energy Future. Smart Grid Renew Energy 2019;10:55–82. https://doi.org/10.4236/sgre.2019.104005.
[226] Vokas G, Lagogiannis K. PV Energy Production Over Greece: Comparison of Predicted and Measured Data of Medium-Scale Photovoltaic Parks 2013;2:3005–11.
[227] Katsoulakos NM. An Overview of the Greek Islands ' Autonomous Electrical Systems : Proposals for a Sustainable Energy Future 2019:55–82. https://doi.org/10.4236/sgre.2019.104005.
[228] RAE. Regulation for Operating the Electrical Systems of Non-Interconnected Islands (NII Regulation). 2018.
[229] International Renewable Energy Agency (IRENA). RENEWABLE GENERATION COSTS IN 2024. Abu Dhab: 2025.
[230] Papoutsis A. ENERGY AUTONOMY IN GREEK ISLANDS USING " ISLAND - SPECIFIC " RENEWABLE ENERGY TECHNOLOGIES . Delft University of Technology, 2023.
[231] Kourtaki A. Greece Inflation Rate 1960-2023. Hell Stat Auth 2023. https://www.statistics.gr/en/home/ (accessed November 5, 2024).

[232] Rawat R, Chandel SS. Simulation and optimization of solar photovoltaic-wind stand alone hybrid system in hilly terrain of India. Int J Renew Energy Res 2013;3:595–604.
[233] PAVAN KUMAR Y V., BHIMASINGU R. Renewable energy based microgrid system sizing and energy management for green buildings. J Mod Power Syst Clean Energy 2015;3:1–13. https://doi.org/10.1007/s40565-015-0101-7.
[234] Frischknecht R, Rebitzer G. The ecoinvent database system: A comprehensive web-based LCA database. J Clean Prod 2005;13:1337–43. https://doi.org/10.1016/j.jclepro.2005.05.002.
[235] Odeh NA, Cockerill TT. Life cycle GHG assessment of fossil fuel power plants with carbon capture and storage. Energy Policy 2008;36:367–80. https://doi.org/10.1016/j.enpol.2007.09.026.
[236] Cui X, Hong J, Gao M. Environmental impact assessment of three coal-based electricity generation scenarios in China. Energy 2012;45:952–9. https://doi.org/10.1016/j.energy.2012.06.063.
[237] Riva A, D'Angelosante S, Trebeschi C. Natural gas and the environmental results of life cycle assessment. Energy 2006;31:138–48. https://doi.org/10.1016/j.energy.2004.04.057.
[238] Yang Y-H, Lin S-J, Lewis C. Life Cycle Assessment of Fuel Selection for Power Generation in Taiwan. J Air Waste Manage Assoc 2007;57:1387–95. https://doi.org/10.3155/1047-3289.57.11.1387.
[239] Song Q, Wang Z, Li J, Duan H, Yu D, Liu G. Comparative life cycle GHG emissions from local electricity generation using heavy oil, natural gas, and MSW incineration in Macau. Renew Sustain Energy Rev 2018;81:2450–9. https://doi.org/10.1016/j.rser.2017.06.051.
[240] Raugei M, Frankl P. Lifcycle impacts and costs of photovoltaic systems: Current state of the art and future outlookse. Energy 2009;34:392–9. https://doi.org/10.1016/j.energy.2009.01.001.
[241] Fthenakis VM, Kim HC. Greenhouse-gas emissions from solar electric- and nuclear power: A life-cycle study. Energy Policy 2007;35:2549–57. https://doi.org/10.1016/j.enpol.2006.06.022.
[242] Kaldellis JK, Apostolou D. Life cycle energy and carbon footprint of offshore wind energy. Comparison with onshore counterpart. Renew Energy 2017;108:72–84. https://doi.org/10.1016/j.renene.2017.02.039.
[243] Raadal, H.L., Vold, B.I., Myhr, A., Nygaard TA. GHG emissions and energy performance of offshore wind power. Renew Energy 2014;66:314–24. https://doi.org/10.1016/j.renene.2013.11.075.
[244] Ingrao C, Bacenetti J, Adamczyk J, Ferrante V, Messineo A, Huisingh D. Investigating energy and environmental issues of agro-biogas derived energy systems: A comprehensive review of Life Cycle Assessments. Renew Energy 2019;136:296–307. https://doi.org/10.1016/j.renene.2019.01.023.
[245] Masanet E, Chang Y, Gopal AR, Larsen P, Morrow WR, Sathre R, et al. Life-Cycle Assessment of Electric Power Systems. Annu Rev Environ Resour 2013;38:107–36. https://doi.org/10.1146/annurev-environ-010710-100408.
[246] Weisser D. A guide to life-cycle greenhouse gas (GHG) emissions from electric supply technologies. Energy 2007;32:1543–59. https://doi.org/10.1016/j.energy.2007.01.008.
[247] Blackett G, Savory E, Toy N, Parke GAR, Clark M, Rabjohns B. An evaluation of the environmental burdens of present and alternative materials used for electricity transmission. Build Environ 2008;43:1326–38. https://doi.org/10.1016/j.buildenv.2006.08.032.
[248] Sinha R, Lennartsson M, Frostell B. Environmental footprint assessment of building structures: A comparative study. Build Environ 2016;104:162–71. https://doi.org/10.1016/j.buildenv.2016.05.012.

[249] Jorge RS, Hertwich EG. Environmental evaluation of power transmission in Norway. Appl Energy 2013;101:513–20. https://doi.org/10.1016/j.apenergy.2012.06.004.
[250] Arvesen A, Hauan IB, Bolsøy BM, Hertwich EG. Life cycle assessment of transport of electricity via different voltage levels: A case study for Nord-Trøndelag county in Norway. Appl Energy 2015;157:144–51. https://doi.org/10.1016/j.apenergy.2015.08.013.
[251] Jones CI, McManus MC. Life-cycle assessment of 11kV electrical overhead lines and underground cables. J Clean Prod 2010;18:1464–77. https://doi.org/10.1016/j.jclepro.2010.05.008.
[252] Bumby S, Druzhinina E, Feraldi R, Werthmann D, Geyer R, Sahl J. Life Cycle Assessment of Overhead and Underground Primary Power Distribution. Environ Sci Technol 2010;44:5587–93. https://doi.org/10.1021/es9037879.
[253] Turconi R, Simonsen CG, Byriel IP, Astrup T. Life cycle assessment of the Danish electricity distribution network. Int J Life Cycle Assess 2014;19:100–8. https://doi.org/10.1007/s11367-013-0632-y.
[254] Harrison GP, Maclean E (Ned). J, Karamanlis S, Ochoa LF. Life cycle assessment of the transmission network in Great Britain. Energy Policy 2010;38:3622–31. https://doi.org/10.1016/j.enpol.2010.02.039.
[255] Santoyo-Castelazo E, Gujba H, Azapagic A. Life cycle assessment of electricity generation in Mexico. Energy 2011;36:1488–99. https://doi.org/10.1016/j.energy.2011.01.018.
[256] Brizmohun R, Ramjeawon T, Azapagic A. Life cycle assessment of electricity generation in Mauritius. J Clean Prod 2015;106:565–75. https://doi.org/10.1016/j.jclepro.2014.11.033.
[257] Rakotoson V, Praene JP. A life cycle assessment approach to the electricity generation of French overseas territories. J Clean Prod 2017;168:755–63. https://doi.org/10.1016/j.jclepro.2017.09.055.
[258] Somorin TO, Di Lorenzo G, Kolios AJ. Life-cycle assessment of self-generated electricity in Nigeria and Jatropha biodiesel as an alternative power fuel. Renew Energy 2017;113:966–79. https://doi.org/10.1016/j.renene.2017.06.073.
[259] Atilgan B, Azapagic A. An integrated life cycle sustainability assessment of electricity generation in Turkey. Energy Policy 2016;93:168–86. https://doi.org/10.1016/j.enpol.2016.02.055.
[260] García-Gusano D, Garraín D, Dufour J. Prospective life cycle assessment of the Spanish electricity production. Renew Sustain Energy Rev 2017;75:21–34. https://doi.org/10.1016/j.rser.2016.10.045.
[261] Quek TYA, Alvin Ee WL, Chen W, Ng TSA. Environmental impacts of transitioning to renewable electricity for Singapore and the surrounding region: A life cycle assessment. J Clean Prod 2019;214:1–11. https://doi.org/10.1016/j.jclepro.2018.12.263.
[262] Kaldellis, J., Spyropoulos, G., Chalvatzis K. The Impact of Greek Electricity Generation Sector on the National Air Pollution Problem. Fresenius Environ Bull 2004:647–56.
[263] Georgakellos DA. Climate change external cost appraisal of electricity generation systems from a life cycle perspective: the case of Greece. J Clean Prod 2012;32:124–40. https://doi.org/10.1016/j.jclepro.2012.03.030.
[264] Theodosiou G, Koroneos C, Stylos N. Environmental impacts of the Greek electricity generation sector. Sustain Energy Technol Assessments 2014;5:19–27. https://doi.org/10.1016/j.seta.2013.10.005.
[265] Orfanos N, Mitzelos D, Sagani A, Dedoussis V. Life-cycle environmental performance assessment

of electricity generation and transmission systems in Greece. Renew Energy 2019;139:1447–62. https://doi.org/10.1016/j.renene.2019.03.009.
[266] PPC. Greek Public Power Corporation 2025. www.dei.gr (accessed June 6, 2025).
[267] Kaldellis JK, Mantelis N, Zafirakis D. Evaluating the ability of Greek power stations to comply with the obligations posed by the second National Allocation Plan concerning carbon dioxide emissions. Fuel 2011;90:2884–95. https://doi.org/10.1016/j.fuel.2011.04.039.
[268] IPTO. Independent Power Transmission Operator S.A. 2025. https://www.admie.gr/en (accessed October 3, 2025).
[269] DAPEEP. Operator of the Greek Electricity Market and Guarantees of Origin 2025.
[270] Minister of Environment Energy & Climate Change. National Renewable Energy Action Plan in the Scope of Directive 2009/28/EC. 2009.
[271] N Lioutas, S Lazarou, G Marmidis, E Pyrgioti DA. Overhead line and cable mapping of the Greek electric transmission system, for the study of transitional overvoltages, using EMTP-ATP. 15th Int. Symp. high Volt. Eng., Elektroinštitut Milan Vidmar, Ljubljana, Slovenia: ISH; 2007, p. 2–6.
[272] Turconi R, Boldrin A, Astrup T. Life cycle assessment (LCA) of electricity generation technologies: Overview, comparability and limitations. Renew Sustain Energy Rev 2013;28:555–65. https://doi.org/10.1016/j.rser.2013.08.013.
[273] Vattenfall. Life Cycle Assessments for Vattenfall ' s electricity generation. 2023.
[274] International Energy Agency (IEA). Electricity information database 2010. https://www.iea.org/statistics/topics/Electricity/ (accessed September 20, 2025).
[275] Meier PJ, Wilson PPH, Kulcinski GL, Denholm PL. US electric industry response to carbon constraint: a life-cycle assessment of supply side alternatives. Energy Policy 2005;33:1099–108. https://doi.org/10.1016/j.enpol.2003.11.009.
[276] Energy Information Administration. Natural Gas 1998: Issues and Trends. Office of Oil and Gas. US Dep Energy, Washingt 1998. http://www.eia.doe.gov/oil_gas/natural_gas/analysis_publications/natural_gas_1998_issues_and_trends/it98.html.
[277] International Energy Agency Statistics. Electric power transmission and distribution losses (% of output) 2014. http://www.iea.org/statistics/statisticssearch/ (accessed October 5, 2025).
[278] Moirasgentis, S., Sarafidis, G., Georgopoulou E. Long Term Plan for the Greek Energy System. 2017.
[279] Siddiqui S, Zerhusen B, Zehetmeier M, Effenberger M. Distribution of specific greenhouse gas emissions from combined heat-and-power production in agricultural biogas plants. Biomass and Bioenergy 2020;133:105443. https://doi.org/10.1016/j.biombioe.2019.105443.
[280] Kanchiralla FM, Brynolf S, Malmgren E, Hansson J, Grahn M. Life-Cycle Assessment and Costing of Fuels and Propulsion Systems in Future Fossil-Free Shipping. Environ Sci Technol 2022;56:12517–31. https://doi.org/10.1021/acs.est.2c03016.
[281] Atilgan B, Azapagic A. Life cycle environmental impacts of electricity from fossil fuels in Turkey. J Clean Prod 2015;106:555–64. https://doi.org/10.1016/j.jclepro.2014.07.046.
[282] Al Rashdi Z, Barghash H, Al Habsi F, Okedu KE. Environmental impact assessment of different power generation strategies in Oman: A comparative life-cycle analysis. Heliyon 2024;10:e37781. https://doi.org/10.1016/j.heliyon.2024.e37781.

[283] Castro-Diaz L, García MA, Villamayor-Tomas S, Lopez MC. Impacts of hydropower development on locals' livelihoods in the Global South. World Dev 2023;169:106285. https://doi.org/10.1016/j.worlddev.2023.106285.
[284] Low Carbon Power. Global Electricity Generation by Source 2024 2024. https://lowcarbonpower.org/ (accessed December 5, 2024).
[285] Gennitsaris S, Sagani A, Sofianopoulou S, Dedoussis V. Integrated LCA and DEA approach for circular economy-driven performance evaluation of wind turbine end-of-life treatment options. Appl Energy 2023;339:120951. https://doi.org/10.1016/j.apenergy.2023.120951.
[286] Vestas. Vestas secures 36 MW order in Greece 2022. https://www.vestas.com/en/media/company-news/2022/vestas-secures-36-mw-order-in-greece-c3537288 (accessed March 31, 2022).
[287] Li Y. Wind Generation. Cyber-Physical Microgrids, Cham: Springer International Publishing; 2022, p. 77–97. https://doi.org/10.1007/978-3-030-80724-5_5.
[288] Tota-Maharaj K, McMahon A. Resource and waste quantification scenarios for wind turbine decommissioning in the United Kingdom. Waste Dispos Sustain Energy 2021;3:117–44. https://doi.org/10.1007/s42768-020-00057-6.
[289] Mone, C., Hand, M., Bolinger, M., Rand, J., Heimiller, D., Ho G. 2015 Cost of Wind Energy Review. 2017.
[290] Gharfalkar M, Court R, Campbell C, Ali Z, Hillier G. Analysis of waste hierarchy in the European waste directive 2008/98/EC. Waste Manag 2015;39:305–13. https://doi.org/10.1016/j.wasman.2015.02.007.
[291] Andersen N. Wind turbine end-of-life: Characterisation of waste material. University of Gävle, 2015.
[292] Vestas. Life Cycle Assessment of Electricity Production from an onshore V110-2 MW Wind Plant. Vestas Wind Syst A/S 2015:129.
[293] Frischknecht, R., Jungbluth, N., Althaus, HJ., Doka, G., Dones, R., Heck, T., Hellweg, S., Hischier, R., Nemecek, T., Rebitzer, G., Spielmann M. The ecoinvent Database: Overview and Methodological Framework (7 pp). Int J Life Cycle Assess 2005;10:3–9. https://doi.org/10.1065/lca2004.10.181.1.
[294] Vo Dong PA, Azzaro-Pantel C, Cadene AL. Economic and environmental assessment of recovery and disposal pathways for CFRP waste management. Resour Conserv Recycl 2018;133:63–75. https://doi.org/10.1016/j.resconrec.2018.01.024.
[295] Yang W, Kim KH, Lee J. Upcycling of decommissioned wind turbine blades through pyrolysis. J Clean Prod 2022;376:134292. https://doi.org/10.1016/J.JCLEPRO.2022.134292.
[296] Psomopoulos CS, Kalkanis K, Kaminaris S, Ioannidis GC, Pachos P. A Review of the Potential for the Recovery of Wind Turbine Blade Waste Materials. Recycl 2019;4:7. https://doi.org/10.3390/RECYCLING4010007.
[297] Yoder C. Cost to Recycle Metal / Desert Metal n.d. http://recycletucson.com/cost-recycle-metal/ (accessed August 25, 2022).
[298] Liu P, Meng F, Barlow CY. Wind turbine blade end-of-life options: An economic comparison. Resour Conserv Recycl 2022;180:106202. https://doi.org/10.1016/j.resconrec.2022.106202.
[299] Ohemeng EA, Ekolu SO. Comparative analysis on costs and benefits of producing natural and recycled concrete aggregates: A South African case study. Case Stud Constr Mater

2020;13:e00450. https://doi.org/10.1016/j.cscm.2020.e00450.
[300] Hoefer M. Wind Turbine Blade Recycling: An Economic Decision Framework. 2015. https://doi.org/10.13140/RG.2.2.28393.90723.
[301] Iqbal Ali A, Seiford LM. Translation invariance in data envelopment analysis. Oper Res Lett 1990;9:403–5. https://doi.org/10.1016/0167-6377(90)90061-9.
[302] Scheel H. Undesirable outputs in efficiency valuations. Eur J Oper Res 2001;132:400–10. https://doi.org/10.1016/S0377-2217(00)00160-0.
[303] WindEurope. Accelerating Wind Turbine Blade Circularity. 2020.